

**DEVELOPMENT AND APPLICATION OF A GEOMORPHIC-BASED VULNERABILITY INDEX FOR
ASSESSING RELATIVE COASTAL VULNERABILITY TO EROSION UNDER WAVE
ENERGY SCENARIOS ASSOCIATED WITH CLIMATE CHANGE**

By Samantha Whitney Page

A Thesis Submitted to
Saint Mary's University, Halifax, Nova Scotia
in Partial Fulfillment of the Requirements for
the Degree of Masters of Science in Applied Science

January, 2015, Halifax, Nova Scotia

Copyright Samantha Whitney Page, 2015

Approved: Dr. Danika van Proosdij
Supervisor
Department of Geography

Approved: Dr. Jeremy Lundholm
Supervisory Committee
Department of Biology

Approved: Dr. Jason Grek-Martin
Supervisory Committee
Department of Geography

Approved: Dr. Don Forbes
External Examiner
Geological Survey of Canada

Date: January 26th, 2015

**DEVELOPMENT AND APPLICATION OF A GEOMORPHIC-BASED VULNERABILITY INDEX FOR
ASSESSING RELATIVE COASTAL VULNERABILITY TO EROSION UNDER WAVE
ENERGY SCENARIOS ASSOCIATED WITH CLIMATE CHANGE**

By Samantha Whitney Page

ABSTRACT

With the projected increase in global mean sea level rise, small coastal communities face formidable challenges as they seek to sustainably manage their coastal assets and resources impacted by sea level rise (SLR). Consequently, it has become increasingly important to assess a community's coastal vulnerability. In collaboration with the Partnership for Canada-Caribbean Community Climate Change Adaptation (ParCA) project, the aim of this research was twofold: 1) develop a tool to assess relative physical coastal vulnerability to erosion, incorporating the geomorphic components of assailing, resistance, and resilience characteristics and 2) apply the tool to Lockeport, Nova Scotia under four wave energy scenarios to simulate how the addition of storm winds and increases in water depths associated with climate change conditions changes the wave energy reaching the shoreline; ultimately allowing for the determination of coastline and building vulnerability to erosion and inundation. The identification of areas and buildings most vulnerable to SLR-induced erosion and inundation, under varying wave energy scenarios, is meant to guide coastal planning and SLR adaptation strategies in the Town of Lockeport, Nova Scotia.

Janauray 26th, 2015

ACKNOWLEDGEMENTS

First and foremost, I would like to thank my supervisor, Dr. Danika van Proosdij for her guidance and support, for trusting me to work so independently, and for providing me with an incredible opportunity to conduct international research. Thank you also to my committee members, Dr. Jason Grek-Martin and Dr. Jeremy Lundholm, for their encouragement and insight, and to Dr. Don Forbes for agreeing to be my external examiner; I am truly honoured and appreciative. I would like to especially thank Cathy Sedge for her incredible assistance with collecting field data for over 60 km of shoreline and walking every inch of it – you were such a trooper. I would also like to thank Matt Christian, my research assistant, for the many hours he spent computing WEMo scenarios and helping to puzzle out GIS analyses, for his unquestionable faith in my GIS abilities, and for the many Samuel moments. Thank you also to Graeme Matheson for your help with flood modeling. Thank you Danika, Jason, Cristian, Hugh, Bob, Philip, Ryan, Will, and Greg, the Geography Department family at SMU, for providing a supportive and inspirational environment in which to work – whether knowingly or not, you have each had an invaluable contribution to this thesis. Thank you Brittany MacIsaac, my fellow masters student, for the many, many hours spent puzzling each other's theses at cafes. Thank you to my biggest cheerleaders; Carianne Johnson, Dad, Jonathan Crevelle, Jay Lunda and especially my Mom – supporter, motivator, and editor extraordinaire! Thank you to my Caribbean family here in NS, for providing a ray of sunshine throughout the dark days of winter and writing (DK, JK, ES, JJ, JG, JL) and to all of my remaining friends and family for their support and encouragement. A huge thank you to the community of Shelburne for hosting me during the field research season and for welcoming me, wholeheartedly into their community. I would also like to thank the Town of Lockeport for their kindness, generosity and assistance in completing my research; especially Bil Atwood, who contributed an incredible amount of his time providing context for my research and for walking all the way to Sam's Point just to ensure I had received some useful documents – your dedication to the community is truly admirable. Thank you also to the Robin Rigby Trust for providing funding for international research and cross-cultural comparisons and to the Faculty of Graduate Studies and Research at SMU for their financial and logistical support – especially Shane Costantino. Last, but not least, thank you to the Partnership for Canada-Caribbean Community Climate Change Adaptation (ParCA) project for providing the necessary funding with which to complete this research and to Dr. Dan Scott for the incredible opportunity to conduct research in Trinidad and Tobago.

ACRONYMS

AR4 – Assessment Report 4

AR5 – Assessment Report 5

BS - Backshore

CCC – Coastal Characteristic Class

CPS – Coastal Protection Structure

CVA – Coastal Vulnerability Assessment

CVI – Coastal Vulnerability Index

DSAS – Digital Shoreline Analysis System

DEM – Digital Elevation Model

FS - Foreshore

GHG – Green House Gas

GIA – Glacial Isostatic Adjustment

GIS – Geographical Information System

GPS – Global Positioning System

GMSLR – Global Mean Sea Level Rise

ICSP – Integrated Community Sustainability Plan

IPCC – Intergovernmental Panel on Climate Change

IRIACC – International Research Initiative on Adaptation to Climate Change

LECZ – Low-elevation Coastal Zone

LiDAR – Light Detection and Ranging

MCCAP – Municipal Climate Change Action Plan

MP_SpARC – Maritime Provinces Spatial Analysis Research Centre

NDBC – National Data Buoy Center

NRCan – Natural Resources Canada

NS – Nearshore

NSTDB – Nova Scotia Topographic Database

NSCS – Nova Scotia Coastal Series
ParCA – Partnership for Canada-Caribbean Community Climate Change Adaptation
PC – Principal Component
PCA – Principal Component Analysis
RCP – Representative Concentration Pathways
RSLR – Relative Sea Level Rise
RWE – Representative Wave Energy
S1 – Wave Energy Scenario 1
S2 – Wave Energy Scenario 2
S3 – Wave Energy Scenarios 3
S4 – Wave Energy Scenario 4
SAR – Synthetic Aperture Radar
SCD – Shoreline Characterization Database
SES – Socio-ecological System
SIDS – Small Island Developing States
SLR – Sea Level Rise
SoCVI – Social Coastal Vulnerability Index
SRES – Special Report on Emissions Scenarios
WAIS – West Antarctic Ice Sheet
WEMo – Wave Exposure Model

TABLE OF CONTENTS

Abstract	ii
Acknowledgements	iii
Acronyms	iv
Table of Contents	vi
List of Tables	ix
List of Figures	x
Chapter 1: Introduction and Literature Review	1
1.1 Research Context	1
1.2 Coastal Zone	5
1.2.1 Coastal Zone Definition	6
1.2.3 Coastal Dynamics & Adaptive Capacity	8
1.3 Sea Level Rise.....	12
1.3.1 Drivers of Sea Level Change	13
1.3.2 Climate Change Projections	16
1.3.3 Sea Level Rise Impacts	19
1.3.3.1 Erosion	20
1.3.3.2 Storm Events.....	22
1.3.3.3 Inundation	23
1.4 Vulnerability	23
1.4.1 Geomorphic Vulnerability	26
1.4.2 Vulnerable Coasts	27
1.5 Assessing Coastal Vulnerability.....	29
1.5.1 Coastal Vulnerability Index (CVI).....	29
1.5.2 Development of a Coastal Vulnerability Index.....	30
1.5.2.1 Environment Type.....	30
1.5.2.2 Event	31
1.5.2.3 System Type.....	31
1.5.2.4 Scale.....	32
1.5.2.5 Data Availability	34
1.5.2.6 Formula & Parameter Weighting.....	34
1.6 Purpose of Study & Objectives	35

Chapter 2: Description of Study Area	38
2.1 Site Selection	38
2.2 Location & Geography	39
2.3 People, Economy, & Assets	42
2.4 Ocean & Climate Impacts	44
2.5 Anthropogenic Intervention & Adaptation.....	48
2.6 Current Climate Change Challenges	52
Chapter 3: Research Design and Methodology	54
3.1 Research Design Overview	54
3.2 CVI Development (Step 1).....	56
3.2.1 <i>CVI Purpose</i>	56
3.2.2 <i>Parameter Selection</i>	56
3.2.3 <i>Data Collection</i>	61
3.2.3.1 Detailed Coastal Mapping.....	61
3.2.3.2 GIS Modeling & Analysis	69
3.2.4 <i>Matrix Creation</i>	76
3.2.4.1 Assailing Parameters.....	78
3.2.4.2 Resistance Parameters	79
3.2.4.3 Resilience Parameters	88
3.2.5 <i>CVI Calculation</i>	92
3.2.6 <i>Coastal Vulnerability & Coastal Characterization Classes</i>	95
3.3 CVI Application (Step 2)	96
3.3.1 <i>Wave Energy Scenario 1</i>	97
3.3.2 <i>Wave Energy Scenario 2</i>	97
3.3.3 <i>Wave Energy Scenario 3</i>	99
3.3.4 <i>Wave Energy Scenario 4</i>	99
3.3.5 <i>Proof of Concept</i>	100
3.3.5.1 Observed Erosion & Areas of Concern.....	100
3.3.5.2 Principal Components Analysis.....	101
3.4 Identification of Vulnerable Buildings (Steps 3 & 4).....	102
3.4.1 <i>Coastal Zone Delineation</i>	103
3.4.2 <i>Buildings Vulnerable to Erosion</i>	103
3.4.3 <i>Buildings Vulnerable to Erosion & Inundation</i>	103
Chapter 4: Results	105
4.1 CVI Development (Step 1).....	105
4.1.1 <i>Matrix Creation</i>	106
4.1.2 <i>Wave Energy Scenarios</i>	106
4.1.3 <i>Coastal Vulnerability and Coastal Characterization Classes</i>	113
4.2 CVI Application (Step 2)	114
4.2.1 <i>Proof of Concept</i>	121
4.2.1.1 Observed Erosion & Areas of Concern.....	121
4.2.1.2 Principal Components Analysis.....	123
4.3 Identification of Vulnerable Buildings (Steps 3 & 4).....	126
4.3.1 <i>Coastal Zone Delineation</i>	126
4.3.2 <i>Buildings Vulnerable to Erosion</i>	127

4.3.3	<i>Buildings Vulnerable to Erosion & Inundation</i>	129
Chapter 5: Discussion	137
5.1	Introduction	137
5.2	Field Based Shoreline Characterization for Assessing Vulnerability	137
5.3	CVI Development	140
5.4	Incorporation of Geomorphic Resilience	143
5.5	CVI Application under Extreme Event Scenarios	148
5.6	Buildings in the Coastal Zone at Risk to Erosion & Inundation	153
5.7	Conclusions & Recommendations	158
5.8	Observations & Recommendations for Lockeport	159
References	164
Appendix A: Shoreline Characterization Charts and Definitions	182
Appendix B: Individual Resistance and Resilience Parameter Contribution to Coastal Vulnerability for Lockeport	190
Appendix C: Permissions	198

LIST OF TABLES

Table 1.1	Equivalent RCP and SRES Scenarios and Associated SLR Projections	17
Table 1.2	Summary of CVIs Applied in Different Countries.....	33
Table 2.1	Percent Coverage of Backshore and Foreshore Features.....	40
Table 2.2	Summary of Select Storms and Hurricanes that Impacted Lockeport.....	46
Table 3.1	Included Parameters and their Frequency of use in 22 Reviewed CVIs	58
Table 3.2	Parameter Selection Process	60
Table 3.3	Data Sources for CVI Matrix Parameters	61
Table 3.4	Geindicator Observations Used to Characterize Sediment Supply State	66
Table 3.5	Attributes Used to Characterize Vegetation State	66
Table 3.6	Attributes Used to Characterize Coastal Protection Structure Point Features....	68
Table 3.7	WEMo Fetch Inputs	71
Table 3.8	Parameters Used in ArcGIS 10.1 Krigging Interpolation Method	74
Table 3.9	Coastal Characterization Class Weighting Process	93
Table 3.10	CVI Calculation for Backshore Segment #87.....	94
Table 3.11	Vulnerability Ranks and Corresponding CVI Ranges	95
Table 3.12	Coastal Characteristic Class (CCC) Ranks and Their Contribution to Coastal Vulnerability Index Scores vs. Actual Coastal Characteristics.....	96
Table 4.1	Relative Coastal Vulnerability Index for Assessing Vulnerability to Erosion in Lockeport, Nova Scotia	108
Table 4.2	CVI Summary for S1 to S4	117
Table 4.3	Principal Components Analysis Loading and Variance	124

LIST OF FIGURES

Figure 1.1	Comparison of Special Report Emission Scenarios (SRES) and Representative Concentration Pathways (RCP) to the year 2100 and RCP Extensions to the Year 2300	17
Figure 1.2	Global Mean Sea Level Rise (GMSLR) Projections for RCP Scenario 2.6, 4.5, 6.0, and 8.5	18
Figure 1.3	Influence of Adaptive Capacity on Exposure, Sensitivity, and Vulnerability.....	25
Figure 2.1	Study Area - Town Of Lockeport, Nova Scotia	41
Figure 2.2	Historical Images of Lockeport	43
Figure 2.3	Little School & Marine Building Museum Flooded from Hurricane Bill Storm Surge	47
Figure 2.4	Calf Island Road Submerged during the February 9 th , 2013 Winter Storm	47
Figure 2.5	The Origins of Crescent Beach	49
Figure 2.6	Calf Island Road Bridge	49
Figure 2.7	Access Stairways by Crescent Beach Centre.....	51
Figure 2.8	Lobster Traps used to Develop Foredune on Crescent Beach	52
Figure 2.9	Observed Locations Vulnerable to climate Change Impacts in Lockeport, Nova Scotia	53
Figure 3.1	Research Design Flowchart.....	55
Figure 3.2	Distribution of Parameter Use from 22 Reviewed CVIs.....	58
Figure 3.3	Coastal Zone Boundaries and Nearshore, Foreshore, and Backshore Characterization Lines	65
Figure 3.4	Method Used to Measure Slope of Coastal Protection Structures.....	69
Figure 3.5	Axes Used to Measure Average Rock Size of Coastal Protection Structures	69

Figure 3.6	Required WEMo Inputs and Resulting Output	73
Figure 3.7	Backshore Segment Mid-points and Foreshore Width Measurement	75
Figure 3.8	Classification and Ranking of Wave Energy	80
Figure 3.9	Ranking of Foreshore Geomorphology	80
Figure 3.10	Ranking of Foreshore and Backshore Slope.....	82
Figure 3.11	Classification and Ranking of Foreshore Width	83
Figure 3.12	Classification and Ranking of Backshore Elevation.....	84
Figure 3.13	Ranking of Vegetation	85
Figure 3.14	Ranking of CPSs.....	87
Figure 3.15	Ranking of Morphological Resilience.....	89
Figure 3.16	Classification and Ranking of Accommodation Space	91
Figure 3.17	Ranking of Sediment Supply	92
Figure 3.18	Wind Rose for Hourly Wind Data from January 1 st , 2011 – December 31 st , 2013	98
Figure 3.19	Wind Rose for Hourly Wind Data from February 9 th , at 1 am – February 10 th , at 11 am, 2013 (February 2013 Storm).....	98
Figure 4.1	Representative Wave Energy Values for Wave Energy Scenario 1	109
Figure 4.2	Representative Wave Energy Values for Wave Energy Scenario 2	109
Figure 4.3	Representative Wave Energy Values for Wave Energy Scenario 3	110
Figure 4.4	Representative Wave Energy Values for Wave Energy Scenario 4	110
Figure 4.5	Contribution of Wave Energy Parameter (Wave Energy Scenario 1) to Coastal Vulnerability	111
Figure 4.6	Contribution of Wave Energy Parameter (Wave Energy Scenario 2) to Coastal Vulnerability	111
Figure 4.7	Contribution of Wave Energy Parameter (Wave Energy Scenario 3) to Coastal Vulnerability	112
Figure 4.8	Contribution of Wave Energy Parameter (Wave Energy Scenario 4) to Coastal Vulnerability	112

Figure 4.9	Theoretical Relationships between Coastal Vulnerability and Coastal Characterization Classes	115
Figure 4.10	Coastal Vulnerability Index for Wave Energy Scenario 1	118
Figure 4.11	Coastal Vulnerability Index for Wave Energy Scenario 2	118
Figure 4.12	Coastal Vulnerability Index for Wave Energy Scenario 3	119
Figure 4.13	Coastal Vulnerability Index for Wave Energy Scenario 4	119
Figure 4.14	Percent of Shoreline Associated with each Vulnerability Rank for Wave Energy Scenarios 1-4	120
Figure 4.15	Coastal Vulnerability Index Values under Wave Energy Scenario 1, Observed Erosion Points, and Noted Areas of Concern for Select Locations in Lockeport, Nova Scotia	122
Figure 4.16	Principal Component Analysis Scores Plot (PC1 vs. PC2)	125
Figure 4.17	Principal Component Analysis Scores Plot (PC1 vs. PC3)	125
Figure 4.18	Principal Component Analysis Scores Plot (PC1 vs. PC4)	126
Figure 4.19	Coastal Zone of Lockeport, Nova Scotia	127
Figure 4.20	Vulnerability of Buildings in the Coastal Zone to Erosion under Wave Energy Scenario 1	131
Figure 4.21	Vulnerability of Buildings in the Coastal Zone to Erosion under Wave Energy Scenario 2	131
Figure 4.22	Vulnerability of Buildings in the Coastal Zone to Erosion under Wave Energy Scenario 3	132
Figure 4.23	Vulnerability of Buildings in the Coastal Zone to Erosion under Wave Energy Scenario 4	132
Figure 4.24	Number of Buildings in the Coastal Zone Vulnerable to Erosion under Wave Energy Scenarios S1 to S4	133
Figure 4.25	Inundation Extent Associated with Wave Energy Scenario 3	134
Figure 4.26	Inundation Extent Associated with Wave Energy Scenario 4	134
Figure 4.27	Vulnerability of Buildings in the Coastal Zone to Erosion and Inundation Associated with Wave Energy Scenario 3	135
Figure 4.28	Vulnerability of Buildings in the Coastal Zone to Erosion and Inundation Associated with Wave Energy Scenario 4	135

Figure 4.29	Number of Buildings in the Coastal Zone Vulnerable to Erosion and Inundation under Wave Energy Scenarios 3 and 4	136
Figure A.1	Backshore Shoreline Characterization Chart	183
Figure A.2	Foreshore Shoreline Characterization Chart	184
Figure A.3	Nearshore Shoreline Characterization Chart	185
Figure A.4	Contribution of Foreshore Geomorphology Parameter to Coastal Vulnerability	193
Figure A.5	Contribution of Foreshore Slope Parameter to Coastal Vulnerability	193
Figure A.6	Contribution of Foreshore Width Parameter to Coastal Vulnerability	194
Figure A.7	Contribution of Backshore Elevation Parameter to Coastal Vulnerability	194
Figure A.8	Contribution of Backshore Slope Parameter to Coastal Vulnerability	195
Figure A.9	Contribution of Backshore Vegetation Parameter to Coastal Vulnerability	195
Figure A.10	Contribution of Coastal Protection Structure Parameter to Coastal Vulnerability	196
Figure A.11	Contribution of Morphological Resilience Parameter to Coastal Vulnerability.	196
Figure A.12	Contribution of Accommodation Space Parameter to Coastal Vulnerability	197
Figure A.13	Contribution of Sediment Supply Parameter to Coastal Vulnerability	197

Chapter 1

INTRODUCTION AND LITERATURE REVIEW

1.1 Research Context

Over the past few decades the coastal zone has been subjected to substantial anthropogenic development and pressure, which has led to a decrease in natural coastal functioning and the deterioration of coastal systems (Mitra, 2011; Wong et al., 2014). The effects of sea level rise (SLR) and extreme events, most notably erosion, inundation, storm surge, and flooding, further exacerbate these anthropogenic impacts (Mitra, 2011) and provide a unique challenge for small coastal communities as they seek to sustainably manage their coastlines. With SLR projected to increase by 2100 (Church et al., 2013), it can be surmised that the vulnerability of the coastal zone and its inhabitants will also increase. It has therefore become increasingly important to assess coastal vulnerability to assist in coastal planning, sea level rise adaptation, and risk management (Palmer et al., 2011). While many approaches exist (Ramieri et al., 2011), the most commonly and extensively applied method of assessing vulnerability are index based coastal vulnerability indices (CVIs).

The vulnerability of any system can be described as a function of exposure, sensitivity,

and adaptive capacity (Engle, 2011; IPCC, 2007; Smit & Wandel, 2006) and can have both a physical and a social aspect. While some CVIs incorporate only physical parameters (Gornitz et al., 1991; Zujar et al., 2009; Ozyurt, 2007; Abuodha & Woodroffe, 2006; Kumar et al., 2010; Torresan et al., 2012; Sousa et al., 2012) and others incorporate only social parameters (Boruff et al., 2005; Cochran et al., 2012), arguments have been made about the importance of including both physical and social in the assessment of vulnerability (Abuodha & Woodroffe, 2010; McLaughlin et al., 2002; Szlafsztein & Sterr, 2007; Adger 2006) which has resulted in CVIs that incorporate both social and physical parameters (Szlafsztein & Sterr, 2007; Palmer et al., 2011; McLaughlin & Cooper, 2010; Orencio & Fujii, 2013; Hedge & Reju, 2007). While the importance of incorporating both components is noted, a coast can be physically vulnerable in places where minimal social vulnerability exists, giving more influence to places where people live and not necessarily to places upon which people depend. To account for this Palmer et al. (2011) assess physical coastal vulnerability *a priori* and socio-economic coastal infrastructure at risk *a posteriori*, allowing for an adequate consideration of the coastal morphological changes which are so essential for integrated management and sustainable development of the coastal zone (Mitra, 2011). In an effort to incorporate the social aspect of vulnerability, this approach will be utilized in this research.

With respect to the physical coastal system, vulnerability is based on the likelihood of geomorphic change. Generally speaking, geomorphic change is a balance between coastal characteristics that induce change (assailing), those that resist change (resistance), and those that allow a system to recover from change (resilience) (Brunsden, 2001), all three relating to the exposure, sensitivity and adaptive capacity components of vulnerability respectively. In these relationships, an increase in assailing forces in turn increases the vulnerability of a system,

but an increase in resistance or resilience components subsequently decreases the system's vulnerability. When assessing physical coastal vulnerability it is therefore important to consider the influence of coastal characteristics as a whole.

Coastal geomorphic vulnerability has, for the most part, been determined by assessing the influence of either resistance parameters (Bush et al., 1999) or the influence of combined assailing and resistance parameters (Shaw et al., 1998) on landform change, but has not incorporated the physical resilience aspect, which ultimately has the ability to reduce vulnerability. Those studies that have considered resilience have done so either independently (Pethick & Crooks, 2000) or have focused on only one aspect of natural resilience (Tibbetts & van Proosdij, 2013). As the geomorphic vulnerability of a coast is not solely dependent on resistance, assailing, or resilience parameters, but on the interconnectivity of all three, the exclusion of the natural adaptive capacity of a coastline is a substantial gap in the literature which could lead to the misrepresentation of vulnerable areas. This research aims to address this gap by developing and applying a physical CVI that incorporates assailing, resistance, and resilience parameters influencing coastal erosion.

The process of coastal erosion is complex and can be influenced by many factors on varying spatial scales but the primary physical mechanism of coastal change at the local scale is wave action (Mitra, 2011). The energy of a wave is directly proportional to the square of its height, thus quadrupling in energy as wave height doubles (Gornitz, 2013). The height of a wave is dependent on wind velocity, water depth, wind direction, and fetch (Gupta, 2011) and it is therefore expected that the combination of rising seas and intense storms will bring higher wave energies, with a greater capacity to erode. Intense storms bring higher winds with the

ability to generate larger waves and a rise in sea level deepens the water column, resulting in the creation of larger waves and a reduction in the ability of the coast to dissipate wave energy. With these concepts in mind, this paper will assess the physical vulnerability of the coast to erosion under four wave energy scenarios with different combinations of water levels and wind conditions associated with climate change. A detailed explanation of each scenario (S1 to S4), including the contributing data, can be found in Sections 3.3.1 to 3.3.4.

The above methodology was applied to the town of Lockeport, Nova Scotia, a small coastal community highly dependent on tourism and fishery activities and very vulnerable to the effects of SLR. The application of this research will illustrate how coastal response differs according to varying wave energy scenarios and will help identify the areas in Lockeport that are at greatest risk to erosion and coastal change, currently, and in the future. Applying the methodology of Palmer et al. (2011), this research will further identify building infrastructure found within the coastal zone that is vulnerable to erosion under each of the wave energy scenarios. As flooding and inundation are the effects of SLR most likely to cause harm to people and infrastructure (Gornitz, 2013), this research will also include the identification of building infrastructure vulnerable to permanent inundation associated with wave energy scenarios that incorporate an increase in water levels (S3 and S4).

The identification of areas and buildings at greatest risk to erosion and inundation will assist coastal managers in Lockeport in building community awareness and adaptive capacity, developing appropriate adaptation strategies, making informed management decisions, and allocating funds to the areas of greatest need. It is important to note that, while the methodology and matrix of this CVI was developed and applied to the Town of Lockeport, it can

easily be adapted and applied to other small coastal communities threatened by the impending impacts of SLR.

1.2 Coastal Zone

Canada's coastal zone is widely recognized as a crucial resource for the country but, for small coastal communities in the Maritimes Provinces, who heavily rely upon coastal resources for their livelihood, the coastal zone becomes their most valuable asset (Environment Canada, 1994; NRCan, 2004). Naturally, the coastal zone provides numerous ecosystem services such as coastal protection from high waves and storm surges (Pernetta, 2004; Gornitz, 2013) and sediment retention and nutrient filtration (Cooper et al., 2009). It is also considered economically important for the role it plays in coastal activities, especially tourism and fisheries (Mitra, 2011; Pendleton et al., 2004).

These coastal benefits are entirely dependent on the integrity of natural coastal resources, which are easily threatened by coastal populations and human activities and further exacerbated by the impacts of climate change. Worldwide, coastal zones are more heavily populated than the interior (Sousa et al., 2012) with more than 50% of the world's population concentrated within 60 km of the coast (Mitra, 2011) and 10% of the population living below 10 m (Nicholls & Cazenave, 2010). This disproportionate development of the coastal zone causes severe conflicts between environmental integrity and the interests of various coastal users. Over the last century the effects of climate change, most notably sea level rise, have exacerbated the effects of human activities on the coast (Kumar et al., 2010). Not only does SLR contribute to more severe coastal impacts, but with increasing development along the coast, a

rise in sea level will result in increased risk to infrastructure, life, and economic investments.

This has led to a need for coastal vulnerability assessments, which are meant to guide the coastal management and adaptation process, and which are the focus of this research. A brief discussion of coastal zone definitions, classification, dynamics, and adaptive capacity will provide context for the discussion of coastal vulnerability assessments.

1.2.1 Coastal Zone Definition

Providing a definition of the coastal zone is a difficult task, as definitions vary between countries and coastal authorities, and boundaries are often arbitrarily defined to suit the purpose for which the definition is being used (Mitra, 2011). Kay & Alder (1999) explain that coastal definitions are often either scientific, where boundaries are demarcated by natural changes in landforms and/or processes, or policy oriented, where boundaries are determined based on the purpose of a particular policy or management plan.

From a natural perspective the coastal zone can be generally described as the area of interface between land and sea (CBCL Limited, 2009; Rochette, 2010; Kay & Alder, 1999), which encompasses shallow coastal waters, as well as the adjacent low-lying shoreline environments (Mitra, 2011; NRCan, 2004; Burke et al., 2001). In addition, this zone is subject to change from natural forces of waves and wind (UNEP/GPA, 2003) or, as the most recent Intergovernmental Panel on Climate Change (IPCC) report (Wong et al., 2014) simply states, all areas near mean sea level. Scientifically the exact landward and seaward limits are purposely not precisely defined, as they can substantially range from coast to coast (Davidson-Arnott, 2010; CBCL Limited, 2009).

Policy oriented definitions are more commonly used and are often based on either

existing jurisdictional boundaries or according to the specific issue being addressed (Mitra, 2011; Greenlaw et al., 2013; Rochette, 2010). Many governments find the use of narrower boundaries encompassing the majority of coastal impacts to be feasible (Environment Canada, 1994). As expected, the use of policy oriented definitions results in an extremely varied range of coastal definitions.

Another important factor to consider when determining the boundaries of a coastal zone is the scale at which a zone is defined. On a global or national level, the entire province of Nova Scotia could be considered a part of the coastal zone (CBCL Limited, 2009). This is often a challenge experienced in small islands where the entire country can be considered part of the coastal zone, as all aspects of island life are influenced by the coast in one way or another (Clark, 1996).

The Province of Nova Scotia has developed a draft Sustainable Coastal Development Strategy and has committed to “taking an integrated, ‘whole of government’ approach to addressing the coastal issues that matter most to Nova Scotians.” (Province of Nova Scotia, 2013). Despite this commitment, to date there is no official Coastal Zone Management policy in Nova Scotia nor a specific definition of the coastal zone. Fanning (2008), who reviewed the importance of a coastal area definition for Nova Scotia, suggested that the definition of the coastal zone, whether scientific or policy based, is best determined by considering the zones of influence and impact of a particular issue or event. Taking this approach into consideration, as well as the fact that it is important for the definition to encompass areas of concern, while at the same time not having such large boundaries that all of Locke Island is considered the coastal zone, the zone of influence of erosion events is considered, for this research, to extend no

further than 50 m seaward and landward from the backshore. Consequently, the definition of the coastal zone for the purpose of this study is as follows: ***the area of land extending 50 m landward and seaward from the backshore; defined as the area that is subject to the farthest reach of waves during exceptionally severe storm conditions and the immediately adjacent landform in the hinterland.***

The coastal zone can be further divided into four zones determined by the presence of different processes occurring along the coastal profile (Figure 3.3). The four zones are: Backshore, Foreshore, Nearshore, and Offshore, however only the first three are relevant to this research. Despite a plethora of existing shorezone definitions, the following will be used in this research:

Backshore Zone (BS): area of the shoreline profile that is subject to the farthest reach of waves during exceptionally severe storm conditions and the immediately adjacent landform in the hinterland (e.g., dune, cliff, slope etc.)

Foreshore Zone (FS): intertidal zone between mean high and low tides

Nearshore Zone (NS): areas of coast bounded by the point at which waves begin to shoal and the low tide line

1.2.3 Coastal Dynamics & Adaptive Capacity

When looking at the overall vulnerability of a coastline to SLR, human aspects and threats must be considered in the context of a coast's natural functions and responses to SLR. The foundation of the geomorphic-based vulnerability assessment, developed and applied in this research, is that physical attributes and processes operating along a coast heavily influence

coastal change and coastal vulnerability. This section will therefore address the basic, but crucial, concept of coastal dynamics in relation to SLR.

It is commonly accepted that, under consistent forcing and no longshore gradients, coastal systems operate under dynamic equilibrium, in which they are constantly working towards some form of equilibrium (Davidson-Arnott, 2010; Woodroffe, 2007), and that “a change in the incident conditions will rapidly be reflected in a predictable change in morphology towards another dynamic equilibrium” (Davidson-Arnott, 2010). Many coastal landforms undergo short-term perturbations such as storm-induced erosion, which encourage morphodynamic change away from the equilibrium but, over time, often return to a form of their “pre-disturbance state” (IPCC, 2007; Woodroffe, 2007), exemplifying the description of coastal resilience. Some landforms also display seasonal variation, with greater change occurring throughout the winter months or the rough seas season (Wong et al., 2014; Crooks, 2004). The rate of change of an ecosystem from basic coastal processes varies based on the energy of the environment and the nature and resistance of the ecosystem material (Trenhaile, 2004; Woodroffe, 2007). For example, due to material resistance, rocky cliffs are less likely to undergo change than easily erodible sandy beaches, and based on wave energy, a low-energy salt marsh system is less likely to undergo drastic change than a high-energy beach or cliff environment. Of the most common ecosystems in Nova Scotia (sandy systems, salt marshes, rocky coasts, and cliffs), sandy systems have the highest rate of change (Pethick & Crooks, 2000). In coastal sandy systems, which include barriers, beaches, and dunes, sediment is constantly moving between system components within a littoral cell: defined as a section of coast that experiences continuous longshore sediment transport and contains sources of sediment input and removal (Davidson-Arnott, 2010). Within a littoral cell, sediment can be added to the system dynamics

through rivers, cliff erosion, coral reefs, etc. and removed through sand mining, or submarine canyons to name a few (Davidson-Arnott, 2010), while some coastal system components act as both sources and sinks (e.g., dune, lagoons, estuaries etc.). Sand dunes store sediment that has been transferred from the beach through processes such as wave and aeolian transport, allowing them to serve as sediment sources for beach recovery.

The coast, although abiotic, operates like a living organism that has the potential to adapt to changes in its environment. It is continually responding to small adjustments and perturbations, but also, under the right conditions, has the ability to adapt to larger perturbations such as SLR. Naturally, coastal systems are capable of adapting to SLR events (Trenhaile, 2004) with the shoreline adjusting form and position as the sea level increases (Gornitz, 2013). The Bruun Rule, developed by Bruun in (1962), is the most commonly and extensively applied model for illustrating the response of a sandy shoreline to a rise in sea level. It demonstrates that for a coast to maintain an equilibrium state, it will undergo a natural translation upwards and backwards on the order of 100 m landward move for every 1 m rise in sea level, and will eventually return to a form of its pre-disturbance state (Cooper et al., 2000; Ozyurt, 2007; Gornitz et al., 1994; Wong et al., 2014). However, recent literature discusses the over-simplification of the Bruun Rule (Gornitz, 2013) and Cooper and Pilkey (2004) highlight that, although the Bruun Rule, in 1962, provided an insight into our understanding of this relationship, advance knowledge of these interactions developed over the past five decades renders the Bruun Rule invalid. Irish et al. (2010) note that it is very likely that the effects of SLR on a coast are more complex than just land retreat.

Despite the complex nature of coastal adjustment to sea level rise, the adaptive capacity

of a coast to rising seas can be said to be highly dependent upon availability of sediment sources, availability of space to be dynamically active (Filho & El-Robrini, 2000; Mitra, 2011) and the morphological resilience of a particular coastal system type (Tibbetts & van Proosdij, 2013).

The amount of sediment available for deposition and the resulting creation or growth of beaches (sandy, gravel, and cobble) and salt marshes depends on the presence of sediment sources such as dunes or other depositional features in the coastal system as well as cliffs, with sediment obtained through erosion processes (Trenhaile, 2004). In Nova Scotia, gravel and cobble beaches are a common feature (Orford et al., 1991), and the large glacial deposits also present along the coast provide a primary source of finer sediment (Trenhaile, 2004). As these types of coastal ecosystems rely so heavily on sediment supply to sustain their form, they are the systems that are naturally at greatest risk from SLR (Australian Department of Climate Change, 2009). Salt marshes adapt to sea level rise primarily through the process of vertical accretion of sediment and organic plant matter (Gornitz, 2013), so long as the rise in sea level does not surpass the rate of marsh accretion. As finer beach material is easily erodible, beach systems can be considered highly vulnerable to SLR. Dunes that back beach systems provide material to replenish beaches after disturbance events (Trenhaile, 2004) and, so long as sediment supply is not inhibited, beaches are very capable of keeping pace with the rising seas (Nicholls et al., 2007). Beaches are also known to display seasonal variation in form and material, where the high-energy waves experienced in winter months result in the creation of a steeper beach profile with coarser material. However, in the summer months, when wave energy decreases, the beach is replenished with finer sediment stored offshore during the winter months. Although sandy systems experience the greatest rates of change they are also

the most resilient.

Morphological resilience, a term used by Tibbetts & van Proosdij (2013), refers to the ability of a landform to return to a state of dynamic equilibrium following a disturbance event. Beach systems are more resilient, as they can easily return to their pre-disturbance state. For example, after extensive erosion from a storm event, the beach will naturally begin to replenish itself in a short time frame. Cliffs on the other hand, have a very low morphological resilience, as material eroded from a cliff cannot return to the cliff face.

With SLR, coastal systems generally undergo a landward translation (Australian Department of Climate Change, 2009), however this retreat can be inhibited by hard immobile structures such as rocky cliffs, coastal protection structures, or other built features (Wong et al., 2014; Australian Department of Climate Change, 2009). When an eroding shoreline runs into a natural or manmade immobile structure, it causes a phenomenon known as coastal squeeze, in which the retreating landform, such as a beach or marsh, will increasingly narrow until it completely disappears (Wong et al., 2014).

In summary, the coast has the ability to naturally adapt to a rise in sea level providing the rate of sea level rise does not exceed the rate of response and recovery. However, the increasing anthropogenic pressure in the coastal zone seriously inhibits the ability of a shore to naturally respond and, as a result, SLR remains one of the greatest threats to the coastal zone (Palmer et al., 2011; IPCC, 2007).

1.3 Sea Level Rise

SLR is one of the greatest impacts affecting the coastal zone in the face of climate

change (Vermeer & Rahmstorf, 2009; Stern, 2007; Nicholls & Cazenave, 2010). Global SLR, often called Global Mean Sea Level Rise (GMSLR), is the absolute rise in water levels around the globe, measured with respect to a geocentric reference ellipsoid (Church et al., 2013). On the other hand, relative sea level change is measured with respect to the earth's land surface (Church et al., 2013) and takes into consideration the local factors that influence changes in sea level, such as tectonic subsidence, isostatic readjustment, sea level fingerprinting and groundwater depletion, which cause deviations from GMSLR projections. Depending on the local conditions, the local rate of sea level change can significantly differ from GMSLR projections (Stocker et al., 2013), and can be positive or negative, resulting in sea level rise, or sea level fall. Although net relative sea level rise (RSLR) is most common, it is important to understand that, in some places, a net fall in sea level can occur. Findings in the newest IPCC reports suggest that RSLR deviates more than 10% from GMSLR for 30% of the ocean, and more than 25% for 9% of the ocean (Stocker et al., 2013), illustrating the potential for large spatial variations on the local scale. In fact, some areas experience SLR rates three times faster than the global average (Nicholls & Cazenave, 2010) and therefore, relative sea level is the most important quantity to examine when considering coastal impacts and adaptation at the local scale (NRCan, 2004; Church et al, 2013).

1.3.1 Drivers of Sea Level Change

The two greatest contributors to SLR are thermal expansion and glacial melt (Nicholls & Cazenave, 2010; Church et al., 2013), followed by ice sheet melt (Stocker et al., 2013). Thermal expansion is the increase in volume of ocean water, caused by a rise in the ocean temperature, with a 0.2-0.6 m rise for every degree Celsius increase (Stocker et al., 2013). As ocean waters

have a large thermal inertia, there is an expected lag time between a change in air temperature and the ocean volume change (Ozyurt, 2007; NRCan, 2004) resulting in a continued rise in sea levels long after Greenhouse Gas (GHG) emissions diminish or stabilize (Gornitz, 2013; Church et al., 2013). During the period 1971 – 2010, thermal expansion proceeded at a rate of 0.8 mm/yr (Stocker et al., 2013) and between 2010 and 2100 it is expected to contribute approximately 35-45% to SLR totals (James et al., 2014).

According to the IPCC (Church et al., 2013), glacial melt refers to the melting of all land ice masses, including mountains and ice caps as well as ice masses adjacent to, but not including, the Greenland and Antarctic ice sheets, and accounts for 22 – 27% of SLR projection totals for 2100 (James et al., 2014). Mountain glaciers, although not as prominent as larger glaciers, are much more sensitive to rising temperatures (Gornitz, 2013). Under the highest emissions scenario (See Section 1.3.2), 35 – 85% of glacier volume is expected to melt by the year 2100 (Stocker et al., 2013), illustrating a substantial contribution from glacial melt by the end of the century. Together, thermal expansion and glacier melt have accounted for 75% of observed GMSLR since 1971 (Stocker et al., 2013). The SLR contribution from melting ice sheets, especially those in Greenland and the West Antarctic, has also increased rapidly over the past two decades (Church et al., 2013), adding 0.4-0.7 mm/yr to SLR within the last decade and 1.3 mm in 2006 alone (Gornitz, 2013). Continued net loss is expected (Stocker et al., 2013).

Land water storage refers to the amount of water being retained on land, not flowing out to sea and therefore has the potential to reduce SLR. It incorporates variations in rainfall and anthropogenic processes that influence the amount of water storage, namely reservoir impoundment and ground water depletion (Stocker et al., 2013; Gornitz, 2013). Impermeable

surfaces and deforestation can cause more water runoff and contribute to a net rise in sea level, while the creation of dams and reservoirs can contribute to a net fall in sea level. Although small, land water storage is expected to account for 1-7% of SLR totals by the end of the century (James et al., 2014). Other important phenomena that influence RSLR include glacial isostatic adjustment (GIA) and sea level fingerprinting. Locally, land can either sink or rise naturally due to isostatic readjustment and tectonic subsidence or uplift as well as from anthropogenic induced subsidence from drainage and groundwater withdrawal (Nicholls & Cazenave, 2010; Gornitz, 2013). Across Canada, James et al. (2014) show GIA rates ranging from 2 mm/yr subsidence in Nova Scotia and 4 mm/yr uplift in Quebec.

Sea level fingerprinting is a relatively new concept that explains the behaviour of sea level changes resulting from the exchange of water between land and sea (Church et al., 2013). At one point, it was assumed that melt water from glaciers and ice sheets resulted in a uniform rise in sea level globally. However, in actuality, melting results in regional sea level variations due to the changes in gravitational attraction between ice and water as glaciers lose mass (Gornitz, 2013), with nearby sea levels dropping and those further away from the melting source, rising (Gornitz, 2013). As Nova Scotia is so close to the Greenland Ice sheet and other meltwater sources, sea level fingerprinting is an important phenomenon to take into account. Due to its proximity to Greenland, Nova Scotia would experience an increase in projected SLR from the melting of the Greenland Ice sheet, and conversely, with the melting of the West Antarctic Ice Sheet (WAIS), Nova Scotia would experience an increase in SLR projections (James et al., 2014).

Using global SLR projections and incorporating the local effects of vertical land motion,

sea level fingerprinting, and regional oceanographic effects, James et al. (2014), provide RSLR projections for 59 stations across Canada and adjacent USA, 22 of which are located in Atlantic Canada and northeastern New England, with values ranging from a 55 cm rise at Sept – Îles, Quebec to a 109 cm rise in Baddeck, Nova Scotia (for RCP8.5max for the period of 2010-2100) - a substantial difference when planning for climate change impacts and adaptation strategies.

1.3.2 Climate Change Projections

Every five to seven years, the IPCC, the leading body on climate change projections produces a set of assessment reports detailing the most recent climate change findings from leading scientists in various climate related fields. The most recent set of reports (Assessment Report 5 – AR5) were published in 2013/2014, providing up-to-date information on global climate change impacts.

One of the biggest changes between Assessment Report 4 (AR4) and AR5 is the replacement of SRES (Special Report Emission Scenarios) scenarios, used to create climate change projections, with RCPs proposed by van Vuuren et al. (2011). SRES projections were based on specific future socio-economic scenarios with variations in economic development, growth rates, and energy sources used (Gornitz, 2013; Cubasch et al., 2013). However, the SRES scenarios did not take into consideration the incorporation of climate mitigation policy (Collins et al., 2013). Thus, in 2010, with an effort to “facilitate interactions between scientific communities working on climate change adaptation and mitigation” (Collins et al., 2013), the IPCC adopted the RCP framework, which is based on profiles of GHG emissions and not socio-economic storylines (Gornitz, 2013, Collins et al., 2013). This method provides GHG emission projections measured in anthropogenic radiative forcing over time, with the idea that any one

projection profile can be realized with many varying socio-economic scenarios (Collins et al., 2013). RCP scenarios range from 2.6 – 8.5, with the associated number referring to net radiative forcing (W/m^2) by 2100 (James et al., 2014). In general, by 2100, the lowest RCP scenario (2.6) peaks and then declines, RCP4.5 and RCP6.0 both rise and stabilize and RCP8.5 continuously rises during this century, but levels out around 2230 (Figure 1.1). For context, Table 1.1 and Figure 1.1 illustrate the equivalent SRES and RCP scenarios.

Table 1.1 - Equivalent RCP and SRES Scenarios and Associated SLR Projections. SLR projection from 2081 – 2100 relative to the reference period of 1986. (Data Compiled from: Collins et al., 2013; James et al., 2014).

RCP scenario	SRES Equivalent (Collins et al., 2013)	SRES Equivalent (James et al., 2014)	SLR Projection (cm) 2081 – 2100 (James et al., 2014)
2.6	None	None	0.26 – 0.55
4.5	B1	B1	0.32 – 0.63
6.0	A1B	B2	0.33 – 0.63
8.5	A2	A1F1	0.45 – 0.82

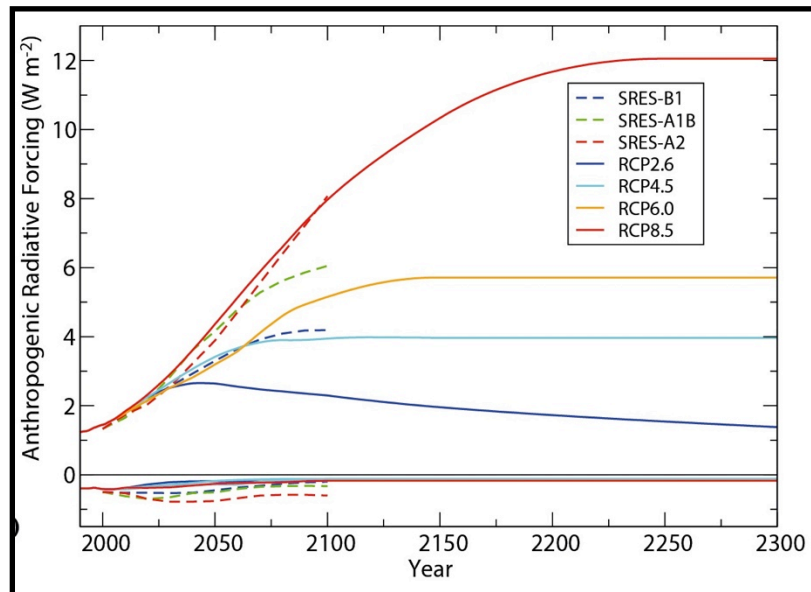


Figure 1.1 Comparison of Special Report Emission Scenarios (SRES) and Representative Concentration Pathways (RCP) to the year 2100 and RCP Extensions to the Year 2300. (Used with authorization from: IPCC Working Group I Assessment Report 5, Chapter 12, Figure 12.3,

Cambridge University Press).

According to AR4, the projected GMSLR for 2100 ranged from 18-59 cm (IPCC, 2007).

The most recent IPCC projections for global SLR for 2100 range from 29 – 66 cm, however if the upper and lower boundaries of the error curves are included the range extends to 23 – 90 cm (James et al., 2014) (Figure 1.2). The upper bound of RCP8.5 is referred to by James et al. (2014) as RCP8.5max.

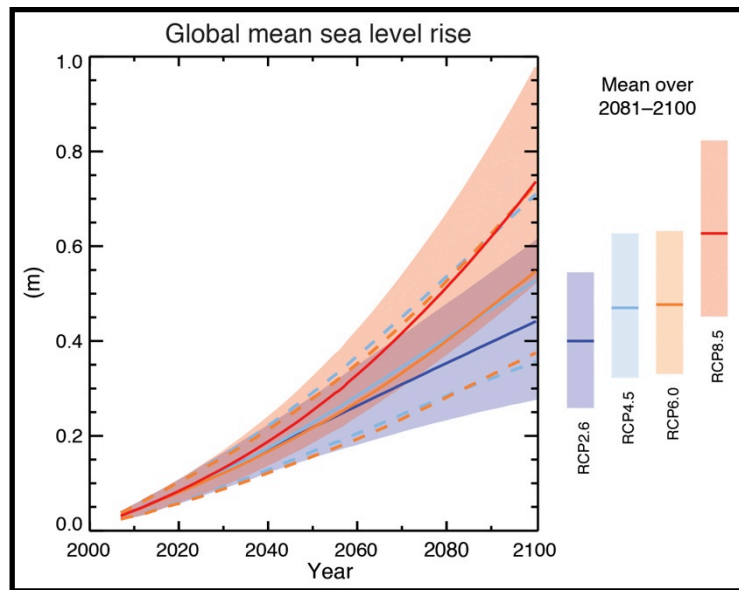


Figure 1.2 Global Mean Sea Level Rise (GMSLR) Projections for RCP Scenario 2.6, 4.5, 6.0, and 8.5. Dashed blue and orange lines and transparent blue and red cones represent the upper and lower boundaries of the error curves for RCP4.5 and RCP6.0 and RCP2.6, and RCP8.5 respectively, and the solid lines of all colours represent the mean. (Used with authorization from: IPCC Working Group I Assessment Report 5, Technical Summary, Figure TS.22, Cambridge University Press).

Despite great advancements in the modeling of ice sheet dynamics over the past decade (Church et al., 2013), the future behavior of the Greenland and Antarctic ice sheets and their contributions is still one of the greatest unknowns when predicting SLR (Gornitz, 2013; Stocker et al., 2013). Although there is consensus that the melting of the WAIS by the end of the century would not likely exceed several tens of cm, lack of consensus exists on the likelihood of

a complete collapse of the WAIS, which would cause a substantial increase in global SLR that exceeds projections for 2100 (Church et al., 2013; Gornitz, 2013; Stocker et al., 2013; James et al., 2014).

As outlined previously, the RSLR projections are the most important to consider when addressing the impacts of SLR on coastal communities, and can substantially deviate from global means. The relative sea level projections calculated in James et al. (2014), incorporate vertical land motion, sea level fingerprinting, and regional oceanographic effects with global SLR values. For Halifax, RSLR values are 28% larger than global values and the median RSLR projections for the time interval 2010-2100 (relative to 1986-2005), range from 52 cm (RCP2.6) – 85 cm (RCP8.5) (James et al., 2014). Although complete melting of the WAIS is unlikely, James et al. (2014) create additional RCP scenarios to take this extreme into consideration by adding an additional 30 cm and 60 cm of SLR to RCP8.5max (95% error boundary of RCP8.5 scenario), which for Halifax is projected, for the time interval 2010-2100 (relative to 1986-2005), to be 179cm (James et al., 2014). While James et al. (2014) did provide RSLR projections for Tusket, which is closer to Lockeport than Halifax, the projections do not greatly differ between the two sites and the RSLR projections for Halifax were extrapolated to Lockeport for this research. Despite the fact that SLR is not likely to exceed the levels of RCP8.5max, the purpose of this research is to assess worst-case scenarios and thus, RCP8.5 and RCP8.5max+60 will be used as SLR scenarios for this research.

1.3.3 Sea Level Rise Impacts

SLR is expected to have extensive negative impacts on the coastal zone and its inhabitants. SLR increases the reach of coastal processes and, while it does not generally create

new hazards, it does exacerbate those already acting on the coast (Shaw et al., 1998; Kumar et al., 2010). Trenhaile (2004) notes that in Atlantic Canada, the effects of SLR will be exacerbated due to the high subsidence rates relative to other areas across the country.

Socio-economic impacts include, but are not limited to, loss of cultural heritage, reduction of tourism, damage to coastal infrastructure, increased property loss, and increased risk of life (Mimura et al., 2007; NRCan, 2004), while physical impacts include extensive coastal inundation, acceleration of beach erosion, saltwater intrusion, rising water tables, degradation of natural coastal defences, loss of coastal habitat, reduced sea-ice cover, and increase in flooding from storm surges (NRCan, 2004; Mimura et al., 2007; Balbus et al., 1998). Of these, the main physical impacts of SLR on the coastal zone are: erosion, inundation, and flooding from storms (Hughes & Brundrit, 1992; Ozyurt, 2007; Balbus et al., 1998; NRCan, 2004; Gornitz, 2013). Erosion is most influenced at the local scale by waves, which are constantly working to change local landforms (Mitra, 2011). Wave energy, which is directly proportional to wave height (Gornitz, 2013), varies with combinations of water depth and wind speed and it can therefore be expected that wave energy scenarios associated with an increase in wave height will have a greater wave energy and, consequently, a greater ability to erode. This research focuses on coastal geomorphic change caused by wave-induced erosion and the examination of wave energies under four scenarios that combine various water levels and wind conditions associated with climate change. But first, it is important to have an understanding of specific SLR impacts.

1.3.3.1 Erosion

Coastal erosion is the physical removal of sediment by current and wave action and

depends on many factors, including coastal slope, sediment transport, landform type, and wave climate (Balbus et al., 1998; Ozyurt, 2007). Gently sloping coasts have a greater ability to dissipate wave energy than their steeper counterparts. Sediment transport influences the amount of sediment reaching the shore and thus the potential for beach replenishment. Landform type, or geomorphology, determines the erodibility of the shoreline, as certain landforms are comprised of sediments with cohesive properties, or are made up of different sized particles. Finally, wave climate influences the wave energy available to act upon the coast (McLaughlin & Cooper, 2010; Balbus et al., 1998, Davidson-Arnott, 2010). Although the erodibility of a coast is dependent on many factors, the primary agent that induces change (assailing factor) is the amount of wave energy reaching the shore, with higher wave energies having a greater potential to induce change than lower wave energies. Waves are dependent on wind velocity, wind direction, and the distance over which wind flows unimpeded, called the fetch (Davidson-Arnott, 2010).

Of the prominent coastal ecosystem types found in Nova Scotia, sandy systems, saltmarshes, rocky coasts, and cliffs, each respond differently to the erosive processes induced by SLR. Beach creation is largely dependent on sediment and waves and the type of beach formed is influenced by factors such as sediment budget, sediment type, wave type, tidal regime, and biota (Short, 2007). However, with all other factors being equal, the erodibility of a beach is dependent on the material size (Gornitz, 2013). Coastal sandy systems are highly susceptible to erosion and, with increasing wave energy along the coast, erosion rates are expected to increase. Barriers are particularly vulnerable to erosion due to their low elevation and narrow width, but do have the ability to retreat landward (Shaw et al., 1998). Salt marshes rely upon an input of sediment into the system, but are able to withstand SLR if the rate of

accretion can keep pace with the rate of SLR (Gornitz, 2013). Like beaches, saltmarshes also migrate landward in response to climate change and their ability to do so depends on slope, sediment supply, and accommodation space (Gornitz, 2013). Rocky coasts and cliffs erode slightly differently, occurring from subaerial slope process (Manson, 2002) or from high wave energy undercutting the base of the cliff. As the cliff is undermined it becomes increasingly unstable, at which point the cliff slumps, depositing material at the base. The material at the cliff base is then either removed by waves, or forms a narrow beach (Gornitz, 2013). The rate of undercutting and erosion depends entirely on the type of cliff material, as hard bedrock is extremely resistant to wave energy and softer limestone cliffs, or cohesive bluffs are less resistant (Shaw et al., 1998).

1.3.3.2 Storm Events

In Nova Scotia, storm events with the ability to cause extensive flooding are generated by two types of storms: tropical cyclones and extra tropical cyclones (Gornitz, 2013). In Atlantic Canada, tropical cyclones occur between the months of June and November (Environment Canada, 2014) and extra tropical storms, also known as nor'easters, occur during the winter months. Compared to nor'easters, hurricanes have stronger wind speeds, but often cover a smaller area of 100-150 km, compared to the 1000 km span common to nor'easters (Gornitz, 2013). In previous IPCC reports, it was suggested that, due to climate change, cyclones were increasing in frequency and intensity (IPCC, 2007). However in AR5 it is suggested that cyclone frequency is likely to remain the same or decrease, but intensity of wind speeds and rain rates are expected to increase (Stocker et al., 2013). In a regional context, Savard et al. (2014) note that the northwestern Atlantic Ocean is one of the stormiest areas in North America.

Flooding from storm surge already has extensive effects on the coastline, but like other coastal impacts, is exacerbated by SLR (Oppenheimer et al., 2014). With an increase in sea level, the effects of storm surge can reach much farther inland and, if a storm coincides with high tide, extensive damage could occur (Davidson-Arnott, 2010; Gornitz et al., 1991).

1.3.3.3 Inundation

Inundation is the permanent submergence of low-lying land and is the most direct effect of SLR (Gornitz, 2013). Often this term is used interchangeably with flooding, however, inundation results in the permanent submergence of land, while flooding from storm surge results in non-permanent submergence of land (Feenstra et al., 1998). The extent of inundation is determined by slope, elevation and the space for systems to migrate inland (Feenstra et al., 1998). Slope or elevation of the coastal system will determine the distance of inland inundation, with gentler slopes and lower elevations resulting in greater inundation distances. Along a coast with no development, a coastal system will more often than not retreat landward as sea level rises. However when development and human influence are present, the ability of a system to retreat is inhibited (Palmer et al., 2011; IPCC, 2007). The effects of inundation on the coast include narrowing of beaches, waves reaching further inland, and an increase in saltwater intrusion into aquifers (Gornitz, 2013). Low-lying coastal areas, with gentle nearshore slope and which are subjected to subsidence, are the most vulnerable to the effects of inundation (Gornitz, 2013).

1.4 Vulnerability

The most recent IPCC report, AR5, defines vulnerability as “the propensity or

predisposition to be adversely affected” (Oppenheimer et al., 2014). Its simplicity and ambiguity speak to the variety of concepts that contribute to vulnerability and the considerably varied definitions and terminology found within the literature (Kumar et al., 2010; McLaughlin & Cooper, 2010; Dow & Downing, 2011; Zujar et al., 2009; Palmer et al., 2011; Smit & Wandel, 2006; Abuodha & Woodroffe, 2010; Adger, 2006; Orenco & Fujii, 2013; Szlafsztein & Sterr, 2007). Although the term vulnerability, in many cases, has been used in literature to refer to the physical vulnerability of coasts (Gornitz et al., 1991), it has been recognized in other studies that vulnerability must also incorporate a socio-economic component, as it is often perceived as the threat to people from a particular hazardous event (Abuodha & Woodroffe, 2010; McLaughlin et al., 2002; Adger, 2006). This is illustrated in the IPCC AR5 report, which explains that vulnerability primarily refers to human or socio-ecological systems, and physical areas are mostly incorporated if human vulnerabilities increase as a result of the reduction of ecosystem services provided by the threatened physical system (Oppenheimer et al., 2014). To account for discrepancy with the use of the term vulnerability, some studies have used the term sensitivity or susceptibility to describe physical vulnerability, employing the term vulnerability only when both physical and socio-economic factors are considered (Shaw et al., 1998; Abuodha & Woodroffe, 2010; Ozyurt, 2007).

Despite the considerable variation among vulnerability definitions, it can be agreed that the vulnerability of any system to an event, whether physical, social, or both, is a function of exposure, sensitivity, and adaptive capacity, where exposure is the extent to which a system is exposed to an event, sensitivity is how affected the particular system is by the event, and adaptive capacity is the ability of the system to cope with the effects of the event (Engle, 2011;

IPCC, 2007).

This relationship was thoroughly explored by Smit and Wandel (2006), who combined exposure and sensitivity into a single factor of “exposure sensitivity” due to their similar characteristics. As illustrated in this relationship, an increase in exposure sensitivity in turn increases the vulnerability of a system, but an increase in adaptive capacity results in a decrease in vulnerability. This relationship is illustrated mathematically and conceptually in Equation 1.1 and Figure 1.3.

Equation 1.1

$$\text{Vulnerability} = \text{Exposure} \times \text{Sensitivity} \times (1/\text{Adaptive Capacity})$$

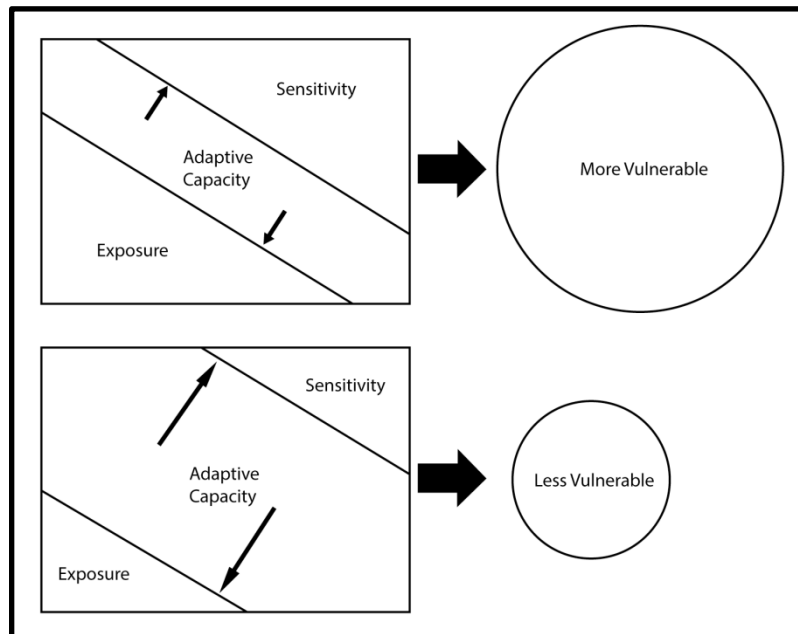


Figure 1.3 Influence of Adaptive Capacity on Exposure, Sensitivity, and Vulnerability.
(Adapted from: Engle, 2011).

This research attempts to assess physical vulnerability of the coastal zone to erosion and then to identify the degree to which building infrastructure, located in pre-identified areas of

high physical vulnerability, is susceptible to inundation. Therefore, even though physical and socio-economic components are not being incorporated into one assessment, the term vulnerability will be used in this research to refer to all aspects of susceptibility, whether physical, social, or both.

1.4.1 Geomorphic Vulnerability

Although both physical and socio-economic components will be addressed to some extent in this research, the primary focus is on the vulnerability of the physical system to erosion under wave energy scenarios with varying combinations of water levels and wind conditions associated with climate change. The vulnerability of the physical system is based on landform change, also called morphodynamics, which is a balance between factors that induce change, those that resist change, and those that allow a system to recover from change. In the comprehensive review of sensitivity in the field of geomorphology, Brunsden (2001) outlines that the stability of a landscape is a function of resisting and disturbing forces, where resisting forces are those with the ability to resist displacement from initial state and disturbing forces are those that apply energy. In his review, the concept of landform resilience was incorporated into the resistance category as system state resistance, representing the degree to which a system can recover from a disturbance (Brunsden, 2001). These basic landform forces that determine geomorphological change will form the basis of the physical coastal vulnerability index in this research. These classes will be called Coastal Characteristic Classes (CCCs), with assailing characteristics defined as those that induce coastal change (such as waves), resistance characteristics defined as those that resist coastal change (such as landform type), and resilience characteristics defined as those that allow a system to cope with and respond to coastal change

(such as sediment supply). Recalling the concept of vulnerability, which can be illustrated by Equation 1.1, it can be seen that in the coastal geomorphic context, assailing, resistance, and resilience characteristics are respectively related to the exposure, sensitivity and adaptive capacity components of vulnerability. While related, the terms sensitivity and resistance are conceptually converse, as sensitivity refers to the susceptibility of a system to change and resistance refers to the ability to resist change. Therefore, it can be inferred that coastal geomorphic vulnerability can be represented by Equation 1.2, such that an increase in coastal resistance or resilience subsequently decreases coastal geomorphic vulnerability.

Equation 1.2

$$\textit{Coastal Geomorphic Vulnerability} = \textit{Assailing} \times (1/\textit{Resistance}) \times (1/\textit{Resilience})$$

To date, no coastal vulnerability assessments have thoroughly incorporated the natural adaptive capacity/resilience of the coastal zone with resistance and assailing parameters. Thus, in an effort to provide a comprehensive geomorphic vulnerability assessment, this research incorporates assailing, resistance and resilience parameters. The approach applied in this research can be applied to any combination of landform and energy inducing event, as the contributing parameters may change, but the geomorphic characteristic classes remain the same, as does their relationship.

1.4.2 Vulnerable Coasts

Coasts can be vulnerable when exposed to physical events such as flooding, inundation and, coastal erosion, but the presence of certain coastal characteristics makes coasts either

more or less vulnerable to these effects. Human and social characteristics that may make a coast more vulnerable to SLR include a high population density (Yin et al., 2012), tourism pressure on the coast and its natural resources (Yin et al., 2012; Hughes & Brundrit, 1992), developments close to the shoreline causing coastal beach squeeze, in which the beach is unable to naturally retreat and re-establish its pre-disturbance profile (Palmer et al., 2011), and low adaptive capacity (Nicholls & Cazenave, 2010). A physically vulnerable coast may be characterized by factors such as an erodible substrate (Gornitz et al., 1991; Hedge & Reju, 2007; Pendleton et al., 2004; Shaw et al., 1998), an open coast and exposure to dominant wave direction (Abuodha & Woodroffe, 2010), a low elevation (Hedge & Reju, 2007; Gornitz et al., 1991; Shaw et al., 1998), current or historical evidence of subsidence or erosion (Gornitz et al., 1991), high energy environment from both tides and waves (Hedge & Reju, 2007; Pendleton et al., 2004), and the absence of biotic protection from vegetation (IPCC, 2007). Other notable characteristics that make a place more vulnerable to shocks belong to low-lying coastal countries such as Small Island Developing States (SIDS). Although the SIDS designation applies only to island countries, other small communities around the world share similar characteristics with SIDS that make them more economically, environmentally, and socially vulnerable to shocks than other communities (UNEP, n.d.; Simpson et al., 2010; IPCC 2007). Some of these characteristics include: relative isolation (Simpson et al., 2010; The Economic Commission for Latin America, 2000), small physical size (Simpson et al., 2010; IPCC, 2007), high concentration of population and infrastructure located in coastal areas (Simpson et al., 2010), a low adaptive capacity (The Economic Commission for Latin America, 2000), high adaptation costs (IPCC, 2007), high exposure to natural hazards (IPCC, 2007), fragile ecosystems, and a heavy reliance on these systems for subsistence and livelihoods (IPCC, 2001). An example of a non-island

community that exhibits many of these characteristics, but which is not designated a SIDS, is the small fishing based coastal community of Lockeport, Nova Scotia.

1.5 Assessing Coastal Vulnerability

A community's ability to adapt to an event such as SLR, begins with the identification of areas that are particularly vulnerable or sensitive to the effects of that event. The purpose of a coastal vulnerability assessment (CVA) is to guide the adaptation process and increase a community's adaptive capacity (McLaughlin & Cooper, 2010). Ramieri et al. (2011) identified four main categories of coastal vulnerability assessments: methods based on dynamic computer models, GIS-based decision support systems, indicator based approaches, and index approaches. Of those, the most commonly and extensively used are coastal vulnerability indices (CVIs) (Doukakis, 2005).

1.5.1 Coastal Vulnerability Index (CVI)

A CVI is one of the pioneer methodologies for coastal vulnerability assessments (Carasco et al., 2012) and its purpose is to simplify a number of key coastal parameters to create a single indicator that is more easily understood and, therefore, more useful for coastal managers (McLaughlin & Cooper, 2010; Sterr, 2008; Perison-Parrish et al., 2012; Wong et al., 2014). In a CVI, the chosen parameters are put into a matrix and ranked according to their contribution to coastal vulnerability. The majority of CVIs have six to nine variables and have five rank categories (*very low, low, moderate, high, and very high*) (McLaughlin & Cooper, 2010). Some CVIs use only four rank categories (*low, moderate, high and very high* [Zujar, 2009]: or *extremely low, low, moderate and high* [Palmer et al., 2011]), and in some cases, three (*low, moderate,*

high) (Sousa et al., 2012). The rank values from each parameter are combined into a CVI and then the range of those CVI values are further divided into three to four categories representing low to high vulnerability. The final CVI score is a dimensionless value, which is only comparable to other CVI scores within the study and not to other coastal vulnerability studies (Pendleton et al., 2004). Although the inability to compare CVIs between studies is a drawback, the dimensionless index allows for both qualitative and quantitative variables in different units to be combined (McLaughlin & Cooper, 2010).

1.5.2 Development of a Coastal Vulnerability Index

The development of a CVI, including the selection of included parameters and its calculation, is guided by the purpose of the assessment, and thus CVIs are widely varied. Table 1.2 provides a summary of some CVIs applied around the world and illustrates their large variation in purpose and application. The factors that determine CVI purpose, and thus the parameters to be incorporated include environment type, event, system type, scale, and data availability and those that influence the calculation of the CVI are choice of formula and parameter weighting. Of the parameters used in the CVIs reviewed in Table 1.2, the top six parameters are: landform morphology, erosion/accretion rate, coastal slope, RSLR, wave height, and tidal range.

1.5.2.1 Environment Type

Environment type refers to the type of systems for which the assessment is taking place and will influence which parameters are appropriate to include in the CVI. For example, Gornitz et al. (1991), who developed the first CVI and applied it to the US coast, included rock type and

landform classes that were characteristic of North America. Similarly in Canada, Shaw et al. (1998) used the same variables as Gornitz et al. (1991), as the environments in the US do not differ greatly from those found in Canada. However, Abuodha & Woodroffe (2006) developed a CVI that focused specifically on the beach environment and consequently replaced relief, rock type and landforms from Gornitz et al. (1991), with dune height, barrier type, and beach type respectively.

1.5.2.2 Event

CVIs assess vulnerability to various events such, as SLR, climate change in general, inundation, and storm surge. The variables that characterize an inundation event may not necessarily characterize a storm surge event and, for this reason, the type of event influences parameter choice. Mendoza & Jimenez (2009) assessed coastal vulnerability of Catalan beaches to storm surge. Ozyurt (2007) developed a CVI for Turkey, which assessed coastal vulnerability to SLR, and included parameters that characterized flooding, coastal erosion, inundation, and saltwater intrusion to groundwater resources and rivers/estuaries. Table 1.2 contains specific variables.

1.5.2.3 System Type

Although many CVIs only calculate physical vulnerability, the importance of incorporating socio-economic data in CVIs has been commonly noted in the literature in recent years (Abuodha & Woodroffe, 2010; McLaughlin & Cooper, 2010; Sterr, 2008; Adger, 2006). The system type refers to the social, economic, environmental, physical and cultural systems, which are potentially vulnerable to different events. Some studies, such as Szlafsztein & Sterr (2007),

incorporate both physical and socio-economic systems in the calculation of a CVI, while others, such as Zujar et al. (2009) and the original CVI from Gornitz et al. (1991), only include the physical system. Palmer et al. (2011) incorporate both physical and socio-economic components, but assesses physical vulnerability *a priori* and socio-economic vulnerability *a posteriori*. Others focus solely on social vulnerability, such as Boruff et al. (2005), who developed the Social Coastal Vulnerability Index (SoCVI), and Cochran et al. (2012).

1.5.2.4 Scale

Spatially, CVIs can be developed for international, national, regional or local scales (Sterr, 2008). There is not a “one size fits all” CVI that can be used at all scales because the variables acting on a coast at a local scale may be too minute to influence coastal vulnerability at a national scale and vice versa (McLaughlin & Cooper, 2010). For example, the rate of SLR would be an important variable when looking at the coastal vulnerability of the entire US; however, when looking at the vulnerability of a single beach, as in the case of Sousa et al. (2012), the rate of SLR may not be as important to include, as sea level is unlikely to change from one end of the beach to the other. McLaughlin & Cooper (2010) investigated the importance of scale in assessing coastal vulnerability and determined that the approach needs to match the level of management for which strategies and decisions will be made (i.e., international management strategies require a global approach). A study conducted by Shaw et al. (1998), discovered that the use of generalized data to assess coastal sensitivity over a long length of coast led to the misrepresentation of the sensitivity of small, but vulnerable sites. Torresan et al. (2012), state that beaches and estuaries are particularly vulnerable ecosystems to the effects of climate change and, consequently, are best studied at the regional or local scale.

Table 1.2 Summary of CVIs Applied in Different Countries Where N= No, Y= Yes, A= CVI₅ - square root of product mean, B= CVI₁ - sum/number of variables, C= CVI₆ - sum of variables, and OT = other formula (Compiled by: Samantha Page, 2013).

Author/Date	Location	Purpose (Vulnerability to....)	Weights	Calculation	Physical Variables														Social Variables			Other Variables		
					Landform Morphology Erosion/Accretion	Dune Height/Presence	Shoreline Exposure	Presence of Rivers/Inlets	Elevation	Soil Permeability	Rock Type	Coastal Slope	Barrier Types	RSR	Wave Height	Tide Range	Storm Frequency	Beach Width	Vegetation	Natural Habitats	Sediment Supply/Budget		Artificial Protection	Population
Abuodha & Woodroffe, 2006	Australia	SLR	N	A	x	x																		Beach Types
Abuodha & Woodroffe, 2010	Australia	SLR	N	A	x	x	x			x	x	x	x	x	x									
Alexandrakis et al., n.d.	Aegean Coast	SLR	N	A	x	x					x	x	x	x										
Doukakis, 2005	Greece	SLR	N	A	x	x					x	x	x	x										
Gaki-Papanastassiou et al., 2010	Greece	SLR	N	A	x	x					x	x	x	x										
Gornitz et al., 1991	US	SLR	N	A	x	x			x				x	x	x									
Guannel et al., 2012	British Columbia	SLR	N	A	x		x	x					x				x							
Thieler & Hammer-Klose, 2000	US	SLR	N	A	x	x					x	x	x	x										
Hedge & Reju, 2007	Managalore, India	Erosion	N	B	x	x					x									x				
Hughes & Brundrit 1992	South Africa	SLR	N	OT	x	x			x			x	x	x							x			
Kumar et al., 2010	India	SLR	N	A	x						x	x	x	x										Tsunami Arrival Height
Mclaughlin & Cooper, 2010	Ireland	Hazard Risk	N	B	x	x			x	x					x					x	x	x		Morphodynamic State, Cultural Heritage
Ojeda-Zujar et al., 2009	Spain	SLR	N	A	x	x					x	x	x	x										
Ozyurt, 2007	Turkey	SLR	Y	OT	x	x			x		x	x	x	x										Proximity to Groundwater, Type of Aquifer, River Discharge, Depth of Watertable, Hydraulic Conductivity
Palmer et al., 2011	South Africa	Erosion & Extreme Weather Events	Y	C		x									x	x								Percentage Rocky Outcrop, Offshore Slope
Pendelton et al., 2004	Virgin Islands National Park	SLR	N	A	x	x					x	x	x	x										
Shaw et al., 1998	Canada	SLR	N	A	x	x					x	x	x	x										
Sousa et al., 2012	Brazil	Erosion	N	OT	x	x	x	x	x	x							x			x	x			
Szlafstein & Sterr, 2007	Brazil	Climate Change	Y	OT	x		x	x												x				Coastline Length, Historical Emergency Relief, Historical Flooded Areas, Non-local Population, Poverty, Wealth
Tibbets & van Proosdij, 2013	Nova Scotia	Storm Surge	Y	A	x	x					x				x	x			x					Morphological Resilience, Freeboard
Torresan et al., 2012	North Adriatic Sea	Climate Change	Y	OT	x	x			x	x					x	x	x	x						Protection Level of Natural Habitats
Yin et al., 2012	China	SLR	Y	C	x	x					x		x	x										

1.5.2.5 Data Availability

One of the biggest limitations in the development of a CVI is the lack of available data, and, because of this, it is common to exclude a useful parameter, the process of which does not always produce accurate results (Sterr, 2008; Hedge & Reju, 2007; Perison – Parrish et al., 2012). Even if data do exist, another challenge arises from the unwillingness of organizations to share data as well as the sheer cost of data acquisition (Sousa et al., 2012). Szlafsztain & Sterr (2007) emphasized that the data that were most lacking in their study were high-resolution elevation data, climatic and oceanographic data, erosion rates, population growth, and population statistics for women. Other challenges identified in the literature include the necessity of expensive, high-resolution data for local scale studies (McLaughlin & Cooper, 2010), the general low spatial resolution of available data (Palmer et al., 2011), and the huge data gap that exists for coastal change and subsidence rates (Hughes & Brundrit, 1992; Shaw et al., 1998).

1.5.2.6 Formula & Parameter Weighting

Once the appropriate variables for a CVI are chosen and ranked, the last step is choosing the best CVI formula. Gornitz et al. (1997) tested multiple formulas for calculating a CVI using samples of 93 randomly selected coastal segments. The following formulas were tested:

CVI₁ = product mean

CVI₂ = modified product mean

CVI₃ = average sum of squares

CVI₄ = modified product mean (2)

CVI₅ = square root of product mean

CVI₆ = sum of products

CVI₃ and CVI₆ were least sensitive to changes in parameters, which did not allow for small, but key changes to be noted. CVI₁, CVI₂, and CVI₄ have the advantage of expanding the range of values, but can be slightly sensitive to extremely small changes. CVI₅, on the other hand, is relatively insensitive to variations in one factor, but is still able to produce useable results when differences occur within more than one factor (Gornitz et al., 1997). Because of this, CVI₅ (Equation 1.3) is the most commonly used formula to calculate a CVI. Of the 22 CVIs reviewed in Table 1.2, two used CVI₁, two used CVI₆, five used various other formulas, and 13 used CVI₅.

Equation 1.3

$$CVI_5 = \sqrt{(a*b*c*d*e*f)/n}$$

Although the square root of the product mean is most commonly used, some studies use the sum of the ranked variables (Yin et al., 2012; Palmer et al., 2011), others use the sum divided by the number of variables (Hedge & Reju, 2007; McLaughlin & Cooper, 2010), and others use linear algebra (Torresan et al., 2012). Some authors also choose to weight their variables, as some factors are perceived to contribute to vulnerability more than others and therefore are assigned weights that give them more prominence over other variables. As is illustrated in Table 1.2, weighting is not a common practice, as it is often viewed as being biased (McLaughlin & Cooper, 2010).

1.6 Purpose of Study & Objectives

This research focuses on the development of a CVI that assesses the physical vulnerability of a coastline while incorporating assailing, resistance, and resilience parameters. The aim of the project is to assess the vulnerability of the coastal zone to erosion and to illustrate the

differences in coastal response under varying wave energy scenarios with different combinations of water levels and wind conditions associated with climate change. Furthermore, the building infrastructure located in highly vulnerable coastal areas will also be identified in an effort to inform local coastal management strategies. This method was applied to the town of Lockeport, Nova Scotia; a small coastal community highly vulnerable to the effects of SLR and was carried out using the following objectives:

1. Develop a field based shoreline characterization database (SCD) for coastal protection structure and observed erosion points and for backshore (BS), foreshore (FS), and nearshore (NS) lines to increase project accuracy and spatial scale.
2. Develop a CVI matrix based on the principles of geomorphology and international literature, which incorporates the natural adaptive capacity of coastal landforms and can be used to assess relative coastal vulnerability to erosion.
3. Apply the developed CVI to Lockeport, Nova Scotia to assess relative coastal vulnerability to erosion under four wave energy scenarios associated with climate change and determine the areas that are at greatest risk to erosion.
4. Identify buildings in the coastal zone that are at risk to erosion under each wave energy scenario (S1, S2, S3, and S4).
5. Identify buildings in the coastal zone that are at risk to erosion and permanent inundation associated with the wave energy scenarios that incorporate an increase in water levels (S3 and S4).

This research is part of the larger ParCA (Partnership for Canada-Caribbean Community Climate Change Adaptation) project, which focuses on assessing current and future exposure sensitivities and adaptive capacities in socio-economic, political and environmental realms across four regions: Nova Scotia, Prince Edward Island, Tobago, and Jamaica. The research outcomes will not only inform coastal managers in Lockeport, but also contribute to the ParCA project knowledge base and provide opportunities for cross-cultural comparisons. The ParCA project, and thus my research, will also contribute to the International Research Initiative on Adaptation to Climate Change (IRIACC), which addresses various knowledge gaps in climate change adaptation research in Canada and across four continents.

Chapter 2

DESCRIPTION OF STUDY AREA

2.1 Site Selection

The primary focus of the ParCA project, to which this research contributes, is to study climate change vulnerability and adaptive capacities of small to medium coastal communities whose main source of income are the tourism and fishery industries. The ParCA team identified a study area along the South Shore, Nova Scotia from Port Clyde to Port Medway and study communities were chosen based on clusters of tourist attractions (accommodations, parks, lighthouses, restaurants, golf courses, historically and culturally important sites, and piping plover sites), fishing wharves accommodating vessels that employ a variety of fishing techniques, and areas that were noted as being particularly vulnerable to the effects of storms and climate change (Municipality of the District of Shelburne, 2013). The identified areas were: Gunning Cove, Birchtown, Shelburne, Lower Sandy Point, Lockeport, Louishead, Summerville, Whitepoint, and Port Mouton. In an effort to enhance the detail of the research for this study, the geographic range was reduced to focus on only one community. The Town of Lockeport, a community increasingly threatened by SLR, was chosen due to the availability of LiDAR (Light

Detection and Ranging) data, the identification of this location as being highly vulnerable to the impacts of climate change, ease of site accessibility, and the documented need for climate change vulnerability assessments (Eshelby, 2010).

This chapter is designed to provide research context by presenting an overview of location, geography, people, economy and community assets, ocean and climate impacts, anthropogenic intervention and adaptation, and finally, identifying locations currently prone to climate change impacts. While some scientific literature has been included to support these topics, indispensable information gathered during the field season from personal interviews and general conversation with knowledgeable community members has also been incorporated.

2.2 Location & Geography

The Town of Lockeport is located in the eastern portion of Shelburne County, approximately 4.5 km into Ragged Island Bay from the tip of Western Head (Taylor, 2009). Initially Lockeport, named as such in 1870 (Mattatall, 1993) included Locke Island only, but in 1907 a section of the mainland along the current Brighton Road was added to the Lockeport jurisdiction in order to meet the necessary population and acreage requirements to be recognized as an official town (Mattatall, 1993) (Figure 1.2). The municipality of the Town of Lockeport, third smallest of 45 municipal districts in Nova Scotia, has a land area of 2.32 km² and a coastline of eight km (Eshelby, 2010; Atwood, 2013). Of the eight km, 3.14 km is owned by the Town of Lockeport, including 0.56 km along Calf Island Road, 0.5 km on the north shore, 1.4 km along Sam's Point, and 0.68 km along the marsh side of the causeway (Atwood, 2013; Anonymous a, 2013).

For its size, the Town of Lockeport consists of widely varied coastal features: sandy and cobble beaches, marshlands, bedrock, sand dunes, and anthropogenic structures. According to coastal characterization data collected for this research during the summer of 2013 (and the resulting SCD [Shoreline Characterization Database] created in 2014), 61.51% of Lockeport’s backshore is organogenic slope (unconsolidated slope covered with organic material [i.e., vegetated]), followed by anthropogenic structures at 19.34%, and the foreshore consisting primarily of beach at 27.14%, anthropogenic structures at 24.63%, and outcrop at 23.62% (Table 2.1). The underlying geology consists of hard bedrock from the Goldenville Formation, consisting of quartz with bands of mica and schist (Keppie, 2000). The presence of hard bedrock underlying the majority of Lockeport is a vital natural asset when it comes to climate change impacts and island longevity.

Table 2.1 Percent Coverage of Backshore and Foreshore Features. Compiled from the Shoreline Characterization Database, created in May, 2014 with data collected during the June and July 2013 field season.

Backshore Type	% Coverage	Foreshore Type	% Coverage
Organogenic Slope	61.51	Beach	27.14
Anthropogenic	19.34	Anthropogenic	24.63
Dune	7.06	Outcrop	23.62
Organogenic Wetland	6.64	Wetland Organogenic	17.01
Clastic Slope	3.00	No Foreshore	3.76
Outcrop	2.44	Platform	2.46
		Clastic Slope	1.38

Of all coastal features in Lockeport, Crescent Beach is considered the most important natural asset to the community (Atwood, 2013). Its economic and social value and its dynamic features identify it as a primary focal point for those concerned with rising seas associated with climate change (Atwood, 2013; Anonymous a, 2013). Crescent Beach is a 0.8 km long bay-head barrier beach, which connects Locke Island to the mainland. The width of the beach, extending

from the front of the foredune to the low tide level, ranges from 53-85 m with a very shallow slope (Taylor, 2009). The beach is located between two bedrock outcrops and is backed by a single dune ridge, behind which is the only access road from the island to the mainland (Crescent Beach Causeway) (Taylor, 2009).



Figure 2.1 Study Area - Town Of Lockeport, Nova Scotia.

2.3 People, Economy, & Assets

The history and development of the Town of Lockeport is a story of economic highs and lows heavily reliant upon and directly related to the unpredictable, ever changing nature of the sea. This has shaped the community into what it is today: a proud and highly resilient group of people with a profound sense of community and spirit - qualities, which have led to the recognition, in the Municipal Climate Change Action Plan (Atwood, 2013), of “Lockporters” as a major asset of the town in the face of climate change.

First settled in 1755 (Mattatall, 1993), Lockeport became a central port for the West Indian Trading outfit in the 1850’s, a period that saw the town become one of the wealthiest settlements in Nova Scotia (Mattatall, 1993). At its peak, the town boasted more than 13 inns and harbored over 50 vessels manned by more than 800 men (Mattatall, 1993; Anonymous a, 2013). A major decline in the West India Trading outfit at the onset of the 1900’s forced Lockeport to become more reliant upon fishing for its survival (Mattatall, 1993). In 1925 a railway “spur line”, consisting of a rail line and two trestles, was constructed, which connected the island to the mainland and provided efficient transport for the fish plants in Lockeport (Atwood, 2013; Mattatall, 1993). In 1979, the Canadian National Railway abandoned service to Lockeport and in the years of 1989, 1993, 1994, and 2008, Lockeport experienced major fish processing plant closures (Eshelby, 2010). With fishing still a major economic focus of the community, the town revived the tourism industry by building a number of small cottages near Crescent Beach in 1990 and 1996, the Crescent Beach Tourism Centre in 1994, and a boardwalk in 1996/97, which is now part of the Lockeport Loop Walking Trail (Town of Lockeport, 2013; Anonymous a, 2013; Mattatall, 1993).

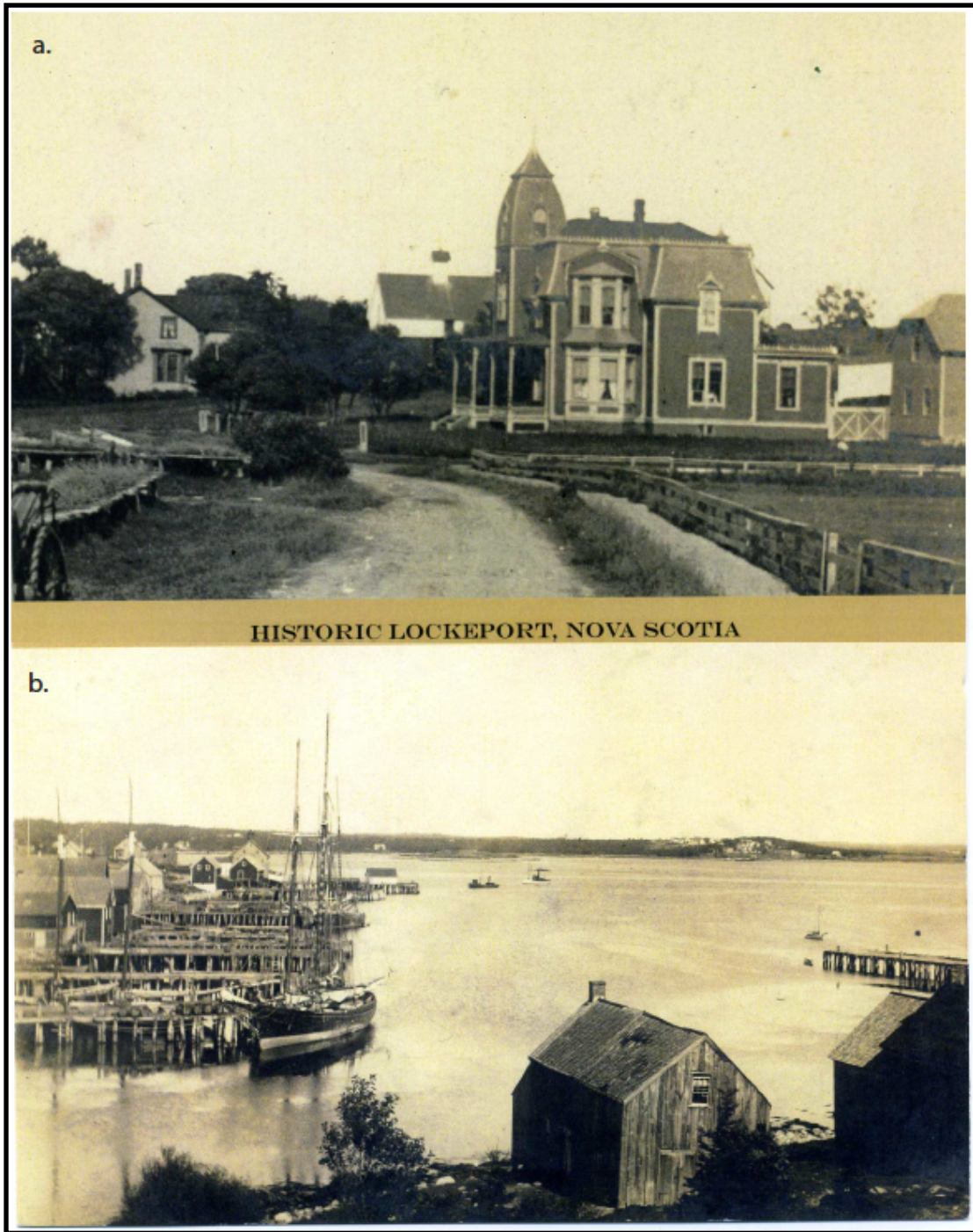


Figure 2.2 Historical Images of Lockeport. a) Locke House c.1907, built for Captain Henry Locke in 1876. Located on the Locke Streetscape it is part of the first provincially designated Streetscape in Nova Scotia (Used with permission from: Peter Swim, Lockeport Town Market). b) Lockeport Waterfront c.1907, with the Old Lockeport Meeting House in the foreground (Used with permission from: Peter Swim, Lockeport Town Market).

Today, Lockeport's population consists of approximately 588 year-round residents with population numbers increasing substantially during the warmer seasons (Atwood, 2013; Anonymous a, 2013). Between 2006-2011, the population decreased by 9%, from 646-588, and the average age was 51.1 years (Government of Canada, 2014; Brown, 2014). With an annual operating budget of 1 200 000 CAD, the town is responsible for 12 buildings/ infrastructure, two sports fields, two public parks and one playground (Atwood, 2013). Despite Lockeport's designation as a declining working waterfront (CBCL Limited, 2009), the fishery remains the primary industry, with the Clearwater lobster processing plant employing approximately 200 people (Atwood, 2013). Tourism is becoming a major focus and Lockeport's beaches are considered the town's most valuable tourism asset (Eshelby, 2010; Atwood, 2013).

2.4 Ocean & Climate Impacts

As a seafaring town, Lockeport is no stranger to high winds and big swells from tropical cyclones, tropical storms and nor'easters (Table 2.2). Its location in Ragged Islands Bay provides little protection against hurricanes and high winds that occur in the Atlantic Ocean, and its open, southerly exposure makes this town even more susceptible to storm winds from the South (Atwood, 2013; Taylor, 2009).

"In the city, the weather really isn't much of a concern; it's whether you should take a raincoat or umbrella to get to a taxi. Here, your livelihood depends on it."

- Lockeport Resident, 2013

While Lockeport has recovered from the impacts of storm events in the past, which included but were not limited to storm surge, erosion, and flooding (Atwood, 2013), with rising sea levels storms are beginning to impact them on a more regular basis, allowing less time for

recovery (Anonymous a, 2013; Anonymous b, 2013) (Table 2.2). The year 2011 alone saw 13 million CAD in storm damage to Nova Scotia coastlines (The Canadian Press, 2011). Although Crescent Beach displays the common cyclical seasonal sediment transport pattern (Crooks, 2004), with sediment levels and beach stability highest in summer months and most scoured in winter, only to be replenished again in the summer, the foredunes along the beach are commonly being wiped out two to three times a year, which does not allow adequate time for foredunes to become sufficiently re-established (Anonymous a, 2013). In the past, the single dune ridge backing Crescent Beach has provided protection along the causeway; however, recent years have seen dune overtopping on a regular basis (three to four times a year), with even small storms causing impacts (Anonymous a, 2013; Anonymous b, 2013). Two of the more recent storms of most notable impact were Hurricane Bill in 2005 and the winter storm of 2013 (Anonymous a, 2013) (Table 2.2, Figure 2.3, and Figure 2.4).

While the town's greatest climate change vulnerability is the storm surge and flooding associated with large storms (Atwood, 2013), Lockeport is also susceptible to erosion events. While the majority of the island is underlain by hard, resistant bedrock, and approximately 23% of the foreshore is bedrock outcrop (this study), high winds and frequent storm surges yield powerful waves with the ability to cause substantial erosion and damage along the remaining 77% (this study) of the shoreline that is not hard bedrock.

Table 2.2 Summary of Select Storms and Hurricanes that Impacted Lockeport. The list of storms is by no means complete and only refers to those found in the literature causing specific damage to Lockeport. (Sources 1=Environment Canada, 2010, 2=Taylor, 2009, 3=Scott, 1991, 4=Atwood, 2013, 5=Atwood, 2009, 6=DeMont et al., 2010, 7=Taylor & Frobel, 2009, 8=Anonymous a, 2013, 9=Anonymous b, 2013).

Date/Name	Additional Info	Impacts/Damage	Source(s)
Aug. 27 th , 1924 Hurricane Three	Category 2, 158 km/hr	great damage to trees and gardens, barns lost roofs in gale	1
Sept. 17 th , 1940 The 1940 NS Hurricane	Category 1, 120 km/hr, made landfall near Lockeport	high tides made Lockeport a temporary island, many homes flooded	1
Oct. 17 th , 1943 Tropical Storm Eight	Tropical Storm, 65 km/hr, but 110 km winds in Nova Scotia	damage to railway lines in Lockeport	1
Sept. 19 th , 1936 Hurricane Thirteen	Category 1, 148 km/hr	reservoir burst from pressing water and a 2.5 m torrent flow to ocean, destroyed buildings and roads	1
Oct. 8 th , 1962 Hurricane Daisy	Category 1, 120 km/hr	Lockeport lost two beaches and sand washed across the causeway	1
Oct. 29 th , 1963 Hurricane Ginny	Category 2, 176 km/hr	dune breach, 15-20 cm of dune sediment washed onto causeway	2, 3
1978	severe sleet storm	unusually high tides, waves breached dunes at eastern end of Crescent Beach	2,3
Oct. 31 st , 1991 The Perfect Storm	Nor'easter	large waves breached dunes and caused flooding	2
Sept. 15 th , 1996 Hurricane Hortense	Category 1, 130 km/hr	dunes were breached, Crescent Beach Centre flooded and filled well with saltwater	2, 4
Nov. 3 rd , 2007 Tropical Storm Noel	Tropical Storm, 120 km/hr	some waves overwashed onto road east of Crescent Beach Centre and near the Old School Museum	2
Sept. 29-30 th , 2008 Hurricane Kyle	Category 1, 120 km/hr	waves overwashed part of beach	2
Sept. 14 th , 2009 Hurricane Bill	Category 2, 140 km/hr	breaching of dunes, closure of causeway for 45min., with pulses of water overwashing the east side dune crest (3.3-3.6 m)	4, 5, 6,7
February 9 th , 2013	Nor'easter	substantial storm surge, and flooding, washed out 10 ft of foredune of beach	8, 9



Figure 2.3 Little School & Marine Building Museum Flooded from Hurricane Bill Storm Surge, 2009. (Used with permission from: Bil Atwood).



Figure 2.4 Calf Island Road Submerged during the February 9th, 2013 Winter Storm. (Used with permission from: Bil Atwood).

2.5 Anthropogenic Intervention & Adaptation

“Whatever we do around here isn’t really because we would like to do it. We do it out of necessity; to adapt to weather impacts.”

-Lockeport Resident, 2013

Adapting to adverse weather conditions is not a new phenomenon for the Lockeport community. However, of all human intervention and adaptation efforts conducted to date, Crescent Beach has received the most attention. Given the high value the community has placed on the beach (Atwood, 2013), a history of its

creation will serve as a useful backdrop for the purposes of this study. The beach and dune owe their existence to the local residents who, over time, have created a highly engineered “natural” system (DeMont et al., 2010). Prior to the 1900s, a transient sand bar connected Locke Island to the mainland, very similar to the one that currently connects Cranberry Island (located east of Lockeport) to Locke Island during low tide. At the turn of the century a wooden cribwork was built across the bar to encourage sediment deposition and foredune creation (Taylor, 2009; Scott, 1991). Over the years the dune was built up using a variety of objects, including old car bodies and animal carcasses, and eventually a vegetated foredune began to form (Anonymous a, 2013). Figure 2.5 shows Locke Island and the beginning of dune formation in the 1920s.

After a fire destroyed the wooden bridge connecting Locke Island to the mainland across the current Calf Island Road (Figure 2.6), a paved road was built, in 1935, along the back side of Crescent Beach to provide access to the mainland (Taylor, 2009; Scott, 1991). As late as the 1960’s, varied objects were still being used to stabilize the dunes (Scott, 1991) until Crescent Beach was placed under the Nova Scotia Beaches Act (Beaches Act. R.S., c.32, s.1) in July 1976 (Government of Nova Scotia, 1989; Taylor, 2009). In the early 1980’s three sets of beach access

stairs were constructed over the top of the dune (Figure 2.7) to decrease foot traffic along the dune crest and reduce dune deterioration (Taylor, 2009; Scott, 1991) and in 1984 a dune



Figure 2.5 The Origins of Crescent Beach. Crescent Beach c.1920's connecting Locke Island to the mainland (Used with permission from: Peter Swim, Lockeport Town Market).



Figure 2.6 Calf Island Road Bridge. Old Bridge c.1907 (Used with permission from: Peter Swim, Lockeport Town Market).

restoration project was undertaken, which included the use of snow fencing along the foredunes and marram grass plantings (Taylor, 2009; Scott, 1991). This program was relatively successful, but storm surge and, in some places dune deflation around the access stairways (Scott, 1991), resulted in a second dune restoration project, which was conducted in 1990, consisting of sand fences placed both higher up the slope of the dune and farther seaward than the program of 1984 (Taylor, 2009; Scott, 1991; Anonymous a, 2013).

After Hurricane Hortense in 1996, which caused substantial flooding and damage to the Crescent Beach Centre, an armour stone revetment was built, extending from the parking lot area of the Crescent Beach Centre 370 m eastward along the foredune (Atwood, 2013; Anonymous a, 2013; Taylor, 2009). In the year following Hurricane Bill in 2009, an additional 390 m of armour stone revetment was built from the corner of South Street and Hall Street westward along the foredune (Atwood, 2013) leaving 90 m of the beach unprotected by revetments. The 2010 revetment project used larger rocks sourced from Birchtown, which were individually placed, as opposed to dumped, and cost approximately 110 000 CAD (Anonymous a, 2013). Most recently (2013), the town of Lockeport has tried using discarded lobster traps, placed in a zigzag pattern just seaward of the base of the dune in an effort to trap sediment and help re-establish the foredune (Anonymous a, 2013) (Figure 2.8). By the end of July 2013, this approach appeared to be quite successful, resulting in the beginning of foredune formation.

Other adaptation measures in Lockeport include the construction of the South Wharf Breakwater in the 1960's and Breakwater widening and heightening in 2009, carried out by the Government of Canada, who invested 1.37 million CAD in six small craft harbours along the South Shore of Nova Scotia from 2008-2009 (Fisheries & Oceans Canada, 2008; Anonymous a,

2013). Shoulder repair and widening along 460 m of Brighton road was completed in 2010 (Atwood, 2013; Anonymous a, 2013) and the Little School Museum was elevated by 0.6 m in 2011 after it was extensively flooded in Hurricane Bill (Atwood, 2013). Coastal protection structures along the coastline of Lockeport range from small groynes and concrete seawalls to large riprap revetments. Including private and town owned structures, they total 81 (this study).



Figure 2.7 Access Stairways by Crescent Beach Centre. (Photographer: Sam Page, 2013).



Figure 2.8 Lobster Traps used to Develop Foredune on Crescent Beach. (Photographer: Sam Page, 2013).

2.6 Current Climate Change Challenges

While the purpose of this research project is to determine the areas that are particularly vulnerable to geomorphic change under varying wave energy scenarios associated with climate change, the Municipal Climate Change Action Plan (MCCAP) (Atwood, 2013) has identified locations of particular concern based on recent observations and experiences with climate change impacts in the community. The following locations have been identified as areas of concern by Atwood (2013), Taylor & Frobel (2009), and Anonymous a (2013): 1) Calf Island Road; 2) South Street (three locations); 3) Chetwynd Lane; 4) Crescent Beach Causeway; 5) Locke Street West; 6) South Water Street; 7) Intersection of North Street and Upper Water Street; 8) the Trestles; 9) Boardwalk; and 10) Nursing Home (Figure 2.9). Of these, the locations with highest risk rankings include Calf Island Road, the intersection of North Street and Upper Water Street, Chetwynd Lane, Locke Street West, and the Crescent Beach Causeway (Atwood, 2013).

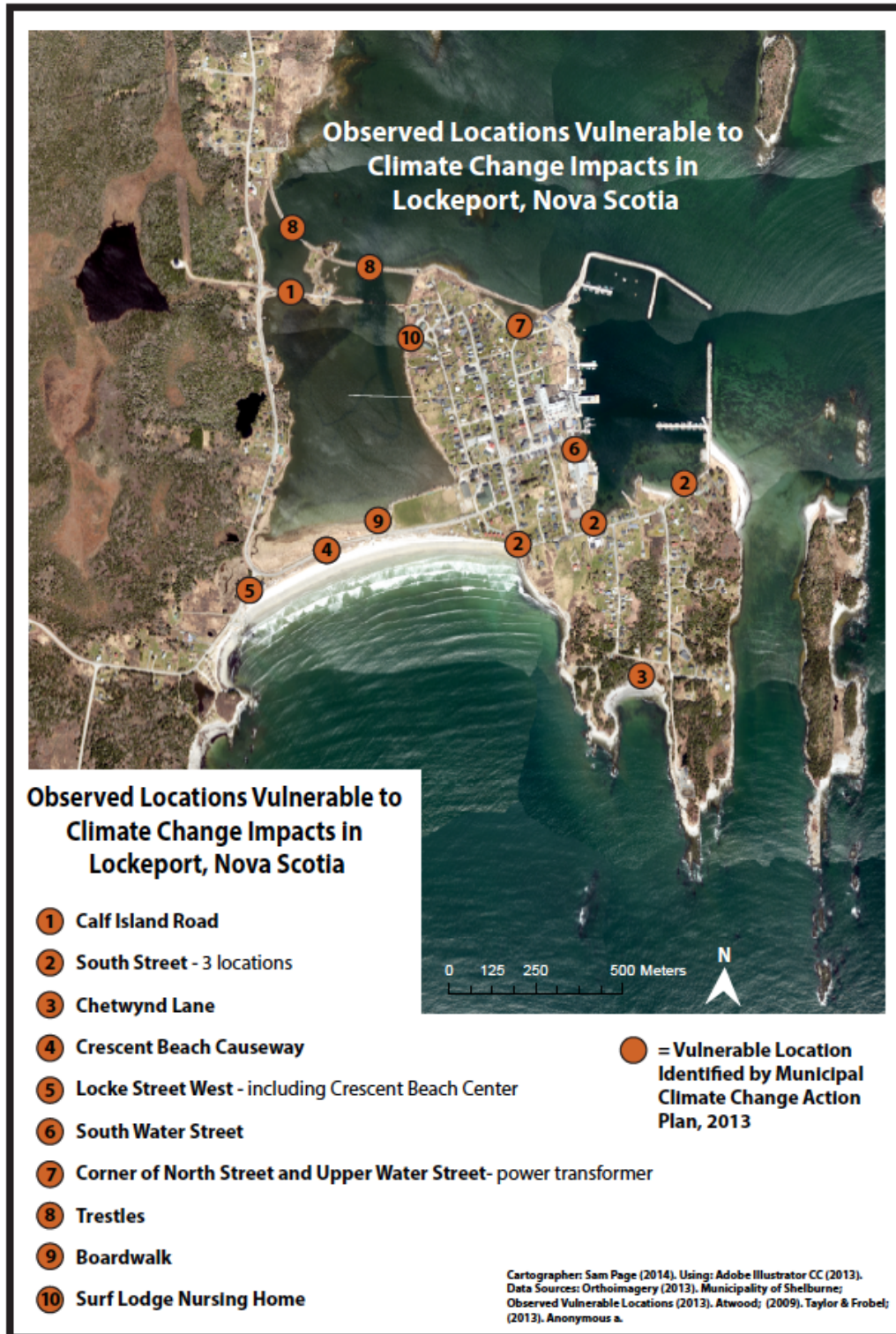


Figure 2.9 Observed Locations Vulnerable to Climate Change Impacts in Lockeport, Nova Scotia. (Noted observations are based on Municipal Climate Change Action Plan for the Town of Lockeport, NS [Atwood, 2013]).

Chapter 3

RESEARCH DESIGN AND METHODOLOGY

3.1 Research Design Overview

The purpose of this research is twofold: first, the goal is to develop a CVI that incorporates assailing, resistance, and resilience parameters and assesses physical vulnerability to erosion; and, second, to apply the CVI to a small coastal community to illustrate the differences in coastal vulnerability under varying wave energy scenarios associated with climate change. Furthermore, this research aims to support coastal management and adaptation decisions in the community by identifying buildings that are vulnerable to erosion under each wave energy scenario as well as those that are also vulnerable to permanent inundation.

To achieve this, a vulnerability matrix was developed by selecting erosion-contributing parameters from peer reviewed coastal vulnerability literature. On-the-ground coastal mapping and data collection was conducted, along with GIS (Geographic Information System) modeling and analysis, and acquisition of spatial datasets to produce the necessary detailed data for CVI matrix creation and calculation. The developed matrix was then applied to the Town of Lockeport, Nova Scotia, and the CVI was calculated for each segment of coastline under four

wave energy scenarios ; each differing in water depth and/or wind conditions. The vulnerability of buildings to erosion in the coastal zone was then identified for S1, S2, S3, and S4 using spatial analysis. Those also vulnerable to inundation from SLR were identified for the scenarios that incorporate a change in water depth (S3 and S4) (Figure 3.1). The identification of areas and buildings vulnerable to erosion and inundation will enable the Town of Lockeport to better address coastal impacts currently and in the future.

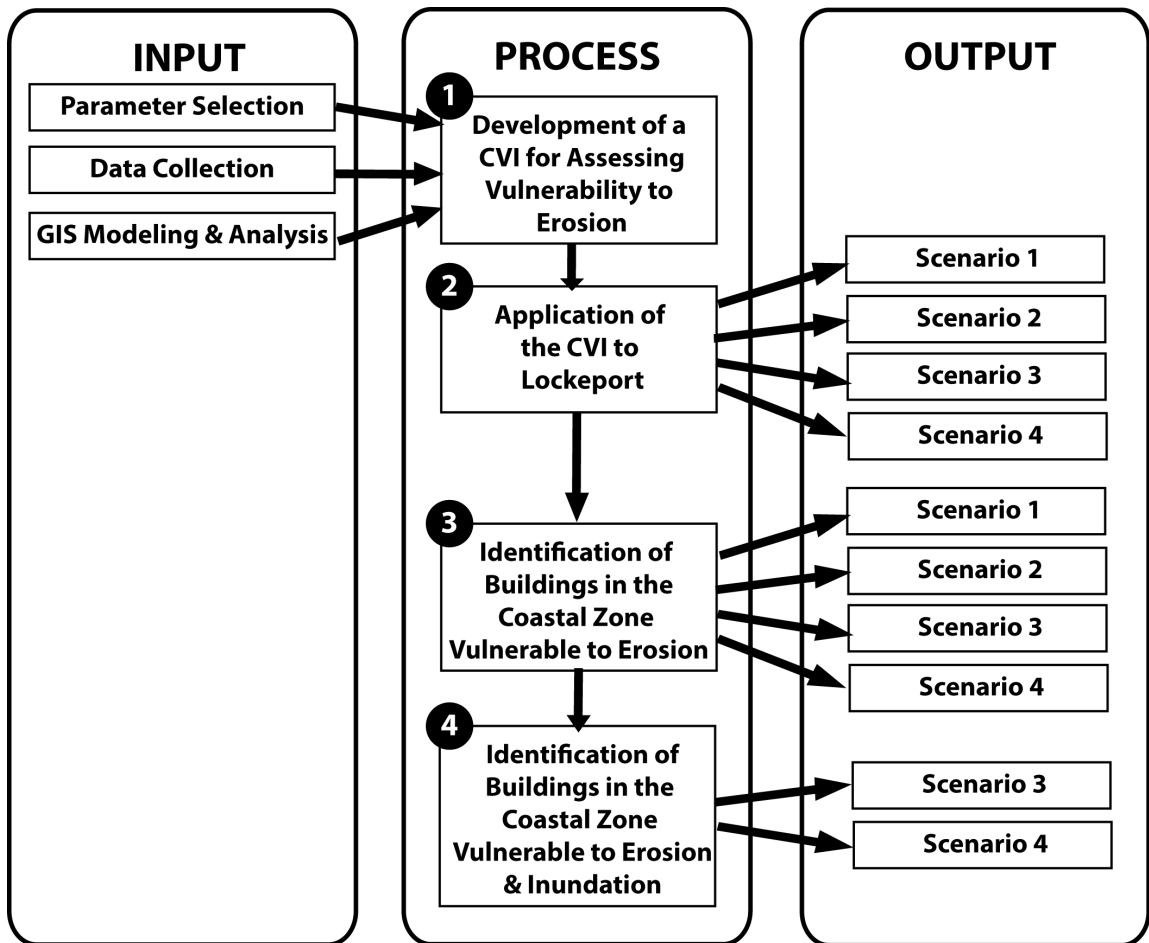


Figure 3.1 Research Design Flowchart. Where each wave energy scenario (S1 to S4) is associated with a different combination of water depth and wind condition.

3.2 CVI Development (Step 1)

After an extensive review of published CVIs, it was found that no existing CVI suited the purpose of this research. The goal of this research was therefore expanded to incorporate the development of a CVI that could be used to assess physical vulnerability to erosion while incorporating assailing, resistance, and resilience characteristics. The development process included parameter selection, data collection (in the form of detailed coastal mapping and GIS modeling and analysis), matrix creation, matrix calculation, and, finally, exploration of the “proof of concept” through observed erosion locations and a principal components analysis.

3.2.1 CVI Purpose

The development of a CVI matrix, including the selection of included parameters and their calculation, is based on the purpose of the assessment and is determined by the following factors: environment type, event, system type, and scale, which are discussed in detail in Sections 1.5.2.1 – 1.5.2.4. When applied to this research, the *environment type* encompasses all coastal features within the South Shore of Nova Scotia, the *event* is erosion under varying wave energy scenarios, the *system type* is physical, and the *scale* is local.

3.2.2 Parameter Selection

The practice of incorporating expert opinion and review of chosen parameters has been used occasionally for the development of matrices in coastal vulnerability literature (Palmer et al., 2011; Yin et al., 2012; Torresan et al., 2012). While this is thought to create a more robust CVI matrix, this practice can also be considered biased (McLaughlin & Cooper, 2010; Yin et al.,

2012) and is not always an option. Although a few informal individual expert reviews were conducted, this project did not include a thorough expert consultation.

Instead, in an effort to develop an accurate, comprehensive CVI, parameters were chosen from existing peer-reviewed and published journal articles. The final list of included parameters was determined through this systematic process:

1. Conduct a thorough review of relevant CVI literature (Table 1.2) and compile the included parameters into a chart.
2. Using this chart, determine the most commonly used parameters in CVI matrices.
3. Identify a few key publications whose assessment purpose is similar to that of this research (i.e., erosion and/or geomorphic change).
4. Compile a list of most commonly used parameters in CVI matrices (from Step #2) as well as the parameters used in the few key publications (from Step #3).
5. Based on the purpose of the research, as well as data availability, determine the final parameters to be used for the CVI matrix that will be applied in this research.

Table 3.1 displays the compilation of parameters from a review of CVI literature (Table 1.2). In Figure 3.2, which illustrates the distribution of parameter use, it can be seen that the data show a bimodal distribution. Using natural breaks, it was determined that the top parameters used in CVIs are any parameters that have been used 13 or more times, which include: Landform Morphology, Erosion/Accretion, RSLR, Wave Height, Tidal Range, and Coastal Slope. A thorough literature review identified five publications with a similar assessment goal to that of this research: Hedge & Reju, 2007, Sousa et al., 2012, Ozyurt, 2007, Shaw et al., 1998,

and Palmer et al., 2011. The parameters used in these publications, along with the most commonly used parameters identified from a thorough literature review as listed above, were compiled into one list (Table 3.2 - C4).

Table 3.1 Compilation of Included Parameters and their Frequency of Use in 22 Reviewed CVIs.
(outlined in Table 1.2).

Parameter	Frequency of Use in Reviewed CVIs	Parameter	Frequency of Use in Reviewed CVIs
Landform Morphology	19	Shoreline Exposure	5
Erosion/Accretion	16	Presence of Rivers/Inlets	5
Relative SLR	14	Barrier Types	4
Wave Height	14	Rock Type	3
Tidal Range	14	Natural Habitats	2
Coastal Slope	13	Sediment Budget	2
Elevation	7	Beach Width	2
Vegetation	5	Storm Frequency	2
Dune Height/Presence	5	Soil Permeability	1

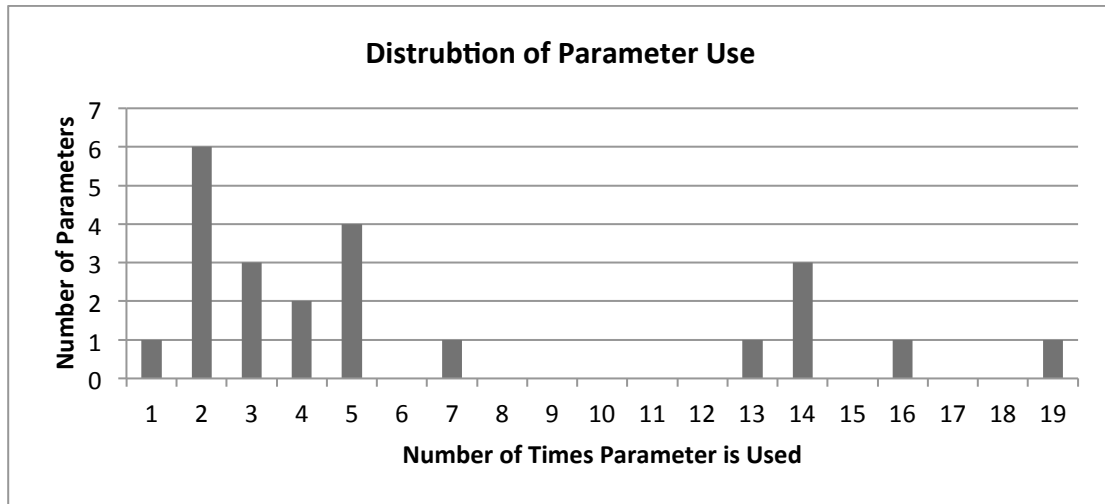


Figure 3.2 Distribution of Parameter Use from 22 Reviewed CVIs. (outlined in Table 1.2).

Parameters from Table 3.2 – C4, were then either included or excluded for use in the CVI matrix used in this research based on their alignment with the purpose of this assessment (Table 3.2 – C5). In addition to these narrowed down parameters, three more parameters were added in order to assess the physical resilience component of vulnerability, which to date has

been incorporated in very few CVIs. These additional resilience parameters include: morphological resilience, accommodation space, and sediment supply (Table 3.2 – C5). The final 11 chosen parameters, from Table 3.2 – C5, were further divided into the CCCs of assailing, resistance, and resilience (Table 3.2 – C6) and form the basis of the CVI matrix for this research.

Table 3.2 Parameter Selection Process.

Source (C1)	Description (C2)	Parameters Used (C3)	Condensed Parameter List (C4)	Final Parameters to be used in CVI (C5)	CCC's	Final Parameters sorted into Coastal Characteristic Classes (C6)
Table 1.2	Chose top parameters based on natural break in data	Landform Morphology Erosion/Accretion RSLR Wave Height Tide Range Coastal Slope	Landform Morphology Erosion/Accretion RSLR Wave Height Tidal Range Coastal Slope Population Dune Height/Presence Shoreline Exposure Presence of Rivers Elevation Soil Permeability Vegetation Artificial Protection Beach Width Offshore Slope % Rocky Outcrop	Wave Energy FS Geomorphology FS Slope FS Width BS Elevation BS Slope BS Vegetation CPS (Coastal Protection Structure) + Morphological Resilience Accommodation Space Sediment Supply	Assailing	Wave Energy
Hedge & Reju, 2007	Assessing coastal vulnerability to erosion	Landform Morphology Erosion/Accretion Coastal Slope Population				Resistance
Sousa et al., 2012	Assessing coastal vulnerability to erosion for beaches	Landform Morphology Erosion/Accretion Dune Height/Presence Shoreline Exposure Presence of Rivers Elevation Soil Permeability Vegetation Artificial Protection			Resistance	
Ozyurt, 2007	Assessing coastal vulnerability to SLR with a specific section on erosion	Rate of SLR Significant Wave Height Tidal Range Sediment budget Landform Morphology Coastal Slope				Resistance
Palmer et al., 2011	Assessing coastal vulnerability to erosion and extreme weather events	Dune Height/Presence Beach Width Vegetation Offshore Slope % of Rocky Outcrop			Resistance	
Shaw et al., 1998	Assessing the degree to which SLR would cause coastal geomorphic change	Relief Rock Type Landform Sea-Level Change Shoreline Displacement Tidal Range Wave Height				

3.2.3 Data Collection

Once the selected parameters were identified for use in the CVI, data were collected for each. Data for some parameters were derived from on-the-ground detailed coastal mapping, which included shoreline characterization, observed vegetation type and state, as well as sediment supply in the backshore. Data were also derived from information collected about Coastal Protection Structures (CPSs) and erosion/flooding sites. Other parameter data were derived from GIS modeling and analysis using available GIS datasets. Table 3.3 shows the parameter data sources.

Table 3.3 Data Sources for CVI Matrix Parameters. (SCD = Shoreline Characterization Database as developed by Pietersma-Perrott & van Proosdij, 2012, F=Additional data collected in the field that was incorporated into the SCD in this research, and GIS = GIS Analysis).

CCC	Parameter	Source
Assailing	Wave Energy	GIS
Resistance	Foreshore Geomorphology	SCD
	Foreshore Slope	SCD
	Foreshore Width	GIS
	Backshore Elevation	GIS
	Backshore Slope	SCD
	Backshore Vegetation	F
	CPS State, Material, & Type	F
Resilience	Morphological Resilience	SCD
	Accommodation Space	GIS
	Sediment Supply	F

3.2.3.1 Detailed Coastal Mapping

The creation of a detailed spatial database highlighting shoreline characteristics and features was the first step in assessing local coastal vulnerability. On-the-ground observations and data collection in the field increased assessment accuracy and allowed for data to be incorporated that may not have been attainable from small-scale spatial imagery, such as aerial

photography or satellite imagery. Detailed shoreline data were collected during the period of June 14th – July 1st, 2013 in Lockeport, Nova Scotia using a robust field computer, the YUMA Trimble, outfitted with ArcGIS 9.3 and a Global Positioning System (GPS) with an accuracy of $\pm 2-5$ m (Pietersma-Perrott & van Proosdij, 2012). Using dynamic segmentation, in which multiple sets of attributes can be assigned to any portion of a linear feature (Environmental Systems Research Institute, 2009), shoreline characterization data for three shorelines (BS, FS, and NS) were collected and input into a spatial geodatabase. The coastline used for characterization was based on the 1:10 000 coastline shapefile from the Nova Scotia Coastal Series (NSCS). However, after the field season, the BS line, which was used for coastal vulnerability assessment, was manipulated, using aerial photography and coastal knowledge gained in the field, so that it depicted the BS more accurately than the NSCS coastline shapefile. Additional BS data (including vegetation state and sediment supply) were also included with each linear BS segment and data associated with coastal protection structures, along with observations of flooding and erosion events were entered as point features.

The incorporation of this information into a geodatabase allowed for easy querying and data analyses. As well, the collection of detailed data from in-the-field observations allowed for a more detailed assessment of coastal vulnerability. Ultimately this resulted in a more accurate identification of at risk areas in Lockeport. The basic steps for detailed coastal mapping were:

1. Walked the shoreline of the study area and observed coastal form and features.
2. For each stretch of coast, noted vegetation state and sediment supply of backshore segments and characterized the backshore, foreshore, and nearshore lines in the ArcGIS geodatabase using decision tree charts (Appendix A).

3. Noted coastal protection structures and locations of observed flooding and erosion events and input into ArcGIS geodatabase as point features.
4. For each line and point feature, took a georeferenced photograph that linked it to the individual feature in the final geodatabase.

Shoreline Characterization

Shoreline characterization is the classification of natural coastal features along a stretch of coastline. Despite the previous application of coastal classification techniques in Canada (e.g., CIS [Sherin, 2000] and CanCoast [Smith et al., 2013]), to date, no approach provides the same level of detailed information as the technique developed by Pietersma-Perrot & van Proosdij (2012), which incorporates on-the-ground characterization for multiple shorelines. Since its development in 2012, this characterization approach has been adapted and successfully applied in Prince Edward Island and tropical locations, including Jamaica, Tobago, Grenada, Mauritius, and Seychelles. For this research, this method has been adapted for mesotidal shorelines characteristic of the South Shore of Nova Scotia. Pietersma-Perrot & van Proosdij (2012), characterized five shorelines: backshore, upper foreshore, middle foreshore, lower foreshore, and nearshore. However, taking into account the much smaller tidal range of this study area compared to the Bay of Fundy, for which the shoreline characterization tool was developed, only three shorezones were chosen for characterization: backshore, foreshore and nearshore (as defined previously in Section 1.2.1).

While the above BS, FS, and NS definitions, used in this research, apply to shore zones, for simplicity, the data collected for coastal characterization were entered as linear features,

such that one line represents the characteristics of the entire zone. For this research, the point within a zone for which characterization data were collected is represented by the landward boundary of each zone (Figure 3.3).

The characterization of the shoreline is facilitated by decision tree flow charts, with a specific chart representing each shorezone (Appendix A) to account for varying forms and features associated with varying parts of the coast. It captures information such as landform type, material, height, slope, vegetation type and density. Characterization data were stored within the attribute table of each linear segment and a photograph was linked to each segment for reference. Within this characterization method, shorelines were segmented into characterization units based on natural changes in form type and/or feature attributes; for this study there were 190 backshore segments, 105 foreshore segments, and 27 nearshore segments. The creation of shoreline segments based on natural changes in coastal forms, as opposed to pre-determined equal interval segments is important, as an over-generalized coastal characterization can lead to misleading results when used in a vulnerability assessment. In summary, the more detailed the characterization, the more accurate the data and the more realistic the vulnerability assessment results. The level of detail with this shoreline characterization method is limited only by the accuracy of the GPS receiver which is $\pm 2-5$ m; thus, any natural changes in form type or attribute that are less than 2-5 m in length were not accurately captured.

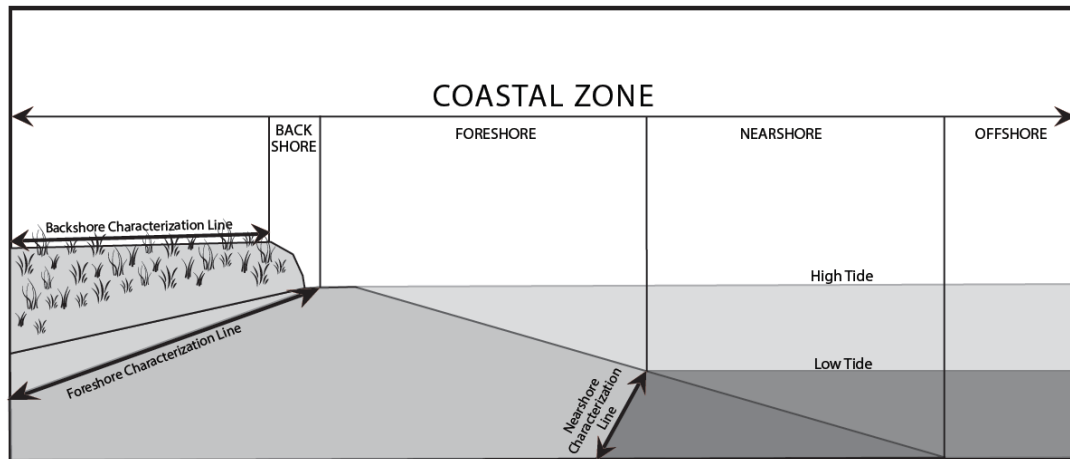


Figure 3.3 Coastal Zone Boundaries and Nearshore, Foreshore, and Backshore Characterization Lines. (Adapted from: Davidson-Arnott, 2010).

Sediment Supply & Vegetation State

In addition to the shoreline characterization data for the backshore, data on sediment supply and vegetation state were also collected and attributed to the linear coastal segments. Sediment supply refers to the availability of sediment within a system and was measured using a checklist of geoindicators developed by Bush et al. (1999) to determine the state of shoreline change along a stretch of coast (Table 3.4). Although the state of shoreline change does not directly measure the availability of sediment, it can be used as a proxy to indicate sediment supply; a shoreline in a state of accretion is an indication of a high availability of sediment and a shoreline in a state of severe erosion is an indication of a low availability of sediment.

Table 3.4 Checklist of Geindicator Observations Used to Characterize Sediment Supply State.

(Recreated from: Bush et al., 1999).

Severe Erosion	Erosion	Accretion/Stable
<p>Dunes absent with overwash common</p> <p>Active wave scarping of bluffs or dune remnants</p> <p>Tidal channels exposed in surf zone</p> <p>Vegetation absent</p> <p>Man-made shoreline structures now on beach or offshore</p> <p>Beach scraping (piled sand) evident</p>	<p>Dunes scarped or breached</p> <p>Bluffs steep with no talus ramp</p> <p>Peat, mud, or tree stumps exposed on beach</p> <p>Beach narrow or no high-tide beach (no dry beach)</p> <p>Overwash passes or fans; artificial gaps (i.e., road cuts)</p> <p>Vegetation ephemeral or topples along scarp line</p>	<p>Dunes and beach ridges robust, unbreached, vegetated</p> <p>Bluffs vegetated with stable (vegetated) ramp at toes</p> <p>Beach wide with well-developed berm</p> <p>Overwash absent</p> <p>Vegetation well-developed from interior maritime forest, to dune shrubs, and pioneer beach grass</p>

Vegetation state refers to the density and type of vegetation present in the backshore segment and was classified using Table 3.5.

Table 3.5 Attributes Used to Characterize Vegetation State.

Density	+	Type
Dense		Tree
Sparse		Shrub
		Grass
Unvegetated		Unvegetated

Observed Erosion

To aid in the validation process of the vulnerability assessment, erosion point features were added to the geodatabase. Collected data included year of event, if known, and a photograph for reference and were collected using personal observations of severe erosion during the field season.


Coastal Protection Structures

In this research context, CPSs refer to any man-made structures designed to protect the shoreline from the negative effects of flooding and/or erosion. Each protection structure, despite condition or size, was input as a point feature and assigned attribute information on structure type, height and width, slope, condition, material, year, purpose, average rock size, angle to shore (Table 3.6), along with a photo for reference. CPS data points were input into the database at the mid-point of the structure.

Height measurements were taken from the base of the protection structure to the highest peak and, width measurements were taken from the farthest seaward extent of the structure to the farthest landward extent. These measurements were obtained using a stadia rod and string, where the stadia rod was placed at the seaward base of the structure and the string placed at its highest landward peak, and measured with a measuring tape (Figure 3.4). A string level was used to ensure accuracy.

For each coastal protection structure three rocks, selected at random, were measured along the longest axis, intermediate axis and shortest axis (Figure 3.5). The average axis size was calculated for each rock and the resulting measurements were then averaged, yielding one final measurement, representing the average rock size of the CPS (Equation 3.1).

Table 3.6 Attributes Used to Characterize Coastal Protection Structure Point Features.

Field	Attribute Explanation
<p>Type</p> <p>(van Proosdij & Page, 2012; CCRM, 2013)</p>	<p>Breakwater – structure attached to land that reduces the amount of wave energy reaching the shoreline</p> <p>Offshore Breakwater – structure detached from land that reduces the amount of wave energy reaching the shoreline</p> <p>Revetment – sloped, on shore structure that protects land from erosion</p> <p>Bulkhead – vertical structure that acts as a retaining wall</p> <p>Dyke – earthen structure that prevents flooding of the land it protects</p> <p>Seawall – vertical onshore structure that breaks wave energy</p> <p>Groyne – structure perpendicular or on a slight angle to the shoreline which help strap sediment</p> <p>Vegetation (Planting) – the use of natural materials to help prevent erosion (e.g., planting trees)</p> <p>Other – any structure that uses unconventional materials (e.g., lobster traps, broken concrete, debris etc.)</p>
<p>Height & Width</p>	<p>Measured in cm</p>
<p>Slope</p>	<p>Calculated from height and width measurements and presented in degrees</p>
<p>Condition</p>	<p>Intact – perfect condition</p> <p>Damaged – performing function, but looks like it could use some repair</p> <p>Failing – needs to be replaced but, if repaired, could perform function</p> <p>Remnant – abandoned, not performing function</p>
<p>Material</p>	<p>Concrete, Earth, Masonry, Metal, Wood, Riprap – an assortment of rock and/or rubble</p> <p>Other – any other material not previously mentioned (e.g., tires, lobster traps, gabion baskets etc.)</p> <p><i>*when two or more materials are present in the same structure, choose dominant material</i></p>
<p>Year</p>	<p>If available, the year the structure was built</p>
<p>Purpose</p>	<p>Armouring – structure constructed to prevent erosion of uplands and mitigate coastal flood effects, resisting waves, scour, and/or overtopping (e.g., seawall, bulkhead, dyke, revetment)</p> <p>Soil Stabilization – structure intended to stabilize or reduce shoreline erosion, which, by doing so, affords some protection to upland areas; holds upland sediment, retards longshore sediment transport (e.g., groyne, offshore breakwater, beach nourishment, planting)</p> <p>Navigation – structure used for navigation which resists waves, current, and/or sedimentation (e.g., offshore breakwater, attached breakwater)</p>
<p>Average Rock Size</p>	<p>Average axes measurements of three rocks, selected at random from structure (Equation 3.1)</p>
<p>Angle To Shore</p>	<p style="text-align: center;"> <i>Perpendicular</i> <i>Parallel</i> <i>Angled</i> <i>Mixed</i> </p>  <p style="text-align: center;">SHORELINE</p>

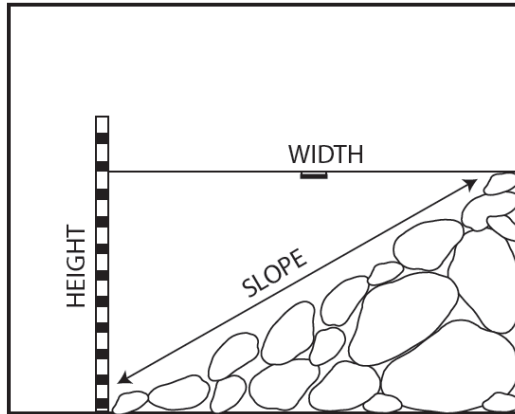


Figure 3.4 Method Used to Measure Slope of Coastal Protection Structures.

Equation 3.1

$$\text{Average Rock Size} = (((A_1 + B_1 + C_1)/3) + ((A_2 + B_2 + C_2)/3) + ((A_3 + B_3 + C_3)/3))/3$$

Where: A= Longest Axis 1=Rock 1
 B= Intermediate Axis 2=Rock 2
 C= Shortest Axis 3=Rock 3

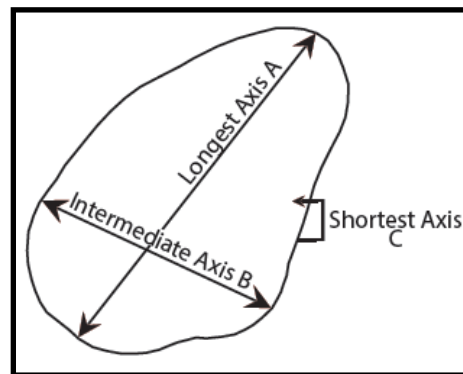


Figure 3.5 Axes Used to Measure Average Rock Size of Coastal Protection Structures.

3.2.3.2 GIS Modeling & Analysis

Along with a spatial geodatabase of shoreline characterization data and other data collected in the field, GIS modeling and analysis were used to derive data for the following parameters: Wave Energy, Foreshore Width, Accommodation Space, and Backshore Elevation

(Table 3.3). The spatial datasets used in these analyses were retrieved from a combination of publicly available online sources (Nova Scotia Coastal Series [NSCS] and NOAA National Buoy Data Center [NDBC]) and, with generous contribution, from the Municipality of the District of Shelburne in the form of recently flown LiDAR data. LiDAR is a method of remote sensing which uses pulsing beams of light to measure the distance to Earth and results in high-resolution digital elevation models (DEMs). Modeling and analyses were conducted using the WEMo (Wave Exposure Model) developed by NOAA and ArcGIS 10.1 developed by ESRI.

Wave Energy

Wave Energy was calculated by Matt Christian of MP_SpARC (Maritime Provinces Spatial Analysis Research Centre) at Saint Mary's University, using the WEMo developed by NOAA, a simple 1D hydrodynamic model designed to predict the effect of coastline exposure to wind-generated waves (Fonseca & Malhotra, 2006). WEMo calculates the average rate at which energy is transmitted in the direction of wave propagation, which in this model is based on shoaling, wave breaking, and bottom friction over fetch. The final calculated values are denoted as representative wave energy (RWE) in J/m and represent "the total wave energy in one wave length per unit wave crest width" (Malhotra & Fonseca, 2007), which is calculated for each point in a pre-defined point grid. WEMo operates under linear (Airy) wave theory and a ray tracing technique in which calculations are carried out as waves propagate along fetch rays. To compute the final RWE values (for each point in the point grid), WEMo determines the effective fetch rays and then calculates the wind frequency and wave height along each fetch ray (Malhotra & Fonseca, 2007).

Fetch is considered as the unimpeded distance from site to land along a compass heading, and the number of fetch rays used in WEMo, which can range from 16-56, depends on the complexity of the shoreline, with non-complex shorelines requiring fewer rays and those with highly irregular coastlines requiring the most. Fetch rays extend from each calculation point in equal intervals, which for 56 rays is every 6.43°, and end when they reach the shoreline or a set distance; whichever comes first (Malhotra & Fonseca, 2007). The input values used in this research are displayed in Table 3.7. In order to account for shoreline irregularities, the fetch is modified by “taking the cosine weighted average of all rays within a sector on either side of a fetch ray, defined by angle φ ” and is called the effective fetch (See [Malhotra & Fonseca, 2007] for specific equation).

Table 3.7 WEMo Fetch Inputs.

Fetch Inputs	Value
No. of calculation points used	5000
No. of fetch rays used	56
Fetch distance (m)	100 000
Distribution of fetch (m)	1000
Bathymetry interrogation distance (m)	100
Alpha Goda’s Formula (m)	0.17
Sensitivity eps.	1 in 1000
Beach slope for Goda’s formula (°)	1.909

Wind speed and frequency were computed for each effective fetch ray, where wind frequency for a particular direction is the “ratio of number of hours the wind blows from that direction and the total number of hours of wind data” (Malhotra & Fonseca, 2007) and therefore it is acceptable to use subsets of data that represent particularly intense wind periods for comparison with larger wind data sets. Wind data with a temporal resolution ranging from one minute to one hour can be used, however hourly wind data were used for this research.

In WEMo, wave height is calculated for each effective fetch ray and depends on wind speed (in the same direction) and water depth. Propagation of waves into shallow water, is carried out in WEMo by shoaling, wave breaking, and bottom friction and the wave height reaching the coast is determined by Equation 3.2 (Malhotra & Fonseca, 2007).

Equation 3.2

$$H = H_w - (H_{S+B+f})$$

Where: H_w = wave height generated by wind alone

H_{S+B+f} = the rest of external physical phenomena contributing to the wave height, which are each computed separately

Where: S = shoaling

B = wave breaking

F = bottom friction

The equation used to calculate shoaling is based on Dean & Dalrymple, 1991, the equation used to calculate wave breaking is based on Goda, 1985 and Wood et al., 2001, and the equation used to calculate bottom friction is based on Putnam & Johnson, 1949 and Bretschneider & Reid, 1954 (Malhotra & Fonseca, 2007).

After computing wave height and wind speed over each of the fetch rays, the RWE value is calculated using Equation 3.3.

Equation 3.3

$$RWE = C \sum_{i=1}^n (H_i^2 T_i^2 \tanh(k_i d_i)) w_i$$

Where: C = constant

H_i = wave height in i^{th} effective fetch ray direction

T_i = wave period in i^{th} effective fetch ray direction

k_i = wave number

d_i = depth

w_i = wind frequency in the i^{th} effective fetch ray direction

To calculate these values, WEMo requires the input of bathymetry values, a shoreline polygon, wind data, and a point grid dictating the frequency at which RWE values are calculated

(Figure 3.6). WEMo calculates wave energy irrespective of datums and the output is a RWE point shapefile with RWE values associated with each point from the point grid (Fonseca & Malhotra, 2006).

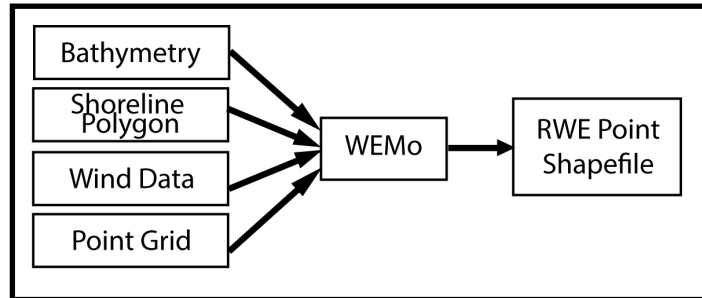


Figure 3.6 Required WEMo Inputs and Resulting Output. (Adapted from: Fonseca & Malhotra, 2006).

For this study, bathymetric data were obtained from the 1:10 000 NSCS water layer using map sheet 20P11 (Chart Datum). Using the “Topo to Raster” function in ArcGIS 10.1, bathymetry lines, soundings, and a coastline polygon, were used to create a hydrologically correct raster surface as its output. Shoreline data, in the form of a polyline, were obtained from the 1:10 000 NSCS land layer using map sheet 20P11 and, using the “Feature to Polygon” function in ArcGIS 10.1, were used to create a shoreline polygon extending the desired length of study area. Wind data were obtained from NOAA National Data Buoy Center (NDBC) from Buoy 44024 located in the northeast channel at 42.331N 65.907W. Finally, the point grid was derived using the “Feature to Raster” and “Raster to Point” features in ArcGIS 10.1 with a grid resolution of 5 m (i.e., 5 m distance between points). Data were input into WEMo and the resulting RWE were displayed as a point shapefile. The point shapefile was then interpolated using krigging (Table 3.8) as a way to effectively visualize the strength and reach of the RWE values. RWE values were extracted from the RWE interpolation to the midpoint of each backshore segment using the “Spatial Join” function in ArcGIS 10.1.

Table 3.8 Parameters Used in ArcGIS 10.1 Krigging Interpolation Method.

Krigging Parameters	
Krigging Method	Ordinary
Semivariogram Model	Spherical
Output Cell Size	5 m
Search Radius	Variable
Number of Points	12

Foreshore Width

For each backshore coastal segment, the width of the foreshore was measured, on imagery, perpendicularly from the mid-point of the seaward boundary of the backshore (e.g. base of foredune) to the shoreline at the time of aerial imagery acquisition (Figure 3.7) and therefore the water level at the time the imagery was taken is used as a surrogate for low tide, in the measurement of Foreshore Width. While the measurement was taken only from the mid point of each backshore segment (the middle of each backshore line) it was used to represent the foreshore width for the entire segment length. Therefore, it is important to note that, in some instances, the foreshore width measurement may be larger or smaller than the foreshore width average for that section. The midpoint of each backshore segment from which the measurements were taken was derived using the “Feature Vertices to Point” function in ArcGIS 10.1. The foreshore width measurements (displayed in meters) were derived manually using the “Ruler Tool” to allow for human interpretation of the orthoimagery. Individual segment interpretation and manual measurement was feasible in this study due to its small geographic size, however a larger study area would require the use of a more automated approach.

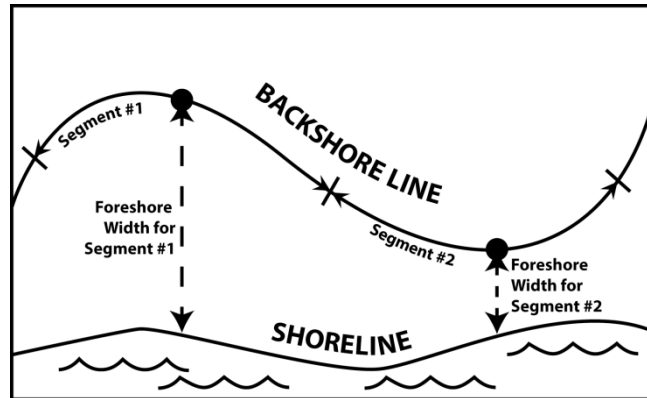


Figure 3.7 Backshore Segment Mid-points and Foreshore Width Measurement.

Accommodation Space

In this research, accommodation space refers to the distance from the backshore to the first immobile structure that could impede shoreline retreat (e.g., buildings, roads, CPSs, etc.). Assuming perpendicular retreat and non-relocation of structures, this distance was measured manually using the “Ruler Tool” for each backshore segment; from the backshore characterization line perpendicularly to the first hard structure before 50 m. Distances greater than 50 m were not measured, as the coastal zone definition in this study extends 50 m landward from the backshore line. It is important to note that the accommodation space measurement value is determined by the closest hard structure and may not extend for the entire backshore segment. Therefore, while shoreline retreat may be impeded in one section of the segment, it does not necessarily mean it would be impeded for the entire backshore segment. However, for this research, it was determined that in the assessment of vulnerability, it is more important to slightly over predict coastal vulnerability than under predict it.

Backshore Elevation

Elevation values for each backshore segment were extracted from a 1 m LiDAR-derived DEM (in CGVD28 – vertical precision not included in DEM metadata) to the midpoint of each backshore segment using the “Extract Multi-Values to Points” function in ArcGIS10.1. The backshore segment lines were aligned with the landward boundary of the backshore (i.e., top of the dune, slope, cliff etc.) (See Figure 3.3). Again, while the value assigned to the midpoint was determined by using the closest elevation unit, the value was used to represent the elevation for the entire backshore segment length.

3.2.4 Matrix Creation

In a CVI matrix, chosen parameters are ranked according to their contribution to the vulnerability of a particular event (which in this research is erosion). The majority of CVI matrices have five rank categories, with lower ranks an indication of low contribution to vulnerability and higher ranks an indication of high contribution to vulnerability. As there was no particular benefit to having four rank classes over five, this matrix continues with the majority and uses five rank classes (*very low, low, moderate, high, very high*). One of the most beneficial aspects of using a ranked approach is that it allows for both qualitative and quantitative parameters in different units to be combined (McLaughlin & Cooper, 2010). In this research, each quantitative parameter was divided into five rank classes using the appropriate data classification method (e.g., natural breaks, equal interval, quantile etc.), based on the distribution of data (Stern et al., 2011). Qualitative parameters were divided into five rank classes by listing all possible options for the target environment and sorting them based on their contribution to vulnerability. Those having the same level of contribution to vulnerability were

included in the same rank category and given an “OR” option. Maps of ranked values were created for each parameter to illustrate their overall contribution to vulnerability (Figures 4.5 – 4.8 and Appendix B).

The matrix for this research is designed to exemplify the relationship of coastal geomorphic vulnerability (Equation 1.2), where high assailing forces, present along the coast, increase vulnerability and high resistance and resilience characteristics, present along the coast, decrease vulnerability. Consequently, in an effort to account for these converse relationships in matrix development, coastal segments with low “actual, on-the-ground” resilience or resistance characteristics (i.e., existing physical characteristics) were given a *high* vulnerability rank, and coastal segments with low “actual, on-the-ground” assailing forces were given a *low* vulnerability rank. Therefore when discussing a coastal segment that has a *very high* resistance or resilience rank, it refers to a coastal segment with “actual, on-the-ground” low resistance or resilience respectively. While seemingly complex, this distinction is crucial to consider throughout this document. However, in an attempt to limit confusion, the terms *very low*, *low*, *moderate*, *high*, and *very high* will be italicized when corresponding to a rank, and will remain non-italicized when corresponding to “actual, on-the-ground” characteristics.

As the ranked classes incorporate ranges and possibilities found in the study area of this research, this matrix is only applicable to this study. However, it is important to note that using the same parameters, this matrix could be adapted for other areas of South Shore, Nova Scotia, or areas with a similar environment, by modifying the ranges and possibilities to suit that particular region. The following sections will discuss each parameter in detail including how it

influences vulnerability, its value range, data classification type, and its importance in assessing vulnerability.

3.2.4.1 Assailing Parameters

Assailing parameters are those that induce coastal change and, for this assessment, include the parameter Wave Energy. Recall that high assailing forces on a coast increase coastal vulnerability. Therefore, an assailing parameter with a *very high* rank (5) represents an actual coastal segment with very high assailing properties.

Wave Energy (a)

Wave Energy can be defined for this research as the total RWE in one wavelength per unit crest width (J/m) reaching the shoreline (Fonseca & Malhotra, 2006) and was derived for each backshore segment using the methodology outlined in Section 3.2.3.2. Other CVIs incorporate the degree of shoreline exposure (Abuodha & Woodroffe, 2010; Guannel et al., 2012; Szlafsztein & Sterr, 2007), which effectively quantifies the orientation of the shore relative to wave direction, with exposed shorelines being more susceptible to erosion than those that are sheltered. However, only one study measured the amount of Wave Energy reaching the coast (Tibbetts & van Proosdij, 2013). In this study, Wave Energy reaching the coast was measured using WEMo (Fonseca & Malhotra, 2006) and it is expected that higher wave energies have greater erosion potential and therefore contribute to a higher vulnerability ranking. The quantitative values of Wave Energy computed in this study ranged from 0-9904 J/m, with the uppermost value of the range associated with a water depth of 6.33 m and a maximum wave height of 0.78 m. The values were divided into five rank categories using quantiles (Stern et al., 2011) and resulted in the rank classes illustrated in Figure 3.8.

3.2.4.2 Resistance Parameters

Resistance parameters are those that resist coastal change and, for this assessment, include the parameters Foreshore Geomorphology, Foreshore Slope, Foreshore Width, Backshore Elevation, Backshore Slope, Backshore Vegetation, and Coastal Protection Structures. Recall that a resistant coast decreases coastal vulnerability. However, in this research, a coastal segment with low resistance characteristics is given a *very high* vulnerability ranking in its contribution to the final coastal vulnerability index. Therefore a resistance parameter with a *very high* rank (5) represents an coastal segment with very low resistance properties.

Foreshore Geomorphology (b)

The presence of certain combinations of foreshore forms create environments that are more or less susceptible to erosion. In this study, the Foreshore Geomorphology parameter combines form and material type to qualify vulnerability to erosion. Hard, immobile forms such as outcrop, platform, and/or anthropogenic structures are highly resistant and therefore receive a *very low* vulnerability rank, while those areas of the coast with no foreshore receive a *very high* vulnerability rank (Figure 3.9). The remaining categories were classified based on the knowledge that smaller particle sizes of non-cohesive sediments require less wave energy to be transported (Masselink et al., 2011). Therefore, clastic slopes and beaches were determined to qualify *low, moderate, or high* vulnerability areas depending on the grain size of material in the foreshore (i.e., boulder, cobble, sand, or gravel), with larger material size resulting in a less susceptible environment to erosion. Dunes and flats are most often composed of sand or gravel and consequently are placed in the *high* rank (4) category. Data on foreshore geomorphology were queried from the SCD using ArcGIS 10.1 and, using the “Field Calculator” function, were assigned corresponding vulnerability ranks.

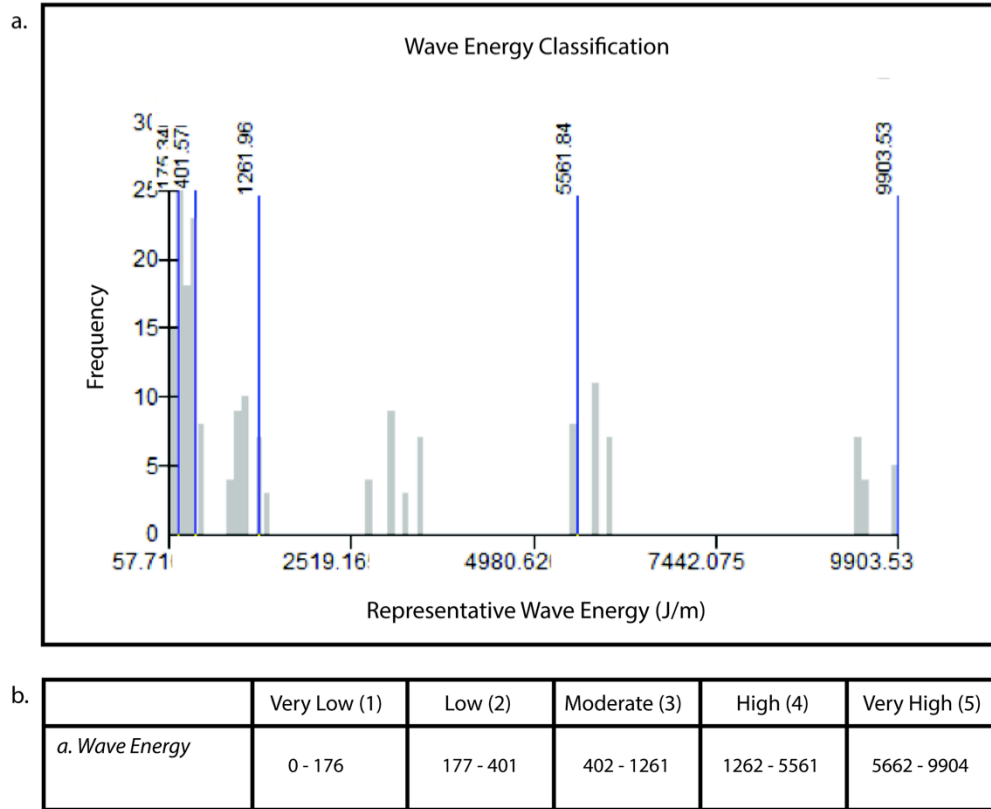


Figure 3.8 Classification and Ranking of Wave Energy. a) Histogram of Wave Energy classification using quantiles. b) CVI categories and associated ranks.

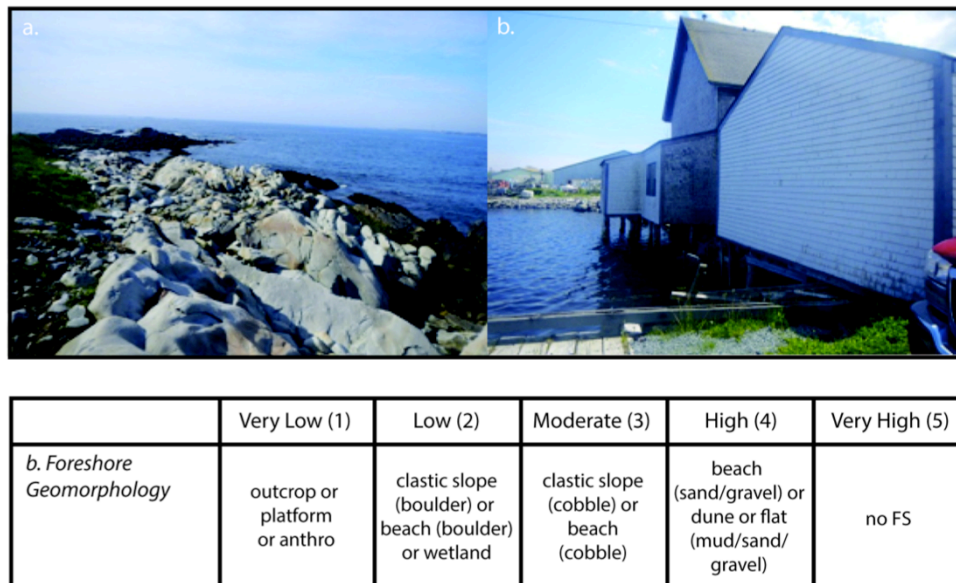
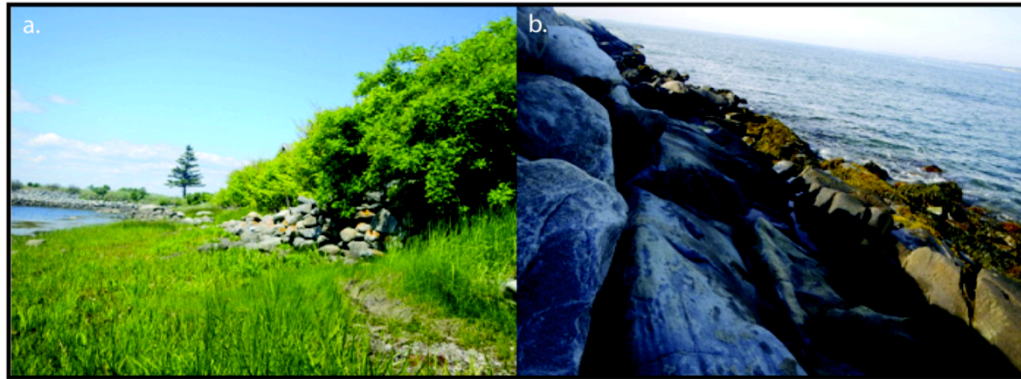


Figure 3.9 Ranking of Foreshore Geomorphology. a) Example of an outcrop in Lockeport (Photographer: Sam Page). b) Example of no FS in Lockeport (Photographer: Sam Page). c) CVI categories and associated ranks.

Foreshore Slope (c) & Backshore Slope (f)

Foreshore and Backshore Slope refer to the gradient of the coastal profile from the seaward to landward limit of the foreshore zone and the seaward to landward limit of the backshore zone respectively. While the parameter coastal slope has been included in many vulnerability matrices as a single parameter (Table 1.2), it was divided into two parameters in this study under the premise that foreshores and backshores do not have the same slope and contribute differently to vulnerability. Whether foreshore or backshore, a steeper slope increases the potential for wave energy to cause erosion, while a gentle slope allows for wave energy to dissipate. Slope rank categories ranged from ramped to high slope corresponding to *very low* and *very high* vulnerability ranks respectively (Figure 3.10). The term ramped refers specifically to wetland environments with sloping morphology, which has a greater potential to decrease vulnerability than a low slope of a dune, beach, platform, outcrop, or organogenic slope. The term cliffed also refers specifically to wetland environments, but with an abrupt cliffed morphology as opposed to a sloping one. Cliffed morphology has a greater potential to contribute to vulnerability than a medium slope of a dune, beach, platform, outcrop, or organogenic slope, but less potential than a high slope. Data on Backshore and Foreshore Slope were queried from the SCD using ArcGIS 10.1 and, using the “Field Calculator” function, were assigned corresponding vulnerability ranks.



c.

	Very Low (1)	Low (2)	Moderate (3)	High (4)	Very High (5)
<i>c. Foreshore Slope</i> <i>f. Backshore Slope</i>	ramped	low slope	medium slope	cliffed	high slope

Figure 3.10 Ranking of Foreshore Geomorphology. a) Example of a ramped slope (Photographer: Sam Page). b) Example of a high slope (Photographer: Sam Page). c) CVI categories and associated ranks.

Foreshore Width (d)

Foreshore Width can be defined in this research as the perpendicular distance from the seaward boundary of the backshore to the shoreline and was measured from each backshore segment using the methodology outlined in Section 3.2.3.2. The foreshore width is of particular importance due to its ability to dissipate waves; a wider foreshore is more likely to decrease wave energy reaching the coast. Consequently, the vulnerability of a coast to erosion is considered lowest along coasts with wide foreshores (often associated with beach environments) and highest along coasts with a small foreshore width. This parameter has been used in the CVI applied by Tibbetts & van Proosdij (2013), when measuring foreshore width of macrotidal environments, and by Palmer et al. (2011), when measuring beach width. The quantitative values of Foreshore Width measured in this study ranged from 0-82 m. The values

were divided into five rank categories using quantiles (Stern et al., 2011) and resulted in the rank classes illustrated in Figure 3.11.

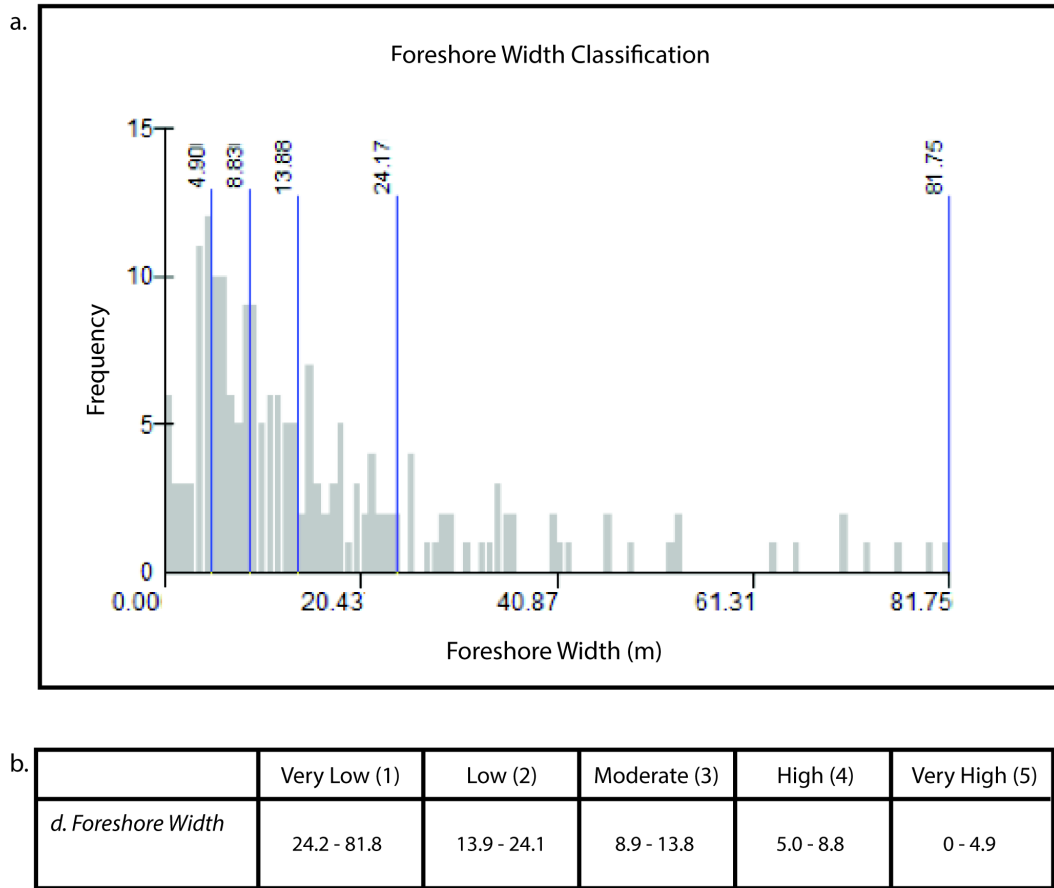


Figure 3.11 Classification and Ranking of Foreshore Width. a) Histogram of Foreshore Width classification using quantiles. b) CVI categories and associated ranks.

Backshore Elevation (e)

The Backshore Elevation parameter is usually incorporated into SLR and flooding vulnerability matrices (Gornitz et al., 1991; Hughes & Brundrit, 1992), as a higher elevation decreases the likelihood of flooding from storm surge and of permanent inundation. However, Sousa et al. (2012) used elevation as a parameter in their vulnerability index to erosion on the premise that permanent inundation from SLR or overwash during storms increases erosion.

Consequently a high elevation in the backshore reduces erosion potential. It is under this premise that Backshore Elevation will be used in this study. Backshore Elevation measurements were taken for each backshore segment using the methodology outlined in Section 3.2.3.2. The quantitative values of Backshore Elevation measured in this study ranged from 0-6.1 m. These values were divided into five rank categories using natural breaks (Stern et al., 2011) and resulted in the rank classes illustrated in Figure 3.12.

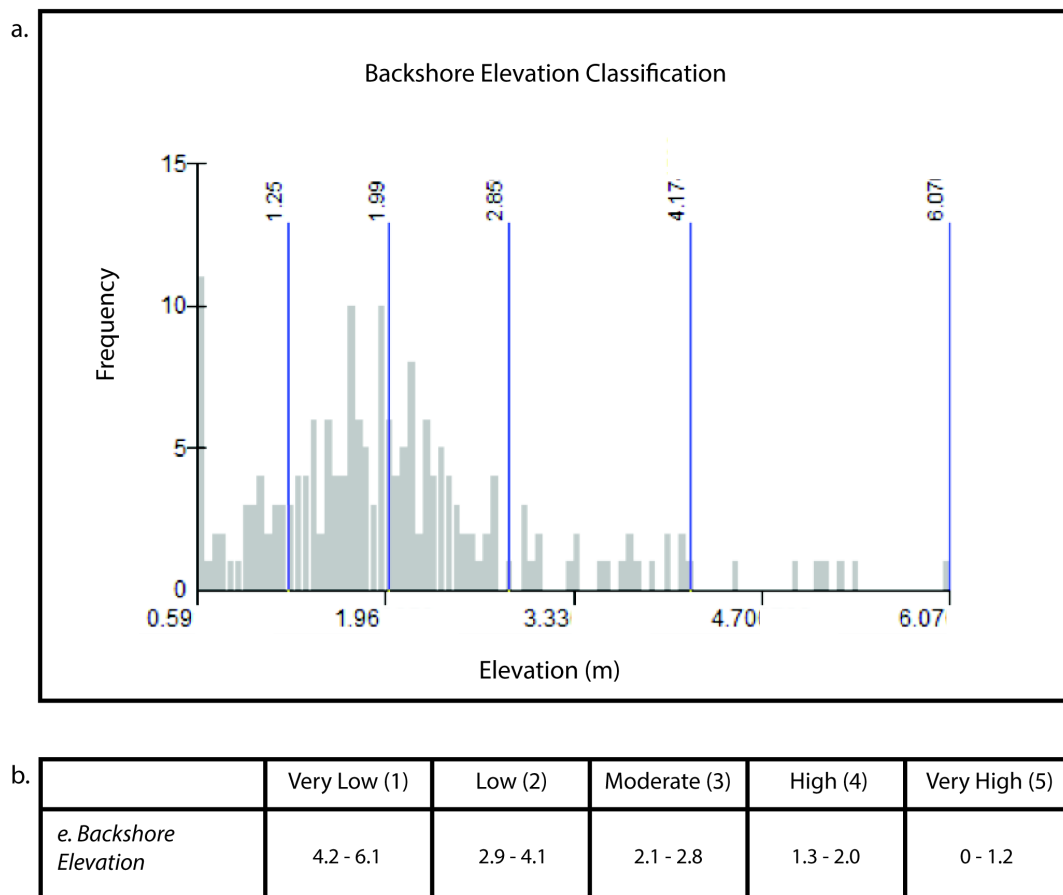
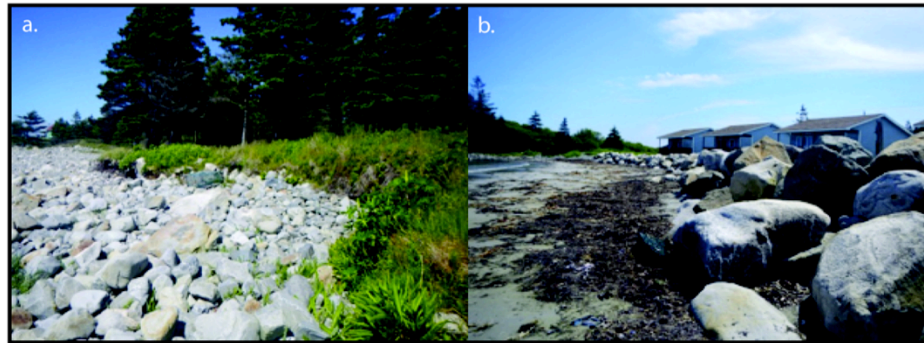


Figure 3.12 Classification and Ranking of Backshore Elevation. a) Histogram of Backshore Elevation classification using natural breaks. b) CVI categories and associated ranks.

Backshore Vegetation (g)

Density and presence of vegetation along the backshore determines the stability of the backshore feature, which in turn influences the likelihood of erosion. While some CVIs use vegetation type to classify vegetation (Torresan et al., 2012; Sousa et al, 2012) and others use distance of vegetation in the backshore (Palmer et al., 2011), this matrix classifies Backshore Vegetation and its contribution to vulnerability based on type and density; ranging from dense tree to unvegetated (Figure 3.13). Although the extent of a root system varies with plant species, it can be generally expected that larger vegetative species have larger root systems and therefore a greater ability to stabilize land. In addition to its well know role as a soil stabilizer, vegetation also has the ability to dissipate wave energy, thus decreasing erosion potential (Möller, 2006). Data on Backshore Vegetation were queried from the backshore attribute table using ArcGIS 10.1 and, using the “Field Calculator” function, were assigned corresponding vulnerability ranks.



c.

	Very Low (1)	Low (2)	Moderate (3)	High (4)	Very High (5)
<i>g. Backshore Vegetation</i>	dense tree	sparse tree or dense shrub	sparse shrub or dense grass	sparse grass	unvegetated

Figure 3.13 Ranking of Backshore Vegetation. a) Example of dense tree backshore in Lockeport (Photographer: Sam Page). b) Example of unvegetated backshore in Lockeport (Photographer: Sam Page). c) CVI categories and associated ranks.

Coastal Protection Structures (h)

Coastal Protection Structures (CPSs) refer to any man-made structures designed to protect the shoreline from the negative effects of flooding and/or erosion and can vary considerably in form and effectiveness. In some CVIs coastal protection structures are ranked under the premise that their presence represents areas of instability and therefore contribute to a *very high* vulnerability ranking (Sousa et al., 2012). On the other hand, some CVIs rank structures under the premise that their presence indicates a state of protection and therefore contributes to a *very low* vulnerability ranking (Torresan et al., 2012; Tibbetts & van Proosdij, 2013; Szlafsztein & Sterr, 2007). The latter viewpoint is adopted in this study. Coastal Protection Structures can vary considerably in form, material type, use, material size, and effectiveness, to name a few, and ranking CPSs is not as simple as noting their presence or absence. This research therefore takes, not only the state of functioning into consideration when ranking a structure's contribution to vulnerability, but also the type and size of material. Within the matrix, the logic is as follows: structures that are intact are less likely to contribute to erosion than an area with a remnant structure, or no structure at all (Figure 3.14), as intact structures are able to perform the function for which they were built. With regards to the type and material, it is recognized that any CPS constructed from riprap is more robust than a solid concrete structure, as riprap is able to absorb wave energy better than solid concrete (Douglass et al., 2011). However, smaller riprap requires less wave energy to initiate material transport than larger riprap and, consequently, CPSs made of small riprap should have a higher vulnerability rank than those made of large riprap (Mangor, 2004). In the vulnerability ranking for this study, all CPS types (e.g., revetments, seawalls, groynes, and breakwaters) are treated equally and to obtain the final ranked score for the CPS parameter, the CPS state(a) and material

type(b) ranks were averaged. Data on CPSs were queried from the backshore attribute table using ArcGIS 10.1 and, using the “Field Calculator” function, were assigned corresponding vulnerability ranks.



e.

	Very Low (1)	Low (2)	Moderate (3)	High (4)	Very High (5)
<i>h. Coastal Protection Structure (CPS)</i>	intact	damaged	failing	remnant	none
<i>*avg score (state + type & material rank)/2</i>	cps large rip rap (75-147)	cps medium rip rap (34-74)	cps small rip rap (0-33)	cps concrete	no cps

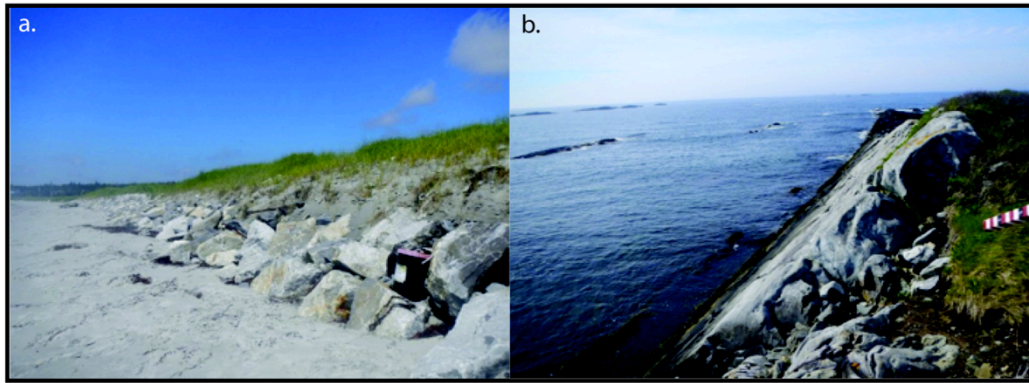
Figure 3.14 Ranking of CPSs. a) Example of an intact CPS in Lockeport (Photographer: Sam Page). b) Example of a remnant CPS in Lockeport (Photographer: Sam Page). c) Example of large riprap CPS in Lockeport (Photographer: Sam Page). d) Example of concrete CPS in Lockeport (Photographer: Sam Page). e) CVI categories and associated ranks.

3.2.4.3 Resilience Parameters

Resilience parameters are those that allow a system to recover from change and, for this assessment, include the parameters Morphological Resilience, Accommodation Space, and Sediment Supply. Recall that resilience decreases coastal vulnerability. However, in this research a coastal segment with low resilience characteristics is given a *very high* ranking in its contribution to the final coastal vulnerability index. Therefore a resilience parameter with a *very high* rank (5) represents a coastal segment with very low resilience properties.

Morphological Resilience (i)

Morphological Resilience refers to the ability of a landform to return to a state of dynamic equilibrium following a disturbance event (Tibbetts & van Proosdij, 2013). Beach systems have a high Morphological Resilience (and therefore a *very low* vulnerability rank) due to their short recovery time and cliffs have a low Morphological Resilience (and therefore a *very high* vulnerability rank) due to their longer recovery time (Penthick & Crooks, 2000). Therefore, it has been assumed that all backshore landforms are more resilient if fronted with a beach. In the vulnerability matrix ranking for this parameter (Figure 3.15), foreshore and backshore forms operate together to influence Morphological Resilience. Backshores consisting of dunes are considered more resilient than a backshore consisting of an outcrop, cliff, or anthropogenic structure. As each backshore is considered to be more resilient when fronted by a beach, a backshore without a beach is ranked one category higher than the same backshore with a beach (e.g., dune + beach = *very low* vulnerability [Rank 1] and dune + no beach = *low* vulnerability [Rank 2]). Data on Morphological Resilience were queried from the shoreline characterization database using ArcGIS 10.1 and, using the “Field Calculator” function, were assigned their corresponding vulnerability rank.



c.

	Very Low (1)	Low (2)	Moderate (3)	High (4)	Very High (5)
<i>i. Morphological Resilience</i>	dune + beach	low slope + beach or dune + no beach	high-med slope + beach or low slope + no beach or wetland	bluff + beach or high-med slope + no beach	outcrop or cliff or anthro with or without beach or bluff + no beach

Figure 3.15 Ranking of Morphological Resilience. a) Example of a dune + beach in Lockeport (Photographer: Sam Page). b) Example of outcrop + no beach in Lockeport (Photographer: Sam Page). c) CVI categories and associated ranks.

Accommodation Space (j)

For the purposes of the CVI, Accommodation Space refers to the distance from the backshore to the first immobile structure that could impede shoreline retreat and was determined using the methodology outlined in section 3.2.3.2. During extreme events, wave energy has the ability to exert its force farther inland, potentially increasing erosion in that particular area and moving the system away from its state of dynamic equilibrium. Naturally, coastal systems, with no immobile structures impeding shoreline retreat, have a greater ability to “absorb” coastal climate change-related impacts, resulting in a greater ability to recover and thus, a higher natural resilience. It is important to note that recovery refers to the return to a dynamic state of equilibrium which could be in a similar position to the original form, but could

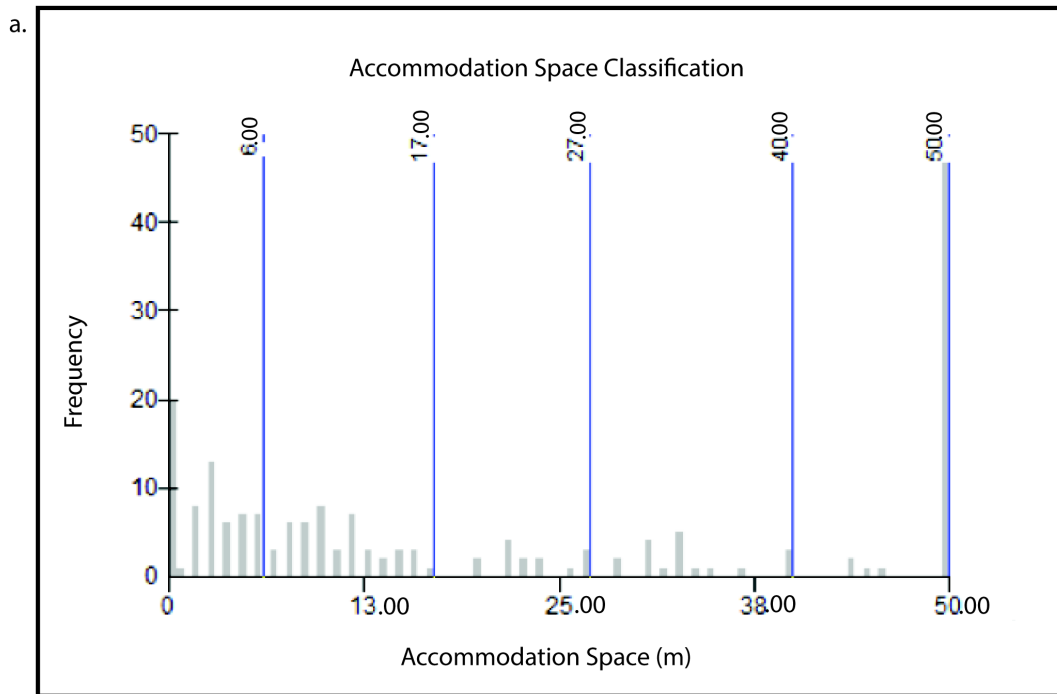
also be translated upward and landward; resulting in the establishment of a new equilibrium state farther inland.

However, a coast with no immobile structures impeding shoreline retreat has a greater ability to recover from extreme events. Consequently, a shoreline with a large Accommodation Space is highly resilient (and therefore has a *very low* vulnerability rank) and a shoreline with a small Accommodation Space is not very resilient (and therefore has a *very high* vulnerability rank). The quantitative values of Accommodation Space measured in this study ranged from 0-50 m. These values were divided into five rank categories using natural breaks (Stern et al., 2011) and resulted in the rank classes illustrated in Figure 3.16.

Sediment Supply (k)

When exposed to an erosion event, a coastline with a sediment source nearby (e.g., dunes or sedimentary cliffs) has a greater likelihood of recovering from the event than a coastline without access to a sediment source. The availability of sediment within a system can be surmised by determining the erosion/accretion state of the shoreline, such that coastlines that are accreting are likely being fed by a nearby sediment source and, conversely, for eroding shorelines. Although there are computationally intensive methods of determining the erosion/accretion state of a coastline, such as the Digital Shoreline Analysis System (DSAS) (Thieler et al., 2009), this study uses a rapid assessment checklist developed by Bush et al. (1999) (Section 3.2.3.1), which allows for qualitative determination of shoreline state. In this matrix, a stable shoreline represents a coast with a high availability of sediment and subsequently a high resilience (and therefore a *very low* vulnerability rank). Conversely, a severely eroding shoreline represents a coast with a lack of sediment availability and subsequently a very low resilience (and therefore a *very high* vulnerability rank) (Figure 3.17).

Data on Sediment Supply were queried from the backshore attribute table using ArcGIS 10.1 and, using the “Field Calculator” function, were assigned corresponding vulnerability ranks.



d.

	Very Low (1)	Low (2)	Moderate (3)	High (4)	Very High (5)
<i>j. Accommodation Space</i>	41 - 50	28 - 40	18 - 27	7 - 17	0 - 6

Figure 3.16 Classification and Ranking of Accommodation Space. a) Histogram of Accommodation Space classification using natural breaks. b) Example of 0 m from backshore to building in Lockeport (Photographer: Sam Page). c) Example of 0 m from backshore to CPS in Lockeport (Photographer: Sam Page). d) CVI categories and associated ranks.

	Very Low (1)	Low (2)	Moderate (3)	High (4)	Very High (5)
<i>k. Sediment Supply</i>	stable		erosion		severe erosion

Figure 3.17 Ranking of Sediment Supply. CVI categories and associated ranks.

3.2.5 CVI Calculation

The two factors that influence the calculation of a CVI are parameter weighting and the formula used. As outlined in detail in 1.5.2, CVI_5 (the square root of the product mean) is the most commonly used equation in CVI calculation. The equation is relatively insensitive to variations in one parameter, while displaying changes when differences occur within more than one, and consequently has been chosen for this research. Despite its less than common use, weighting has also been incorporated on the CCC level as opposed to the individual parameter level. It has been assumed that each CCC contributes to vulnerability equally and, consequently, each class received an equal weight whether it contained one, three, or seven contributing parameters. The uneven number of parameters in each class could easily lead to results that favored the resistance CCC, containing the most assessed parameters, while not giving enough importance to the assailing CCC, containing only one parameter. Weights were assigned using the following process:

1. A mock assessment was completed where every parameter was given the maximum rank of 5, and the product mean was calculated for each CCC, resulting in a CCC Rank (Table 3.9).
2. The Assailing CCC Rank was given a weight of 1, as it contained only one contributing parameter.

3. The subsequent CCC weights were determined by dividing the assailing CCC Rank by the CCC Rank for each other class (e.g., assailing CCC Rank/Resistance CCC Rank). The final weights are displayed in Table 3.9.

Table 3.9 Coastal Characterization Class Weighting Process.

CCC	CCC Rank <i>*calculated using max rank (5) for all parameters</i>	Weight Calculation	Weight
Assailing	5	N/A	1
Resistance	11160.71	5/1160.71	0.0004
Resilience	41.67	5/41.67	0.12

Using the CVI₅ formula, along with the weighted CCCs, a CVI was calculated for each of the 190 backshore segments. The backshore segment was chosen as the cell size for assessment because, of the backshore, foreshore, and nearshore, it was the coastline which changed the most and thus had the greatest number of segments. While the backshore line provides the assessment cell size, the developed CVI assess both backshore and foreshore features within each zone bounded by the backshore segment. This provided a comprehensive assessment of the coastal vulnerability for that particular area. It is also important to note that, in the few instances where the foreshore changed within a backshore segment, the backshore line was cut to match the foreshore. While many studies use pre-set, equal cell sizes to assess coastal vulnerability (Hedge & Reju, 2007; Palmer et al., 2011; Kumar et al., 2010; McLaughlin & Cooper, 2010; Abuodha & Woodroffe, 2010) this study uses segment sizes based on natural backshore changes determined from the shoreline characterization database. This is a key benefit in this research, as the use of pre-defined cell widths for assessment can lead to generalization of coastal features within a cell and can ultimately, albeit unintentionally, misrepresent the actual vulnerability of an area.

The process of CVI calculation is outlined in Table 3.9, using backshore segment #87 as an example. For each backshore segment, each parameter from *a-k* was ranked according to its contribution to vulnerability for that segment (Table 3.10 - C2). The product mean was calculated for each CCC using the equations in Table 3.10 - C3, which produced a single rank for each CCC (Table 3.10 - C4). This CCC rank was then multiplied by the CCC weight (Table 3.10 - C5), which produced a weighted rank for each class (Table 3.10 -C6). The square root of the product mean (CVI_s) was then used to calculate the final CVI score (Table 3.10 – C7 & C8). The final CVI is a dimensionless, relative value, only comparable to other CVI scores in this study and not to other coastal vulnerability studies (Pendleton et al., 2004).

Table 3.10 CVI Calculation for Backshore Segment #87.

CCC	Parameter (C1)	Rank (C2)	Equation (C3)	CCC Rank (C4)	CCC Weight (C5)	Weighted CCC Rank (C6)	Equation (C7)	Final CVI Score (C8)
Assailing	a. Wave Energy	3	$(a)/1$	3	$\times 1$	3	$\sqrt{((\text{weighted assailing rank} \times \text{weighted resistance rank} \times \text{weighted resilience rank})/3)}$	0.46
	Resistance	b. Foreshore Geomorphology	1	$(b \times c \times d \times e \times f \times g \times h)/7$	535.71	$\times 0.0004$		
c. Foreshore Slope		2						
d. Foreshore Width		5						
e. Backshore Elevation		5						
f. Backshore Slope		3						
g. Backshore Vegetation		5						
h. Coastal Protection Structures		5						
Resilience		i. Morphological Resilience	5					
	j. Accommodation Space	5						
	k. Sediment Supply	1						

Once the CVI values were calculated for each backshore segment, the values were divided into five levels of vulnerability ranging from *very low* (1) to *very high* (5). In this study the CVI values ranged from 0-2.99 and were divided into five classes of vulnerability using quantiles (Stern et al., 2011) (Table 3.11).

Table 3.11 Vulnerability Ranks and Corresponding CVI Ranges.

Level of Vulnerability	Corresponding CVI Range
Very Low	0-0.089
Low	0.090-0.157
Moderate	0.158-0.243
High	0.244-0.370
Very High	0.371-2.99

3.2.6 Coastal Vulnerability & Coastal Characterization Classes

As this research is one of the first physical coastal vulnerability assessments to incorporate assailing, resistance, and resilience parameters, it is important to look at the theoretical relationships between these CCCs and coastal vulnerability scores. Visualizing the relationships before applying real-world data is beneficial to the overall understanding of the interactions between these components.

Under the assumption that coastal geomorphic vulnerability is a function of assailing, resistance, and resilience, as depicted in Equation 1.2, and that each CCC contributes equally to the vulnerability of a coast, CVI scores were calculated for varying combinations of CCC ranks. Recall that, while the coastal geomorphic vulnerability relationship is a function of assailing x 1/resistance x 1/resilience, the calculation of an index requires the inversion of the resistance and resilience CCCs such that a *very high* vulnerability rank, and thus contribution to

vulnerability, corresponds to a coastline with low “actual” resistance or resilience characteristics (Table 3.12).

In an effort to simplify the theoretical exploration of the relationships, it was also assumed that each CCC had only one contributing parameter and therefore there was no need for weighting. The square root of the product mean was calculated, using equation 3.4, for each possible rank outcome for each CCC, using potential ranks from 1-5 (e.g. Assailing Rank =1, Resistance Rank = 1, and Resilience Rank = 1; 1-1-2; 1-1-3; 1-1-4; 1-1-5 etc.), the result of which represents a theoretical coastal vulnerability score. The scores were then categorized, using equal interval classification, into classes representing *low, moderate, or high* vulnerability.

Equation 3.4

$$\text{Theoretical Coastal Vulnerability} = \sqrt{((\text{Assailing Rank} \times \text{Resistance Rank} \times \text{Resilience Rank})/3)}$$

Table 3.12 Coastal Characteristic Class (CCC) Ranks and Their Contribution to Coastal Vulnerability Index Scores vs. Actual Coastal Characteristics.

CCC	Rank	Contribution to Coastal Vulnerability Index Score	“Actual, On-the –Ground” Characteristics
Assailing	5	<i>very high</i> vulnerability	very high assailing properties
	1	<i>very low</i> vulnerability	very low assailing properties
Resistance	5	<i>very high</i> vulnerability	very low resistance properties
	1	<i>very low</i> vulnerability	very high resistance properties
Resilience	5	<i>very high</i> vulnerability	very low resilience properties
	1	<i>very low</i> vulnerability	very high resilience properties

3.3 CVI Application (Step 2)

The developed CVI matrix was applied to the Town of Lockeport, Nova Scotia to assess the current vulnerability of the coastline to erosion (Scenario 1). In an effort to identify areas at risk to future erosion, this CVI was applied under three additional wave energy scenarios with varying associated water depths and wind conditions. In each case, the resistance and resilience

parameter ranks remained the same, while the Wave Energy parameter associated with the assailing CCC, was manipulated. As explained in Section 3.3.3.2, the calculation of RWE values required the input of bathymetry data, wind data, and coastline shape and therefore a change in one input changes the amount of wave energy reaching the coast. In this study, wave energy scenarios were meant to be sequential and were manipulated by changing either water depth or wind condition. The resulting CVIs calculated for each scenario, shown on individual CVI maps, illustrate the differences in coastal response with varying wave energy scenarios associated with climate change. The scenarios will be discussed in greater detail in the sections to follow.

3.3.1 Wave Energy Scenario 1

In Scenario 1 which represents current wave energy conditions, the following inputs were used to calculate the RWE values: 1:10 000 coastline shapefile from the NSCS, 1:10 000 bathymetric data (in CD) from the NSCS, and hourly wind data from the NOAA NDBC using buoy 44204 for the period of January 1st, 2011 – December 31st, 2013. A wind rose illustrating the distribution of wind speed and direction at buoy 44204 during this time period is shown in Figure 3.18.

3.3.2 Wave Energy Scenario 2

This wave energy scenario predicts the wave energy reaching the coastline for a large storm event. In this scenario, the wind data used is characteristic of a notable storm event that severely impacted the South Shore of Nova Scotia on February 9th, 2013. The following inputs were used to calculate the RWE values for Scenario 2: 1:10 000 coastline shapefile from the NSCS, 1:10 000 bathymetric data (in CD) from the NSCS, and hourly wind data from the NOAA

NDBC using buoy 44204 for the period of February 9th at 1 am – February 10th at 11 am, 2013. A wind rose illustrating the distribution of wind speed and direction at buoy 44204 during this time period is shown in Figure 3.19.

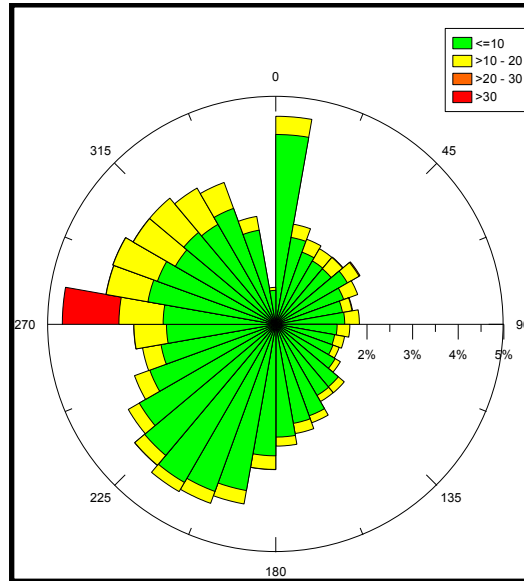


Figure 3.18 Wind Rose for Hourly Wind Data from January 1st, 2011 – December 31st, 2013.
Derived using Golden Software Grapher 4.

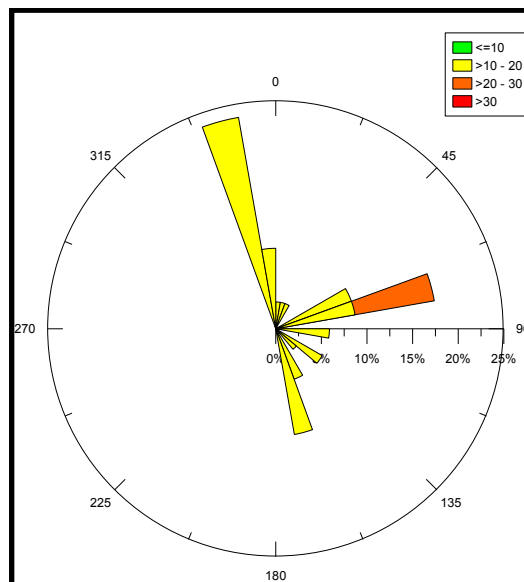


Figure 3.19 Wind Rose for Hourly Wind Data from February 9th at 1am – February 10th at 11am (February 2013 Storm). Derived using Golden Software Grapher 4.

3.3.3 Wave Energy Scenario 3

In addition to the storm winds included in Scenario 2, Scenario 3 incorporates a 2.21 m increase in water depth, facilitated in WEMo by “lowering” the sea floor by this amount, thus allowing for the coastline to remain static. The 2.21 m increase in water depth incorporates the 0.85 m RCP8.5 RSLR projection for Halifax for the time interval 2010-2100 (James et al., 2014) and a value of 1.36 m \pm 0.02 m, which represents the 2-year return level high water-level scenario for Halifax Harbour in 2100 (based on the annual extremes analysis of water levels for Halifax Harbour [1920 – 2007]) (Forbes et al., 2009). The following inputs were used to calculate the RWE values for Scenario 3: 1:10 000 coastline shapefile from the NSCS, 1:10 000 bathymetric data (in CD) from the NSCS + a 2.21 m increase in water levels, and hourly wind data from the NOAA NDBC using buoy 44204 for the period of February 9th at 1 am – February 10th at 11 am, 2013.

3.3.4 Wave Energy Scenario 4

In addition to the storm winds included in Scenario 2, Scenario 4 incorporates a 3.10 m increase in water depth, facilitated in WEMo by “lowering” the sea floor by this amount, thus allowing for the coastline to remain static. The 3.10 m increase in water depth incorporates the 1.74 m RCP8.5max+60 RSLR projection for Halifax for the time interval 2010-2100 (James et al., 2013 *In Review*) and a value of 1.36 m \pm 0.02 m, which represents the 2-year return level high water-level scenario for Halifax Harbour in 2100 (based on the annual extremes analysis of water levels for Halifax Harbour [1920 – 2007]) (Forbes et al., 2009). In James et al. (2014), the RSLR projection referred to above was modified to 1.79 m and was released after the analysis was completed. Since it is only a difference of 0.05 m, it is within the range of error and the

impacts will be minor. The following inputs were used to calculate RWE values for Scenario 4: 1:10 000 coastline shapefile from the NSCS, 1:10 000 bathymetric data (in CD) from the NSCS + a 3.10 m increase in water levels, and hourly wind data from the NOAA NDBC using buoy 44204 for the period of February 9th at 1 am – February 10th at 11 am, 2013.

3.3.5 Proof of Concept

Since the matrix is newly developed, it is important to ensure that it adequately assesses vulnerability to erosion. A statistical matrix validation, which would be useful, requires an independent set of quantitative erosion data, which does not exist for this research and, the practice of incorporating expert consultation for parameters selection was also not incorporated. Despite these limitations, the matrix parameters were systematically chosen from peer-reviewed literature, and the ability of the matrix to assess vulnerability to erosion was explored using on-the-ground erosion observations. Furthermore, a principal components analysis was used to identify the parameters that together contribute to higher vulnerability scores for Scenario 1.

3.3.5.1 Observed Erosion & Areas of Concern

Along the coastline, areas identified in the field as being susceptible to erosion, along with areas of concern noted in the Town of Lockeport MCCAP (Atwood, 2013), were qualitatively compared with areas identified by the CVI, for Scenario 1, as being vulnerable to erosion.

3.3.5.2 Principal Components Analysis

A principal components analysis (PCA) was completed for the 11 parameters incorporated in this research using the statistical program R. A PCA is a multivariate analysis technique that takes a set of possibly correlated parameters and, using an orthogonal transformation, transforms them into a set of linearly uncorrelated, composite parameters, called principal components (PCs), that best describe the variance of the dataset (Dunteman, 1989). Essentially, a PCA aims to reduce the dimensionality of a data set with minimal loss of information (Holland, 2008; Smith, 2002), as a smaller set of uncorrelated parameters are much easier to use in further analyses as composite variables, or to interpret, enabling underlying relationships within the data to be discovered (Dunteman, 1989). The interest in this study is to reduce the dimensionality of the data set to help determine the parameters that are driving the high coastal vulnerability scores.

Principal components, also known as eigenvectors, and their associated variance (λ), also called eigenvalues (Dunteman, 1989), were derived from a covariance matrix using R. The resulting PCs are each individual, uncorrelated variables that are a combination of the 11 input parameters the contributions of which are determined by the associated loadings. The first PC accounts for the largest variance in the data set, PC two accounts for the next largest variance in the data set (under the condition that it is orthogonal to the first PC), the third PC accounts for the next largest variance etc (Holland, 2008). The proportion of variation explained by each PC was calculated by dividing the variance of each PC by the number of PCs (Dunteman, 1989). In a PCA, the number of derived PCs equal the number of original variables, and account for all of the variance in the data set (Dunteman, 1989). However, as the goal of a PCA is to reduce data dimensionality, there is no advantage in keeping all PCs (Dunteman, 1989) and therefore the PCs

that account for very little variance in the data can be removed with minimal loss of information (Holland, 2008).

There are many methodologies developed to determine the number of PCs to retain (Dunteman, 1989; Holland, 2008; Jackson, 1993), however the most commonly used methodology in ecology is the Kaiser-Guttman “stopping rule” which suggests that all PCs with a $\lambda > 1$ should be retained (Jackson, 1993). The Kaiser-Guttman stopping rule was applied in this PCA.

In an effort to interpret the relationships among the PCs, PC1 was plotted against each of the remaining PCs on a biplot, depicting the loadings and magnitudes of each input parameter. The size of the loadings reflect how much a particular variable contributes to that PC and the length of the arrows determines the importance of that variable in explaining the variability in that PC. Using the biplots, in combination with original data, the parameters most likely driving the high coastal vulnerability scores for this study were determined.

3.4 Identification of Vulnerable Buildings (Steps 3 & 4)

A community’s ability to adapt begins with the identification of areas that are particularly vulnerable. Thus far, the areas of coast that are physically vulnerable to erosion have been identified under varying wave energy scenarios. However, following the methodology of Palmer et al. (2011), this section will identify building infrastructure (utilities, residences, and commercial properties) located within the coastal zone vulnerable to erosion and inundation. To achieve this, the coastal zone of Lockeport was delineated, followed by the identification of infrastructure vulnerable to erosion under each wave energy scenario (S1 to S4)

and finally the identification of infrastructure vulnerable to the combined effects of erosion and permanent inundation associated with the wave energy scenarios that incorporate an increase in water depth (S3 and S4).

3.4.1 Coastal Zone Delineation

The focus of this section is to identify the vulnerability of buildings within the coastal zone that, for this study, encompasses all land and water residing within 50 m either side of the backshore line. Using the “Buffer” tool in ArcGIS 10.1, a buffer extending 50 m either side of the backshore line was created for Lockeport. Next, using the “Select by Location” function, buildings within the coastal zone were identified from the Nova Scotia Topographic Database (NSTDB) 1:10 000 buildings dataset.

3.4.2 Buildings Vulnerable to Erosion

In order to identify buildings within the coastal zone vulnerable to erosion under each wave energy scenario, CVI values representative of each scenario were extracted from the nearest backshore line to each building point feature within Lockeport using the “Spatial Join” function in ArcGIS 10.1. For each scenario (S1 to S4), buildings located within the coastal zone were associated with a particular vulnerability rank from *very low* vulnerability (1) to *very high* vulnerability (5) and were subsequently displayed on maps.

3.4.3 Buildings Vulnerable to Erosion & Inundation

As flooding and inundation are the effects of SLR most likely to cause harm to people and infrastructure, buildings vulnerable to erosion and inundation were also identified. As

inundation is associated only with the wave energy scenarios linked to an increase in water levels, building vulnerability is only identified for scenarios 3 and 4 with an associated 2.21 m and 3.10 m of increase in water depth respectively. Inundation polygons were created for each scenario by reclassifying 1 m DEM data using the “Reclassify” function in ArcGIS 10.1. Next, using the “Select by Location” function, buildings located within the coastal zone and within the inundation polygon were identified and associated with a particular vulnerability rank ranging from *very low* vulnerability (Rank 1) to *very high* vulnerability (Rank 5). The results were displayed on maps.

Chapter 4

RESULTS

To address the purpose and objectives of this research, this chapter presents the outcomes of the development of a CVI to assess vulnerability to erosion, its application under wave energy scenarios S1 to S4, and the identification of buildings vulnerable to erosion and inundation.

4.1 CVI Development (Step 1)

The development of a CVI matrix includes the process of selecting appropriate parameters that match the CVI purpose, collecting data, creating the matrix, and determining the CVI calculation method. Chapter 3 extensively outlines the data collection, CVI calculation method, and parameter selection components of this process, with Table 3.2 - C5 listing the final parameters chosen for the CVI assessment. The following sections will illustrate the resulting CVI matrix, the contribution of wave energy under each wave energy scenario and will examine the theoretical relationships between CCCs and coastal vulnerability scores.

4.1.1 Matrix Creation

The relative CVI for assessing vulnerability to erosion in Lockeport (Table 4.1) groups the 11 parameters into the CCCs, of assailing, resistance, or resilience, according to their role as a parameter that induces change (assailing), resists change (resistance), or allows the coast to recover from change (resilience). It was assumed that each CCC contributes equally to coastal vulnerability and therefore each was given an equal weight despite the number of contributing parameters. Using the matrix, the 11 parameters were ranked on their individual contribution to vulnerability with a rank of 1 representing a *very low* contribution and a rank of 5 representing a *very high* contribution. As explained in chapter 3, qualitative parameters were divided into rank classes by listing all possible options and sorting those options based on their contribution to vulnerability, while quantitative parameters were divided using appropriate data classification methods. The method of solely using data from Lockeport to determine rank classes means that this is a relative vulnerability matrix, where the final CVI scores are comparable only to other CVI scores in this research.

4.1.2 Wave Energy Scenarios

Using the WEMo program, RWE was calculated for four scenarios for the area surrounding Lockeport, Nova Scotia (Figure 4.1, 4.2, 4.3, and 4.4). In S1 and S2, the highest wave energies are concentrated between the south and east areas of Lockeport, with S2 showing a higher concentration of wave energy approaching The Anchorage. Scenarios 3 and 4 illustrate that the locations of highest energy are primarily to the south of Lockeport, with a slight moderate wave energy reaching the north part of the study area. In all scenarios, Crescent Beach experiences comparatively lower wave energy and the Back Harbour along with

the area between Locke Island and Cranberry Island appear to be most sheltered from wave energy.

The contribution of Wave Energy to the CVI for each wave energy scenario is shown in Figures 4.5-4.8 and display Wave Energy rank relative to the most extreme scenario: Wave Energy Scenario 4. Overall, the percent of shoreline experiencing *low* Wave Energies (Ranks 1 and 2) decreases with each scenario, with S1, S2, S3, and S4 showing a combined percent shoreline coverage of 87%, 69%, 50%, and 37% respectively. The highest vulnerability rank is 3 in S1, 4 in S2 and S3, and 5 in S4, with 16% of the shoreline experiencing *very high* Wave Energy (Rank 5) in S4.

As each scenario progresses, the areas of coast shown to have exposure to the highest Wave Energies include the west end of Crescent Beach, the north side of Locke Island, the historic portion of South Street, the north part of The Anchorage and the north part of Brighton Road. The only part of the coastline that experiences a decrease in Wave Energy reaching the coast as each scenario progresses is the stretch between Rood's Head and the Wastewater Treatment Facility. With respect to Crescent Beach, S1 indicates that the entire length of the beach has a rank of 2, with the west part of the beach increasing to a rank of 4 in S2. While S3 and S4 exhibit no rank increase for the farthest west portion of the beach, a rank increase from 2 to 4 and from 2 to 3 is experienced for the central and eastern parts of the beach respectively. Maps depicting individual parameter contribution for the remaining parameters can be found in Appendix B.

Table 4.1 Relative Coastal Vulnerability Index for Assessing Vulnerability to Erosion in Lockeport, Nova Scotia. (Created by: Sam Page, 2014).

CCC	Variable	Sub-Variable	Vulnerability Rank				
			1 <i>Very Low</i>	2 <i>Low</i>	3 <i>Moderate</i>	4 <i>High</i>	5 <i>Very High</i>
ASSA ILIN	a. Wave Energy (RWE values in J/m)		0 – 176	177 - 401	402 – 1261	1262– 5561	5562 – 9904
	b. Foreshore Geomorphology		outcrop or platform or anthro	clastic slope (boulder) or beach (boulder) or wetland	clastic slope (cobble) or beach (cobble)	beach (sand/gravel) or dune or flat (mud/sand/gravel)	no FS
RESISTANCE	c. Foreshore Slope		ramped	low slope	medium slope	cliffed	high slope or no FS
	d. Foreshore Width (m)		24.2-81.8	13.9-24.1	8.9 – 13.8	5.0-8.8	0-4.9
	e. Backshore Elevation (m)		4.2 – 6.1	2.9– 4.1	2.1– 2.8	1.3 – 2.0	0 – 1.2
	f. Backshore Slope		ramped	low slope	medium slope	cliffed	high slope
	g. Backshore Vegetation		dense tree	sparse tree or dense shrub	sparse shrub or dense grass	sparse grass	unvegetated
	h. Coastal Protection Structure (CPS) <i>*take average score</i>	a. State	intact	damaged	failing	remnant	none
		b. Type & Material (cm)	cps large riprap (75-147)	cps medium riprap (34-74)	cps small riprap (0-33)	cps concrete	no cps
	RESILIENCE	i. Morphological Resilience (as a system combining BS and FS)		a. dune + beach	a. low slope + beach b. dune + no beach	a. high-med slope + beach b. low slope + no beach c. wetland	a. bluff+ beach b. high-med slope + no beach
j. Accommodation Space (m)			41-50	28-40	18-27	7-17	0-6
k. Sediment Supply			stable		erosion		severe erosion

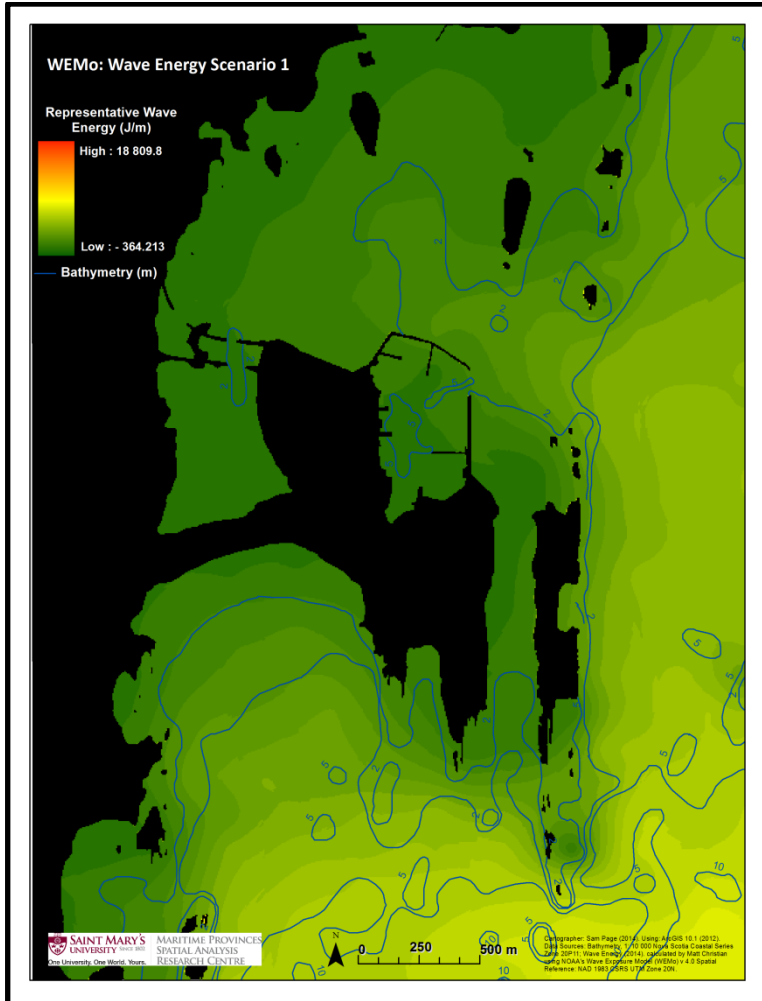


Figure 4.1 Representative Wave Energy Values for Wave Energy Scenario 1. RWE values are relative to S4.

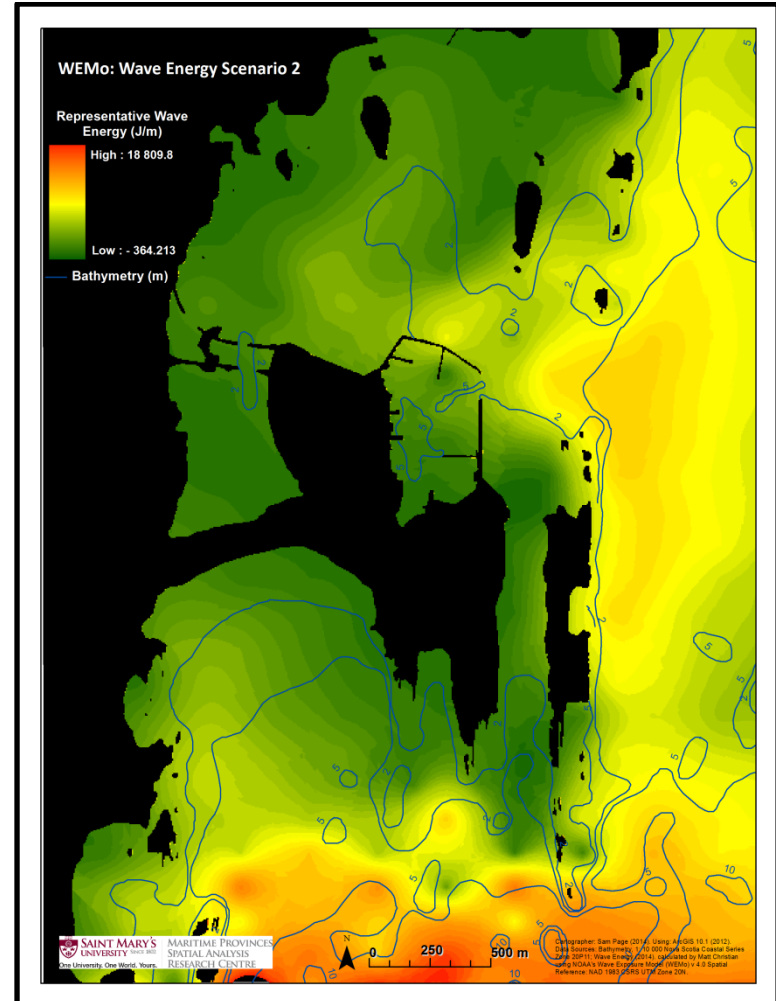


Figure 4.2 Representative Wave Energy Values Wave Energy Scenario 2. RWE values are relative S4.

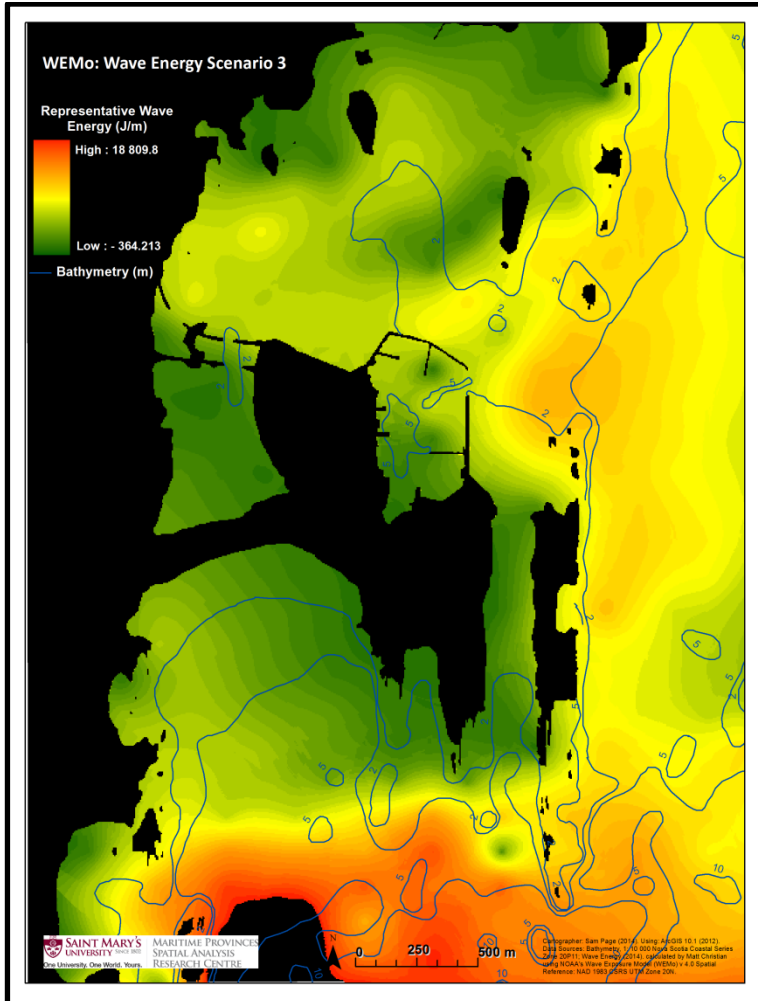


Figure 4.3 Representative Wave Energy Values Wave Energy Scenario 3. RWE values are relative to S4.

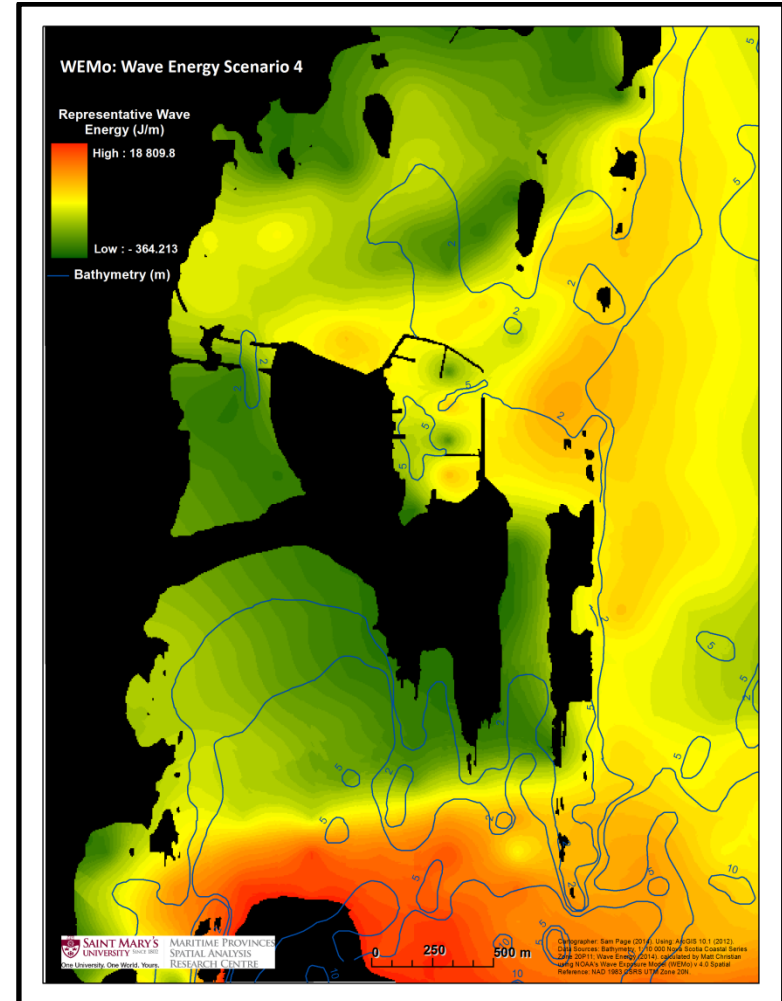


Figure 4.4 Representative Wave Energy Values for Wave Energy Scenario 4. RWE values are relative to S4.

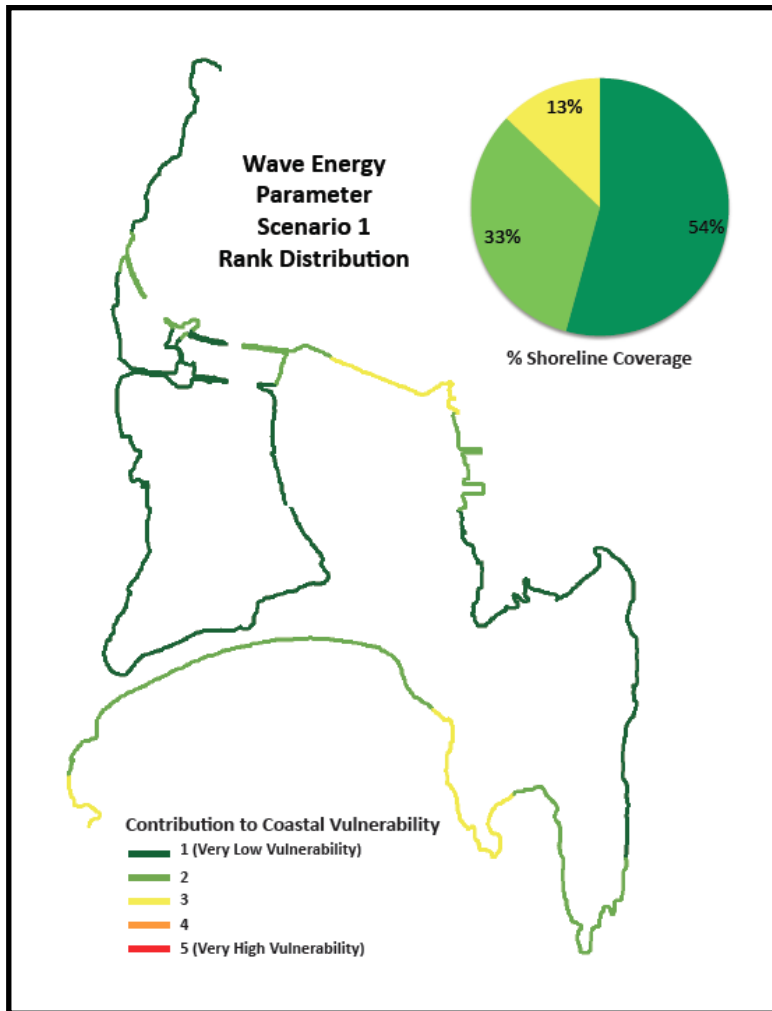


Figure 4.5 Contribution of Wave Energy Parameter (Wave Energy Scenario 1) to Coastal Vulnerability. Where % Shoreline Coverage = percent of shoreline associated with each vulnerability rank.

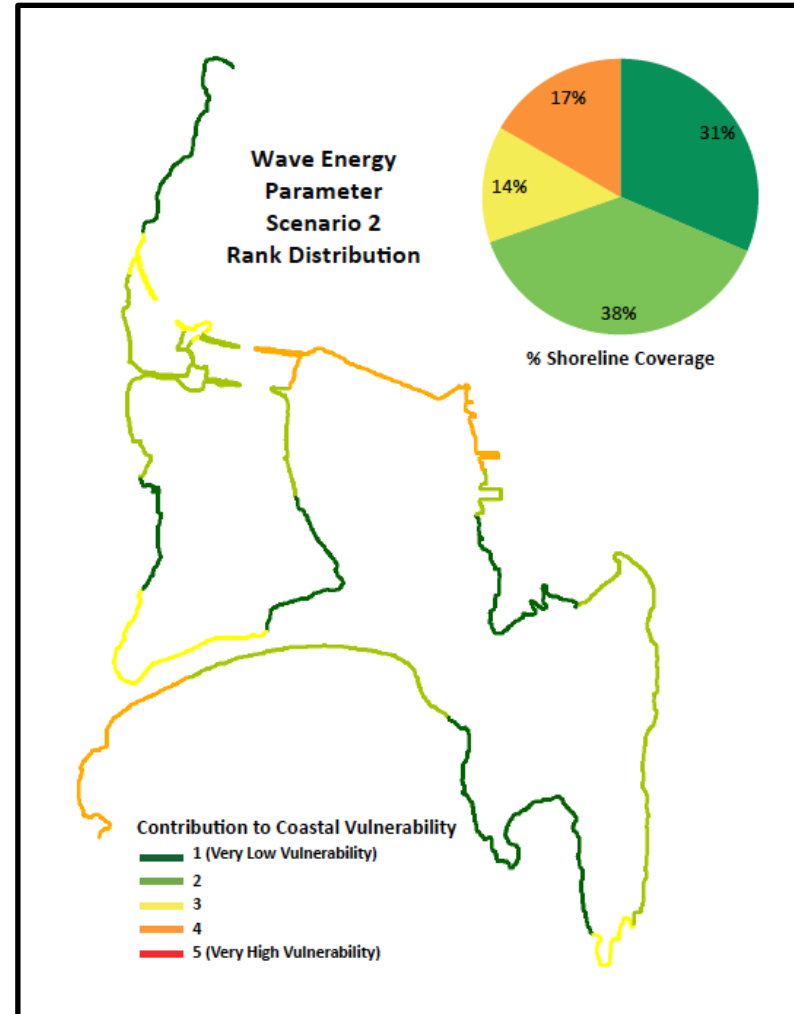


Figure 4.6 Contribution of Wave Energy Parameter (Wave Energy Scenario 2) to Coastal Vulnerability. Where % Shoreline Coverage = percent of shoreline associated with each vulnerability rank.

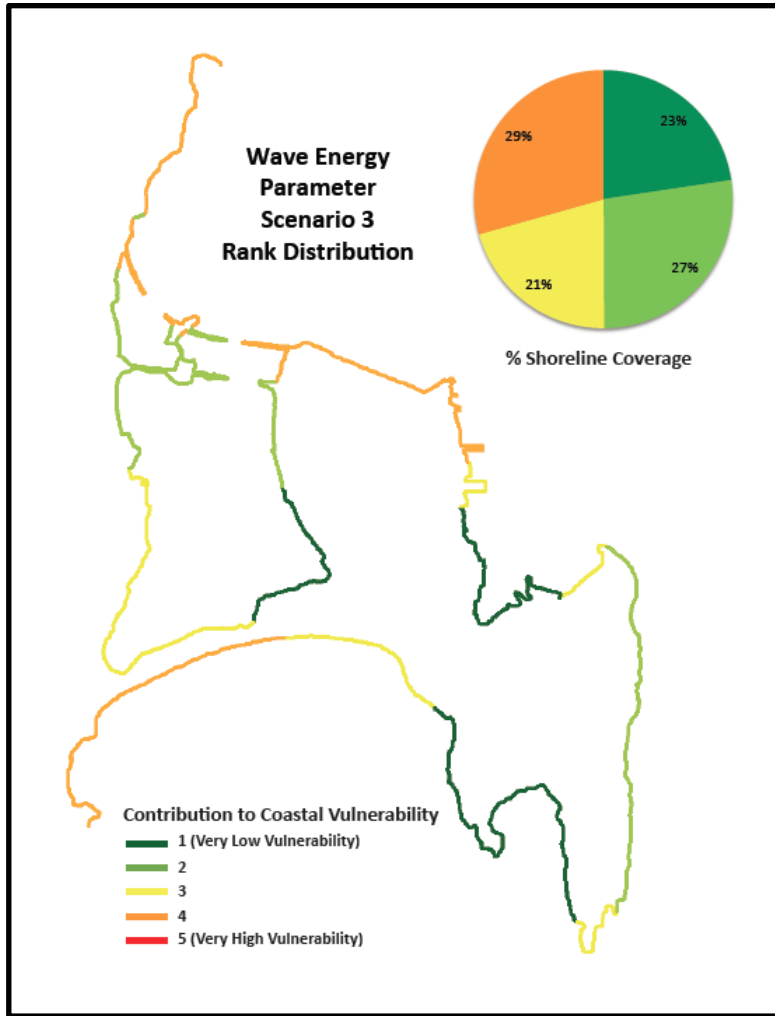


Figure 4.7 Contribution of Wave Energy Parameter (Wave Energy Scenario 3) to Coastal Vulnerability. Where % Shoreline Coverage = percent of shoreline associated with each vulnerability rank.

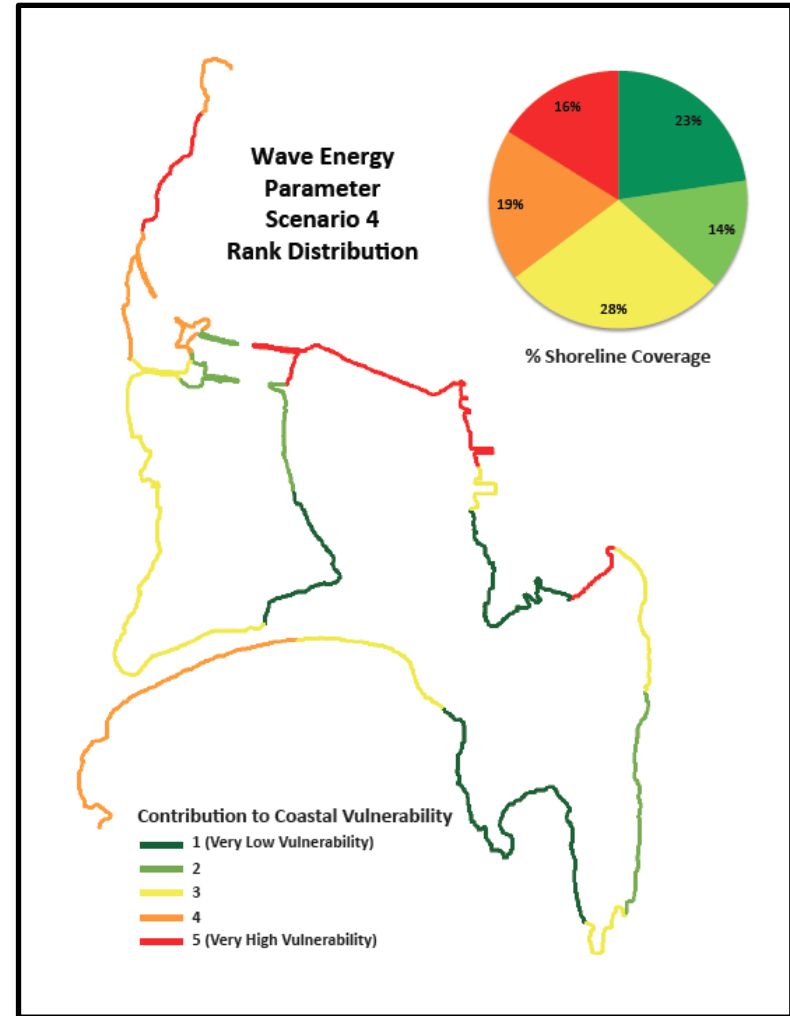


Figure 4.8 Contribution of Wave Energy Parameter (Wave Energy Scenario 4) to Coastal Vulnerability. Where % Shoreline Coverage = percent of shoreline associated with each vulnerability rank.

4.1.3 Coastal Vulnerability and Coastal Characterization Classes

An examination of theoretical coastal vulnerability scores derived from various combinations of assailing, resistance, and resilience ranks, is beneficial for understanding the relationships between coastal vulnerability and CCCs. Before interpreting these relationships recall that the resistance and resilience classes have an inverse relationship with vulnerability, such that a high coastal resistance or resilience results in a low coastal vulnerability rank (1), as displayed in Table 4.1, and a *very high* resistance or resilience rank (5) represents a coast with very low resistance or resilience (See Table 3.11 for reference).

With this in mind, the conceptual diagram (Figure 4.9) illustrates that coastal vulnerability increases with increasing resilience rank (i.e., decreasing actual resilience) with the most vulnerable coastline resulting from a combination of 5-5-5 (Assailing Rank =5, Resistance Rank=5, and Resilience Rank=5 [i.e., very high actual assailing, and very low actual resistance and resilience]). Conversely, the least vulnerable coastline results from a combination of 1-1-1 (Assailing Rank = 1, Resistance Rank = 1, and Resilience Rank = 1 [i.e., very low actual assailing and very high actual resistance and resilience]). While these observations are fairly basic, Figure 4.9 also shows that coasts with a *very low* resilience rank of 1 (i.e., very high actual resilience), for the most part, have *low* coastal vulnerability scores, despite the increase in resistance and assailing ranks, and never contribute to *high* coastal vulnerability. Despite various combinations of resistance and assailing parameters, coasts with a *low* resilience rank of 2 also do not contribute to *highly* vulnerable coastlines. Even with a resilience rank of 3 (*moderate*), high coastal vulnerability scores only result where there is also a *very high* rank (5) of assailing and resistance. Another notable relationship is that coasts with *high* resistance and assailing ranks (4 and 5) do not always result in *highly* vulnerable shorelines, but *low-moderate* resistance and

assailing ranks (1,2, and 3) always result in *lowly* vulnerable shorelines, despite the change in resilience. Overall, it can be said that *highly* vulnerable coastlines tend to occur when assailing ranks are *moderate* to *high* (3-5) and actual coastal resistance and resilience are relatively low (Rank 3-5).

This conceptual diagram and associated theoretical CVI scores are meant to provide a “stand alone” insight into the relationships between CCCs and coastal vulnerability and, while the explored relationships provide context, the theoretical values are not incorporated in the application of the developed CVI matrix (Table 4.1) to Lockeport.

4.2 CVI Application (Step 2)

The developed CVI was applied to the Town of Lockeport under each wave energy scenario and the resulting CVI scores are displayed in Figures 4.10-4.13. Overall, the percent of *highly* and *very highly* vulnerable coastline increases from S1 to S4 (Figure 4.14). However, as scenarios progress, Ranks 4 and 5 show an increase in percent shoreline coverage from S1 to S2, a decrease from S2 to S3, and an increase again from S3 to S4; the opposite is true for Ranks 1, 2, and 3 (Table 4.2). Of all scenarios, S4 has the largest percent of *highly* and *very highly* vulnerable coastline and S1 has the largest percent of *lowly* and *very lowly* vulnerable coastline.

From S1 to S4, the greatest net change, which is 10%, occurs in Rank 5, from 10% coverage to 20% coverage. Rank 4 and Rank 2 have a +9% and -9% net change respectively, from S1 to S4 and both Rank 1 and Rank 3 show a 5% net decrease in shoreline coverage. However, from one scenario to another, the largest percent shoreline coverage change is +7%, which occurs in Rank 4 from S1 to S2 (Table 4.2). The top three smallest percent shoreline

coverage change, from one scenario to another occur between S2 to S3, with 0% change for Rank 2, 1% change for Rank 5, and 2% change for Rank 3 (Table 4.2). In fact, combined absolute change in percent shoreline coverage is smallest between S2 and S3 and is substantially smaller than combined absolute change between S1 and S2 and S3 and S4.

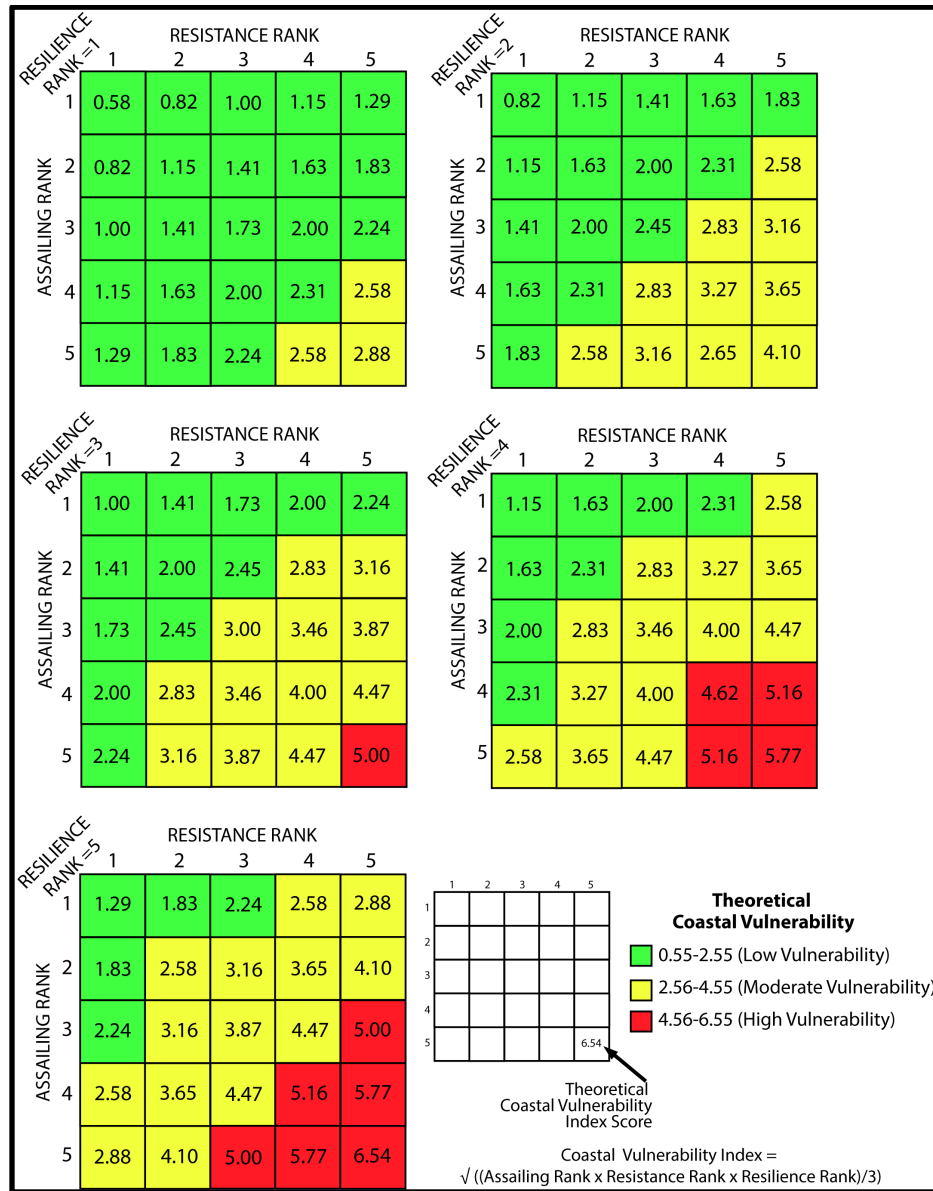


Figure 4.9 Theoretical Relationships between Coastal Vulnerability and Coastal Characterization Classes.

With respect to specific locations (Figures 4.10-4.13), the majority of shorelines show either an increase in vulnerability or no change in vulnerability with increasing scenarios. However, the stretch of coastline extending from Rood's Head to the Wastewater Treatment Facility on John Street, excluding the section of Chetwynd Lane, decreases in vulnerability from S1 to S2, and remains that way throughout the remaining scenarios. Chetwynd Lane, the west end of Crescent Beach, a small section parallel to Cranberry Island, Sam's Point and sporadic sections of Brighton Road all remain *very lowly* vulnerable throughout all scenarios. On the other hand, the majority of Water Street and the land portion of North Wharf remain *very highly* vulnerable throughout all scenarios.

From S1 to S2, the Trestles and Locke Street West become *very highly* vulnerable and Calf Island Road becomes *highly* vulnerable. From S2 to S3 there is only a 1% change in shoreline coverage for Rank 5, which can be largely accounted for by the western portion of Crescent Beach, but which also includes a small portion of historic South Street and small stretches of Brighton Road. From S3 to S4 the change in *very highly* vulnerable shoreline is mostly concentrated around Calf Island Road. With respect to Crescent Beach, the western and some central sections of the beach are deemed to have a *very low* vulnerability and the eastern and some central sections are deemed to have a *moderate to high vulnerability* (Ranks 3, 4, and 4) in S1. Along Crescent Beach, the shoreline does not change in vulnerability between S1 and S2 or S3 and S4, but does change from S2 to S3 with some central and western portions increasing in vulnerability. Generally shoreline vulnerability between scenarios did not increase by more than one rank, however between S2 and S3, vulnerability ranks for portions of the northern part of Brighton Road did increase by more than one rank.

Table 4.2 CVI Summary for S1 to S4. Where % Coverage= % of shoreline associated with each vulnerability rank, Change = the change of % coverage between scenarios, Absolute Change = the total combined, absolute, change between scenarios, and Net Change = the net change in % coverage between S1 and S4.

Rank	S1 % Cov.	Change from S1 to S2	S2 % Cov.	Change from S2 to S3	S3 % Cov.	Change from S3 to S4	S4 % Cov.	Net Change S1 to S4
5	10	+6	16	-1	15	+5	20	+10
4	10	+7	17	-4	13	+6	19	+9
3	21	-4	17	+2	19	-3	16	-5
2	29	-6	23	0	23	-3	20	-9
1	30	-3	27	+3	30	-5	25	-5
Absolute Change		26		10		22	S4	

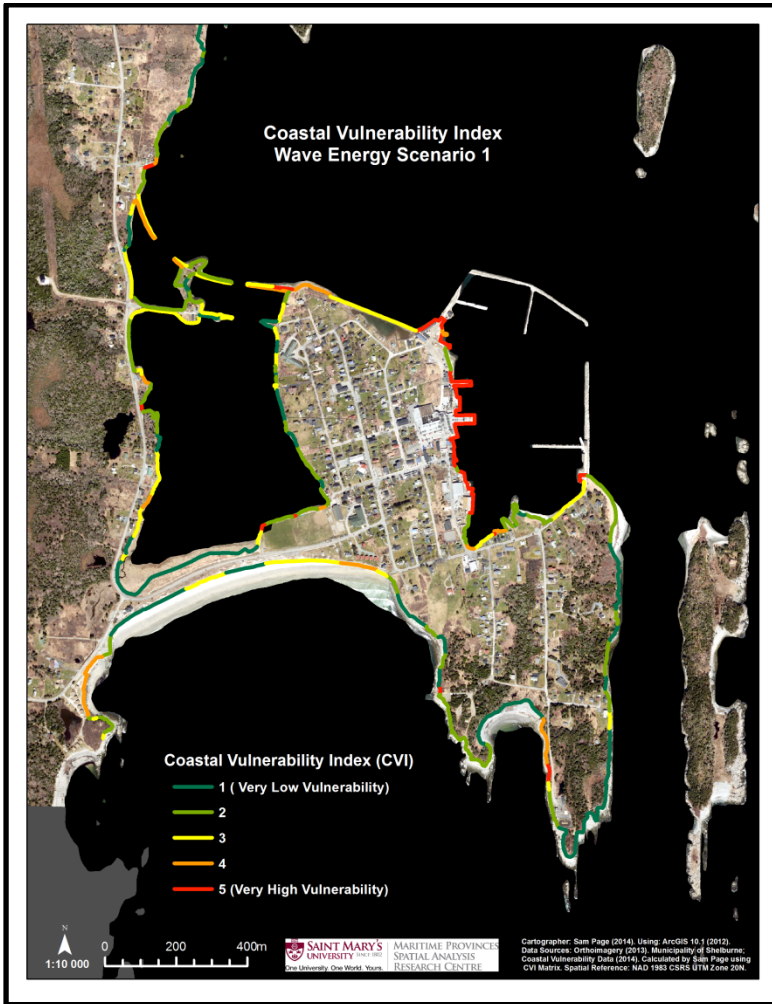


Figure 4.10 Coastal Vulnerability Index for Wave Energy Scenario 1. CVI values are derived using the CVI Matrix (Table 4.1).

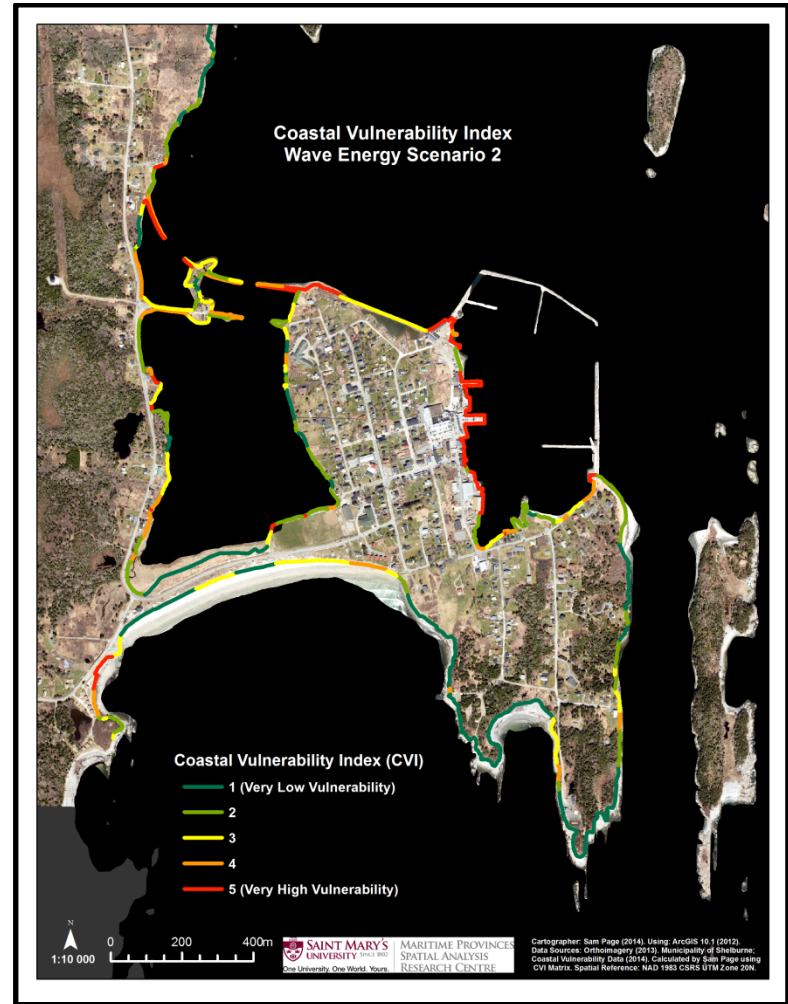


Figure 4.11 Coastal Vulnerability Index for Wave Energy Scenario 2. CVI values are derived using the CVI Matrix (Table 4.1).

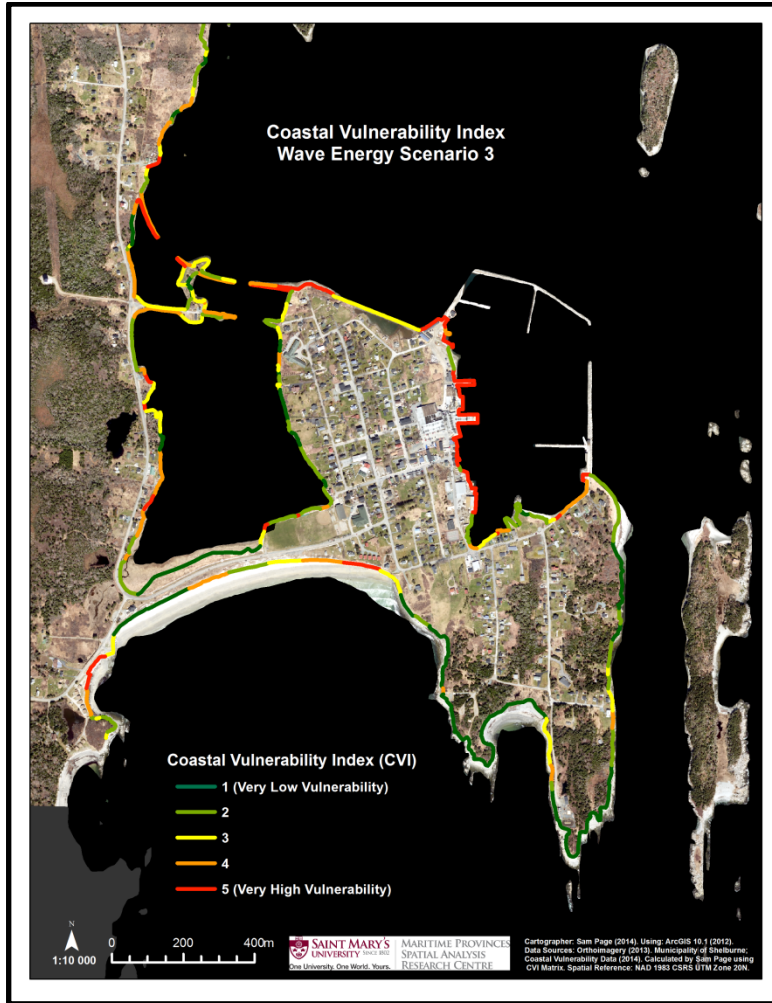


Figure 4.12 Coastal Vulnerability Index for Wave Energy Scenario 3. CVI values are derived using the CVI Matrix (Table 4.1).

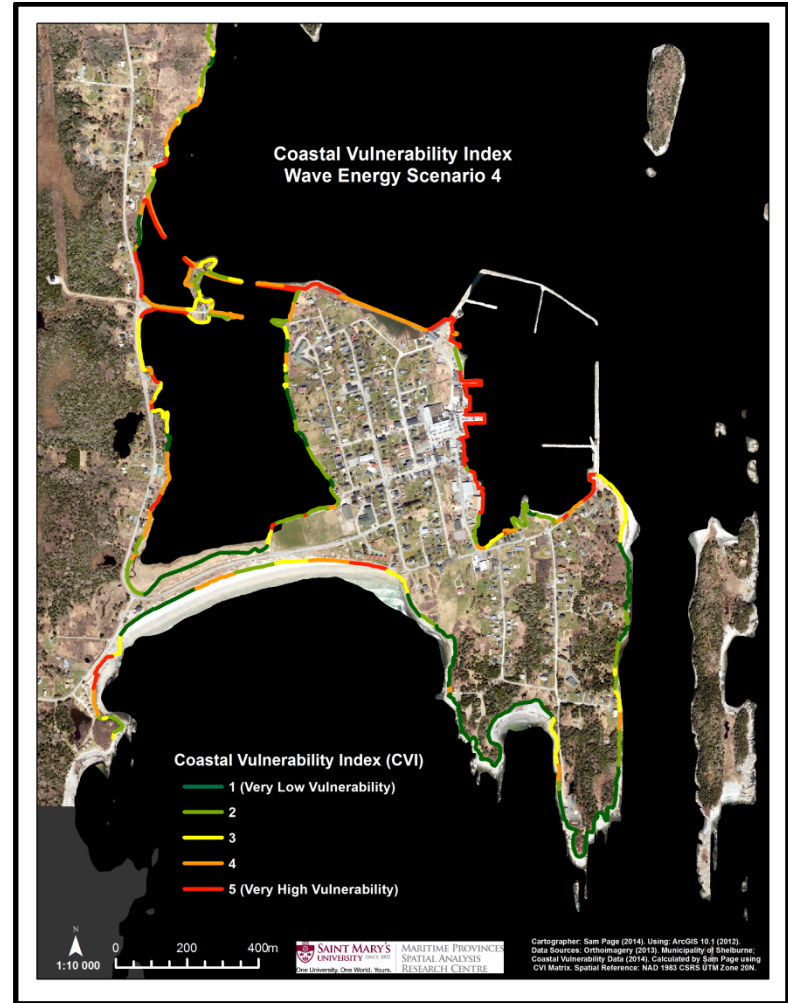


Figure 4.13 Coastal Vulnerability Index Wave Energy Scenario 4. CVI values are derived using the CVI Matrix (Table 4.1).

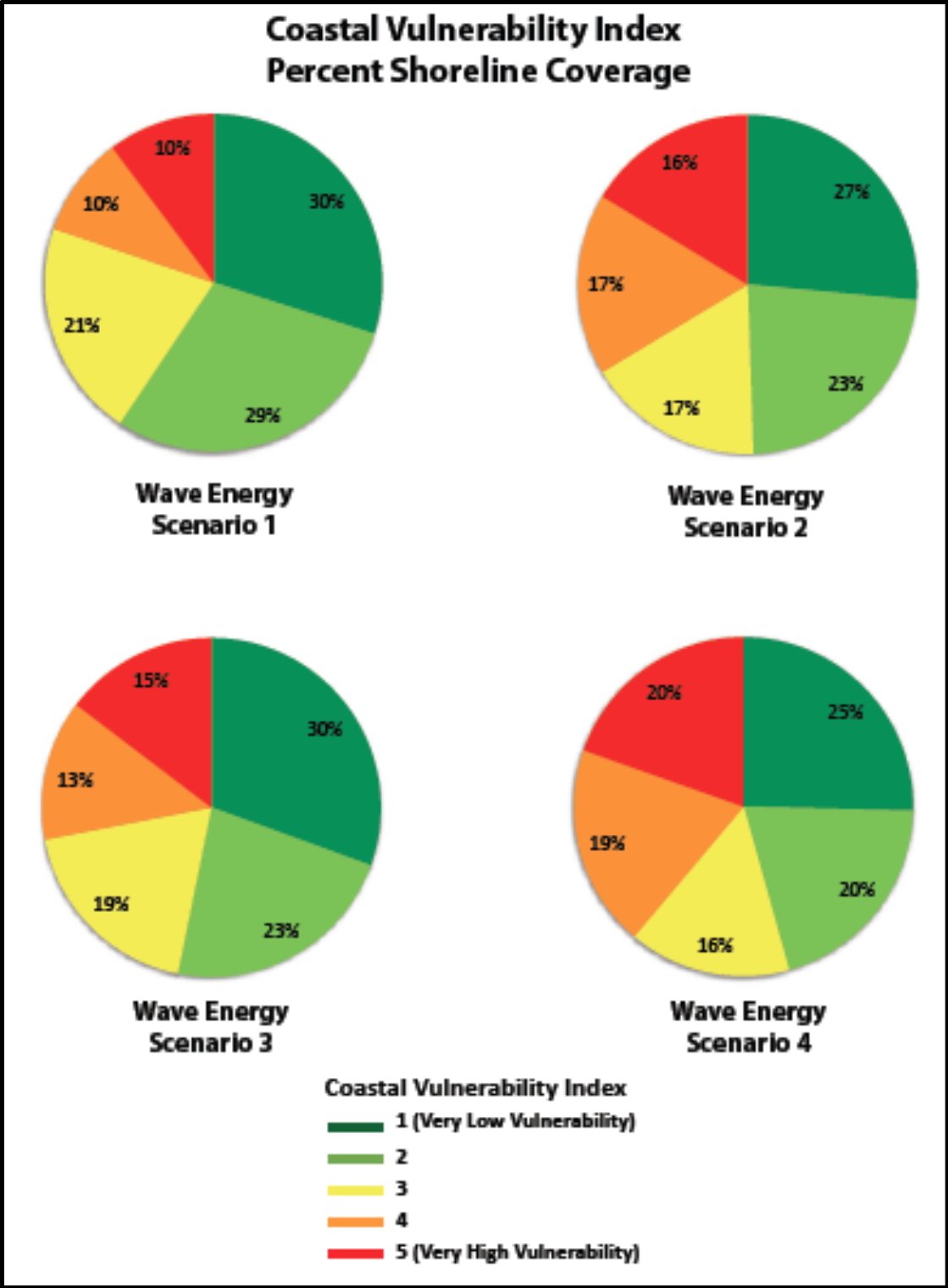


Figure 4.14 Percent of Shoreline Associated with each Vulnerability Rank for Wave Energy Scenarios 1 to 4.

4.2.1 Proof of Concept

Comparisons of identified vulnerable shorelines with observed erosion points and areas of concern noted in the MCCAP (Atwood, 2013) were made to help illustrate the validity of the matrix. Furthermore, a PCA was used in an effort to interpret relationships between parameters and to help identify parameters that contribute to high vulnerability scores in this study.

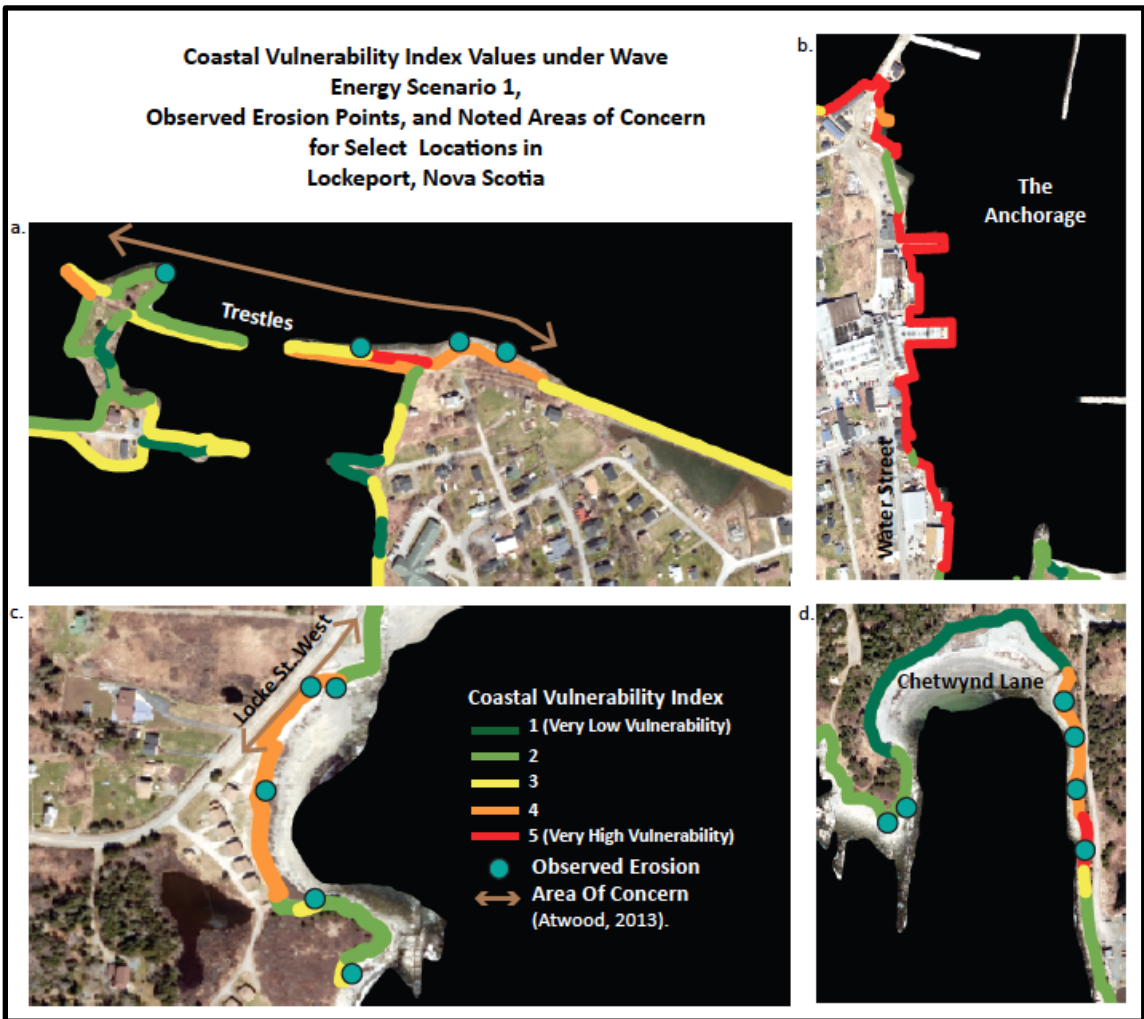
4.2.1.1 Observed Erosion & Areas of Concern

Before describing the relationships between areas of concern, vulnerable shorelines, and observed erosion points in this study, it is important to understand that the areas of concern noted by Atwood (2013) are primarily focused on their risk to storm surge and flooding, and secondly that the observed erosion points collected in the field do not necessarily account for every point of erosion for the shoreline of Lockeport. Therefore the lack of erosion points along a stretch of shoreline does not absolutely indicate that the segment is not susceptible to erosion.

With that in mind, the most vulnerable stretch of shoreline identified for S1 was located along North and South Water Street within the confines of the two large Breakwaters (Figure 4.24b), however it does not correspond with any observed erosion points. The Trestles (Figure 4.24a) illustrate a stretch of shoreline that is an area of concern, has observed erosion points, and is an identified vulnerable shoreline, although not as much as North and South Water Street. Similar to the Trestles, Locke Street West, depicted in Figure 4.24c, shows a convergence of a noted area of concern, observed erosion points and a *highly* vulnerable shoreline. This location is low-lying and has an erodible backshore bounded by two hard outcrop formations. The other site chosen for observation is Chetwynd Lane (Figure 4.24d). The MCCAP (Atwood,

2013) notes Chetwynd Lane as a primary area of concern when it comes to flooding, however this study illustrates that from an erosion perspective, this area is not *highly* vulnerable. The MCCAP (Atwood, 2013) also notes that the shoreline east of Chetwynd Lane is susceptible to erosion events, which also aligns with the CVI scores calculated for that stretch of shoreline as well as with observed erosion points.

Figure 4.15 Coastal Vulnerability Index Values under Wave Energy Scenario 1, Observed Erosion Points, and Noted Areas of Concern for Select Locations in Lockeport, Nova Scotia. (Area of Concern is based on MCCAP report (Atwood, 2013), coastal vulnerability values derived by Sam Page using CVI matrix, and erosion points observed in the field.)



4.2.1.2 Principal Components Analysis

A PCA is used to reduce dimensionality of data with a goal to either use the simplified principle components (PCs) in further data analyses or to interpret relationships and patterns within the data set, the latter of which was employed in this research. The statistical program R returned 11 eigenvectors (Table 4.3) that account for the entire variation in the data. Of the 11 PCs, four had eigenvalues greater than 1 and, using the Kaiser-Guttman (Jackson, 1993) stopping rule, these four PCs accounted for the majority of variance within the original data set. The proportion of variability accounted for by PC1, PC2, PC3, and PC4 was 20.11%, 18.04%, 13.00%, and 10.98% respectively, for a cumulative total of 62.13%. The bi-plots depicted in Figures 4.16, 4.17, and 4.18, show that, in all cases, the three highest CVI scores (represented by the largest circles) are more or less clustered together, indicating that the same parameters are contributing to the *very high* vulnerability score. Looking at the original data set, it can be seen that the backshore segments with *very high* vulnerability scores (BS #77, BS #82, and BS #83) all have *very high* ranks of Morphological Resilience, Foreshore Geomorphology, Foreshore Slope, Backshore Vegetation, and Accommodation Space (i.e., very low actual Morphological Resilience, Foreshore Geomorphology, Foreshore Slope, Backshore Vegetation, and Accommodation Space), illustrating that these parameters are most likely driving the *very high* vulnerability scores in this study. Conversely, these shorelines have relatively low ranks of Sediment Supply, and Wave Energy (i.e., *high* to *very high* actual Sediment Supply and *low* to *very low* actual Wave Energy), indicating that these parameters do not likely drive high vulnerability scores in this study.

Table 4.3 Principal Components Analysis Loadings and Variance. Where PC = Principal Component.

		PC1	PC2	PC3	PC4	PC5	PC6	PC7	PC8	PC9	PC10	PC11
		Loadings										
Original Parameters	Wave Energy	-0.06	-0.54	0.07	-0.05	0.20	-0.12	0.51	-0.56	0.09	-0.18	0.15
	FS Geomorphology	0.02	-0.09	-0.23	-0.78	-0.12	-0.08	-0.37	-0.24	0.06	0.16	0.30
	FS Slope	0.06	-0.17	0.33	-0.20	-0.83	-0.04	0.27	0.11	-0.15	-0.04	-0.16
	FS Width	0.36	0.28	0.21	0.25	-0.14	-0.45	-0.20	-0.53	-0.07	0.34	0.11
	BS Elevation	0.14	0.52	0.19	-0.20	0.05	0.35	0.05	-0.38	0.06	-0.52	-0.30
	BS Slope	0.05	-0.48	0.34	0.05	0.08	-0.14	-0.62	-0.01	0.18	-0.26	-0.36
	BS Vegetation	0.42	-0.04	0.16	-0.41	0.42	-0.15	0.25	0.20	-0.22	0.33	-0.42
	Coastal Protection Structures	-0.44	0.15	0.30	-0.17	0.18	-0.36	-0.08	0.07	-0.60	-0.27	0.22
	Morphological Resilience	0.31	-0.17	0.46	0.13	0.11	0.58	-0.08	0.06	-0.25	0.10	0.46
	Accommodation Space	0.54	0.05	-0.08	-0.07	0.01	-0.36	0.07	0.34	0.21	-0.50	0.40
	Sediment Supply	0.30	-0.21	-0.55	0.16	-0.10	0.09	-0.12	-0.15	-0.63	-0.23	-0.17
	λ (variance)	2.2123	1.9847	1.4301	1.2029	0.9631	0.8306	0.6588	0.5092	0.4506	0.4087	0.3473
	% of Variation Explained	20.11	18.04	13.00	10.98	8.75	7.55	5.99	4.63	4.09	3.71	3.15
	Cumulative % of Variation Explained	20.11	38.15	51.15	62.13	70.88	78.43	84.42	89.05	93.14	96.85	100

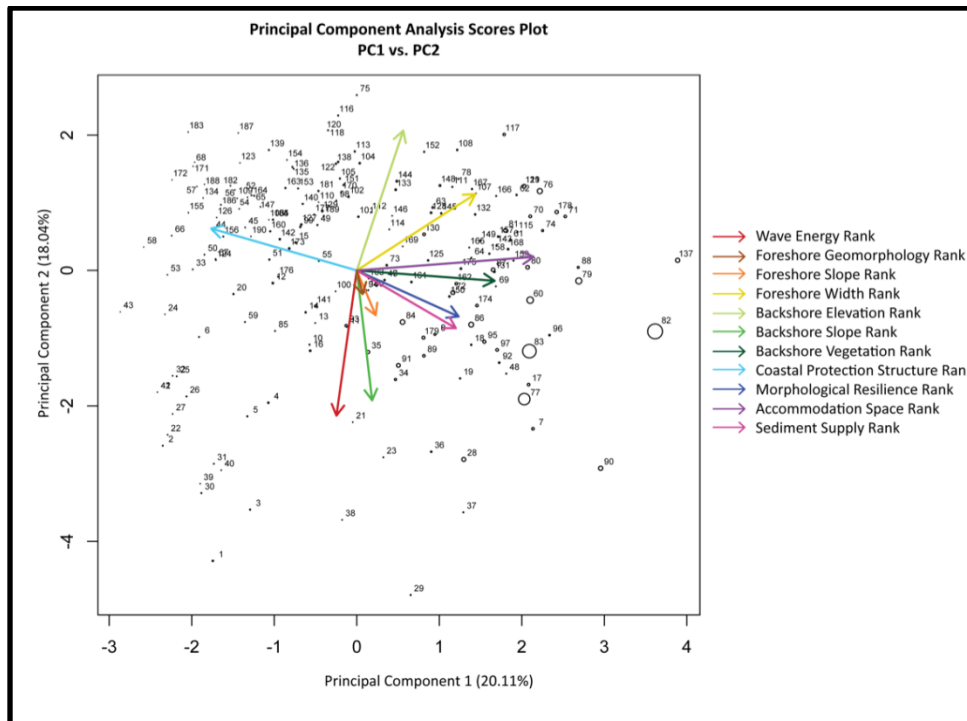


Figure 4.16 Principal Component Analysis Scores Plot (PC1 vs. PC 2). Graphs derived using R stats program. Circles depict CVI scores for each BS segment, with larger circles representing higher CVI scores and smaller circles representing lower CVI scores.

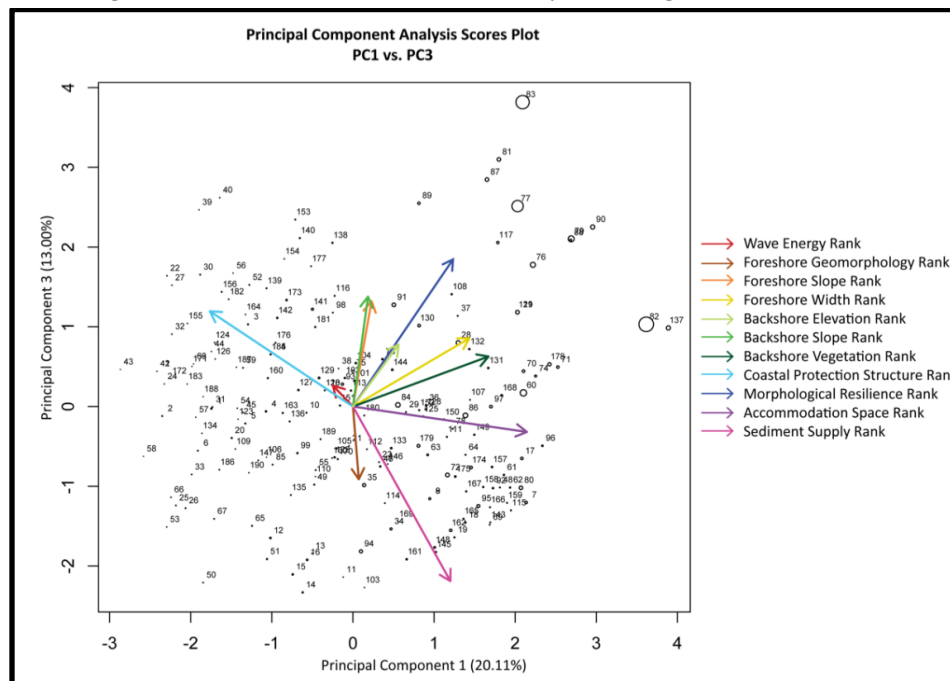


Figure 4.17 Principal Component Analysis Scores Plot (PC1 vs. PC 3). Graphs derived using R stats program. Circles depict CVI scores for each BS segment, with larger circles representing higher CVI scores and smaller circles representing lower CVI scores.

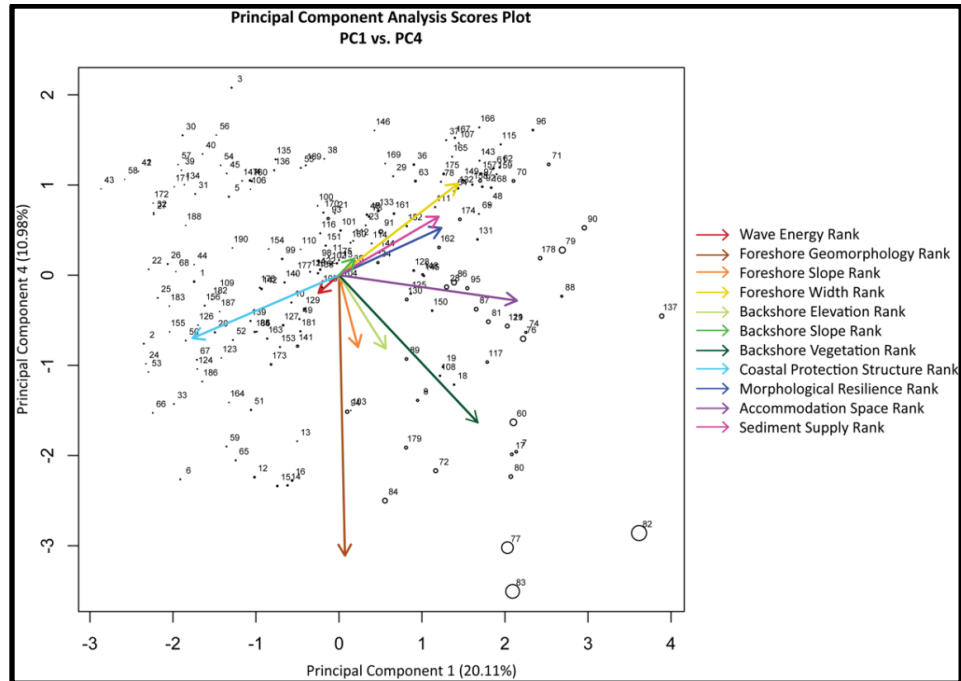


Figure 4.18 Principal Component Analysis Scores Plot (PC1 vs. PC 4). Graphs derived using R stats program. Circles depict CVI scores for each BS segment, with larger circles representing higher CVI scores and smaller circles representing lower CVI scores.

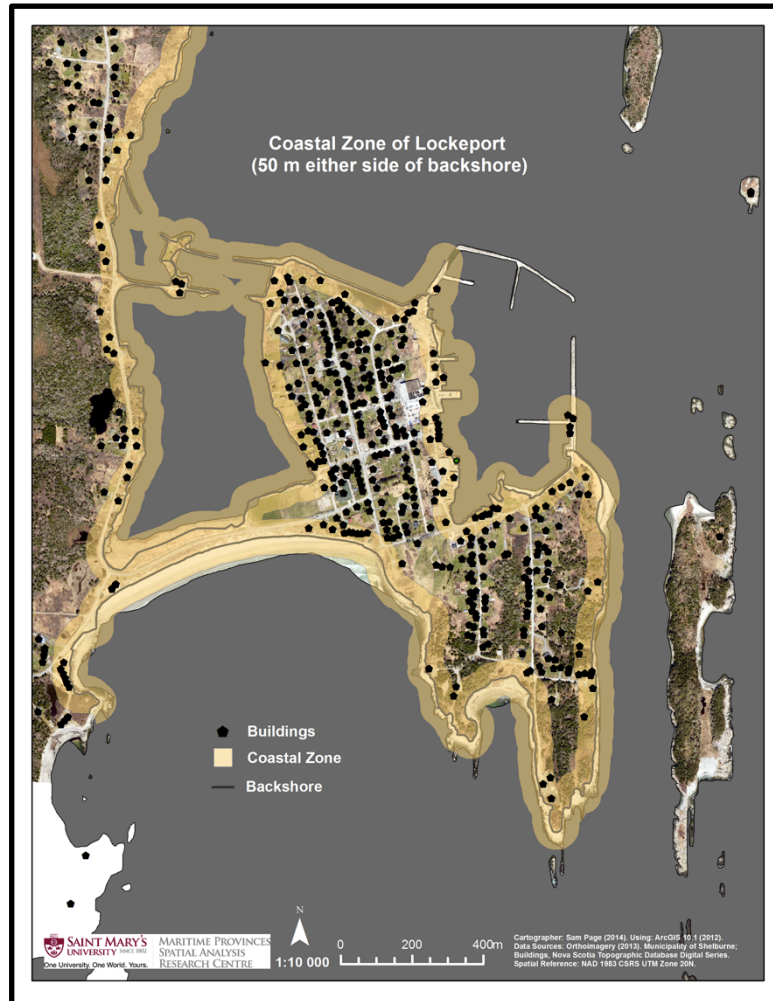
4.3 Identification of Vulnerable Buildings (Steps 3 & 4)

The vulnerability of buildings located within the coastal zone was determined for wave energy scenarios S1, S2, S3, and S4 by delineating the coastal zone for Lockeport, identifying buildings vulnerable to erosion and separately, identifying buildings vulnerable to both erosion and inundation.

4.3.1 Coastal Zone Delineation

The coastal zone, defined for this research as the *area of low-lying land extending 50 m landward and seaward from the backshore*, was delineated for Lockeport, Nova Scotia (Figure 4.19). Using that definition, the coastal zone of Lockeport encompasses a large extent of Brighton Road, all of Crescent Beach, Crescent Beach Causeway and the marsh directly adjacent,

the Trestles, Calf Island Road, Water Street, historic South Street and associated residences, Rood's Head, and the majority of the wharves, and includes 122 buildings. It does not however encompass the majority of the Breakwaters nor the Electricity Substation.



4.19 Coastal Zone of Lockeport, Nova Scotia. For this research the coastal zone is defined as the area 50 m either side of the backshore line.

4.3.2 Buildings Vulnerable to Erosion

As scenarios progress, from S1 to S4, the number of *very highly* vulnerable buildings increases and the number of both *moderate* and *low* vulnerability buildings decreases (Figure

4.20-4.23). For the lowest vulnerability rank (Rank 1) the number of included buildings remains the same across all four scenarios.

The largest net change in number of buildings associated with a rank, occurs for Rank 5, which experiences a net increase of 26 buildings from S1 to S4. Rank 3 and Rank 2 both experience a net decrease in number of vulnerable buildings from S1 to S4 with an overall loss of nine and fourteen buildings respectively. From one scenario to another, the greatest change in building numbers occurs between S2 and S3 with a gain of ten buildings for Rank 5.

With respect to specific locations (Figures 4.21-4.24), the majority of vulnerable buildings in S1 are located along Water Street and the North and South Wharves. From S1 to S2, only two buildings, located on the north side of Locke Island, progress to a *very high* vulnerability designation, which are located on the north side of Locke Island. In S3, the Ocean Mist Cottages become *very highly* vulnerable along with a few residences on Brighton Road. In the final wave energy scenario (S4), three additional houses along Brighton Road, and one on the historic South Street become *very highly* vulnerable. Throughout all scenarios, the buildings which remain *very lowly* vulnerable to erosion include those located near Rood's Head, Sam's Point, a few along the east side of Back Harbour, one along the coast facing Cranberry Island and the Crescent Beach Center and its adjacent buildings. Across all scenarios the pockets of buildings with *moderate* to *high* vulnerability ranks are focused around Crescent Beach (with the exclusion of the Crescent Beach Centre), sporadically along Brighton Road, the north side of Locke Island, historic South Street, Calf Island Road, and a few on the east side of Locke Island.

4.3.3 Buildings Vulnerable to Erosion & Inundation

Inundation associated with Wave Energy Scenario 3 (2.21 m increase in water level) and Wave Energy Scenario 4 (3.10 m increase in water level) is illustrated in Figures 4.26 and 4.27 respectively. Inundation from a 2.21 m increase in water levels does not flood Crescent Beach Causeway or Brighton Road, but does appear to cause damage to portions of South Street, Chetwynd Lane, the Breakwaters, and completely submerges Calf Island Road and Upper Water Street. Inundation associated with a 3.10 m increase in water levels causes substantially more damage to the Town of Lockeport, with Crescent Beach Causeway, portions of Brighton Road, all of Calf Island, the Trestles, all of historic South Street and South Water Street being affected by water. This scenario also results in the division of Locke Island between John Street and Church Street all the way from Chetwynd Lane to The Anchorage. Additionally, an increase in water levels of 3.10 m results in overtopping of the entire extent of both Breakwaters.

Buildings which are located within the coastal zone and which are vulnerable to erosion and inundation increase from 16 to 47 under S3 and S4 respectively (Figure 4.39), with a net positive change across all ranks. Of the 16 buildings vulnerable under S3, 10 have a *very high* vulnerability rank and are located along Water Street and the North and South Wharves (Figure 4.28). The remaining six buildings include residences on Calf Island, South Street, and Point Street along with the Crescent Beach Centre. In this scenario, the only building that is susceptible to inundation but not found within the coastal zone is the Electricity Substation located at the corner of Upper Water Street and North Street. Under S4, associated with 3.10 m of inundation, an additional nine buildings are designated as being *very highly* vulnerable, including more buildings on Water Street, and three more buildings along Locke Street (Figure 4.29). The remaining 26 buildings with vulnerability ranks of 4 or lower are found along Locke

Street, including the Little School Museum, the east side of Back Harbour, Calf Island and a few along South Street. In this scenario the very few buildings that are vulnerable to inundation, but do not fall within the coastal zone include the Electricity Substation, a private residence at the corner of Upper Water Street and North Street, and three private residences between John Street and Church Street.



Figure 4.20 Vulnerability of Buildings in the Coastal Zone to Erosion under Wave Energy Scenario 1.



Figure 4.21 Vulnerability of Buildings in the Coastal Zone to Erosion under Wave Energy Scenario 2.



Figure 4.22 Vulnerability of Buildings in the Coastal Zone to Erosion under Wave Energy Scenario 3.

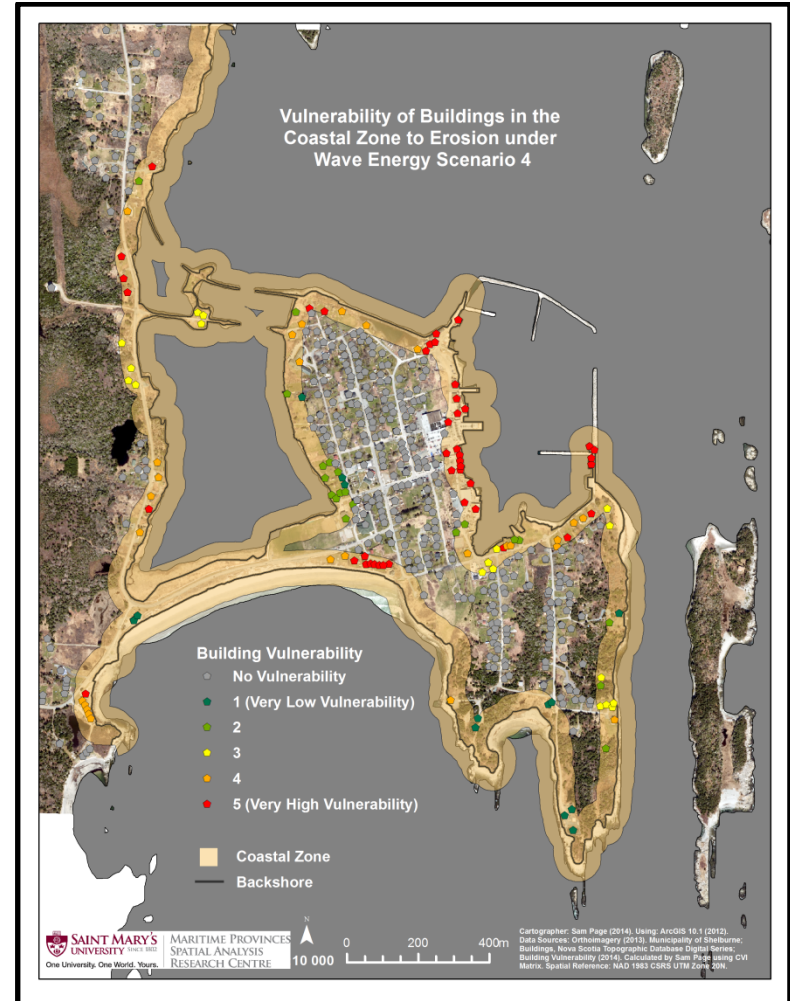


Figure 4.23 Vulnerability of Buildings in the Coastal Zone to Erosion under Wave Energy Scenario 4.

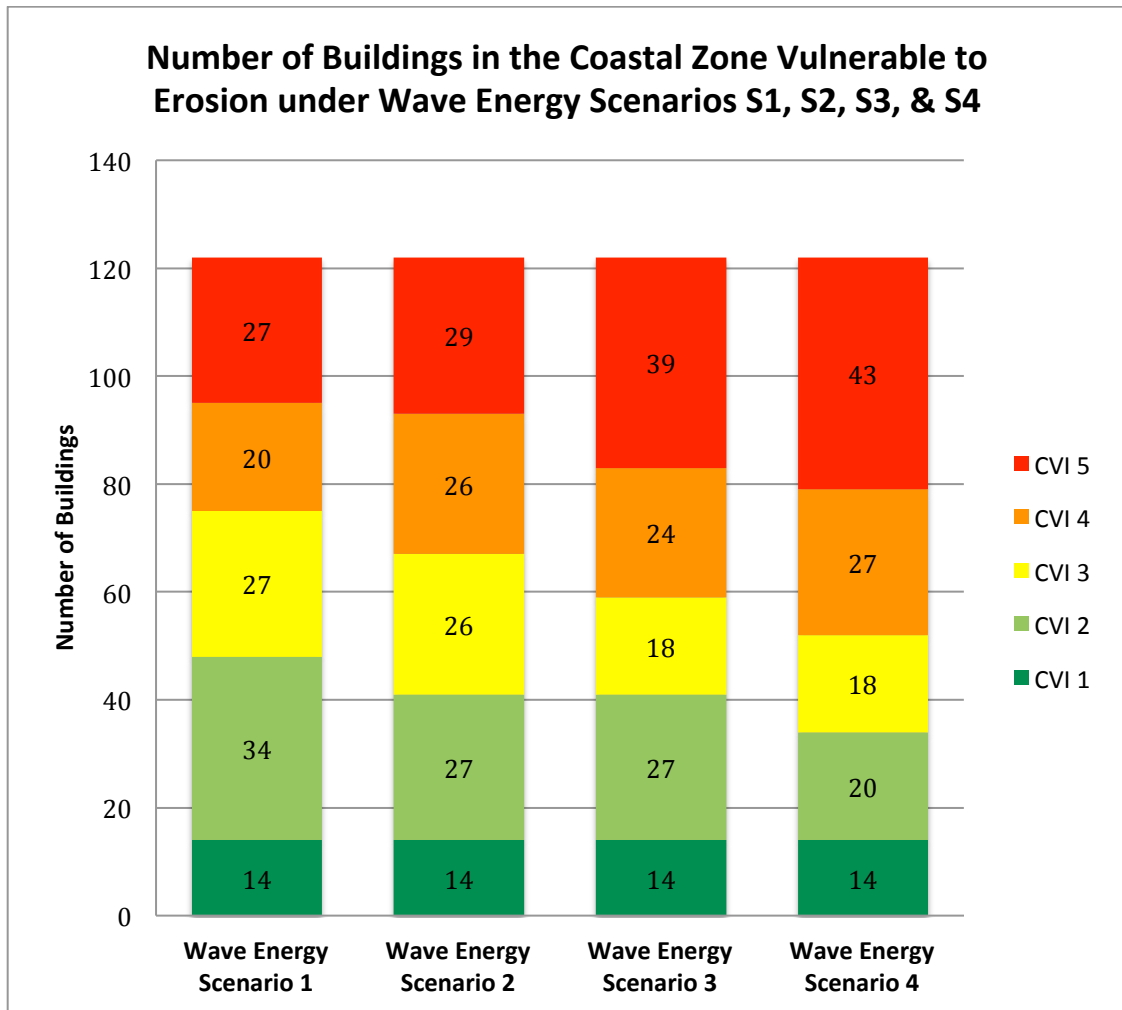


Figure 4.24 Number of Buildings in the Coastal Zone Vulnerable to Erosion under Wave Energy Scenarios 1 to 4.

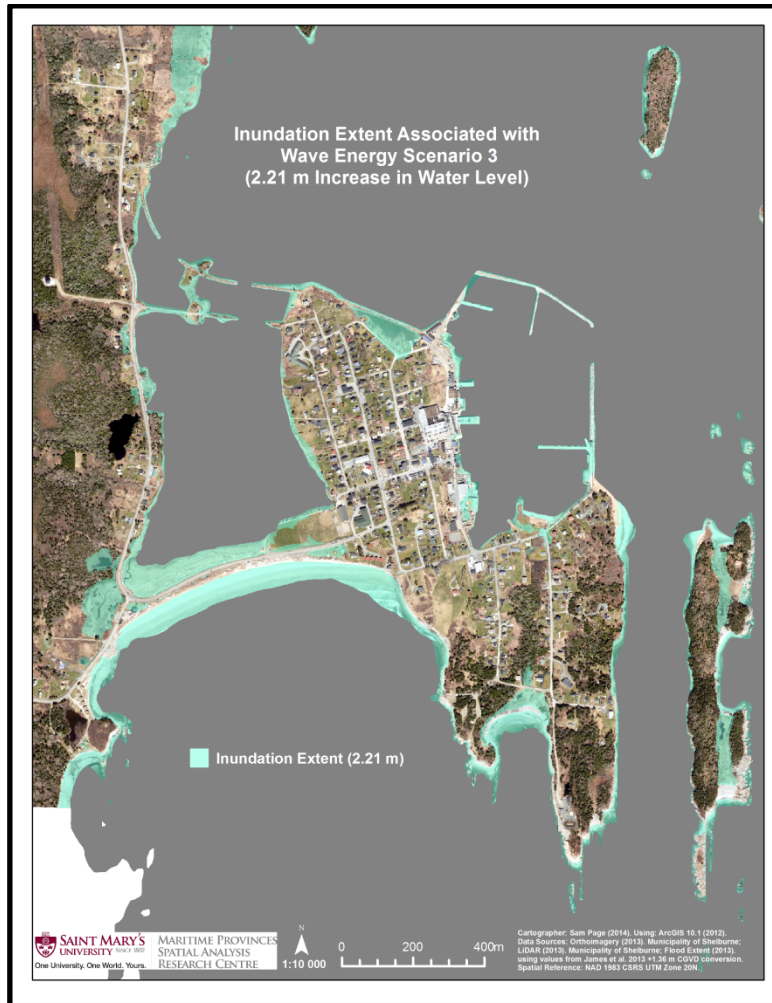


Figure 4.25 Inundation Extent Associated with Wave Energy Scenario 3. Inundation extent associated with a 2.21 m increase in water levels.

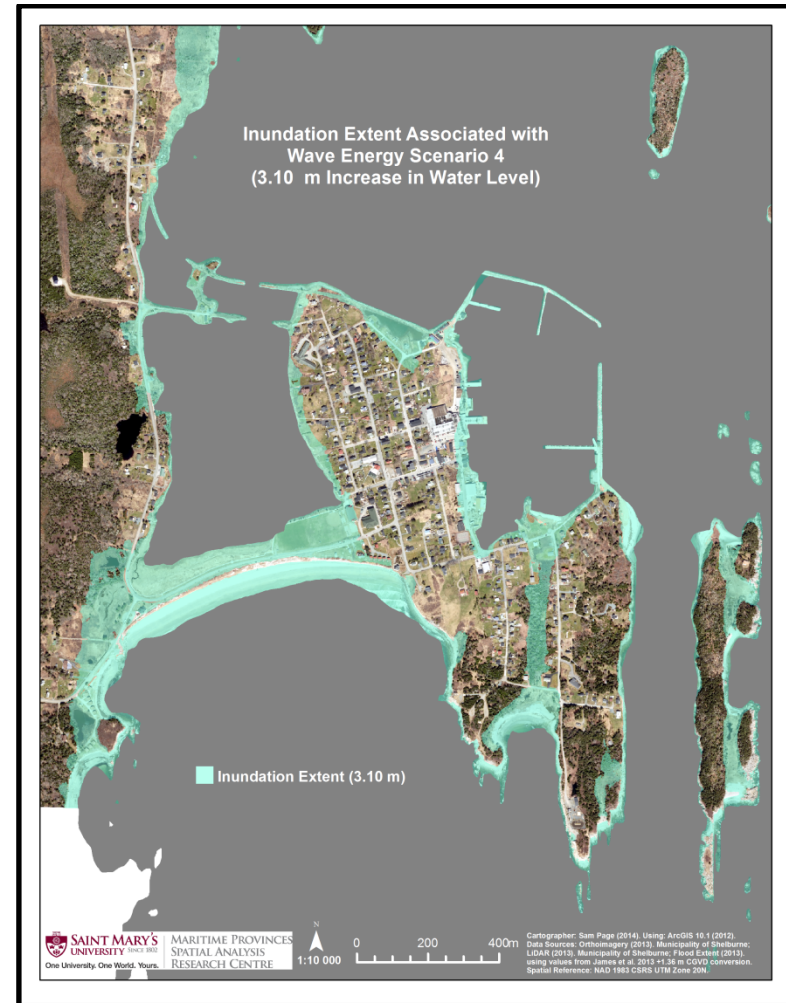


Figure 4.26 Inundation Extent Associated with Wave Energy Scenario 4. Inundation extent associated with a 3.10 m increase in water levels.

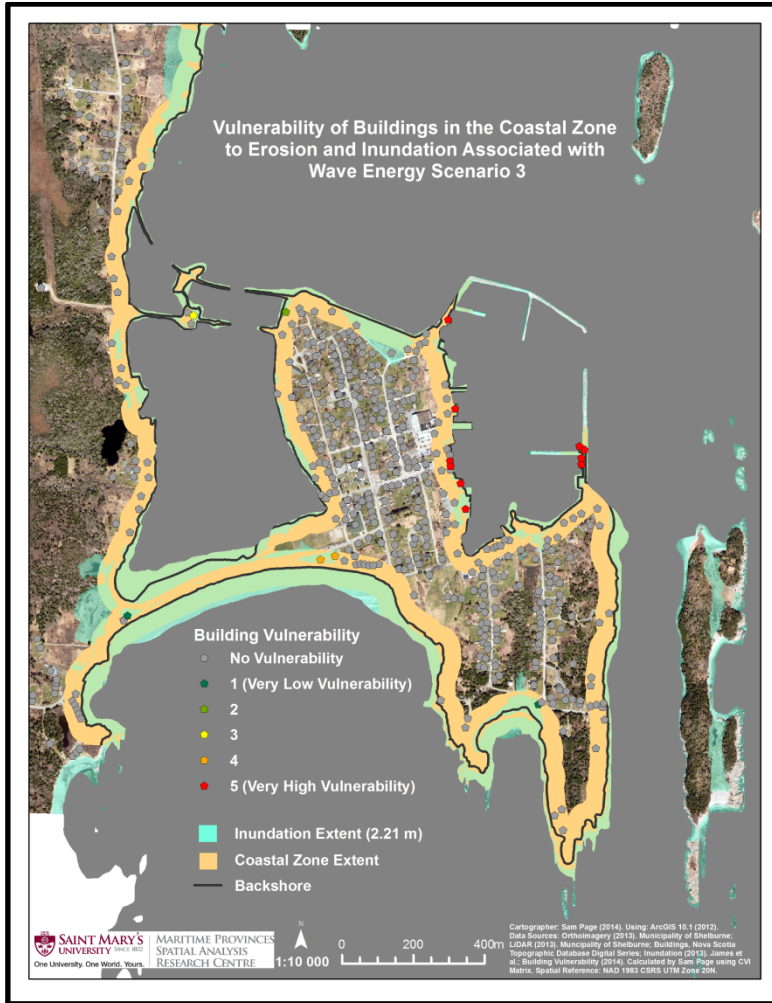


Figure 4.27 Vulnerability of Buildings in the Coastal Zone to Erosion and Inundation Associated with Wave Energy Scenario 3.

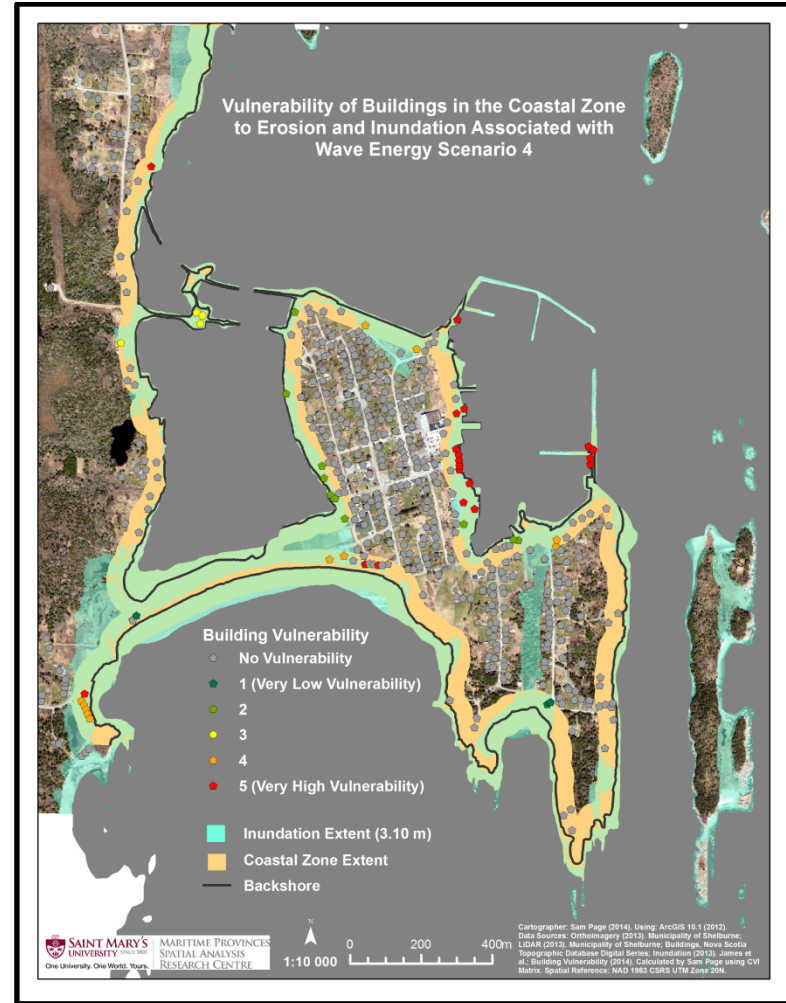


Figure 4.28 Vulnerability of Buildings in the Coastal Zone to Erosion and Inundation Associated with Wave Energy Scenario 4.

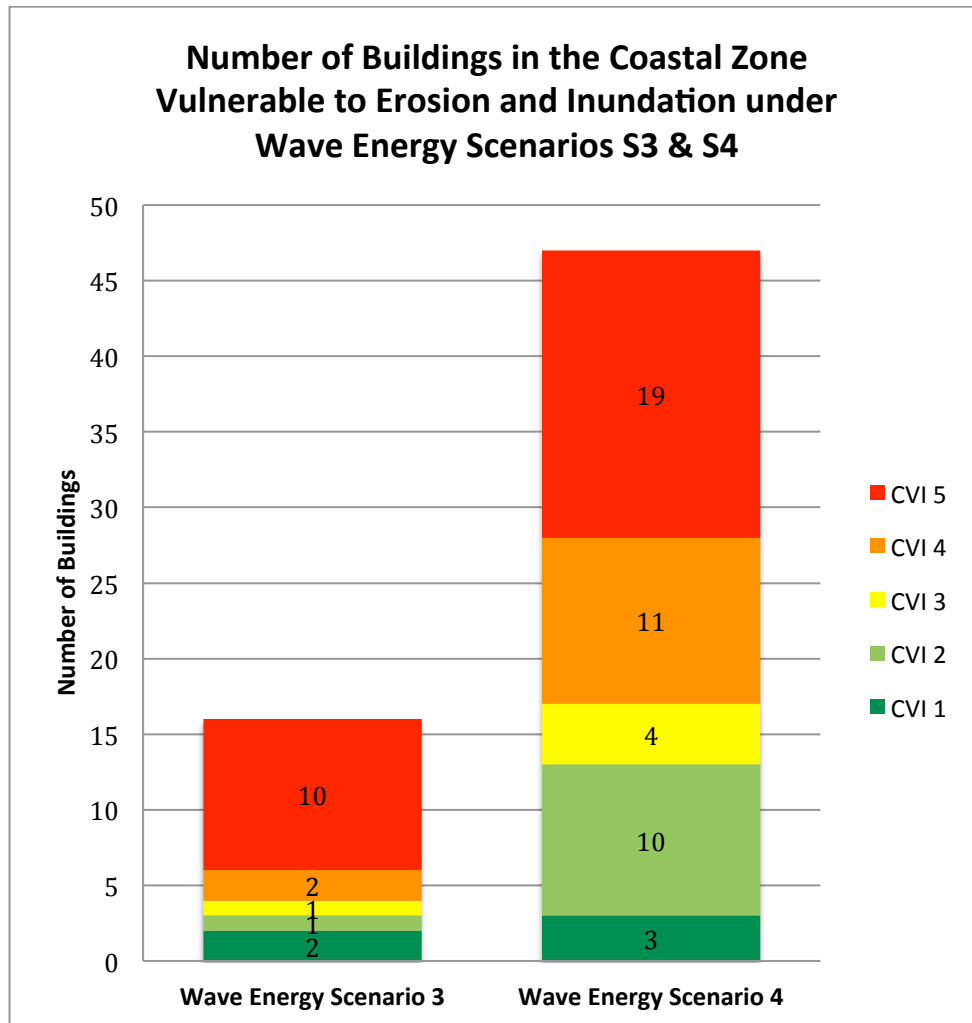


Figure 4.29 Number of Buildings in the Coastal Zone Vulnerable to Erosion and Inundation under Wave Energy Scenarios 3 and 4

Chapter 5

DISCUSSION

5.1 Introduction

This chapter frames the results of this research within the context of the research objectives outlined in Section 1.6. Additionally, specific recommendations are made for the areas of Lockeport found to be most vulnerable to current and future SLR induced erosion and/or inundation.

5.2 Field Based Shoreline Characterization for Assessing Vulnerability

One challenge with coastal characterization is that the needs of one classification technique do not necessarily meet the needs of another, resulting, over time, in the development of multiple coastal classification techniques. Techniques vary based on the methodology used to collect and interpret the data (e.g., LiDAR, GIS, field-based etc.) and the way in which a coast is classified, such as noted by Inman and Nordstrom (1971), who proposed that coastal morphology could be classified according to its position on varying types of tectonic plates, or Davies (1972), who classified coasts according to the differences in wave environments (Trenhaile, 2004; Short, 2007).

Often coasts are characterized using spatial imagery, including the use of aerial coastal video and imagery to collect data on geomorphic form and material composition of coastal features (Jenner et al., 2003), the use of historical Landsat imagery and Digital Shoreline Analysis System (DSAS) to characterize shoreline change (Gomez et al., 2014), and more recently, the use of hyper spectral imagery (Bachmann et al., 2012; Bachmann et al., 2010a; Bachmann et al., 2010b), and LiDAR (Woolard & Colby, 2002). While these techniques allow for large areas to be characterized in a relatively short time period and may provide sufficient detail at a regional to national scale, such as with the Canadian Coastal Information System developed by Sherin in 1994 and the CanCoast national spatial database developed by NRCan (Natural Resources Canada) in 2001 (Smith et al., 2013), the use of these techniques for local level vulnerability assessments can lead to the misrepresentation of vulnerable areas.

In this study, the use of the field-based shoreline characterization technique for assessing coastal vulnerability, developed by Pietersma-Perrot & van Proosdij (2012), resulted in the collection of very detailed coastal characterization data, which in turn facilitated a comprehensive assessment of coastal vulnerability. This methodology, which uses a YUMA Trimble outfitted with GIS and GPS, has a measurement accuracy of $\pm 2-5$ m (Pietersma-Perrott & van Proosdij, 2012). Additionally, the method of collecting data in the field allowed for a better estimation of height of features (e.g., cliffs and bluffs), the identification of areas of erosion and type/presence of CPSs not visible with aerial imagery, and a decrease in the likelihood of mis-characterizing coastline formations. For example, Lockeport has over 80 CPSs, which are sometimes quite hard to differentiate from clastic slopes, and, additionally, it is not feasible to obtain measurements of individual armour stones or state of functioning, which in Lockeport, ranges from abandoned to intact. It is cases like these that truly showcase the

invaluable strengths of the field-based SCD. This methodology also incorporated the collection of data for multiple shoreline vectors, allowing for the shorezone to be treated as a comprehensive, interacting unit as opposed to a static line.

While this field based method, which requires researchers to walk along the entire shoreline, can be challenging along coastlines comprised of cliffs or a headland-bay morphology, and time consuming for larger study areas, the detail of data derived from this technique is extremely useful at the local scale. The use of a video-boat surveying technique (Shoreline Video Assessment Method), developed for use in the Mangrove Watch program to monitor the health of mangrove ecosystems (Mackenzie & Duke, 2012), could be adapted for use in characterizing inaccessible coasts and decreasing characterization time, thus allowing for larger areas to be surveyed.

For smaller scale assessments (e.g., regional, provincial, or national), which do not require as much detail, the field-based characterization method may not be the best option, especially where the use of LiDAR or hyper spectral imagery (Bachmann et al., 2012; Woolard & Colby, 2002) may supply sufficient detail. While LiDAR can be costly and not always available, it provides very detailed measurements for the creation of DEMs (± 0.2 m in the vertical direction and ± 0.5 m in the horizontal direction) and can be rapidly collected (Horne, 2013; Woolard & Colby 2002). However, in this study, the combination of field based shoreline characterization and LiDAR allowed for detailed on-the-ground data to be collected, while still providing the ability to determine precise elevation and foreshore width values from the detailed orthoimagery. Combining techniques was successful in another study that used a multi-sensor approach to coastal characterization combining thermal imagery, synthetic aperture radar

(SAR), LiDAR, and hyper spectral imagery (Bachmann et al., 2012). In summary, there is no one best technique for coastal characterization and, in fact, the best results come from the combination of multiple techniques to suit the particular needs of the characterization. However, at a local scale, the detail provided by the field based characterization methodology is invaluable.

5.3 CVI Development

The purpose of a CVA is to identify people and places that are vulnerable to an event and to use this knowledge as a guide in adaptation and decision making processes with a view to increasing a community's adaptive capacity (McLaughlin & Cooper, 2010; Luers, 2005). While an approach that predicts the precise effects of a climate change -related event, such as a rise in sea level, does not yet exist, the relative vulnerability of a coast to any event can be assessed using parameters (Thieler & Hammar-Klose, 2000). Literature suggests that CVAs are a key step in the adaptation process; they help determine how to best manage risk (Palmer et al., 2011), are advantageous in minimizing socio-economic impacts from SLR (Koutrakis et al., 2011), serve as a rapid assessment of a large area, which helps to identify areas that require a more detailed study, and provide a valuable framework to help managers allocate limited funds to areas in greatest need (Abuodha & Woodroffe, 2010; Hedge & Reju, 2007). While many assessment methodologies exist (Ramieri et al., 2011), the benefits of CVIs in particular, include their ability to incorporate both qualitative and quantitative data and to simplify a number of key coastal parameters to create a single indicator that is more easily understood (McLaughlin & Cooper, 2010; Sterr, 2008), ultimately aiding in the dissemination of complex scientific concepts to policy makers and community members (Hinkel, 2011).

While vulnerability indices can be extremely useful in their ability to simplify complex systems into a single score, the choice of parameters included, the interpretation of the parameter contribution to vulnerability, the choice of formula used for calculation, the weighting of parameters, and the division of parameter characteristics and/or values into classes that rank their contribution to vulnerability can vary extensively with individual study purposes and researchers. For example, with varying CVIs, the presence of CPSs solicits a *very high* or *very low* vulnerability rank based on the way in which the researcher views the parameter's contribution to vulnerability (Sousa et al., 2012; Torresan et al., 2012; Tibbetts & van Proosdij, 2013; Szlafsztein & Sterr, 2007). Though this decision process may appear seemingly arbitrary, the decisions surrounding these choices are generally based on published and peer reviewed literature and knowledge of the processes and landforms present in the coastal zone, which is the case in this research. It is important however, for users of the indices to understand that CVIs are not an absolute measure of vulnerability, but are scores based on various assumptions and conditions. Furthermore, Hinkel (2011), who identified six recurring themes in the vulnerability literature regarding indicator purpose, discovered that the use of indicators was appropriate for only one of these themes: the identification of vulnerable areas and people at the local scale, resulting in the discovery that there is often a disconnect between the problems meant to be solved by indicators and what the indicator truly indicates.

With these concepts in mind, it is important to understand that the vulnerability matrix developed in this research is meant to, at the local scale, identify areas of the coast that are physically vulnerable to erosion, after which the socio-economic infrastructure located in these physically vulnerable areas can be determined. It does not, however, assess the vulnerability of humans to erosion, which would incorporate aspects such as population density, perception of

risks, education, age etc. While the difference between these two interpretations may seem minute, differentiating between the two becomes crucial when interpreting the index properly.

Additionally, the defined assumptions and conditions of this study are that:

1. the chosen parameters contribute to vulnerability as designated in the CVI matrix
2. there are no synergistic relationships between parameters
3. the square root of the product mean provides the best calculation of vulnerability
4. each CCC contributes equally to vulnerability of the coast
5. the human/ socio-economic component of the coast does not affect coastal vulnerability to erosion
6. quantitative parameters were classified using the most appropriate classification technique
7. the final CVI score is relative and therefore not comparable to other studies
8. the matrix assesses physical coastal vulnerability to erosion/geomorphic change

While these challenges could be looked upon as a negative consequence of using vulnerability indices, in actuality, vulnerability indices and their ability to simplify complex, often interrelated parameters are extremely useful, as long as the use of the index in adaptation planning matches the intent for which it was created as long as and managers and community members who use the index, use it with an understanding of the acknowledged assumptions and conditions.

5.4 Incorporation of Geomorphic Resilience

Ignoring the discrepancies in terminologies and precise definitions, which have been thoroughly reviewed by Adger (2006), Folke (2006), and Smit & Wandel (2006), it can be said that the vulnerability of a system has essentially three defining components: exposure, sensitivity, and adaptive capacity (Adger, 2006; Engle, 2011; IPCC, 2007). Over the past two decades, the coastal system has increasingly been recognized in the literature as a system with biophysical and socio-economic components that are intrinsically interconnected and evolve together (Phillips, 2009; Klein et al., 1998; Gallopín, 2006). This has led to the call for holistic vulnerability assessments that incorporate both the natural and socio-economic components (Nicholls & Branson, 1998; Gallopín, 2006). An attempt at this has been made with the development and use of socio-ecological systems (SEs) in vulnerability assessment literature (Gallopín, 2006; Adger, 2006; Folke, 2006; Gallopín, 1991). Despite its widespread application, upon closer review of literature employing this concept, it was found that these studies focus more on the vulnerability of the socio-economic component within the physical environment and do not do justice to the vulnerability of the physical system itself. They also frame the resilience aspect of the SES solely around social resilience, incorporating parameters such as access and distribution of resources, technology, information and wealth, risk perceptions, social capital, education, information, and skills (Dolan & Walker, 2004; Luers, 2005; Adger, 2006). While there is no doubt that social and ecological systems operate jointly and that together they can provide a holistic assessment of vulnerability, it is important to understand how the individual components of the socio-ecological system operate and interact prior to integrating them into one assessment. A conceptual diagram for the assessment of coastal vulnerability developed by Klein and Nicholls (1999) illustrated that a successful analysis of

socio-economic vulnerability requires prior understanding of the natural system. Hinkel (2011) and Gallopín (2006) both note that the individual study of either the social or physical components of a vulnerable system is a commonly used approach and can provide integral understanding of the individual components. Thus, this research has set out to develop a physical CVI based on the principles of geomorphology to assess vulnerability of the coastal zone to erosion, with a view to being integrated into a vulnerability assessment of both human and physical systems in future research.

In the field of geomorphology, which essentially studies the responses and changes of landforms to persistent or discrete disturbances (Phillips, 2009), the stability of a landscape and hence its vulnerability to geomorphic change has been described by Brunsden (2001) and Klein et al. (1998) as being a function of resisting, disturbance (exposure) and resilience components. Due to the interconnected nature of the coastal system, successful vulnerability assessments of geomorphic change require a holistic approach (Woodroffe, 2007), where all landscape stability components are taken into consideration - the importance of which is outlined by Crooks (2004). Phillips (2009) specifically notes the importance of a holistic approach in the application of frameworks and analyses for assessing geomorphic change.

In this research, the terms assailing, resistance, and resilience were used to denote the aforementioned disturbance, resistance and resilience components of landscape stability and the theoretical relationships between coastal vulnerability. These individual components (called CCCs in this study) were explored in section 4.1.3 and Figure 4.9. This conceptual model shows that a coast with very low actual resistance and resilience (i.e., *very high* vulnerability rank), is *very highly* vulnerable when exposed to very high disturbance events (i.e., *very high* vulnerability

rank). It also illustrates that despite the level of resilience, coastlines with *very low* ranked assailing forces (i.e., very low actual assailing) and resistance forces (i.e., very high actual resistance), result in a coast with *very low* vulnerability. However, the role of resilience in reducing overall coastal vulnerability is evident; a notion supported by Nicholls & Branson (1998). More importantly the conceptual model highlights the interconnectivity of all three characterization classes, further supporting the call for a holistic approach in the assessment of vulnerability to geomorphic change.

In the coastal vulnerability assessment literature, many studies have individually assessed the vulnerability to perturbations incorporating various combinations of resistance, assailing, and resilience parameters, but few have incorporated all three. Bush et al., (1999) introduced a rapid vulnerability assessment checklist using geoindicators of coastal change, which included parameters that assessed resistance. Shaw et al. (1998) conducted a sensitivity assessment in which they looked at the degree to which a rise in sea level would result in geomorphological changes, namely erosion. Their study considered parameters that fell under the resistance and assailing CCCs but did not incorporate resilience. Pethick and Crooks (2000) proposed a preliminary coastal vulnerability index from a geomorphological perspective. Their review focused on the concept of landform resilience, such that a landform's vulnerability is dependent upon the frequency of a major event and the time it takes for a coastal feature to recover its form after the event passes, called relaxation time. According to Klein et al. (1998), Baan et al., (1997) used potential coastal dynamics as an indicator of morphological resilience. However, the geomorphic vulnerability of a coast is not solely dependent on resistance, assailing, or resilience parameters, but the interconnectivity of all three. Phillips (2009) suggests that a combination of hazard evaluation and landscape sensitivity would be beneficial for

assessing geomorphic change, which could be measured as a function of the 4 Rs (Response, Resistance, Resilience, Recursion). Tibbetts & van Proosdij (2013), in their study of macro-tidal environments, were the first to incorporate all three CCCs in a vulnerability assessment. In their research, Tibbetts & van Proosdij (2013) used the parameter “morphological resilience” to express the ability of a particular coastal feature to return to a form of its pre-disturbance state following a major event, very similar to the definition of morphological resilience first proposed by Baan et al. (1997).

While geomorphic resilience is obviously not a new concept in geomorphology (Wang et al., 2005; Phillips, 2009; Woodroffe, 2007; Bernatchez et al., 2011; Naylor et al., 2010; Nicholls & Branson, 1998; Klein et al., 1998; Pethick & Crooks, 2000), and its importance in the functioning of coastal systems has been well documented (Klein et al., 1998; Nicholls & Branson, 1998; Phillips, 2009), it is the view of this research that the exclusion, in most cases, of the resilience of the physical system in the assessment of coastal vulnerability is a substantial gap in literature and an oversight that needs to be explored before the physical system can be incorporated in a combined assessment of the socio-ecological system.

In this research, the parameters Morphological Resilience, Sediment Supply, and Accommodation Space were chosen to exemplify the resilience of the physical coastal zone. Morphological resilience refers to the ability of a landform to return to some state of dynamic equilibrium following a disturbance event. As outlined by Pethick & Crooks (2000), the ability of landforms to recover after a perturbation (called the relaxation time) varies with varying landform type and similarly, Phillips (2009) notes the importance of considering the possibility of reversibility. For example, the erosion of beaches is theoretically reversible, while rocky coasts,

once eroded, are unable to replace material (Naylor et al., 2010). Similarly material eroded from slopes cannot climb back up the slope (Phillips, 2009). In Lockeport, this concept of Morphological Resilience makes the greatest difference in coastal vulnerability along coastlines composed of, or fronted with, sand beaches, especially along Crescent Beach and Freddy's Beach, which are backed by dunes (Figure A.11). Sediment Supply refers to the availability of mobile sediment within the system, which has been recognized as a crucial component of the recovery of depositional features and the resiliency of the coast (Houser & Hamilton, 2009; Crooks, 2004; Klein et al., 1998). In Lockeport, (Figure A.13), Sediment Supply has a *very low* vulnerability rank (i.e., very high actual Sediment Supply) along the marsh areas in Back Harbour and the beach parallel to Cranberry Island. Crescent Beach, while having a sediment source in the form of dunes, also is fronted by revetments, which according to Bush et al.'s (1999) geoinicator checklist, indicates an area of severe erosion. The final parameter, Accommodation Space, refers to the availability of space for shorelines to be naturally dynamic, a parameter deemed important by Crooks (2004) and Pethick & Crooks (2000). In a study conducted by Wang et al. (2005), which looked at the recovery of a beach after a storm event, it was found that beaches rapidly returned to a state of equilibrium, but were translated 15-40 m landward from the original position and, in another study examining post-storm beach recovery, a direct correlation existed between the presence of immobile shorelines and the lack of beach sediment, both illustrating the value of Accommodation Space. In Lockeport (Figure A.12), the areas with the greatest Accommodation Space and, consequently, a *very low* contribution to vulnerability, are located primarily along the northern portions of Brighton Road and from Rood's Head to Chetwynd Lane. While portions of these areas have large Accommodation Space due to lack of infrastructure present, other portions do contain residences, but ones

which were built far enough from the coastline to theoretically allow for natural coastal functioning. While not incorporated in this study, the case can be made for the inclusion of event frequency in further studies (Pethick & Crooks, 2000; Houser & Hamilton, 2009; Morton, 2002; Forbes et al., 2004), as insufficient time to recover, despite the Morphological Resilience ability, will affect the overall coastal resilience and consequently its vulnerability.

In summary, the incorporation of resilience in the assessment of geomorphic vulnerability is crucial in understanding the vulnerability of a coastal system and has reduced coastal vulnerability index scores along Rood's Head, Chetwynd Land, parts of Brighton Road, Freddy's Beach and Crescent Beach in this study. This holistic approach to assessing geomorphic change, which includes assailing, resistance, and resilience components, is necessary for effective coastal zone planning and management. Future studies could incorporate additional resilience parameters, however this first attempt at combining physical assailing, resistance and resilience components provides a holistic framework that can be incorporated into future assessments of the SES.

5.5 CVI Application under Wave Energy Scenarios

The developed CVI matrix was applied to the coast of Lockeport, Nova Scotia under four wave energy scenarios with varying combinations of water levels and wind conditions associated with climate change. As Wave Energy was the only parameter manipulated, the differences in CVI scores between scenarios can largely be accounted for by differences in this parameter. Prior to discussing the differences between scenarios, the common characteristics of *very high* and *very low* stretches of shorelines will be examined for Scenario 1.

The parameters with the highest percentage of shoreline characterized by Rank 5 are: Coastal Protection Structures (61%), Sediment Supply (41%), and Accommodation Space (36%). On the other hand, the parameters with the highest percentage of shoreline characterized by Rank 1 are: Wave Energy (54%), Foreshore Geomorphology (50%), and Foreshore Width (31%). This does not mean that these parameters contribute most or least to coastal vulnerability, only that of the 11 parameters, these ones have the highest percent of shoreline that falls within a *very high* and *very low* vulnerability rank respectively. The principal components analysis conducted for this research illustrated that the segments with the highest CVI scores (BS #77, BS #82, and BS #83), all had similar characteristics contributing to their *very high* vulnerability rank and not multiple combinations of parameters. Looking at the data, the aforementioned highly vulnerable coastal segments all have *very high* ranks in the parameters Morphological Resilience (*outcrop or cliff or anthro with or without beach*), Accommodation Space (*0-6.00 m*), Backshore Vegetation (*unvegetated*), Foreshore Slope (*high slope or no FS*), and Foreshore Geomorphology (*no FS*) (i.e., low actual Morphological Resilience, Accommodation Space, Backshore Vegetation, Foreshore Slope, and Foreshore Geomorphology). The parameters that, in this study, contribute least to a *very highly* ranked vulnerable coastline are Sediment Supply and Wave Energy (i.e., low actual Wave Energy and high actual Sediment Supply). While these parameters contribute most and least to the vulnerable coastline in this study, it does not mean that they will also contribute the most or least to the vulnerability of another study area.

In shallow water, Wave Energy is directly proportional to the square of wave height (Gornitz, 2013). The height of a wave in deep water is dependent on wind speed, wind duration, and fetch (Gornitz, 2013; Gupta, 2011); however as a wave propagates into shallow water there are numerous processes that influence wave transformation, including shoaling, refraction,

diffraction, dissipation due to bottom friction and/or percolation into the bed, breaking, additional growth due to wind, wave-current and/or wave-wave interaction, run-up, reflection, and dispersion (Davidson-Arnott, 2010; Hobbs, 2012).

In this study the WEMo, developed by NOAA, was used to determine the amount of Wave Energy reaching the coast. As would be expected, modelling the incredibly complex interactions of wave propagation in shallow coastal waters comes with some limitations. WEMo does not take into account refraction and diffraction, however it does incorporate shoaling and dissipation over fetch (Fonseca & Malhotra, 2006). While the processes of wave refraction and diffraction can result in waves reaching parts of the coastline that are at a different orientation to the direction of wind and wave propagation, the integration of these processes would drastically increase computation time, which in this research already ranged from 7-12 days.

Observations from the Wave Energy calculated for each wave energy (Figures 4.1-4.4) showed that higher Wave Energies extend around the north end of Locke Island in S2, S3, and S4. This occurrence is most likely due to the direction of storm winds that were used in S2, S3, and S4, which vary from the ones used in S1. Although the fetch for the storm winds is not as long as the fetch that would result for waves coming off the open ocean, it is still enough to create substantial Wave Energy. Another observation is that Back Harbour and the area between Locke Island and Cranberry Island have comparatively low Wave Energies throughout all four scenarios, probably due to the sheltering effect of the islands. However, if refraction and diffraction were incorporated into the WEMo, these areas may experience higher wave energies due to the potential ability of waves to reach parts of the coastline that are at a different orientation to the direction of wind and wave propagation. In S1, S2, and S3, The

Anchorage experiences relatively low Wave Energies, however, in S4, higher Wave Energies appear to enter this protected area. This occurrence can largely be attributed to an increase in water levels in S4 that surpasses the height of the current Breakwaters, rendering their protective capacity ineffective. Additionally, submerged natural or anthropogenic barriers can enhance Wave Energy by reducing the depth of the water, thus increasing wave height and consequently Wave Energy (Morton & Sallenger, 2003). Along Crescent Beach Wave Energies appear to be relatively low across all scenarios, most likely due to the attenuation capacity of the gently sloping nearshore that continues offshore for quite a distance (DeMont et al., 2010). However, over the scenarios, Crescent Beach does become slightly more vulnerable between S2 and S3, due to the increase of water depth, which decreases shoaling and dissipation effects allowing for greater Wave Energy to reach the beach. Across all scenarios, the area of coastline from Rood's Head to the Wastewater Treatment Facility on John Street is the only section that illustrates a decrease in vulnerability, which occurs between S1 and S2. This decrease is most likely attributable to the differences in wind data used for S1 and S2. The data chosen for S2 represents the February 9th, 2013 winter storm and therefore, if a different storm were chosen to depict storm winds, the vulnerability of this section of coastline could change.

Once the other parameter data were included and the CVI was calculated, the results illustrated that the largest percent change in shoreline coverage between scenarios occurred between S1 and S2 for Rank 4 (+7%) and that the top three smallest percent changes in shoreline coverage between scenarios occurred between S2 and S3 for Ranks 2 (0%), 5 (-1%), and 3 (+2%), revealing that the inclusion of wind in S2 contributes substantially to an increase in vulnerable shorelines and that the inclusion of a small increase in water levels on top of storm winds does not create as much of an impact on the coast. The percent change between S3 and

S4, while not the highest, still shows substantial contribution to an increase in shoreline vulnerability for Rank 4 (+6%) and 5 (+5%), demonstrating that while storm winds and a moderate increase in water levels does not have a great effect on coastal vulnerability, a considerable increase in water levels does. The substantial increase in shoreline vulnerability from S1 to S2 can most likely be attributed to the included storm winds, as storm winds result in higher waves and thus greater Wave Energy. Additionally, large storm waves have the ability to disturb the bottom at greater depths, thus increasing the effects of shoaling (Hobbs, 2012). While dissipation removes some energy from a wave, a wave with greater overall energy, such as storm waves, will reach the coast with higher energy than smaller waves. From S2 to S3 the coastal vulnerability does not change considerably, most likely resulting from a small increase in water depth, which does not substantially reduce the effects of shoaling. Finally, the considerable increase in *highly* vulnerable (Rank 4 and 5) shoreline from S3 to S4 can most likely be attributed to the large increase in water levels, which limits shoaling and dissipation, allowing for higher Wave Energies to reach the shore.

The shore segments having the largest changes in CVI scores from S1 to S4 are those that are most influenced by the Wave Energy parameter and include sections of north Brighton Road, historic South Street, and the Trestles. Conversely, those having the smallest changes in CVI scores from S1 to S4 are not highly influenced by the Wave Energy parameter. The shoreline segments exhibiting a *very low* vulnerability throughout all scenarios include areas along Chetwynd Lane, west Crescent Beach, east Locke Island, Sam's Point and areas along Brighton Road which, for the most part, have the following parameters in common: Foreshore Geomorphology (*outcrop, platform, or anthro*) and Backshore Vegetation (*dense tree*). On the other hand, the shoreline segments exhibiting a *very high* vulnerability throughout all scenarios

include areas along Water Street and North Wharf which, for the most part, have the following parameters in common: Foreshore Width (0-4.9 m), Backshore Vegetation (*unvegetated*), Coastal Protection Structures (*no CPS*), and Accommodation Space (0-6 m).

In summary, storm winds have a large impact on vulnerable shorelines and a moderate increase in water levels does not result in substantial changes. However, a large increase in water levels in addition to storm winds does cause substantial coastal vulnerability. Therefore, in the short term, residents should be more concerned about storms causing erosion than an increase in water levels. Additionally, the areas that are most vulnerable to erosion currently are primarily located along Water Street and the North Wharf, which extends to include the Trestles, Locke Street West, and Calf Island Road in S2, historic South Street in S3, and more of Calf Island Road in S4. While the MCCAP (Atwood, 2013) report focuses primarily on storm surges and flooding, some of the areas of concern identified in the report match the areas of concern identified in this research and include: the Trestles, Water Street, Locke Street West, Calf Island Road, and historic South Street. Therefore, these areas are not only susceptible to storm effects as presented in the MCCAP (Atwood, 2013) report, but also susceptible to current and/or future geomorphic change. For this study the CVI scores are a relative assessment of vulnerability such that the scores are comparable only to each other and not to other studies. Therefore, it is impractical to compare the results of this study to others in the literature.

5.6 Buildings in the Coastal Zone at Risk to Erosion & Inundation

The buildings located within the coastal zone that are at risk to erosion under each wave energy scenario were identified. Separately, buildings located within the coastal zone, that are

at risk to both erosion and permanent inundation associated with S3 and S4 were also identified.

As no coastal zone definition exists for Nova Scotia, coastal zone delineation was a crucial aspect in the determination of “at risk” buildings. It was important that the definition encompassed areas of concern, but did not have such large boundaries that all of Locke Island was considered the coastal zone. As outlined in 1.2.1, a plethora of coastal zone definitions exist, and often studies use the term coastal zone arbitrarily without providing a definition (Crowell et al., 2007). While most coastal zone definitions are defined on a nation-to-nation basis, there has been growing use of the LECZ (low-elevation coastal zone) definition (Wong et al., 2014), which was developed with respect to sea level rise by Lichter et al., (2011), and encompasses the areas of land and population up to 10 m in elevation. Although useful in the absence of a national coastal zone definition, when applied to the study area of Lockeport, the majority of the town would be considered the coastal zone, thus rendering the delineation of the coastal zone futile. Therefore in light of the fact that no coastal zone definition exists for Nova Scotia, Fanning’s (2008) suggestion to consider the zones of influence and the impact of a particular issue or event was used for this research. While topographic contours are often used as coastal zone boundaries, erosion events are not necessarily restricted by elevation, as would be the case with a flooding event. The zone of influence for an erosion event is not expected to be greater than 50 m from the beginning of the backshore and therefore, the coastline was defined in this research as *the area of land extending 50 m landward and seaward from the backshore*. When applied to the Town of Lockeport, the use of the coastal zone boundaries, as defined above, appeared to be a good choice, as they encompassed the majority of areas that have been noted as areas of concern in the MCCAP (Atwood, 2013) for Lockeport as well as the

buildings located on the wharves. Although defined for erosion events, when overlaid with inundation, the delineated coastal zone encompassed all buildings that were affected by the inundation, except for the Electricity Substation in S3, and the majority of buildings that were affected by the inundation associated with S4, save for the Electricity Substation again, along with two residences located off of South Street between John Street and Church Street. Overall, the use of this coastal definition is considered appropriate for this study and incorporated 122 buildings.

Similar to the approach employed by Palmer et al. (2011), this research identifies coastlines at risk *a priori* and the infrastructure located within those vulnerable areas *a posteriori*. Although the approach does not specifically incorporate the human component of coastal vulnerability, it makes an effort to better inform management and adaptation strategies by incorporating “at risk” buildings. Palmer et al. (2011) chose to identify assets at risk (e.g., piers, roads, turtle nesting sites, subsistence fishing areas, swimming beaches, sports fields etc.) instead of just buildings at risk, as was done with Lockeport. However, in an asset mapping workshop held in Lockeport in 2009, community members identified five asset categories (natural, built, social, economic, and service) (Millier Dickinson Blais, 2013) which in future, could easily be added to this study to allow for identification of all assets at risk to erosion, as well as proportions of assets at greatest risk.

Using the CVI shoreline segment scores, all buildings located within the coastal zone, of which there are 122, were identified as being *very lowly* to *very highly* vulnerable to erosion for each wave energy scenario. As the scenarios are progressive, the buildings with a *high* (Rank 4 or 5) risk designation in S1 are the most important to address immediately, while those with a

high (Rank 4 or 5) risk designation in S2 are important to address currently or in the very near future, and those identified as being *highly* (Rank 4 or 5) at risk in S3 and S4 are those to address in future planning measures, as they incorporate SLR projections for the year 2010 -2100.

Overall the number buildings that are *very highly* vulnerable to erosion increase with each increasing scenario, with 27 *very highly* vulnerable buildings identified in S1 and 16 additional buildings identified by S4. The greatest change in building numbers occurs for Rank 5 between S2 and S3. While the progression from S2 to S3 was noted in Section 5.5 as not substantially increasing the amount of vulnerable coastline, the large number of buildings added between these two scenarios can be attributed to the fact that there are a lot of houses located within the small sections of shoreline that became *very highly* vulnerable, which includes residences along Brighton Road and Ocean Mist Cottages. In S1, the *very highly* vulnerable buildings are located primarily along Water Street, North Wharf, and South Wharf along with one residence on Brighton Road and a building along the coast near Rood's Head. In S2, additional buildings along west Locke Street (1 of the Seaside Cottages), and the north side of Locke Island are identified and in S3 more houses along Brighton Road, the remaining Ocean Mist Cottages, and a house along historic South Street are added to the *very high* vulnerability rank. Scenario 4 sees the incorporation of additional houses along Brighton Road and historic South Street. In summary, across all scenarios, pockets of *moderate* to *very highly* vulnerable buildings are primarily concentrated along Crescent Beach, Calf Island Road, North and South Wharves, historic South Street and sporadically along Brighton Road.

Inundation extent associated with S3 and S4 was incorporated for these scenarios and buildings located within the coastal zone, that are at risk to both erosion and inundation, were

identified. In this discussion it is important to recall that inundation is not the same as flooding, as the former refers to enduring water levels and flooding refers to temporary water accumulation. Therefore the buildings identified in this section are not being assessed for vulnerability to flooding and storm surge. However, with higher water levels, storm surge does have the capacity to reach farther inland. The inundation extent for these scenarios illustrates that, with a 2.21 m increase in water levels, Calf Island Road, the Trestles, South Street, and a portion of the South Wharf experience submersion and that a 3.10 m increase in water levels results in complete submersion of Crescent Beach Causeway, the Trestles, Calf Island Road, South and North Water Street, historic South Street as well as both Breakwaters which protect The Anchorage from the effects of storms. Additionally, S4 results in the division of Locke Island between John Street and Church Street as well as Cranberry Island, a phenomenon that occurred centuries ago when Cranberry Island was “separated” from Locke Island (Atwood, 2013).

The total number of buildings located with the coastal zone that are vulnerable to both erosion and inundation increase from 16 to 47 for S3 and S4 respectively. In Scenario 3, ten buildings were ranked *very highly* vulnerable which included buildings along North and South Wharves and Water Street. In S4 an additional nine buildings were recognized as being *very highly* vulnerable, including more along Water Street, one on west Locke Street (Seaside Cottages), two on east Locke Street (Ocean Mist Cottages), and one along north Brighton Road. The only building affected by inundation for both scenarios, but which is not located within the coastal zone, is the Electricity Substation located at the corner of Upper Water Street and North Street. This piece of infrastructure has been noted as being very vulnerable to flooding events and, if the coastal zone definition in this research extended to 55 m instead of 50 m, the

Electricity Substation would be considered *highly* vulnerable to erosion and inundation. In summary, the buildings that are most vulnerable to erosion and flooding in both scenarios are concentrated along Water Street and the North and South Wharves.

5.7 Conclusions & Recommendations

The developed matrix is successful in incorporating the assailing, resistance, and resilience components of geomorphic change and in providing a preliminary attempt at a holistic assessment of physical coastal vulnerability to erosion. It also provides researchers with a framework that can be applied to other physical environments and impacts in future studies. It would be beneficial to validate the matrix using independently collected erosion data and modify the matrix accordingly. As a system can only be resilient if it has enough time to recovery from a perturbation (Pethick & Crooks, 2000), it is highly recommended that future assessments of geomorphic resilience also incorporate event frequency as a contributing parameter. Additionally it is crucial for future vulnerability assessments, especially those concerning SESs, to incorporate the physical geomorphic resilience aspect of coastal vulnerability to account for the natural ability of a coastal system to recover from disturbance events, instead of solely incorporating the social aspect of resilience. The data obtained through the use of the field based coastal characterization methodology was crucial in the assessment of physical coastal vulnerability to erosion at the local level as the use of aerial imagery would have diminished the level of detail obtained for included parameters (e.g., CPSs).

The application of the developed CVI matrix illustrated that the vulnerability of Lockeport's shoreline is highly affected by storm conditions, exemplified by an increase in wind data, whereas an additional moderate increase in water levels does not have as much of an

impact. However storm winds, along with a large increase in water levels, do appear to have a large impact on the presence of *highly* (Rank 4 and 5) vulnerable coastlines in this study. While the *highly* (Rank 4 and 5) vulnerable coastlines of this research had *very highly* ranked Morphological Resilience, Accommodation Space, Backshore Vegetation, Foreshore Slope, and Foreshore Geomorphology (i.e., low actual Morphological Resilience, Accommodation Space, Backshore Vegetation, Foreshore Slope, and Foreshore Geomorphology), it would be interesting to apply the developed matrix to other study sites to determine if the parameters contributing to *very high* vulnerability in this research are the same as other sites, or if they vary with varying sites.

In Lockeport the areas that remained *very lowly* vulnerable to erosion across all scenarios were Chetwynd Lane, west Locke Street, east Locke Island, Sam’s Point, and areas along Brighton Road, most of which had common Foreshore Geomorphology and Backshore Vegetation. On the other hand, the areas that have been identified as being most vulnerable to erosion and inundation under the wave energy scenarios are: Crescent Beach, the Trestles, Calf Island Road, Water Street, historic South Street and parts of Brighton Road. Recommendations for some of these areas will be presented in the following section.

5.8 Observations & Recommendations for Lockeport

“Lockeport recognizes the potential threat caused by climate change and associated extreme weather events and is committed to protecting municipal infrastructure, residents and property through use of partnerships and effective strategies.” – Eshelby, 2010 pg. 10

The results of this research, in combination with related reports, have led to the following recommendations for the study area of Lockeport, Nova Scotia:

1. The Town of Lockeport should seriously consider a secondary access from the mainland to Locke Island. Despite the ability of the gently sloping foreshore slope of Crescent Beach to attenuate energy, the expected increases in SLR will allow for waves with greater energy, and thus erosion potential, to reach the beach. In addition, a dune-beach system is meant to be dynamic, where sediment constantly shifts with small or larger perturbations and the system is able to translate upwards and backwards to accommodate rises in sea level. The process of “fixing” Crescent Beach in place goes against coastal sandy system dynamics and results in a system that is increasingly unstable and unable to naturally accommodate a rise in sea level (DeMont et al., 2010). The Integrated Community Sustainability Plan (ICSP) (Eshelby, 2010) noted that a goal for Lockeport is to “have access and egress by vehicle in all weather conditions,” and the more recent MCCAP (Atwood, 2013) has recognized the establishment of a secondary access as a main priority, as without island access, “the social stability of Lockeport and surrounding areas are at risk.” Options for a secondary access are either the Rails to Trails walkway or Calf Island Road. In either case the secondary access would have to be in the form of a bridge so as not to cut off water flow into the Back Harbour (doing so would likely starve the salt marsh of sediment and result in further subsidence of that area). While some reports suggest that the emergency access is possible across the Rails to Trails path, a recent structural assessment of the Trestles suggested that upgrades are required (Atwood, 2013). It is the view of this research that a primary access be placed along Calf Island Road to Bridge Street on Locke Island, where a bridge formerly existed.

2. A cost-benefit analysis considering cost of beach and dune upkeep versus cost of building or reinforcing a secondary access should be undertaken. Despite the physical support for the creation of a secondary access, it may be more feasible to continue substantial upkeep of

armouring along Crescent Beach than to build a secondary access. However, if taking into consideration the initial cost of full beach armouring, which DeMont et al. (2010) have estimated at 1.5 million CAD, in addition to the cost of upkeep as well as increasing height to keep up with a rise in sea level, which requires an increase in revetment base width too, as well as the requirement of frequent planting programs to encourage sediment accumulation and foredune development and the cost of ploughing sand off the Crescent Beach Causeway from frequent overtopping events, it is expected that the price of a secondary access across Calf Island Road would be in a similar, if not lower, price range. The main difference between the two options would be that dune and beach stability cannot be guaranteed, whereas a secondary access could ensure “access and egress” to vehicles in most weather conditions.

3. The Town of Lockeport should consider “managed retreat” or “limited intervention” options for Crescent Beach as opposed to the current “hold the line” approach. *Hold the line* is considered a fairly maladaptive approach when it comes to coastal climate change adaptation strategies, as it prevents coasts from being naturally dynamic. A natural coast is considered a resilient coast, which is as was presented in this research, a crucial part of decreasing the vulnerability of a coast to erosion. Often *hold the line* approaches are employed when there is absolutely no other option; however, the fact that a secondary access point is plausible, abandoning the *hold the line* approach for Crescent Beach would result in a more resilient coastline in the face of impending increases in SLR and storminess. The report by van Proosdij & Page (2012) reviews the *managed retreat* and *limited intervention* adaptation options.

4. The Trestles operate as a good emergency access corridor, but will require investment of funds to cover revetment upkeep and top up as water levels increase.

5. Calf Island Road is highly susceptible to erosion and inundation events and requires implementation of appropriate adaptation strategies in the near future. Calf Island Road is highly vulnerable to erosion and inundation and, according to the MCCAP (Atwood, 2013), also flooding and storm surge. In the future, residents run the risk of being cut off from Brighton Road. As the Town of Lockeport is responsible for this section of Lockeport's coastline, it is recommended that, in order to preserve funds, the secondary access route be placed along Calf Island Road. With this option, the protection required for Calf Island Road can be integrated within the larger secondary access project, thus reducing the overall financial requirements. If the secondary access is not placed here, Calf Island Road will require the building of revetments along both sides.

6. The creation or upgrading of any coastal protections structures should consider the coast as a whole so as not to cause increased erosion for properties or infrastructure further down the shoreline.

7. The Electricity Substation located on the corner of Upper Water Street and North Street requires immediate attention. While this piece of infrastructure was not identified as being vulnerable to erosion, due to its inland location, which is only slightly greater than the designated 50 m for the coastal zone, it was identified as being susceptible to an increase in water levels in S3 and S4 and it also noted in several reports as an area of great concern (DeMont et al., 2010; Atwood, 2013).

8. A by-law regulating future development within vulnerable areas should be implemented, stipulating necessary vertical allowances and/or horizontal setbacks and limiting further development within certain high-risk zones. A recent report by Zhai et al., (2014) suggests sea

level allowances on the scale of 0.32 -0.38 m for 2050/2099 respectively for RCP4.5 scenario and 0.78 -1.11 m for 2050/2099 respectively for the RCP8.5 scenario, which is the same one used in S3 in this research. The distance of a horizontal setback, to accommodate sea level allowances as outlined above, depends on elevation (i.e., however far landward it takes to reach a set elevation, which in this case would be the sea level allowance heights). However, more feasible for Lockeport would be the incorporation of building codes (e.g., minimum floor elevations) that accommodate a vertical sea level allowance of a set amount. If horizontal setbacks or vertical allowances are not incorporated, at the very least, waivers should be signed indicating that developers or home owners understand that they are building in a vulnerable area, are aware of the potential associated risks, and release the town of responsibility for any incurred damage.

9. With the influx of climate change research from the ParCA project, a detailed climate change management plan needs to be developed for the Town of Lockeport. This plan should include participation of community members, town council and relevant scientists/researchers, and incorporate specific options along with quotes and contacts.

REFERENCES

- Abuodha, P. A. O. & Woodroffe, C. D. (2006). *Assessing vulnerability of coasts to climate change: A review of approaches and their application to the Australian coast*. University of Wollongong Faculty of Science Papers. Retrieved from: <http://ro.uow.edu.au/scipapers/> [accessed December 30th, 2012].
- Abuodha, P. A. O. & Woodroffe, C. (2010). Assessing vulnerability to sea-level rise using a coastal sensitivity index: a case study from southeast Australia. *Journal of Coastal Conservation*, 14: 189-205.
- Adger, W. N. (2006). Vulnerability. *Global Environmental Change*, 16: 268-281.
- Alexandrakis, G., Karditsa, A., Poulos, S. E., Ghionis, G., & Kampanis, N. A. (n.d.). An Assessment of the Vulnerability to Erosion of the Coastal Zone Due to a Potential Rise of Sea Level: The Case of the Hellenic Aegean Coast. In *Encyclopaedia of Life Support Systems (ELOSS)*. Paris, France: Eolss Publishers.
- Anonymous a. (2013). *Personal Communication*. May 6th, May 17th, and June 14th, 2013.
- Anonymous b. (2013). *Personal Communication*. May 6th, 2013.
- Atwood, B. (2009). *Hurricane Bill's Greatest Hits*. YouTube video. Retrieved from: <https://www.youtube.com/watch?v=yr-CWbMy8Wg> [accessed November 12th, 2014].
- Atwood, B. (2013). *Municipal Climate Change Action Plan Town of Lockeport*.
- Australian Department of Climate Change. (2009). *Climate Change Risks to Australia's Coast: A First Pass National Assessment*. Australian Government. Retrieved from: http://www.climatechange.gov.au/sites/climatechange/files/documents/03_2013/cc-risks-full-report.pdf [accessed November 24th, 2014].

- Baan et al. (1997) Veerkracht van de kust-ontwikkeling en operationalisering van een 'veerkracht-meter'. In R. J. T. Klein, M. J. Smit, H. Goosen, & C. H. Hulsbergen. (1998) Resilience and Vulnerability: Coastal Dynamics or Dutch Dikes?. *The Geographical Journal*, 164(3): 259-268.
- Bachmann, C. M., Abeley, A., Philpot, W., Nichols, C. R., Smith, G., Korwan, D., Gardner, J., Sletten, M., Musser, J. A., Fusina, R. A., Vermillion, M., Parrish, C. E., Li, R. R., Sellar, J., White, S., van Roggen, E., & Doctor, K., (2012). *A Multi-Sensor Approach to Coastal Characterization*. Optical Remote Sensing of the Environment, Monterey, California, June 24-28th, 2012.
- Bachmann, C., Nichols, C. R., Montes, M. J., Fusina, R. A., Fry, J. C., Li, R., Gray, D., Korwan, D., Parrish, C., Sellars, J., White, S. A., Woolard, J., Lee, K., McConnon, C., & Wende, J. (2010a). *Coastal Characterization from Hyperspectral Imagery*. Imaging and Applied Optics Congress, OSA Technical Digest (CD) (Optical Society of America), paper OMD2.
- Bachmann, C. M., Nichols, C. R., Montes, M. J., Fusina, R. A., Li, R., Gross, C., Fry, J. C., Parrish, C., Sellers, J., White, S. A., Jones, C. A., & Lee, K. (2010b). *Coastal Characterization from hyperspectral imagery: An intercomparison of retrieval properties from three coast types*. Geoscience and Remote Sensing Symposium (IGARSS), Honolulu, Hawaii, July 25-30th, 2010.
- Balbus, J. M., Baker, B., Brody, M., Burton, I., Cohen, S. J., Feenstra, J. F., Hlohowskyi, I., Hulme, M., Iglesias, A., Klein, R. J. T., Lenhard, S., Linder, S., Malcolm, J. R., Nicholls, R. J., Parry, M. L., Rosenzweig, C., Scholes, R. J., Smith, J. B., Stern, F., Strzepek, K. M., & Tol, R. S. J. (1998). *Handbook on Methods for Climate Change Impact Assessment and Adaptation Strategies*. UNEP. Retrieved from: <http://dspace.ubvu.vu.nl/bitstream/handle/1871/10440/f1.pdf?sequence=1> [accessed November 24th, 2014].
- Bernatchez, P., Fraser, C., Lafaivre, D., & Dugas, S. (2011). Integrating anthropogenic factors, geomorphological indicators and local knowledge in the analysis of coastal flooding and erosion hazards. *Ocean & Coastal Management*, 54: 621-632.
- Boruff, B. J., Emrich, C., & Cutter, S. L. (2005). Erosion Hazard Vulnerability of US Coastal Counties. *Journal of Coastal Research*, 21(5): 932-942.
- Bretschneider, C. L. & Reid, R. O. (1954). *Modification of Wave Height Due to Bottom Friction, Percolation, and Refraction*. U.S. Army Corps of Engineers, Beach Erosion Board, Washington D.C.

- Brown, S. (2014). *Nova Scotia South Shore Fisheries CBVA Report*. Partnership for Canada-Caribbean Community Climate Change Adaptation. Unpublished document.
- Brunsdon, D. (2001). A critical assessment of the sensitivity concept in geomorphology. *Catena*, 42: 99-123.
- Bruun, P. (1962). *Sea-level Rise as a Cause of Shore Erosion*. *Journal of Waterways and Harbors*. ASCE, 88: 117-130.
- Burke, L., Yumiko, K., Kassem, K., Revenga, C., Spalding, M., & McAllister, D. (2001). *Pilot Analysis of Global Ecosystems: Coastal Ecosystems*. World Resource Institute. Retrieved from: <http://www.wri.org/publication/pilot-analysis-global-ecosystems-coastal-ecosystems> [accessed November 15th, 2013].
- Bush, D. M., Neal, W. J., Young, R. S., & Pilkey, O. H. (1999). Utilization of geoinicators for rapid assessment of coastal-hazard risk and mitigation. *Ocean & Coastal Management*, 42: 647-670.
- Carrasco, A. R., Ferreira, O., Matias, A., & Freire, P. (2012). Flood hazard assessment and management of fetch-limited coastal environments. *Ocean & Coastal Management*, 65: 15-25.
- Center for Coastal Resources Management (CCRM). (2013). *Currently Defended Shorelines – Definitions*. Retrieved from: [Decision Tree Tool](#) [accessed October 15th, 2014].
- Church, J. A., Clark, P. U., Caxenave, A., Gregory, J. M., Jerejeva, S., Levermann, A., Merrifield, M. A., Milne, G. A., Nerem, R. S., Nunn, P. D., Payne, A. J., Pfeffer, W. T., Stammer, D., & Unnikrishan, A. S. (2013). Sea Level Change. In T. F. Stocker, D. Qin, G. K. Plattner, M. Tignor, S. K. Allen, J. Boschung, A. Nauels, Y. Xia, V. Bex, & P. M. Midgley (Eds.), *Climate Change 2013: The Physical Science Basis. Contribution of Working Group 1 to the Fifth Assessment Report of the Intergovernmental Panel on Climate Change* (pp.1137-1216). Cambridge, UK and New York, NY, USA: Cambridge University Press.
- CBCL Limited. (2009). *The 2009 State of Nova Scotia's Coast Technical Report*. Province of Nova Scotia. Retrieved from: https://www.novascotia.ca/coast/documents/state-of-the-coast/WEB_SummaryReport.pdf [accessed November 26th, 2014].
- Clark, J. R. (1996). *Coastal Zone Management Handbook*. Boca Raton, Florida: CRC Press LLC.

- Cochran, M., Manuel, P., & Rapaport, E. (2012). *Social Vulnerability to Climate Change in Yarmouth, Nova Scotia*. Atlantic Climate Adaptation Solutions (ACAS). Retrieved from: <http://atlanticadaptation.ca/sites/discoveryspace.upei.ca.acasa/files/B%20Michaela%20CochranSECURED.pdf> [accessed November 24th, 2014].
- Collins, M., Knutti, R., Arblaster, J., Dufresne, J.-L., Fichet, T., Friedlingstein, P., Gao, X., Gutowski, W. J., Johns, T., Krinner, G., Shongwe, M., Tebaldi, C., Weaver, A. J., & Wehner, M. (2013). Long-term Climate Change: Projections, Commitments and Irreversibility. In T. F. Stocker, D. Qin, G. K. Plattner, M. Tignor, S. K. Allen, J. Boschung, A. Nauels, Y. Xia, V. Bex, & P. M. Midgley (Eds.), *Climate Change 2013: The Physical Science Basis. Contribution of Working Group 1 to the Fifth Assessment Report of the Intergovernmental Panel on Climate Change* (pp.1029-1136). Cambridge, UK and New York, NY, USA: Cambridge University Press.
- Cooper, E., Burke, L., & Bood, N. (2009). *Coastal Capital: Belize The Economic Contribution of Belize`s Coral Reefs and Mangroves*. World Resources Institute. Retrieved from: [Belize's Coastal Capital | World Resources Institute](#) [accessed October 13th, 2013].
- Cooper, J. A. G. & Pilkey, O. H. (2004). Sea-level rise and shoreline retreat: time to abandon the Bruun Rule. *Global and Planetary Change*, 43: 157-171.
- Cooper, N. J., Leggett, D. J., & Lowe, J. P. (2000). Beach-Profile Measurement, Theory and Analysis: Practical Guidance and Applied Case Studies. *JCIWEM*, 14: 79-88.
- Crooks, S. (2004). The effects of sea-level rise on coastal geomorphology. *Ibis*, 146(Suppl.1): 18-20.
- Crowell, M., Edelman, S., Coulton, K., & McAfee, S. (2007). How Many People Live in Coastal Areas?. *Journal of Coastal Research*, 23(5): iii-vi.
- Cubasch, U., Wuebbles, D., Chen, D., Facchini, M. C., Frame, D., Mahowald, N., & Winther, J. D. (2013). Introduction. In T. F. Stocker, D. Qin, G. K. Plattner, M. Tignor, S. K. Allen, J. Boschung, A. Nauels, Y. Xia, V. Bex, & P. M. Midgley (Eds.), *Climate Change 2013: The Physical Science Basis. Contribution of Working Group 1 to the Fifth Assessment Report of the Intergovernmental Panel on Climate Change* (pp.119-158). Cambridge, UK and New York, NY, USA: Cambridge University Press.
- Davidson-Arnott, R. G. D. (2010). *Introduction to Coastal Processes and Geomorphology*. Cambridge, UK: Cambridge University Press.

- Davies, J. L. (1972). *Geographical Variation in Coastal Development*. Edinburgh, Scotland: Oliver and Boyd.
- Dean, R. G. & Dalrymple, R. A. (1991). *Water wave mechanics for engineers and scientists*. Singapore: World Scientific Publishing.
- DeMont, G., Finck, P., & Utting, D. (2010). *Lockeport, Nova Scotia – Observations and Recommendations Relating to Erosion of Crescent Beach*. Nova Scotia Department of Natural Resources. Unpublished document.
- Dolan, A. H. & Walker, I. J. (2004). Understanding vulnerability of coastal communities to climate change related risks. *Journal of Coastal Research*, SI39: ICS 2004 Proceedings.
- Douglass, S. L., Krolak, J., Chen, Q., McNeill, L., Reid, C., Keith, P., Richards, J., & Shaw, J. (2008). *Highways in the Coastal Environment: Second Edition*. US Department of Transportation. Publication No. FHWA-NHI-07-096, Hydraulic Engineering Circular No. 25. Retrieved from: <http://www.fhwa.dot.gov/engineering/hydraulics/pubs/07096/07096.pdf> [accessed November 14th, 2014].
- Doukakis, E. (2005). Coastal Vulnerability and Risk Parameters. *European Water*, 11/12: 3-7.
- Dow, K. & Downing, T. (2011). *The Atlas of Climate Change: Mapping the World's Greatest Challenge* (3rd ed.). Berkeley, California: University of California Press.
- Dunteman, G. H. (1989). *Principal Components Analysis*. Sage University Paper Series: Quantitative Applications in the Social Sciences, No. 69. Newbury Park, California: Sage Publications.
- Engle, N. L. (2011). Adaptive capacity and its assessment. *Global Environmental Change*, 21: 647-656.
- Environment Canada. (1994). *Reviewing CEPA The Issues #4: Coastal Zone Management in Canada*. Catalogue No.: En40-224/4-1994.
- Environment Canada. (2010). *Detailed Storm Impacts Summaries*. Retrieved from: <http://www.ec.gc.ca/hurricane/default.asp?lang=En&n=1B2964ED-1> [accessed November 12th, 2014].

- Environment Canada. (2014). *Canadian Hurricane Centre – FAQ*. Retrieved from: <http://www.ec.gc.ca/ouragans-hurricanes/default.asp?lang=En&n=3F0FD4CF-1#wsAAE4CD59> [accessed: January 5th, 2015].
- Environmental Systems Research Institute. (2009). *Dynamic segmentation*. Retrieved from: http://webhelp.esri.com/arcgisdesktop/9.3/index.cfm?pid=6120&topicname=Dynamic_segmentation [accessed January 28th, 2015].
- Eshelby D. (2010). *Town of Lockeport Integrated Community Sustainability Plan: A Growing Community Process*. Retrieved from: <http://lockeport.ns.ca/docs/icsp.pdf> [accessed November 24th, 2014].
- Fanning, L. (2008). *Towards a Coastal Area Definition for Nova Scotia*. Workshop June 11th, 2008, Dalhousie University, Halifax.
- Feenstra, J. F., Burton, I., Smith, J. B., & Tol, R. S. T. (1998). *Handbook on Methods for Climate Change Impact Assessment and Adaptation Strategies*. UNEP. Retrieved from: <http://lib.icimod.org/record/13767/files/7157.pdf> [accessed November 4, 2012].
- Folke, C. (2006). Resilience: The emergence of a perspective for social-ecological systems analyses. *Global Environmental Change*, 16: 253-267.
- Fonseca, M. S. & Malhotra, A. (2006). *WEMo (Wave Exposure Model) for use in Ecological Forecasting*. Applied Ecology and Restoration Research Branch, NOAA, National Ocean Service Center for Coastal Fisheries and Habitat Research (CCFHR). Retrieved from: http://www.ccfhr.noaa.gov/docs/wemo_v3_manual.pdf [accessed November 24th, 2014].
- Forbes, D.L., Parkes, G.S., Manson, G.K., & Ketch, L.A. (2004). Storms and shoreline retreat in the southern Gulf of St. Lawrence. *Marine Geology*, 210: 169-204.
- Forbes, D. L., Manson, G. K., Charles, J., Thompson, K. R., Taylor, R. B. (2009). *Halifax Harbour Extreme Water Levels In the Context of Climate Change: Scenarios for a 100-Year Planning Horizon*. Geological Survey of Canada, Open File 6346. Retrieved from: <http://www.halifax.ca/regionalplanning/documents/OF6346final.pdf> [accessed January 29th, 2015].
- Filho, P. W. M. E. S. & El-Robrini, M. (2000). Geomorphology of the Braganca Coastal Zone, Northeastern Para State. *Revista Brasileira de Geociencias*, 30(3): 522-526.

- Fisheries and Oceans Canada. (2008). *Gerald Keddy, M.P. Announces Funding For Six Nova Scotia Harbours*. Retrieved from: <http://www.geraldkeddy.ca/media/riding-news/gerald-keddy,-m.-p.-announces-funding-for-six-nova-scotia-harbours> [accessed November 6th, 2014].
- Gaki-Papanastassiou, K., Karymbalis, E., Poulos, S. E., Seni, A., & Zouva, C. (2010). Coastal vulnerability assessment to sea-level rise based on geomorphological and oceanographical parameters: the case of Argolikos Gulf, Peloponnese, Greece. *Hellenic Journal of Geosciences*, 45: 109-121.
- Gallopin, G. C. (1991). Human dimensions of global change: linking the global and the local processes. *International Social Science Journal*, 130: 797-718.
- Gallopin, G. C. (2006). Linkages between vulnerability, resilience, and adaptive capacity. *Global Environmental Change*, 16: 293-303.
- Goda, Y. (1985). *Random Seas and Design of Maritime Structures*. Tokyo, Japan: University of Tokyo Press.
- Gomez, C., Wulder, M. A., Dawson, A. G., Ritchie, W., & Green, D. R. (2014). Shoreline Change and Coastal Vulnerability Characterization with LandSat Imagery: A Case in the Outer Hebrides, Scotland. *Scottish Geographical Journal*, 130(4): 279-299.
- Gornitz, V. M. (2013). *Rising Seas: Past, Present, Future*. New York, NY: Columbia University Press.
- Gornitz, V. M., White, T. W., & Cushman, R. M. (1991). Vulnerability of the US to future sea-level rise. In O. Magoon, H. Converse, V. Tippie, T. Tobin, & D. Clark (Eds.), *Coastal Zone'91: Proceedings of Seventh Symposium on Coastal and Ocean Management* (pp. 2354-2368). New York, NY: ASCE.
- Gornitz, V. M., Daniels, R. C., White, T. W., & Birdwell, K. R. (1994). The Development of a Coastal Risk Assessment Database: Vulnerability to Sea-Level Rise in the US Southeast. *Coastal Hazards: Perception, Susceptibility and Mitigation*, SI12: 327 – 338.
- Gornitz, V. M., Beaty, T. W., & Daniels, R.C. (1997). *A Coastal Hazards Data Base for the US West Coast*. Environmental Sciences Division Publication No. 4590. Retrieved from: <http://cdiac.esd.ornl.gov/epubs/ndp/ndp043c/43c.htm> [accessed December 24th, 2014].

- Government of Canada. (2014). *Population and dwelling counts, for Canada, provinces and territories, and census subdivisions (municipalities), 2011 and 2006 censuses*. Retrieved from: <http://www12.statcan.gc.ca/census-recensement/2011/dp-pd/hlt-fst/pd-pl/Table-ableau.cfm?LANG=Eng&T=302&SR=1&S=51&O=A&RPP=9999&PR=12&CMA=0> [accessed November 10th, 2014].
- Government of Nova Scotia. (1989). *Beaches Act. R.S., c.32, s.1. Revised 1989, amended 1993, c.9.s.9*. Retrieved from: <http://nslegislature.ca/legc/statutes/beaches.htm> [accessed November 12th, 2014].
- Greenlaw, M. E., Gromack, A. G., Basquill, S. P., MacKinnon, D. S., Lynds, J. A., Taylor, R. B., Utting, D. J., Hackette, J. R., Grant, J., Forbes, D. L., Savoie, F., Berube, D., Connor, K. J., Johnson, S. C., Coombs, K. A., & Henry, R. (2013). *A Physiographic Coastline Classification of the Scotian Shelf Bioregion and Environs: The Nova Scotia Coastline and the New Brunswick Fundy Shore*. Department of Fisheries and Oceans Canada, Canadian Science Advisory Secretariat, Research Document 2012/051. Retrieved from: <http://www.dfo-mpo.gc.ca/Library/347999.pdf> [accessed November 24th, 2014].
- Guannel, G., Arkema, K., Papenfus, M., Verutes, G., Bernhardt, J., Guerry, A., Kim, C-K., Ruckelshaus, M., & Toft, J. (2012). *Coastal Vulnerability Model: Mapping the Coastal Protection Benefits Provided by the Natural Environment*. Retrieved from: http://ncp-dev.stanford.edu/~dataportal/training_feb2012_stanford/CVModel.pdf [accessed November 24th, 2014].
- Gupta, A. (2011). *Tropical Geomorphology*. Cambridge, UK: Cambridge University Press.
- Hedge, A. V. & Reju, V. R. (2007). Development of Coastal Vulnerability Index for Mangalore Coast, India. *Journal of Coastal Research*, 23(5): 1106-1111.
- Hinkel, J. (2011). "Indicators of vulnerability and adaptive capacity": Towards a clarification of the science-policy interface. *Global Environmental Change*, 21: 198-208.
- Hobbs, C. H. (2012). *The Beach Book: Science of the Shore*. New York, NY: Columbia University Press.
- Holland, S. M. (2008). *Principal components Analysis (PCA)*. Department of Geology, University of Georgia, Athens, GA. No. 30602-2501. Retrieved from: <http://strata.uga.edu/software/pdf/pcaTutorial.pdf> [accessed December 7th, 2014].

- Horne, P. A. (2013). *Characterization of Intertidal Geomorphology Based on Multi-scale Analysis of Airborne LiDAR Data*. (Master of Science Dissertation). Saint Mary's University, Halifax, Nova Scotia.
- Houser, C. & Hamilton, S. (2009). Sensitivity of post-hurricane beach and dune recovery to event frequency. *Earth Surface Processes and Landforms*, 34: 613-628.
- Hughes, P. & Brundrit, G. B. (1992). An index to assess South Africa's vulnerability to sea level rise. *South African Journal of Science*, 88: 308-311.
- Irish, J. L., Frey, A. E., Rosati, J. D., Olivera, F., Dunkin, L. M., Kaihatu, J. M., Ferreira, C. M., & Edge, B. L. (2010). Potential implications of global warming and barrier island degradation on future hurricane inundation, property damages and population impacted. *Ocean and Coastal Management*, 53: 645 – 657.
- Inman, D. L. & Nordstrom, C. E. (1971). On the Tectonic and Morphologic Classification of Coasts. *The Journal of Geology*, 79(1): 1-21.
- IPCC. (2001). *Third Assessment Report: Working Group II*. Retrieved from: http://www.ipcc.ch/publications_and_data/publications_and_data_reports.shtml#UQtBxo5-E0w [accessed October 4th, 2012].
- IPCC. (2007). *Fourth Assessment Report: Working Group II*. Retrieved from: http://www.ipcc.ch/publications_and_data/publications_ipcc_fourth_assessment_report_wg2_report_impacts_adaptation_and_vulnerability.htm [accessed October 4th, 2012].
- Jackson, D. A. (1993). Stopping Rules in Principal Components Analysis: A Comparison of Heuristical and Statistical Approaches. *Ecology*, 74(8): 2204-2214.
- James, T. S., Henton, J. A., Leonard, L. J., Darlington, A., Forbes, D. L., Craymer, M. (2014). *Relative Sea-level Projections in Canada and the Adjacent Mainland United States*. Geological Survey of Canada, Open File 7737.
- James, T., Leonard, L., Darlington, A., Henton, J., Mazzotti, S., Forbes, D., & Craymer, M. (2013). *Relative sea-level projections for 22 communities on the east coast of Canada and the adjacent United States*. Unpublished Draft Report In Review.
- Jenner, K. A., Sherin, A. G., & Horsman, T. (2003). The use of dynamic segmentation in the Coastal Information System: Adjacency Relationships from Southeastern Newfoundland.

In: D. Green & S. King (Eds.), *Coastal Marine Geo-Information Systems 4* (pp. 371-384). Netherlands: Kluwer Academic Publishing.

Kay, R. & Alder, J. (1999). *Coastal Planning and Management*. London, UK: E & FN Spon.

Keppie, J. D. (2000). *Geological Map of the Province of Nova Scotia*. Nova Scotia Department of Natural Resources Minerals and Energy Branch Map ME 2000-1, 1:500 000.

Klein, R. J. T., Nicholls, R. J. & Mimura, N. (1999). Assessment of coastal vulnerability to climate change. *Ambio*, 28(2): 182-187.

Klein, R. J. T., Smit, M. J., Goosen, H., & Hulsbergen, C. H. (1998). Resilience and Vulnerability: Coastal Dynamics or Dutch Dikes?. *The Geographical Journal*, 164(3): 259-268.

Koutrakis, E., Sapounidis, A., Marzetti, S., Marin, V., Roussel, S., Martino, S., Fabiano, M., Paoli, C., Rey-Valette, H., Povh, D., & Malvarez, C. G. (2011). ICZM and coastal defence perception by beach users: Lessons from the Mediterranean coastal area. *Ocean & Coastal Management*, 54: 821-830.

Kumar, T. S., Mahendra, R. S., Nayak, S., Radhakrishnan, K., & Sahu, K. C. (2010). Coastal Vulnerability Assessment for Orissa State, East Coast of India. *Journal of Coastal Research*, 26(3): 523-534.

Lichter, M., Vafeidis, A., Athanasios, T., Nicholls, R. J., & Kaiser, G. (2011). Exploring Data-Related Uncertainties in Analyses of Land Area and Population in the "Low-Elevation Coastal Zone" (LECZ). *Journal of Coastal Research*, 27(4): 757-768.

Luers, A. L. (2005). The surface of vulnerability: An analytical framework for examining environmental change. *Global Environmental Change*, 15: 214-223.

Mackenzie, J. & Duke, N. (2012). *Mangrove Watch: Shoreline Video Assessment (S-VAM)*. First Annual Forum on Building Coastal Resilience in Viet Nam, Cambodia, and Thailand, Cahanthaburi, Thailand, February 28th – March 2nd, 2012. Retrieved from: http://cmsdata.iucn.org/downloads/parallel_session_i_s_vam_presentation_1.pdf [accessed December 24th, 2014].

Malhotra, A. & Fonseca, M. S. (2007). *WEMO (Wave Exposure Model): Formulation, Procedures and Validation*. NOAA Technical Memorandum, NOS NCCOS #65. Retrieved from: http://products.coastalscience.noaa.gov/wemo/_assets/docs/NOS_NCCOS_65.pdf [accessed February 5th, 2015].

- Mangor, K. (2004). *Shoreline Management Guidelines*. Denmark: DHI Water & Environment.
- Manson, G.K. (2002). Subannual Erosion and Retreat of cohesive Till Bluffs, McNab's Island, Nova Scotia. *Journal of Coastal Research*, 18(3): 421-432.
- Masselink, G., Hughes, M. G., & Knight, J. (2011). *Introduction to Coastal Processes & Geomorphology (2nd Ed.)*. London, UK: Hodder Education.
- Mattatall, P. (1993). *Highlights of Lockeport's History*. Unpublished document.
- McLaughlin, S. & Cooper, J. A. G. (2010). A multi-scale coastal vulnerability index: A tool for coastal managers?. *Environmental Hazards*, 9(3): 233-248.
- McLaughlin, S., McKenna, J., & Cooper, J. A. G. (2002). Socio-economic data in coastal vulnerability indices: constraints and opportunities. *Journal of Coastal Research*, S136: 487-497.
- Mendoza, E.T. & Jiménez, J.A. (2009) Regional geomorphic vulnerability analysis to storms for Catalan beaches. *Proceedings of the Institution of Civil Engineers, Maritime Engineering*, 162(3): 127-135.
- Millier Dickinson Blais. (2013). Economic Development Council South West Nova: Five-Year Strategic Economic Development Plan. Retrieved from:
<http://lockeport.ns.ca/docs/Five%20Year%20Strategic%20Economic%20Development%20Plan.pdf> [accessed December 20th, 2014].
- Mimura, N., Nurse, L., McLean, R. F., Agard, J., Briguglio, L., Lefale, P., Pavet, R., & Sem, G. (2007). Small Islands. In M. L. Parry, O. F. Canziani, J. P. Palutikof, P. J. van der Linden, & C. E. Hanson (Eds.), *Climate Change 2007: Impacts, Adaptation and Vulnerability. Contribution of Working Group II to the Fourth Assessment Report of the Intergovernmental Panel on Climate Change* (pp. 687-716). Cambridge, UK: Cambridge University Press.
- Mirzaei, A., Tangang, F., & Juneng, L. (2014). Wave energy potential along the east coast of Peninsular Malaysia. *Energy*, 68: 722-734.
- Mitra, D. S. (2011). Remote Sensing and GIS for Coastal Zone Management: Indian Experience In S. Anbazhagan, S. Subramanian & X. Yang (Eds.), *Geoinformatics in Applied Geomorphology* (pp. 63-85). Boca Raton, Florida: CRC Press.

- Möller, I. (2006). Quantifying saltmarsh vegetation and its effect on wave height dissipation: Results from a UK East coast saltmarsh. *Estuarine Coastal and Shelf Science*, 69(3-4): 337-351.
- Morton, R. A. (2002). Factors Controlling Storm Impacts on Coastal Barriers and Beaches: A Preliminary Basis for near Real-Time Forecasting. *Journal of Coastal Research*, 18(3): 486-501.
- Morton, R. A. & Sallenger, A. (2003). Morphological Impacts of Extreme Storms on Sandy Beaches and Barriers. *Journal of Coastal Research*, 19(3): 560-573.
- Municipality of the District of Shelburne. (2013). *Observed Vulnerability Area Maps*. Unpublished document.
- Natural Resources Canada (NRCan). (2004). *Coastal Zone*. Retrieved from: <http://www.nrcan.gc.ca/environment/resources/publications/impacts-adaptation/reports/assessments/2004/ch7/10207> [accessed September 9th, 2014].
- Naylor, L. A., Stephenson, W. J., & Trenhaile, A. S. (2010). Rock coast geomorphology: Recent advances and future research directions. *Geomorphology*, 114: 3-11.
- Nicholls, R. J. & Branson, J. (1998). Coastal Resilience and Planning for an Uncertain Future: An Introduction. *The Geographical Journal*, 164(3): 255-258.
- Nicholls, R. J. & Cazenave, A. (2010). Sea-Level Rise and its Impact on Coastal Zones. *Science*, 328(5985): 1517-1520.
- Nicholls, R. J., Wong, P. P., Burkett, V. R., Condignotto, J. O., Hay, J. E., McLean, R. F., Ragoonaden, S., & Woodroffe, C. D. (2007). Coastal systems and low-lying areas. In M. Parry, O. F. Canziani, J. P. Palutikof, P. J. van der Linden, & C. E. Hanson (Eds.), *Climate Change 2007: Impacts, Adaptation and Vulnerability. Contribution of Working Group II to the Fourth Assessment Report of the Intergovernmental Panel on Climate Change* (pp. 315-356). Cambridge, UK: Cambridge University Press.
- Orford, J.R., Carter, R.W.G., & Forbes, D.L. (1991). Gravel Barrier Migration and Sea Level Rise: Some Observations From Story Head, Nova Scotia, Canada. *Journal of Coastal Research*, 7(2): 477-488.
- Oppenheimer, M., Campos, M., Warren, R., Birkman, J., Luber, G., O'Neill, B., & Takahashi, K. (2014). Emergent Risks and Key Vulnerabilities. In C. B. Field, V. R. Barros, D. J. Bokken, K. J. Mach, M. D. Mastrandres, T. E. Bilir, M. Chatterjee, K. L. Ebi, Y. O. Estrada, R. C.

- Genova, B. Girma, E. S. Kissel, A. N. Levy, S. MacCracken, P. R. Mastrandrea, & L.L. White (Eds.), *Climate Change 2014: Impacts, Adaptation, and Vulnerability. Part A: Global and Sectoral Aspects. Contribution of Working Group II to the Fifth Assessment Report on the Intergovernmental Panel on Climate Change* (pp. 1039-1099). Cambridge, UK and New York, NY, USA: Cambridge University Press.
- Orencio, P. M. & Fujii, M. (2013). An Index to Determine Vulnerability of Communities in a Coastal Zone: A Case Study fo Baler, Aurora, Philippines. *Ambio*, 42(1): 61-71.
- Ozyurt, G. (2007). *Vulnerability of Coastal Areas to Sea Level Rise: A Case Study on Goksu Delta* (Master of Science Dissertation). School of Natural and Applied Science of Middle East Technical University.
- Palmer, B. J., Van der Elst, R., Mackay, F., Mathers, A. A., Smith, A. M., Bundy, S. C., Thackeray, Z., Leucl, R., & Parak, O. (2011). Preliminary coastal vulnerability assessment for KwaZulu-Natal, South Africa. *Journal of Coastal Research*, SI64: 1390-1395.
- Pendleton, E. A., Thieler, E. R., & Williams, S. J. (2004). *Coastal Vulnerability Assessment of Virgin Islands National Park (VIIS) to Sea-Level Rise*. USGS. Retrieved from: <http://pubs.usgs.gov/of/2004/1398/images/pdf/report.pdf> [accessed November 24th, 2014].
- Pethick, J. S. & Crooks, S. (2000). Development of a coastal vulnerability index: a geomorphological perspective. *Environmental Conservation*, 27(4): 359-367.
- Perison-Parrish, E. M., Runyan, R. M., Siemer, K. W., Jackson, C. W. Jr., Bush, D. M., Llerandi-Roman, P. A., & Neal, W. J. (2012). *A Modified Coastal Vulnerability Index for Small Associated Islands of Puerto Rico and the US Virgin Islands*. 2012 GSA Annual Meeting in Charlotte, Paper No. 92-46. Retrieved from: <https://gsa.confex.com/gsa/2013SE/webprogram/Paper216506.html> [accessed November 24th, 2014].
- Pernetta, J. (2004). *Guide to the Oceans*. New York, NY: Firefly Books Ltd.
- Phillips, J. D. (2009). Changes, perturbations, and responses in geomorphic systems. *Progress in Physical Geography*, 33(1): 17-30.
- Pietersma-Perrott, B. & van Proosdij, D. (2012). Shore Zone Characterization for Climate Change in the Bay of Fundy. Atlantic Climate Adaptation Solutions (ACAS). Retrieved from:

http://atlanticadaptation.ca/sites/discoveryspace.upei.ca/acasa/files/ACAS%20Shorezone%20Classification_0.pdf [accessed November 24th, 2014].

Province of Nova Scotia (2013). *Coastal Management in Nova Scotia*. Retrieved from: <http://www.novascotia.ca/coast> [accessed September 8th, 2014].

Putnam, J. A., & Johnson, J. W. (1949). The Dissipation of Wave Energy by Bottom Friction. *Transactions of the American Geophysical Union*, 30: 67-74.

Ramieri, E., Hartley, A., Barbanti, A., Duarte Santos, F., Gomes, A., Hilden, M., Laihonon, P., Marinova, N., & Santini, M. (2011). *Methods for Assessing Coastal Vulnerability to Climate Change*. European Environment Agency: European Topic Centre on Climate Change Impacts, Vulnerability and Adaptation, ETC CCA Technical Paper 1/2011. Retrieved from: http://cca.eionet.europa.eu/docs/TP_1-2011 [accessed November 24th, 2014].

Rochette, J. (2010). *Coastal zone definition and geographic coverage of the ICZM Protocol Issues*. Institute for Sustainable Development and International Relations (IDDRI), 2nd Ad hoc Legal and Technical Working Group meeting on the ICZM Protocol December 6-7th, 2010, Mombasa, Kenya. Retrieved from: http://www.unep.org/NairobiConvention/docs/Coastal_zone_definition_and_geographic_coverage_of_the_ICZM_Protocol-Julien_Rochette.pdf [accessed December 24th, 2014].

Savard, J., van Proosdij, D., O'Carroll, S., Bernatchez, P., Bell, T., Drezja, S., Quintin, C., Desjarlais, C., Leclerc, L., Martel, N., Morneau, F., Robinson, C., Warburton, A., Charles, T. (2014). *Perspective on the East Coast Region*. Unpublished draft report.

Scott, D. M. (1991). *The Dynamic Dunes of Crescent Beach, Lockeport, Nova Scotia: 1978 to 1990* (Honours Dissertation). Saint Mary's University, Halifax, Nova Scotia.

Shaw, J., Taylor, R. B., Forbes, D. L., Ruz, M. H., & Solomon, S. (1998). *Sensitivity of the Coasts of Canada to Sea-Level Rise*. Geological Survey of Canada Bulletin 505.

Sherin, A. (2000). Linear Reference Data Models: Dynamic Segmentation and Application to Coastal and Marine Data. In: D. Wright & D. Bartlett (Eds.). *Marine and Coastal Geographical Information Systems* (pp. 95-166). London, UK: Taylor & Francis.

Short, A. D. (2007). *Beaches of the New South Wales Coast: A Guide to their Nature, Characteristics, Surf and Safety*. Sydney, Australia: Sydney University Press.

- Simpson, M. C., Scott, D., Harrison, M., Sim, R., Silver, N., O'Keeffe, E., Harrison, S., Taylor, M., Lizcano, G., Ruddy, M., Stager, H., Oldham, J., Wilson, M., New, M., Clarke, J., Day, O., Fields, N., Georges, J., & Waithe, R., McSharry, P. (2010). *Quantification and Magnitude of Losses and Damages Resulting from the Impacts of Climate Change: Modelling the Transformational Impacts and Costs of Sea Level Rise in the Caribbean*. UNDP. Retrieved from: <http://caribbean.intasave.org/documents/Publications/Reports/Climate-Change-Science-Policy-and-Practice/Quantification-of-Losses-and-Damages-Resulting-from-the-Impacts-of-Climate-Change/Transformational-Impacts-Full-Report.pdf> [accessed November 24th, 2014].
- Smit, B. & Wandel, J. (2006). Adaptation, adaptive capacity and vulnerability. *Global Environmental Change*, 16: 282-292.
- Smith, L. I. (2002). *A tutorial on Principal Components Analysis*. Retrieved from: http://www.cs.otago.ac.nz/cosc453/student_tutorials/principal_components.pdf [accessed December 7th, 2014].
- Smith, C. D., Manson, G. K., Couture, N. J., James, T. L., Lemmen, D. S., Forbes, D. L., Fraser, P., Frobel, D., Jenner, K. A., Lynds, T. L., Szlavko, B., Taylor, R. B., & Whalen, D. (2013). CanCoast: A national-scale framework for characterising Canada's marine coasts. In: R. Devillers, C. Lee, R. Canessa, & A. Sherin (Eds.), *CoastGIS Conference Proceedings 2013: Monitoring and Adapting to Change on the Coast* (pp. 39-41). The 11th International Symposium for GIS and Computer Cartography for Coastal Zone Management, Victoria, British Columbia, Canada June 18-21, 2013. Retrieved from: <http://coinatlantic.ca/coastgis2013/docs/proceedings.pdf> [accessed November 24th, 2014].
- Sousa, P. H. G. D., Siegle, E., & Tessler, M. G. (2012). Vulnerability assessment of Massaguacu Beach (SE Brazil). *Ocean & Coastal Management*, 77: 24-30.
- Stern, N. (2007). *The Economics of Climate Change: The Stern Review*. Cambridge, UK: Cambridge University Press.
- Stern, B., Hurni, L., Wiesmann, S., & Ysakowski, Y. (2011). *Statistics for Thematic Cartography*. Geographic Information Technology Training Alliance. Retrieved from: <http://www.gitta.info/Statistics/en/text/Statistics.pdf> [accessed November 24th, 2014].
- Sterr, H. (2008). Assessment of Vulnerability and Adaptation to Sea-Level Rise for the Coastal Zone of Germany. *Journal of Coastal Research*, 24(2): 380-393.

- Stocker, T. F., Qin, D., Plattner, G.-K., Alexander, L. V., Allen, S. K., Bindoff, N. L., Breon, F.-M., Church, J. A., Cubasch, U., Emori, S., Forster, P., Friedlingstein, P., Gillett, N., Gregory, J. M., Hartmann, D. L., Jansen, E., Kirtman, B., Knutti, R., Kumar, K., K. Lemke, P., Marotzke, J., Masson-Delmotte, V., Meehl, G. A., Mokhov, I. I., Piao, S., Ramaswamy, V., Randall, D., Rhein, M., Rojas, M., Sabine, C., Shindell, D., Talley, L. D., Vaughan, D. G., & D., Xie, S.-P. (2013). Technical Summary. In F. Stocker, D. Qin, G. K. Plattner, M. Tignor, S. K. Allen, J. Boschung, A. Nauels, Y. Xia, V. Bex, & P. M. Midgley (Eds.), *Climate Change 2013: The Physical Science Basis. Contribution of Working Group I to the Fifth Assessment Report of the Intergovernmental Panel on Climate Change* (pp. 33-116). Cambridge, UK and New York, NY, USA: Cambridge University Press.
- Szlafsztein, C. & Sterr, H. (2007). A GIS-Based Vulnerability Assessment of Coastal Natural Hazards, State of Para, Brazil. *Journal of Coastal Conservation*, 11(1): 53-66.
- Taylor, R. B. (2009). *Crescent Beach, Lockeport, Nova Scotia (Site 2015)*. Geological Survey of Canada. Unpublished document.
- Taylor, R. B. & Frobel, D. (2009). *2009 Hurricane Bill Aug 23, 2009 Lockeport Beach Surveys*. Geological Survey of Canada. Unpublished document.
- The Canadian Press. (2011). *Damage from recent Nova Scotia storms totals \$13M*. Retrieved from: <http://www.ctvnews.ca/damage-from-recent-nova-scotia-storms-totals-13m-1.593356> [accessed November 14th, 2014].
- The Economic Commission for Latin America (2000). *The Vulnerability of the Small Island Developing States of the Caribbean*. Retrieved from: <http://www.eclac.org/publicaciones/xml/8/8118/G0588.html> [accessed November 24th, 2014].
- Thieler, E. R., Himmelstoss, E. A., Zichichi, J. L., & Ergul, A. (2009). *Digital Shoreline Analysis System (DSAS) version 4.0: An ArcGIS extension for calculating shoreline change*. United States Geological Survey. Open File Report 2008-1278. Retrieved from: <http://woodshole.er.usgs.gov/project-pages/DSAS/> [accessed November 24th, 2014].
- Thieler, E. R. & Hammar-Klose, E. S. (2000). National Assessment of Coastal Vulnerability to Sea-Level Rise: Preliminary Results for the US Gulf of Mexico Coast. USGS. Retrieved from: <http://pubs.usgs.gov/dds/dds68/reports/gulfrep.pdf> [accessed November 24th, 2014].

- Tibbetts, J. R. & van Proosdij, D. (2013). Development of a relative coastal vulnerability index in a macro-tidal environment for climate change adaptation. *Journal of Coastal Conservation*. 17(4): 775-797.
- Torresan, S., Critto, A., Rizzi, J., & Marcomini, A. (2012). Assessment of coastal vulnerability to climate change hazards at the regional scale: the case study of the North Adriatic Sea. *Natural Hazards Earth System Science*, 12: 2347-2368.
- Town of Lockeport. (2013). *Things to Do*. Retrieved from: <http://www.lockeport.ns.ca/thingsinlockeport.php> [accessed November, 12th, 2014].
- Trenhaile, A. S. (2004). *Geomorphology: A Canadian Perspective (2nd ed.)*. Oxford, England: Oxford University Press.
- United Nations Environment Programme (UNEP)/Global Programme of Action for the Protection of the Marine Environment from Land-based Activities (GPA). (2003). *Diagnosis of the Erosion Processes in the Caribbean Sandy Beaches*. Environmental Agency, Ministry of Science, Technology and Environment, Government of Cuba. Retrieved from: http://faculty.kfupm.edu.sa/CHEM/thukair/ENVS%20590/Hand%20out/F2/diagnosis_of_the_erosion-17.pdf [accessed November 24th, 2014].
- United Nations Environment Programme (UNEP). (n.d.). *Why UNEP Is Focusing on Small Island Developing States*. Retrieved from: <http://www.unep.org/PDF/SIDS/SIDS-Booklet-4March.pdf> [accessed November 4th, 2012].
- van Proosdij, D. & Page, S. W. (2012). Best Management Practices for Climate Change Adaptation in Dykelands: Recommendations for Fundy ACAS sites. Atlantic Climate Adaptation Solutions (ACAS). Retrieved from: <http://atlanticadaptation.ca/sites/discoveryspace.upei.ca/acasa/files/Best%20Management%20Practices%20for%20Climate%20Change%20Adaptation%20in%20Dykelands.0.pdf> [accessed November 24th, 2014].
- van Vuuren, D. P., Edmonds, J., Kainuma, M., Riahi, K., Thomson, A., Hibbard, K., Hurtt, G. C., Kram, T., Krey, V., Lamarque, J., Masui, T., Meinshausen, M., Nakicenovic, N., Smith, S. J., & Rose, S. K. (2011). The representative concentration pathways: an overview. *Climatic Change*, 109: 5-31.
- Vermeer, M. & Rahmstorf, S. (2009). Global sea level linked to global temperature. *PNAS*, 106(51): 21527-21532.

- Wang, P., Kirby, J. H., Haber, J. D., Horwitz, M. H., Knorr, P. O., & Krock, J. R. (2006). Morphological and Sedimentological Impacts of Hurricane Ivan and Immediate Poststorm Beach Recovery along the Northwestern Florida Barrier-Island Coasts. *Journal of Coastal Research*, 22: 238-258.
- Wong, P. P., Losada, I. J., Gattuso, J.-P., Hinkel, J., Khattabi, A., McInnes, K. L., Saito, Y., & Sallenger, A. (2014). Coastal Systems and Low-Lying Areas. In C. B. Field, V. R. Barros, D. J. Bokken, K. J. Mach, M. D. Mastrandres, T. E. Bilir, M. Chatterjee, K. L. Ebi, Y. O. Estrada, R. C. Genova, B. Girma, E. S. Kissel, A. N. Levy, S. MacCracken, P. R. Mastrandrea, & L.L. White (Eds.), *Climate Change 2014: Impacts, Adaptation, and Vulnerability. Part A: Global and Sectoral Aspects. Contribution of Working Group II to the Fifth Assessment Report on the Intergovernmental Panel on Climate Change* (pp. 361-409). Cambridge, UK and New York, NY, USA: Cambridge University Press.
- Wood, J. D., Muttray, M., & Oumeraci, H. (2001). The SWAN model used to study wave evolution in a flume. *Ocean Engineering*, 28: 805-823.
- Woodroffe, C. D. (2007). The Natural Resilience of Coastal Systems: Primary Concepts. In L. McFaden, E Penning-Rowell, R. Nicholls (Eds.), *Managing Coastal Vulnerability* (pp.45-60). Amsterdam, The Netherlands: Elsevier.
- Woolard, J. W. & Colby, J. D. (2002). Spatial characterization, resolution, and volumetric change of coastal dunes using airborne LIDAR: Cape Hatteras, North Carolina. *Geomorphology*, 48: 269-287.
- Yin, J., Yin, Z., Wang, J., & Xu, S. (2012). National assessment of coastal vulnerability to sea-level rise for the Chinese coast. *Journal of Coastal Conservation*, 16: 123-133.
- Zhai, L., Greenan, B., Hunter, J., James, T., Han, G., Rhomson, R., & MacAulay, P. (2014). *Estimating Sea-level Allowances for the Coasts of Canada and the Adjacent United States Using the Fifth Assessment Report of the IPCC*. Canadian Technical Report of Hydrology and Ocean Sciences 300.
- Zujar, J. O., Francoso, J. I. A., Cajaraville, D. M., & Jurado, P. F. (2009). El uso de las tecnologías de la información geográfica para el cálculo del índice de vulnerabilidad costera (CVI) ante una potencial subida del nivel del mar en la costa andaluza (España). *GeoFocus*, 9: 83-100.

APPENDIX A

SHORELINE CHARACTERIZATION CHARTS AND DEFINITIONS

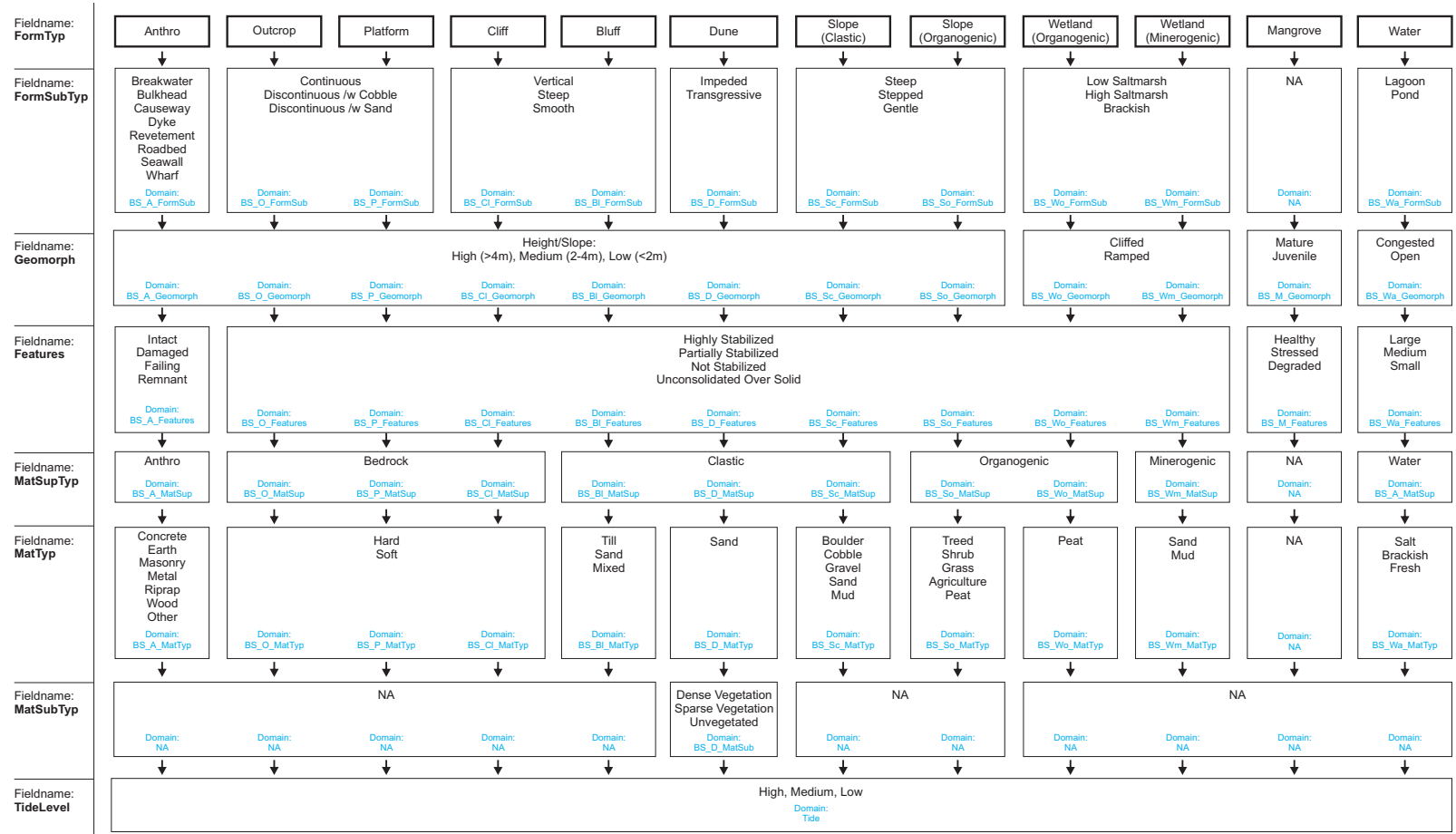


Figure A.1 Backshore Shoreline Characterization Chart.

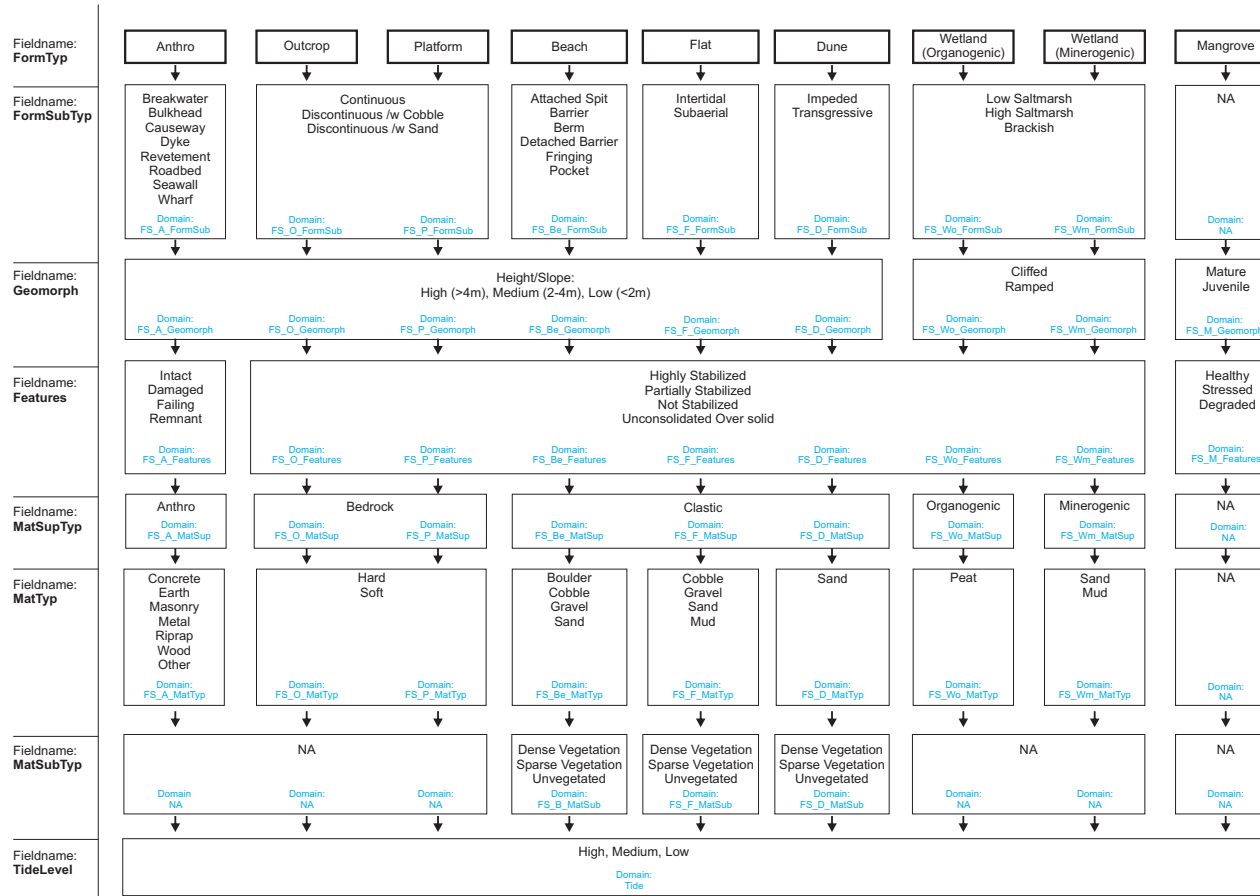


Figure A.2 Foreshore Shoreline Characterization Chart.

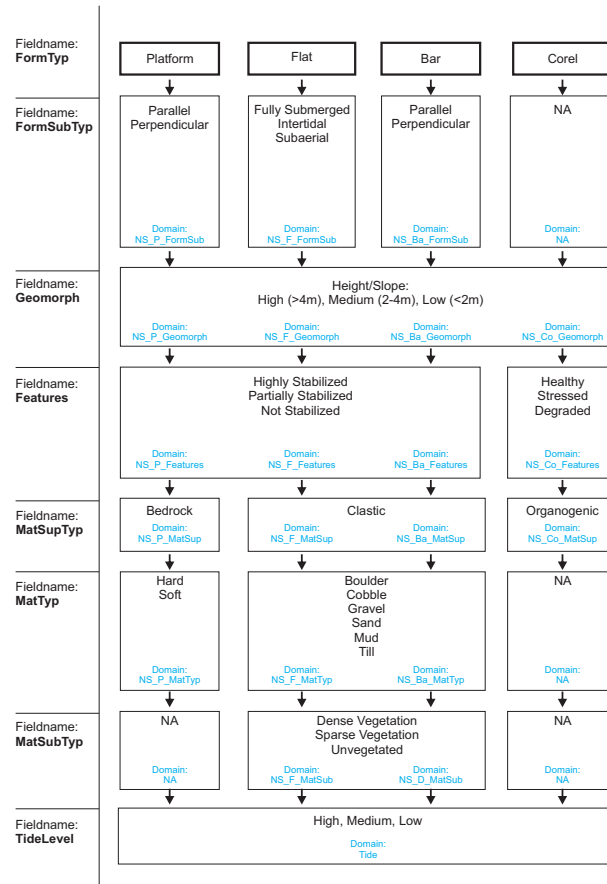


Figure A.3 Nearshore Shoreline Characterization Chart.

Simplified Definitions for Shoreline Characterization

Backshore – extent of farthest possible wave advance in a storm

Foreshore – immediately in front of the backshore (area over which a storm wave would travel)

Nearshore – what is in front of the foreshore (in the water)

BACKSHORE

FormType

Anthro – anything man-made

Outcrop – cliff that is less than 40deg

Platform – bedrock platform (like stepping onto a stage-small cliff)

Cliff – rockface steeper than 40deg (always bedrock)

Bluff – lower angle and very little bedrock, unconsolidated cliff with a few bits of bedrock (boulders)

Dune – a large mound of sand

Slope – unconsolidated material, shallower bluff, equivalent to platform, but unconsolidated

Clastic – non living

Organogenic – living ie: lawn, sod

Wetland – vegetation and wet

Organogenic – living, root mats with plants

Minerogenic – plants, some roots, mostly sand

Water

FormSubType

Breakwater – hardened structure at angle to the shore that stops waves energy before it reaches the shore and protects the shoreline

Bulkhead – retaining wall, generally made out of wood or steel

Causeway – specifically for road, with body water behind

Dyke – earthen/concrete structure to prevent flooding. Land behind dyke is almost always lower

Revetment – sloped structure along shore to prevent erosion

Road – road

Seawall – vertical structure that goes down to bed and breaks wave energy. Generally made of Concrete

Wharf – water passing underneath with mooring of boats

note: for a Gabion basket and living shoreline/soft structure, if rise>run = seawall and if rise<run = revetment

Continuous – all bedrock

Discontinuous – bedrock mixed with cobble or sand in a finger like pattern

Vertical (cliff, bluff) – Can't climb without rope

Steep (cliff, bluff) – need hands to scramble up slope

Smooth (cliff, bluff) – Polished surface (could be vertical or steep)

Impeded – stuck, stable

Transgressive – moving, active

Steep (slope) – need hands to walk up

Gentle (slope) – can walk up

Stepped (slope) – like stairs

Low Saltmarsh – dominated by spartina alterniflora

High Saltmarsh – dominated by spartina patens

Lagoon – historically open at some point, more often open than not, behind a barrier

Pond – pool of water, more often closed than not

Geomorph

Height: High (>4m) – equivalent to 13ft and is greater than height of normal room

Medium (2-4m) – equivalent to 6.3 -13ft

Low (<2m) – equivalent to 6.3ft

Slope: High (>4m) – need hands to climb up it

Medium (2-4m) – can walk up it without using hands

Low (<2m) – very shallow gradient

Cliffed – straight

Ramped - sloped

Congested – full of submerged vegetation, no swimming

Open - swimming

Features

Intact – perfect condition

Damaged – performing function, but looks like it could use some repair

Failing – needs to be replaced, but if repaired, could till go back to function

Remnant – abandoned, not performing function

Highly Stabilized (outcrop, cliff, bluff, plat, wetland) – no erosion, no talus, no recent debris

Partially Stabilized (outcrop, cliff, bluff, plat, wet) – some rock fall

Not Stabilized (outcrop, cliff, bluff, plat, wet) – actively eroding, slumping

Unconsolidated over Solid (outcrop, cliff, bluff, plat, wet) – bedrock base, but unconsolidated over base

Highly Stabilized (dune) – no sand, trees

Partially Stabilized (dune) – some undercutting, movements

Not Stabilized (dune) – blowout, no vegetation

Large – bay = day trip = field

Medium – do a tour = building

Small – useless to put in a canoe = big room

MatSupType

Anthro

Bedrock

Clastic

Organogenic

Minerogenic

Water

MatType (dominant material type)

Concrete – Solid

Masonry – blocks cemented together

Riprap – boulders or others

Metal

Wood

Other – *Living, Gabion Basket*

Hard – granite

Soft – sedimentary (limestone)

Till – sticky, kind of muddy, wet, smaller grain size

Sand – granules

Mixed – mix of sand and till or others

Boulder – can't pick up

Cobble - pick up with two hands

Gravel – much smaller

Sand – granules

Mud – very fine, stuck together

Treed – well established forest

Shrub – bushes, with a few trees

Grass – primarily grass

Agriculture – farmland

Peat – spongy, root mats

MatSubType

Dense Vegetation – 75-100%

Sparse Vegetation – 25-75%

Unvegetated – 0-25%

Tide Level

Is there a high tide line above you? Exposed shells and other organisms?

FORESHORE

MatSubTyp

Beach – deposit of sediment

Flat – platform that is clastic

Geomorph

Attached Spit – large spit attached to land

Barrier – attached at two ends

Detached Barrier – detached at both ends

Fringing – relatively uniform, long distance

Berm – bumpy beach

Pocket Beach – crescent shaped

Intertidal – exposed at tide

Subaerial – mostly exposed

NEARSHORE

FormTyp

Bar – if any bar within 10m of shore, classify as a bar (breaking waves)

APPENDIX B

**INDIVIDUAL RESISTANCE AND RESILIENCE PARAMETER CONTRIBUTION TO COASTAL
VULNERABILITY FOR LOCKEPORT**

Resistance Parameters

With respect to Foreshore Geomorphology (Figure 4.10), the majority (76%) of the coastline has a low contribution to vulnerability with *outcrop, platform, and anthro* (Rank 1) representing 50% of the shoreline and *boulder clastic slope, boulder beach, and wetland* (Rank 2) representing 27% of the shoreline. Three percent of the shoreline has highly vulnerable foreshore geomorphology represented by *no FS*.

Over half of the coastline of Lockeport has a low (Rank 1 & 2) contribution to coastal vulnerability when it comes to the Foreshore Slope parameter with 6% characterized as *ramped* (Rank 1) and 47% as *low slope* (Rank 2). Similar to the Foreshore Geomorphology parameter, only 3% of the shoreline has highly vulnerable Foreshore Slope represented by areas with *high slope or no FS*.

The percent coverage of each Foreshore Width (Figure 4.11) rank is much more evenly distributed than the previous parameters, with the greatest contribution represented by a large width (Rank 1) at 31% and the second greatest contribution represented by a very small width (Rank 5) at 20%. Rank 2, 3, and 4 account for 13%, 17%, and 19% respectively. The largest foreshore widths, which range from 53.47-81.75 m, occur primarily along stretches of coast associated with beaches and wetlands.

The majority of Lockeport's coastline is represented by relatively low Backshore Elevation (Figure 4.12), with 30% of the shore contributing to a medium vulnerability rank (Rank 3), 38% contributing to a high vulnerability rank (Rank 4), and 16% contributing to a very high vulnerability rank (Rank 5), illustrating that 84% of the coastline is below 2.85 m. The remaining 16% has elevation values ranging from 2.86 – 6.10 m, with only 3% of the coastline having a backshore elevation greater than 4.17 m.

With respect to Backshore Slope (Figure 4.13), over 60% of the shoreline indicates a low contribution to vulnerability with 58% of that representing low slope (Rank 2). The low slope designation is prominent along Brighton Road, Back Harbour, Calf Island Road. A large portion of the coast (28%) indicates a medium contribution to vulnerability and a combined 10% is characterized by cliffed wetlands (Rank 4) and high slopes (Rank 5).

Dense grass and sparse shrub (Rank 3) account for almost 50% of Lockeport's shoreline with respect to the Vegetation parameter (Figure 4.14), while 10% of the shoreline is unvegetated (Rank 5). The areas with dense shrub and dense/sparse trees, which have a low contribution to vulnerability, are located along portions of Brighton Road, Roods Park, Sam's Point, and along the shoreline parallel to Cranberry Island, and account for 40% of the shoreline.

Figure 4.15 illustrates the contribution of Coastal Protection Structures (CPSs) to coastal vulnerability. Over 60% of the shoreline is characterized by no CPSs (Rank 5) and the remaining 39% is characterized by a combination of intact, damaged, failing, and remnant structures made of concrete and rip rap of varying sizes. Because this parameter value is derived using the

average ranks of CPS state and CPS material and type, it is difficult to precisely interpret the individual contribution of these attributes.

Resilience Parameters

With respect to Morphological Resilience (Figure 4.16), 85% of the coastline has a medium to very high contribution to vulnerability. The medium rank (Rank 3) encompasses stretches of shoreline consisting of wetlands, a high to medium backshore slope with a fronting beach, or a low slope with no fronting beach. This accounts for 46% of Lockeport's coast and is very prominent along Brighton Road and Back Harbour. Parts of the coast characterized by outcrops, cliffs, and anthro structures contribute to a high vulnerability rank (Rank 5) and account for 23% of the shoreline. The most concentrated area of high vulnerability ranked coastline, for this parameter, is found along Water Street, while the very low vulnerability ranked coastline is found along Crescent Beach and Freddy's Beach and represent 7% of Lockeport's coast.

Over half of Lockeport's shoreline is represented by a relatively high ranked Accommodation Space parameter (Figure 4.17) with 20% of the shore contributing to a high vulnerability rank (Rank 4) and 36% contributing to a very high vulnerability rank (Rank 5), illustrating that 56% of the shoreline has an accommodation space less than 18 m. However, almost a quarter of the shoreline, primarily along Roods Park and Sam's Point, is characterized by an accommodation space of 41-50 m, which contributes to a very low vulnerability rank (Rank 1)

The Sediment Supply parameter has only three rank classes: stable (Rank 1), erosion (Rank 3), and severe erosion (Rank 5). According to Figure 4.18, a quarter of Lockeport's coast is stable, 31% is in a state of erosion and 44% is in a state of severe erosion. The most sediment stable locations are found along the marsh in Back Harbour, sporadically along Brighton Road, and the northern stretch of the coast parallel to Cranberry Island. Conversely, the locations subject to the most severe erosion include the majority of Crescent Beach, Calf Island Road, the historic section of South Street, and the Trestles.

In summary, the three parameters with the largest amount of shoreline contributing to very high vulnerability include Coastal Protection Structures, Sediment Supply and Accommodation Space with 61%, 44%, and 36% shoreline coverage respectively. On the other hand, the three parameters with the largest amount of shoreline contributing to very low vulnerability include Wave Energy for S1 at 54% coverage, Foreshore Geomorphology at 50% coverage and Wave Energy for S2 along with Foreshore Width at 31% coverage each.

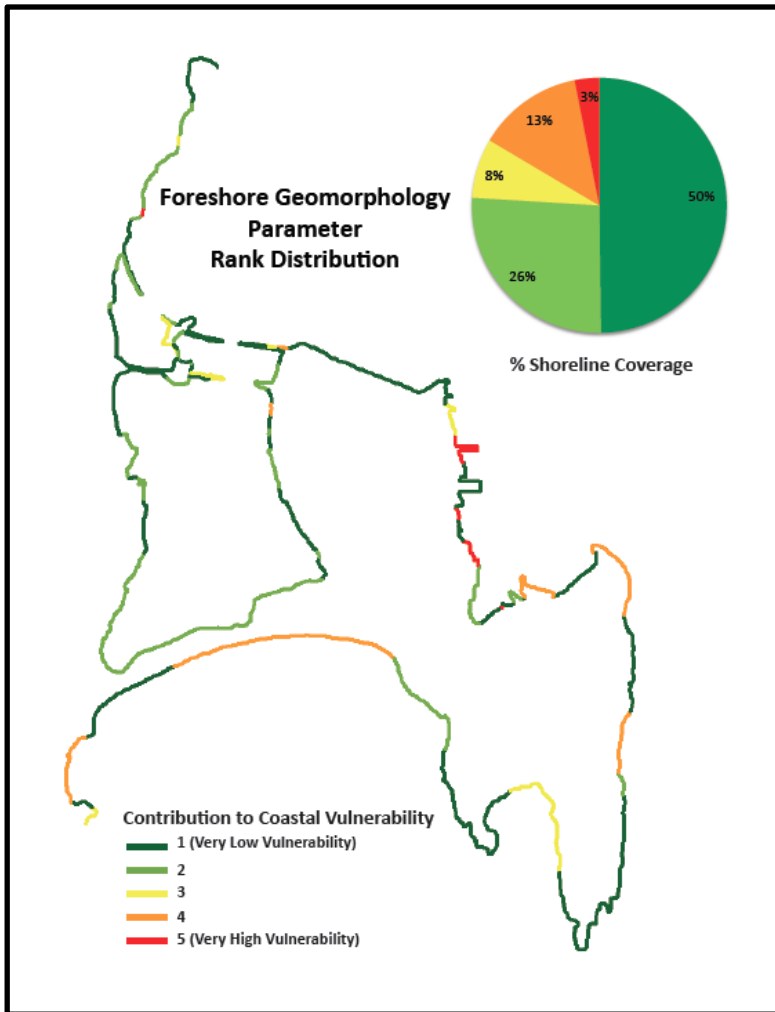


Figure A.4 Contribution of Foreshore Geomorphology Parameter to Coastal Vulnerability. Where % Shoreline Coverage = percent of shoreline associated with each vulnerability rank.

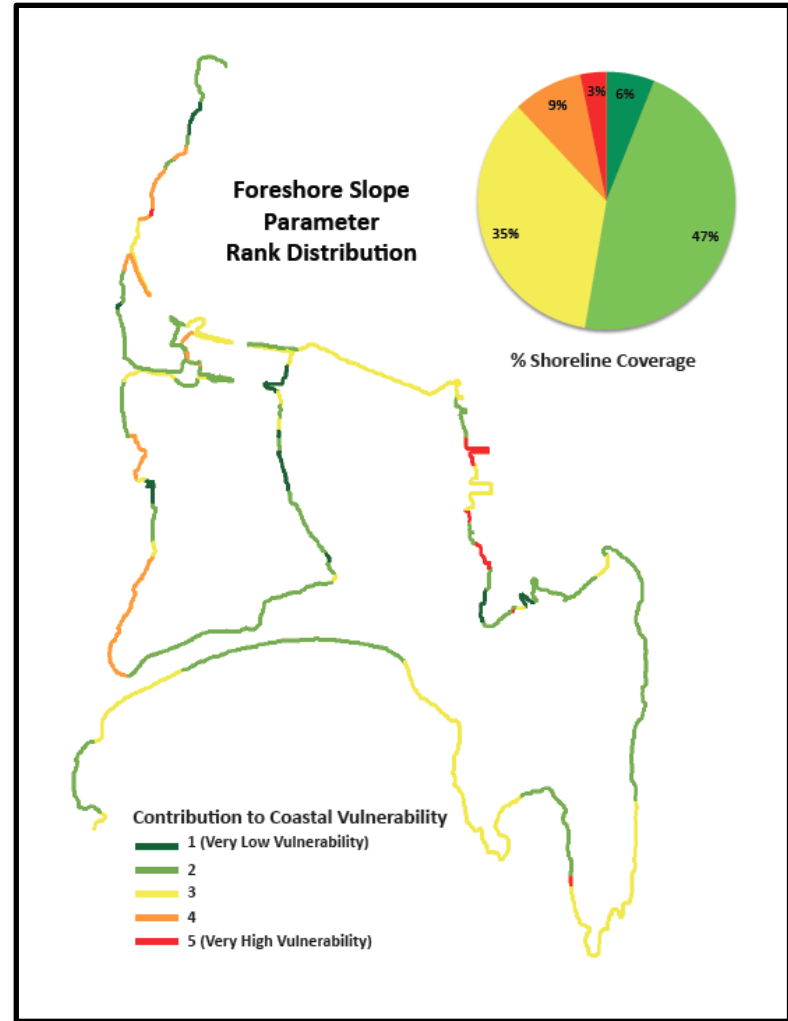


Figure A.5 Contribution of Foreshore Slope Parameter to Coastal Vulnerability. Where % Shoreline Coverage = percent of shoreline associated with each vulnerability rank.

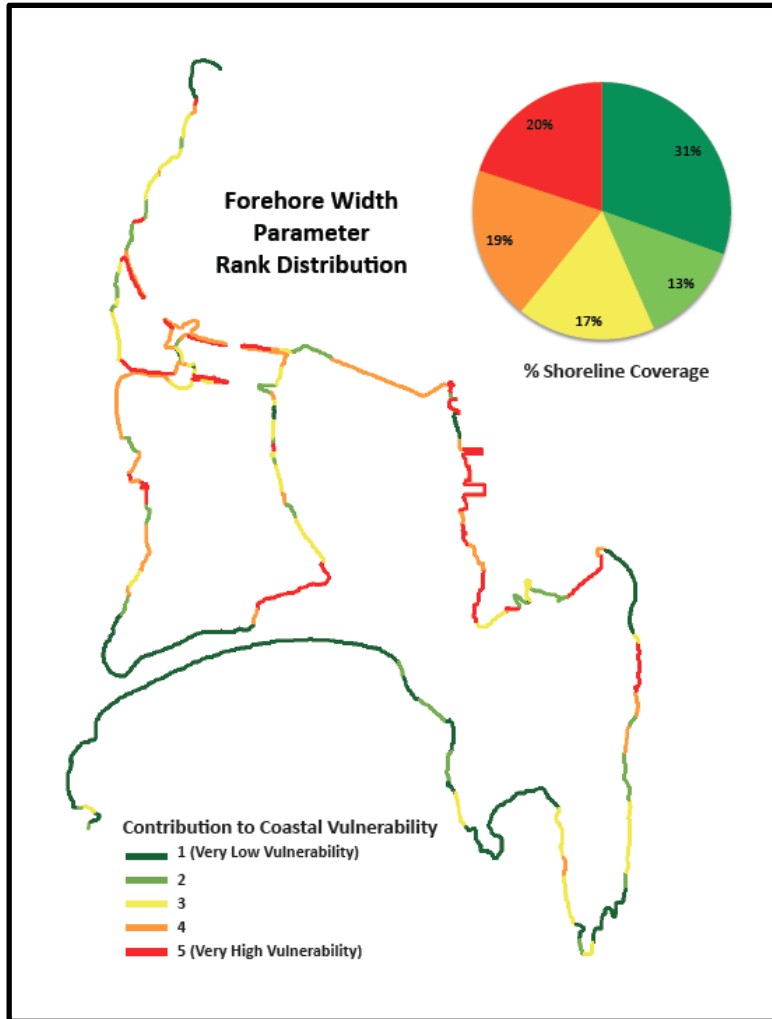


Figure A.6 Contribution of Foreshore Width Parameter to Coastal Vulnerability. Where % Shoreline Coverage = percent of shoreline associated with each vulnerability rank.

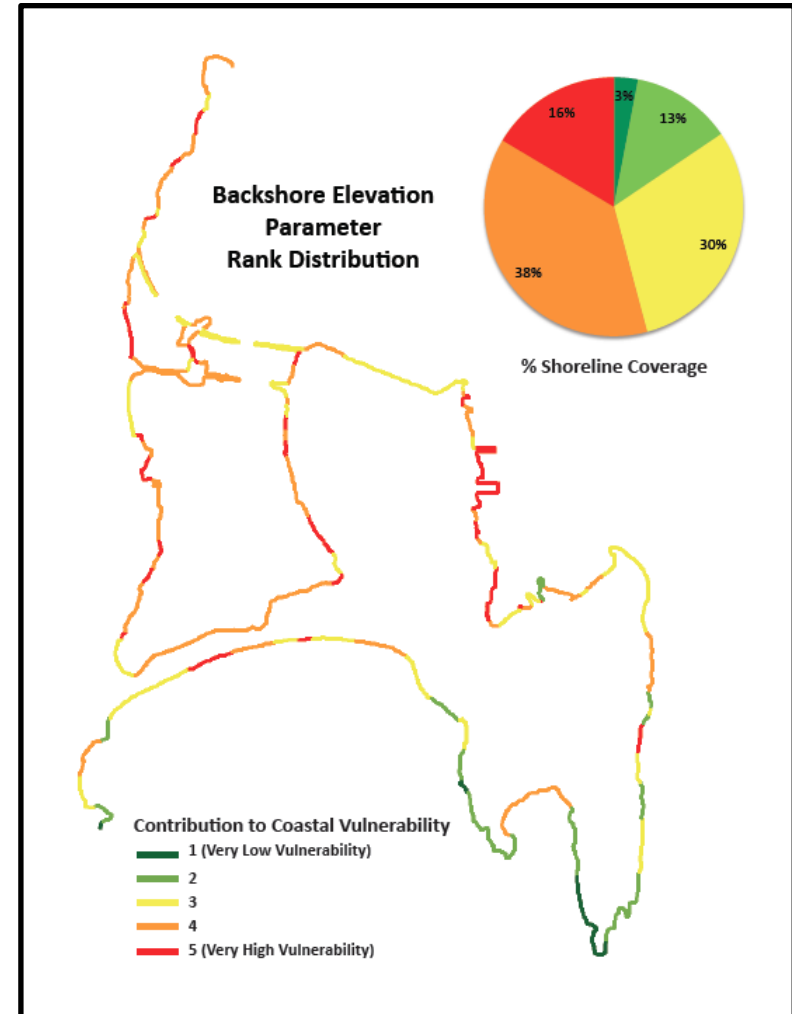


Figure A.7 Contribution of Backshore Elevation Parameter to Coastal Vulnerability. Where % Shoreline Coverage = percent of shoreline associated with each vulnerability rank.

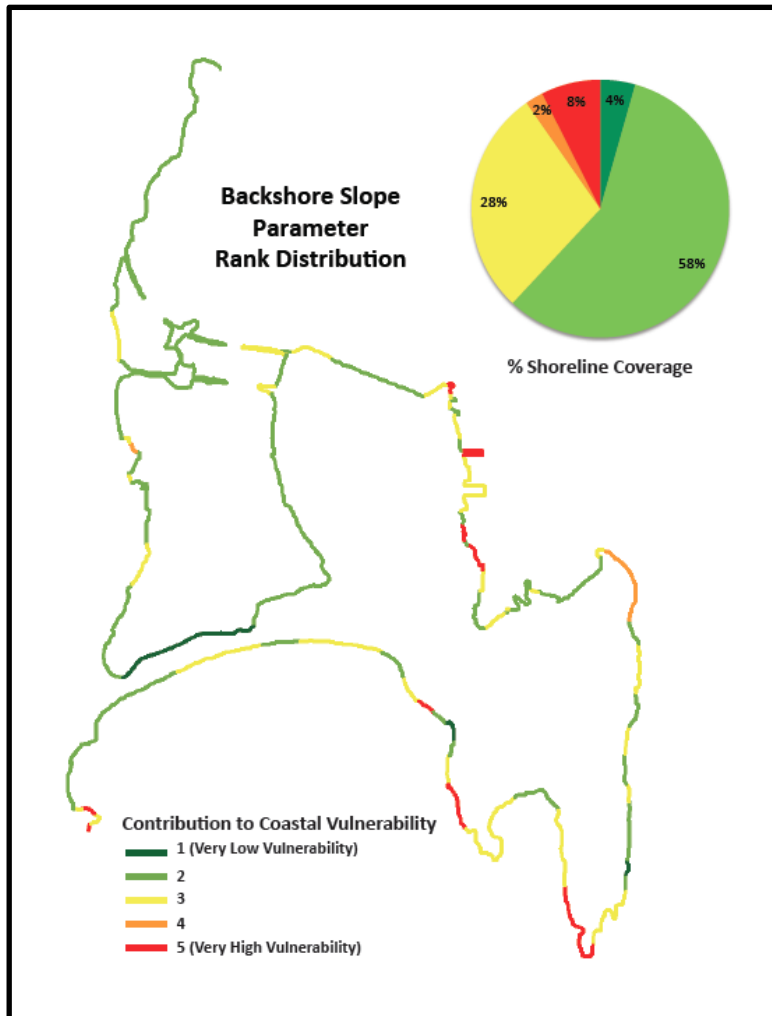


Figure A.8 Contribution of Backshore Slope Parameter to Coastal Vulnerability. Where % Shoreline Coverage = percent of shoreline associated with each vulnerability rank.

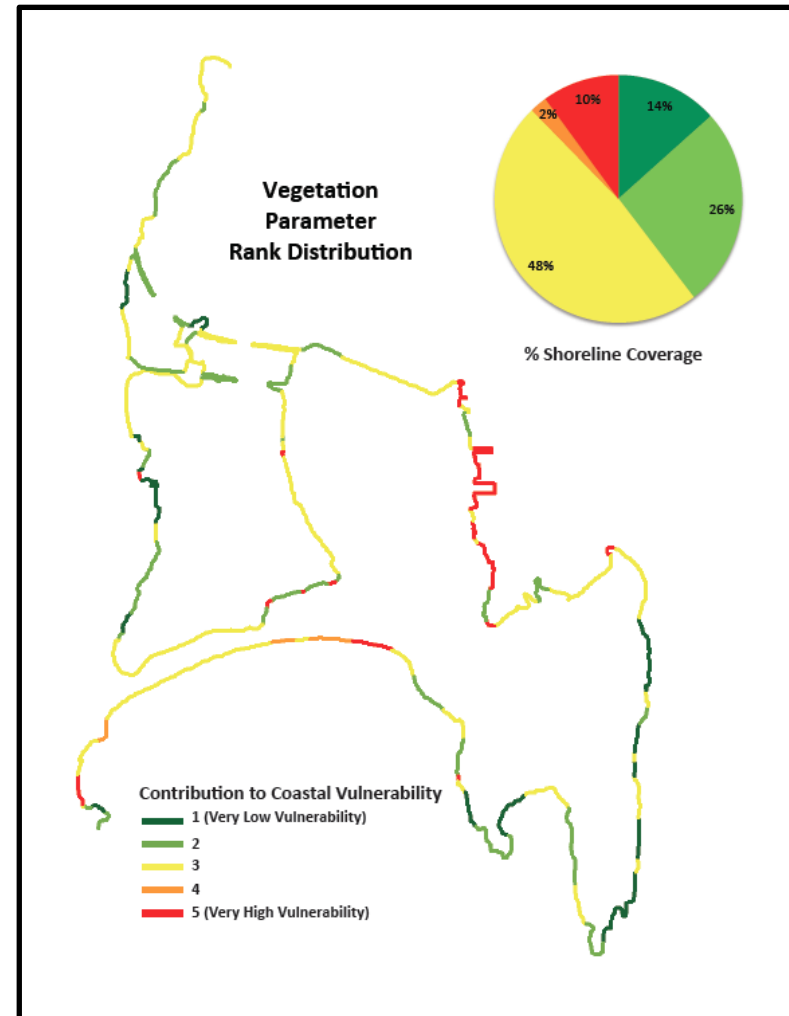


Figure A.9 Contribution of Backshore Vegetation Parameter to Coastal Vulnerability. Where % Shoreline Coverage = percent of shoreline associated with each vulnerability rank.

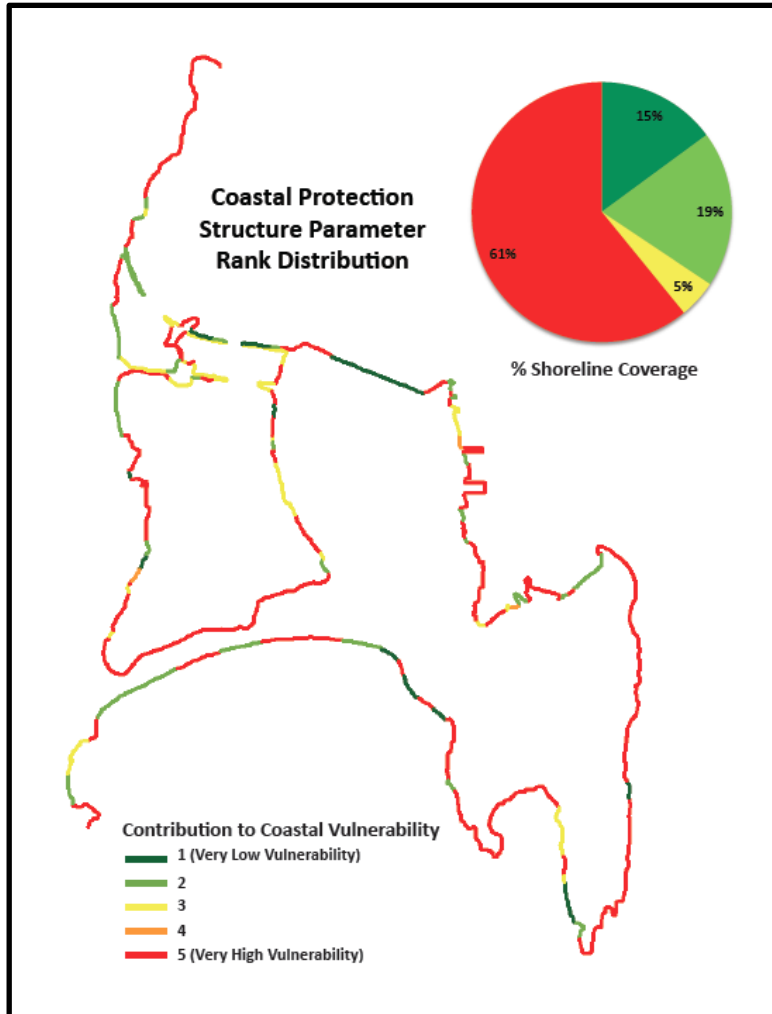


Figure A.10 Contribution of Coastal Protection Structure Parameter to Coastal Vulnerability. Where % Shoreline Coverage = percent of shoreline associated with each vulnerability rank.

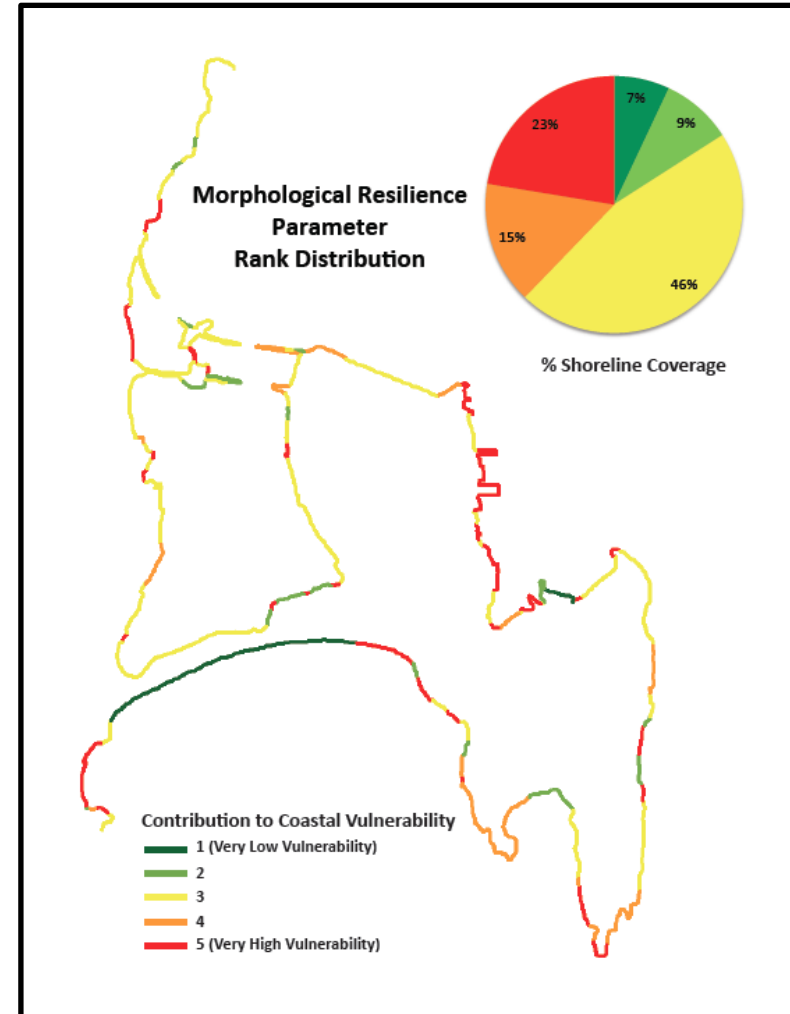


Figure A.11 Contribution of Morphological Resilience Parameter to Coastal Vulnerability. Where % Shoreline Coverage = percent of shoreline associated with each vulnerability rank.

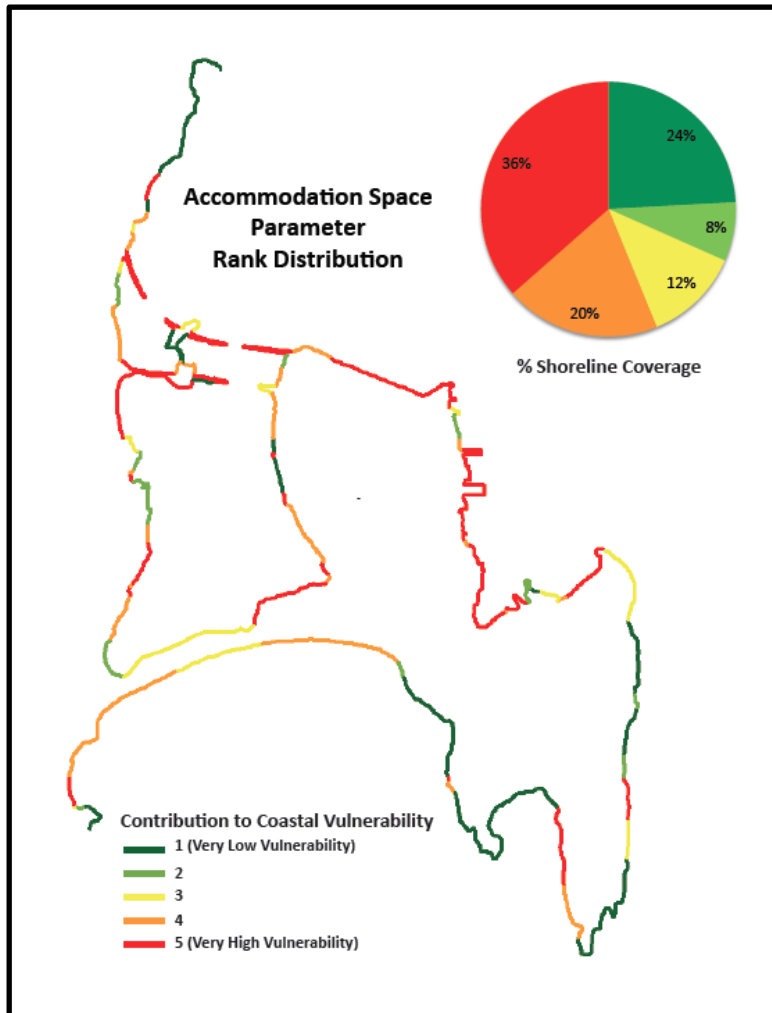


Figure A.12 Contribution of Accommodation Space Parameter to Coastal Vulnerability. Where % Shoreline Coverage = percent of shoreline associated with each vulnerability rank.

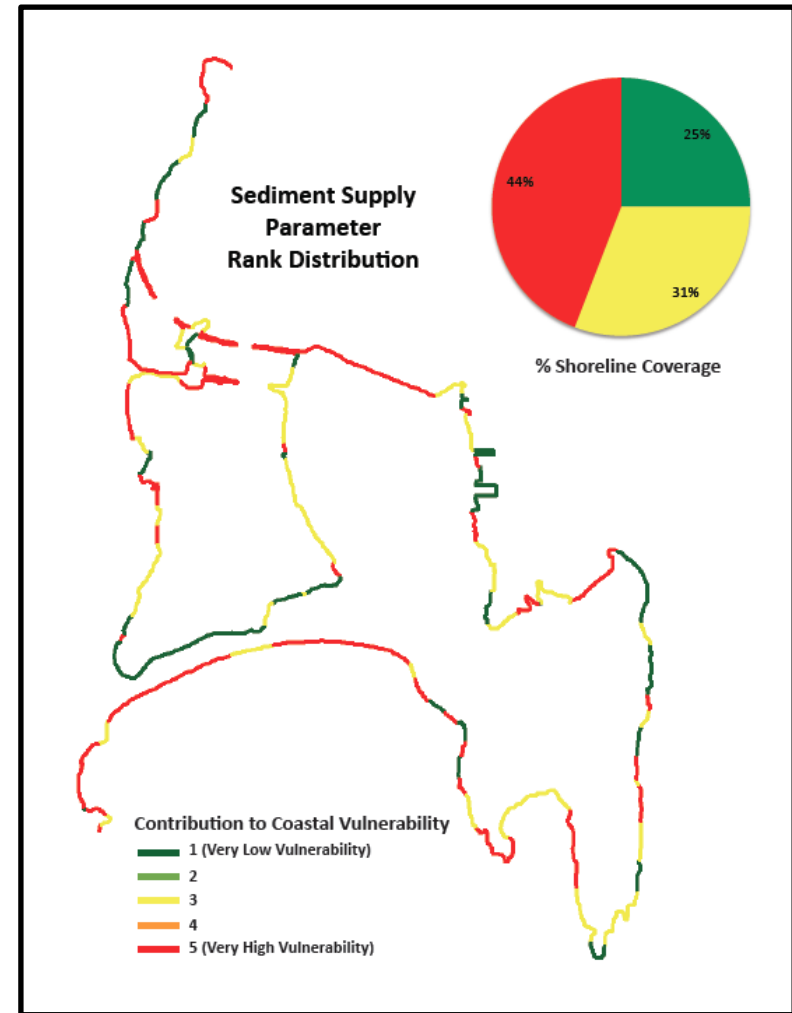


Figure A.13 Contribution of Sediment Supply Parameter to Coastal Vulnerability. Where % Shoreline Coverage = percent of shoreline associated with each vulnerability rank.

APPENDIX C

PERMISSIONS

Bil Atwood
Municipal Climate Change Action Plan Coordinator/Lockeport Resident
Picture Permission for Figures 2.3 and 2.4

Samantha Page
To: Bil Atwood
13/11/2014
Subject: Picture Permission

Hi Bil,

I hope this email finds you and your family doing well! I realize that the MCCAP position with the town ended at the end of December last year, and I understand that it is no longer your duty to liaise with the researchers or ParCA project, however I was hoping that you would give me permission to use two of your pictures (see attached) from the MCCAP report in my thesis. Please let me know if this is ok.

On another note, since I know how interested you are about Lockeport and the climate change impacts its facing, I wanted to let you know that I have done some coastal vulnerability assessments under different scenarios for the entire town of Lockeport and have included a simple analysis of buildings at risk to erosion and inundation from sea level rise. I am currently finishing the writing of my thesis, but if you are interested in receiving a copy, I would be more than happy to pass one along. Danika and I are also planning on meeting with Joyce in January/February to present our results, and while I can respectfully appreciate if you are not interested in joining us, I thought I would extend the invitation just in case.

All the best,
Sam

Samantha W. Page
MSc. Candidate at Saint Mary's University
Coastal Geomorphology and Integrated Coastal Zone Management

Geography Department
923 Robie Street
Halifax, Nova Scotia
B3H 3C3

Bil Atwood
To: Samantha Page
14/11/2014
Subject: Permission granted

Hey Sam!!

Good to hear from you. How are you? All good here.

Yep, it's been almost a year since I have completed the MCCAP.

Sure you can use the pictures or whatever else you need. I'm willing to contribute whenever I can. When you come down in the new year, let me know or Joyce will get in touch with me , I would like to be there. I would like a copy of your thesis..that would be great!!

I believe over the next year some huge political changes will give CC and all of the issues the final push to the forefront. Good on you and all involved for the hard work at such an important time.

Take care,

Bil

IPCC Copyright Policy

Retrieved from: http://www.ipcc.ch/home_copyright.shtml [accessed January 3rd, 2015]

Figure Permission for Figures 1.1 and 1.2

Unless otherwise stated, the information available on this website, including text, logos, graphics, maps, images, audio clips or electronic downloads is the property of the IPCC and is protected by intellectual and industrial property laws. You may freely download and copy the material contained on this website for your personal, non-commercial use, without any right to resell or redistribute it or to compile or create derivative works there from, subject to more specific restrictions that may apply to specific materials. Reproduction of limited number of figures or short excerpts of IPCC material is authorized free of charge and without formal written permission provided that the original source is properly acknowledged, with mention of the complete name of the report, the publisher and the numbering of the page(s) or the figure(s). Permission can only be granted to use the material exactly as it is in the report. Please be aware that figures cannot be altered in any way, including the full legend. For media use it is sufficient to cite the source while using the original graphic or figure. In line with established Internet usage, any external website may provide a hyperlink to the IPCC website or to any of its pages without requesting permission. For any other use, permission is required. To obtain permission, please address your request to the Secretary of the IPCC in a signed letter with all relevant details using official letterhead and fax it to: +41 22 730 8025. All communications by mail should be addressed to:

IPCC Secretariat
World Meteorological Organization
7bis Avenue de la Paix, P.O. Box No. 2300
CH-1211 Geneva 2,
Switzerland

Peter Swim
Lockeport Town Market
Postcard Permission for Figures 2.2, 2.5, and 2.6

Phone Conversation with Seeblick Printing on November 14th, 2014.